

Expression of sigma receptors in human cancer cell lines and effects of novel sigma-2 ligands on their proliferation

Item Type	Thesis or dissertation
Authors	Abbas, Haider
Download date	2026-03-16 10:59:58
Link to Item	http://hdl.handle.net/2436/621768

**EXPRESSION OF SIGMA RECEPTORS IN HUMAN
CANCER CELL LINES
AND
EFFECTS OF NOVEL SIGMA-2 LIGANDS ON THEIR
PROLIFERATION**

Dr. Haider Abbas MBBS

A thesis submitted for the degree of Doctor of Philosophy
University of Wolverhampton

August 2018

This work on any part thereof has not previously been presented in any form to the University or any other body whether for the purpose of assessment, publication or for any other purpose (unless otherwise indicated). I confirm that the intellectual content of the work is the result of my own efforts and of no other person.

The right of Haider Abbas to be identified as author of this work is asserted in accordance with ss.77 and 78 of the Copyright, Designs and Patents act 1988. At this date copyright is owned by the author.

Signature

Date

Declaration

I Dr. Haider Abbas confirm that the work presented in this thesis is my own. Where information has been derived from other sources, I confirm that this has been indicated in the thesis.

Signature

Date

Abstract

Sigma receptors originally thought to be an opioid receptor is now categorized as a distinct class of receptor. There are two main subtypes, the sigma-1 receptor and an uncharacterised binding site, named the sigma-2 binding site. The presence of the sigma-2 binding site shows high correlation with proliferation of cells and is associated with cancer.

I have categorized sigma-1 and sigma-2 binding sites in 11 human tumour cell lines. I have demonstrated that tumour cell lines from a range of tissues express both sigma-1 and sigma-2 binding sites. One exception is the MCF7 breast cancer cell line, which lacks sigma-1 receptors. I show that the quantitation of sigma-2 binding sites using the "masking" protocols are flawed, significantly overestimating levels of sigma-2 binding sites. I propose novel protocols to determine levels of sigma-1 receptors and sigma-2 binding sites in cell lines and tissue.

Using radioligand binding assays in MCF7 cells, I have characterised novel sigma-2 ligands. These ligands are simple ammonium salts containing a single nitrogen atom. They are simpler than the previously recognised pharmacophore for the sigma-2 site. I have shown that these simple ammonium salts show graded affinity for the sigma-2 binding site. The highest affinity ligands were dihexylammonium (pK_i 7.58) and dioctylammonium (pK_i 7.9).

I have used these ammonium salts and previously characterised ligands to determine sigma-2 binding site biology. I have shown that the biological activity of these drugs is related neither to their hydrophobicity nor their ability to effect calcium signalling in cells. I propose that the Hill slope of binding is inversely related to the efficacy of a ligand to inhibit metabolic activity of cancer cells. Furthermore, I offer an explanation as to why concentrations of sigma-2 ligands far higher than their determined binding affinities are required to inhibit metabolic activity.

Acknowledgement

I would like to thank Dr Steve Safrany for his supervision, support and guidance throughout the past four years. I would also like to express my sincere gratitude to Prof. David Ferry for his encouragement and help during my research. Without their expert guidance I would not have managed to achieved as much as I have and for that I am truly grateful.

I would like to thank Dudley group of hospitals NHS trust and New Cross Hospital NHS trust for providing the funding for my research.

I would like to thank all my wonderful friends that I have made at the University of Wolverhampton.

I would never have made it this far without the unconditional support and encouragement of my parents and siblings.

Finally I would like to express my love and appreciation for my wife Saadia, daughter Anaya and son Azlan, without their love, affection and patience all this would not have been possible.

Table of Contents

Chapter 1. INTRODUCTION.....	17
1.1 The importance of receptors and receptor theory	18
1.2 History of the sigma-2 binding site	22
1.3 Sigma-2 binding site structure and function	23
1.4 Sigma-2 binding site distribution and cellular proliferation	25
1.5 Sigma-2 binding sites and cancer	26
1.6 Sigma-2 binding sites and their role in non-invasive imaging of cancer	28
1.7 Sigma-2 binding sites and apoptosis in tumour cells	33
1.8 Sigma-2 binding site ligands.....	36
1.8.1 6,7-dimethoxytetrahydroisoquinoline derivatives	37
1.8.2 Tropane and Granatane derivatives	39
1.8.3 Indole derivatives	41
1.8.4 Cyclohexylpiperazine derivatives.....	43
1.8.5 Miscellaneous compounds with high affinity for sigma-2 binding sites.....	45
1.9 The Sigma-2 binding site ligand pharmacophore	47
1.10 Sigma-2 binding sites and lipid rafts	48
1.11 Sigma-2 binding sites and PGRMC1	50
1.12 Aim of my thesis	51
Chapter 2. MATERIALS & METHODS	53
2.1 General Materials.....	54
2.2 Tissue Culture	54
2.3 Cell propagation and storage.....	55
2.4 General Ligand preparation	56
2.5 General Radioligand binding	59
2.5.1 Saturation binding assays	60
2.5.2 Pentazocine	60
2.5.3 DTG	61
2.6 Competition binding assay	61
2.7 Protein measurement.....	62
2.8 MTS cell proliferation assay	62
2.9 Fura-2 Calcium measurement.....	63
2.10 Data analysis	65
Chapter 3. CHARACTERISATION OF SIGMA-1 RECEPTORS AND SIGMA-2 BINDING SITES IN HUMAN CANCER CELL LINES	70
3.1 Background	71
3.2 Expression of sigma-1 receptor	73
3.3 Oesophageal cancer cell lines (FLO-1, OE21 and OE33)	74
3.4 Breast cancer cell lines (MCF7, MDA-MB-468)	76
3.5 Colorectal cancer cell lines (Caco-2, HCT 116, HT-29 and SW480) ..	77
3.6 Human embryonic kidney cell line (293)	79
3.7 Lung cancer cell line (A549).....	80
3.8 Measurement of pan-sigma binding	82
3.9 Oesophageal cancer cell lines (OE21, OE33 and FLO-1)	97
3.10 Breast cancer cell lines (MCF7, MDA-MB-468)	99
3.11 Colorectal cancer cell lines (Caco-2, SW480, HT-29 and HCT 116).....	101

3.12 Human embryonic kidney cell line (293)	103
3.13 Lung cancer cell line (A549)	103
3.14 Competition binding	106
3.14.1 Oesophageal cancer cell lines	106
3.14.2 Breast cancer cell lines	108
3.14.3 Colorectal cancer cell line	110
3.14.4 Human embryonic kidney (293) and lung cancer (A549) cell lines.	111
3.15 Discussion	115
Chapter 4. AFFINITY OF AMMONIUM SALTS AND SIGMA-2 LIGANDS TO THE SIGMA-2 BINDING SITE.	124
4.1 Background	125
4.2 Saturation [³H] DTG binding in MCF7 cells	128
4.3 Simple straight chain ammonium salts	129
4.4 Primary ammonium salt affinity for the sigma-2 binding site	129
4.5 Secondary ammonium salt affinity for the sigma-2 binding site	131
4.6 Tertiary ammonium salt affinity for the sigma-2 binding site	133
4.7 Quaternary ammonium salt affinity for the sigma-2 binding site ...	135
4.8 Simple branched chain ammonium salts	136
4.9 Primary branched chain ammonium salt affinity for sigma-2 binding site affinity	137
4.10 Secondary branched chain ammonium salt affinity for the sigma-2 binding site	138
4.11 Tertiary branched chain ammonium salt affinity for the sigma-2 binding site	140
4.12 Sigma-2 ligands affinity for the sigma-2 binding site	141
4.13 Discussion	143
4.13.1 Primary ammonium salts.....	143
4.13.2 Secondary ammonium salts.....	144
4.13.3 Tertiary and quaternary ammonium salts.....	145
4.13.4 Commercially available sigma ligands.....	147
4.14 Summary	149
Chapter 5. BIOLOGICAL ACTIVITY OF SIGMA-2 BINDING SITE LIGANDS	150
5.1 Background	151
5.1.1 Effects on electrically stimulated bladder	151
5.1.2 MTS cell “viability” assays.....	151
5.1.3 Lactate dehydrogenase (LDH) assays	152
5.1.4 Calcium homeostasis	153
5.1.5 Caspase activation assays	155
5.2 Results	155
5.2.1 Effects of ammonium salts on cellular proliferation.....	155
5.2.2 Physiochemical properties of primary ammonium salts.....	158
5.2.3 Physiochemical properties of secondary ammonium salts	161
5.2.4 Physiochemical properties of tertiary ammonium salts.....	163
5.2.5 Physiochemical properties of quaternary salts.....	164
5.2.6 Physiochemical properties of commercial ligands	164
5.2.7 Effects of ligands on intracellular calcium	167
5.2.8 Is there evidence for sigma-1 receptor and sigma-2 binding site cross talk?.....	177

5.3 Discussion	179
5.3.1 Definition of agonist and antagonist at the Sigma-2 binding site	179
5.3.2 Correlation between Hill slope and agonistic behaviour	185
5.3.3 Do Sigma-2 ligands meet Lipinski's rule of Five	189
Chapter 6. Discussion	199
6.1 Correct designation of sigma-1 and sigma-2 levels in cells and tissue.	200
6.2 Identification of simple, high-affinity ligands.	201
6.3 Biologically active drugs have a low Hill slope	202
6.4 Sigma-2 activity is not related to calcium or lipophilicity	202
6.5 Desensitisation of sigma-2 binding sites raises the affinity.	202

Table of figures

Figure 1-1: The two-state model of receptors.....	20
Figure 1-2: Example of dose response curve to different types of ligands.....	21
Figure 1-3: Crystal structure of the sigma-1 receptor.....	24
Figure 1-4: Hallmarks of cancer.....	26
Figure 1-5: The role of calcium and cytochrome C in cellular apoptosis (Mattson and Chan, 2003).....	35
Figure 1-6: Hypothetical sigma-2 binding site binding model.....	48
Figure 2-1: Fluorescence excitation spectra of Fura-2.....	64
Figure 3-1: Saturation binding of [³ H] (+) pentazocine to oesophageal cancer cell lines (A: FLO-1, B: OE21 and C: OE33).....	75
Figure 3-2: Saturation binding of [³ H] (+) pentazocine to MDA-MB-468 cells ...	76
Figure 3-3: Saturation binding of [³ H] (+) pentazocine to colorectal cancer cell lines (A: Caco-2, B: HCT 116, C: HT-29 and D: SW480).....	78
Figure 3-4: Saturation binding of [³ H] (+) pentazocine to 293 cells.....	79
Figure 3-5: Saturation binding of [³ H] (+) pentazocine to A549 cells.....	80
Figure 3-6: Binding profile of a ligand.....	83
Figure 3-7: Binding profile of sigma receptors in the best case scenario.....	84
Figure 3-8: Binding profile of sigma receptors in the worst case scenario.....	85
Figure 3-9: Percentage change in (+) pentazocine displacement with increasing DTG concentration.....	86
Figure 3-10: (+) Pentazocine displacement with increasing DTG concentration.....	87
Figure 3-11: Percentage displacement of (+) pentazocine with increasing DTG concentration.....	88
Figure 3-12: Displacement of (+) pentazocine form sigma-2 binding site with increasing concentration of DTG.....	88
Figure 3-13: Calculated binding dextrallorphan to sigma-2 sites.....	90
Figure 3-14: Binding of dextrallorphan at two different affinities.....	91
Figure 3-15: Displacement of dextrallorphan with increasing concentration of DTG.....	92

Figure 3-16: Percentage displacement of dextralorphan with increasing DTG concentration.	93
Figure 3-17: Saturation binding of [³ H] DTG in oesophageal cancer cell lines (A: FLO-1, B: OE21 and C: OE33).....	98
Figure 3-18: Saturation binding of [³ H] DTG in breast cancer cell lines (A: MCF7, B: MDA-MB-468).....	100
Figure 3-19: Saturation binding of [³ H] DTG to colorectal cancer cell lines (A: Caco-2, B: HCT 116, C: HT-29 and D: SW480).....	102
Figure 3-20: Saturation binding of [3H] DTG to 293 cells	103
Figure 3-21: Saturation binding of [³ H] DTG in A549	104
Figure 3-22: Competition binding between [³ H] DTG and (+) pentazocine in oesophageal cancer cell lines.	107
Figure 3-23: Competition binding between [³ H] DTG and (+) pentazocine in breast cancer cell lines.	109
Figure 3-24: Competition binding between (+) pentazocine and [³ H] DTG in colorectal cancer cell lines.	110
Figure 3-25: Competition binding of (+) pentazocine and [³ H] DTG in human embryonic and lung cancer cell lines.	112
Figure 3-26: Summary of the relative ratio of sigma-1 and sigma-2 binding sites in a range of cells.....	113
Figure 3-27: Relationship between K _d and off rate.....	118
Figure 3-28: Comparison of sigma-1 B _{max} calculated by two methods.....	122
Figure 4-1: Hypothetical sigma-2 binding site pharmacophore.....	127
Figure 4-2: Saturation binding of [³ H] DTG in MCF7 cells.....	128
Figure 4-3 Summary of primary ammonium salt binding to the sigma-2 binding site.....	130
Figure 4-4: Summary of Secondary ammonium salt binding to the sigma-2 binding site	132
Figure 4-5: Summary of tertiary ammonium salts binding to the sigma-2 binding site.....	134
Figure 4-6: Summary of quaternary ammonium salt binding to the sigma-2 binding site	136

Figure 4-7: Summary of simple primary branched chain primary ammonium salt binding to the sigma-2 binding site.....	137
Figure 4-8: Summary of the simple secondary branched chain ammonium salts to the sigma-2 binding site.....	139
Figure 4-9: Summary of the simple tertiary branched chain ammonium salts to the sigma-2 binding site.....	140
Figure 4-10: Summary of affinity of sigma-2 ligands to the sigma-2 binding site	142
Figure 5-1: Correlation between affinity for the sigma-2 binding site and calcium response	154
Figure 5-2: Change in fluorescence following addition of rimcazole and octylammonium.....	168
Figure 5-3: Effects of octylammonium and decylammonium on intracellular calcium.	169
Figure 5-4: Effects of dihexylammonium and trihexylammonium on intracellular calcium.	170
Figure 5-5: Effects of AG-205 on intracellular calcium.	171
Figure 5-6: Effects of AG-205 and PB28 on Fura-2's ratiometric signal.....	172
Figure 5-7: Effects of progesterone and (+) pentazocine on intracellular calcium.	173
Figure 5-8: Effects of Progesterone on intracellular calcium.....	174
Figure 5-9: Effects of SM21 and PB28 on intracellular calcium	174
Figure 5-10: Effects of ifenprodil and haloperidol on intracellular calcium.	175
Figure 5-11: pIC ₅₀ and calcium response in MCF7 cells with sigma-2 binding site ligands.	177
Figure 5-12: Relationship between Hill slope (nH) and log (IC ₅₀ /K _i) in MCF7 cells.	187
Figure 5-13: log (IC ₅₀ /K _i) and clogD of sigma-2 binding site ligands.	197

List of tables

Table 1-1: Sigma-2 binding site-selective 6,7-Dimethoxytetrahydroisoquinoline analogue ligands.....	38
Table 1-2: Sigma-2 binding site-selective granatane or tropane analogue ligands.....	40
Table 1-3: Sigma-2 binding site-selective indole analogue ligands	42
Table 1-4: Sigma-2 binding site-selective cyclohexylpiperazine analogue ligands.....	44
Table 1-5: Sigma-2 binding site-selective ligands - miscellaneous structures ..	46
Table 2-1: Simple amine structure, salt and where it was purchased.	59
Table 3-1: Expression of sigma receptors in human cancer cell lines.....	72
Table 3-2: Binding parameters of sigma-1 receptors in various human tumour cell lines.	81
Table 3-3: Summary of range of (+) pentazocine binding to sigma binding sites.	94
Table 3-4: Summary of range of dexrallorphan to sigma binding sites.	94
Table 3-5: Displacement of (+) pentazocine or dexrallorphan by DTG.	95
Table 3-6: Displacement of (+) pentazocine or dexrallorphan by DTG (256nM).	95
Table 3-7: Calculation of sigma-2 binding site density.....	105
Table 3-8: Calculation of sigma-1 and sigma-2 binding sites based on competition binding assay.	114
Table 3-9: Calculation of sigma-1 and sigma-2 binding sites based on competition binding assay.	121
Table 4-1: Affinity of primary ammonium salts for the sigma-2 binding site. ...	143
Table 4-2: Affinity of secondary ammonium salts for the sigma-2 binding site.	145
Table 4-3: Affinity of tertiary ammonium salts for the sigma-2 binding site.	146
Table 4-4: Affinity of commercially available sigma ligands for the sigma-2 binding site.....	148
Table 5-1: Primary ammonium salts characteristics.....	157
Table 5-2: Secondary ammonium salts characteristics.....	160

Table 5-3: Characteristics of tertiary ammonium salts.	162
Table 5-4: Characteristic of quaternary ammonium salts.	164
Table 5-5: characteristics of commercially available sigma-1 and sigma-2 binding site ligands.	166
Table 5-6: Summary of pIC ₅₀ and calcium response to sigma-2 binding site ligands.	176
Table 5-7: Summary of sigma-1 receptor and sigma-2 binding affinities and pIC ₅₀ values for inhibition of metabolic activities in MCF7, MDA-MB-468 and A549 cells.	178
Table 5-8: Summary of characteristics of sigma-2 binding site ligands.	183
Table 5-9: Physiochemical properties of all the ligands.	194
Table 5-10: log (IC ₅₀ /K _i) and clogD of sigma-2 binding site ligands.	196

Abbreviations

Abbreviation	Full name
(+)pentazocine	(1S,9S,13S)-1,13-dimethyl-10-(3-methylbut-2-en-1-yl)-10-azatricyclotrideca-2,4,6-trien-4-ol
σ -1 receptor	Sigma-1 receptor
σ -2	Sigma-2 binding site
[Ca ²⁺]	Calcium ion concentration
A549	Human epithelial alveolar adenocarcinoma
B _{max}	Maximum binding of a ligand to a receptor
Caco-2	Human epithelial colorectal adenocarcinoma
CI	Confidence intervals
CO ₂	Carbon Dioxide
DMEM	Dulbecco Modified Eagle's minimum essential media
DMSO	Dimethyl sulfoxide
EC ₅₀	Effective concentration of a drug to cause 50% maximal response
EDTA	Ethylenediaminetetraacetic acid
FCS	Foetal Calf serum
FLO-1	Human oesophageal adenocarcinoma
G-Protein	guanosine triphosphate-binding protein
HCl	Hydrochloric acid
HCl•	Hydrochloride salt

HCT 116	Human epithelial colorectal adenocarcinoma
293	Human Embryonic Kidney cell line
HT-29	Human epithelial colorectal adenocarcinoma
IC ₅₀	Concentration required to cause a 50% drop in maximal response.
IP ₃	Inositol 1,4,5-trisphosphate
IPAG	1-(4-Iodophenyl)-3-(2-adamantyl)guanidine
K ₅₀	Equilibrium dissociation constant for binding that does not follow the laws of mass action
K _d	Equilibrium Dissociation Constant derived from saturation binding
K _i	Equilibrium Dissociation Constant derived from competitive radio ligand binding
KLB	Krebs' –like buffer
MCF7	Human breast adenocarcinoma
MDA-MB-468	Human breast adenocarcinoma cell line
mM	Millimolar concentration
MTS	3-(4,5-dimethylthiazol-2-yl)-5-(3-carboxymethoxyphenyl)-2-(4-sulfophenyl)-2H-tetrazolium
nH	The Hill coefficient (slope factor) of competitive binding curves
nM	NanoMolar concentration
PBS	Phosphate Buffered saline

OE21	Human oesophageal squamous cell carcinoma
OE33	Human oesophageal adenocarcinoma
pH	The negative logarithm of the concentration of Hydrogen ions in a solution in moles per litre
pIC ₅₀	Negative logarithm of the dose required to reduce a response by half.
pK ₅₀	Negative logarithm of the concentration of ligand required to occupy 50% of receptors when the binding does not follow the laws of mass action
pK _d	Negative logarithm of the equilibrium dissociation constant that is derived from saturation binding assays
pK _i	Negative logarithm of the equilibrium dissociation constant that is derived from competitive binding assays
Rimcazole	9-(3-((3R,5S)-3,5-dimethylpiperazin-1-yl)propyl)-9H-carbazole
RPMI	Roswell Park Memorial Institute
SD	Standard deviation
SEM	Standard Error of the mean (SD/\sqrt{n})
SW480	Human epithelial colorectal adenocarcinoma
TBS	Tris(hydroxymethyl)aminomethane buffered saline
Tris	Tris(hydroxymethyl)aminomethane

μM

Micromoles per litre concentration

Chapter 1. INTRODUCTION

1.1 The importance of receptors and receptor theory

A receptor is a small protein molecule usually embedded in the cell membrane, which transduces a chemical signal from an extracellular environment to the intracellular environment and hence helps the cell to respond to various stimuli. When a chemical signal binds to a receptor it results in transformational change, which further results in some form of cellular response. Although the majority of receptors are found on the cell membrane, they are also found in the cytoplasm and in the nucleus. A general overview on receptors can be found in all pharmacology textbooks, including Rang and Dale's Pharmacology (Rang & Dale's Pharmacology, 8th Edition, Authors: Ritter, Flower, Henderson and Rang, Paperback ISBN: 9780702053634, pp22-49). Based on their structure, receptors can be broadly classified into the following categories:

Type 1 - Ligand-gated ion channels (Ionotropic receptors): These receptors are usually targets of neurotransmitters like GABA and acetylcholine (working through nicotinic acetylcholine receptors). Activation of these receptors by ligands results in the movement of ions across the cell membrane through the same protein. Several examples of cell surface (e.g. nicotinic and 5-hydroxytryptamine (Wu *et al.*, 2015) and intracellular (e.g. inositol 1,4,5-trisphosphate (IP₃) and ryanodine receptors (Seo *et al.*, 2015) exist, allowing the flood of ions down a concentration gradient in an energy-independent manner.

Type 2 - G protein-coupled receptors: This is the largest family of receptors and is composed of proteins containing seven transmembrane alpha helices. The ligand-binding site for larger peptides is usually present on the extracellular domain. Endogenous ligands are usually different types of hormones (examples include histamine and acetylcholine (working through muscarinic acetylcholine receptors (Haga, 2013)) .

Type 3 - Kinase related receptors are composed of extracellular component, which binds to the ligand and intracellular component, which is linked with various downstream signalling pathways. Two subclasses of these receptors exist: those which intrinsic kinase activity, an example of which would include the insulin receptor (Taniguchi *et al.*, 2006) and those without kinase activity that recruit an intracellular kinase following activation by a ligand, examples of which would include cytokine receptors (Abate *et al.*, 2010) .

Type 4 - Nuclear receptors, which can, again, be divided up into two major groups. Homodimeric nuclear receptors are usually found in the cytoplasm. Their endogenous ligands include testosterone and oestrogen (Mauvais-Jarvis, 2011). Upon stimulation with a ligand, dimerization occurs and these receptors are trafficked into the nucleus, where they bind specific response elements on the DNA and regulate protein synthesis. Heterodimeric nuclear receptors pre-exist as dimers with the retinoid X receptor (RXR) and are found in the nucleus. Examples of ligands include thyroid hormone (Rastinejad *et al.*, 1995) and free fatty acids (Johnson *et al.*, 1996). Upon stimulation with a ligand, dissociation from a co-repressor occurs and these receptors bind specific response elements on the DNA and regulate protein synthesis.

Other receptors exist with different structures. Examples include the tumour necrosis factor (TNF) receptor (Tang *et al.*, 1996) and the sigma-1 receptor (Schmidt *et al.*, 2016), both of which exist as trimers.

Binding of an agonist to the receptor results in a conformational change (Couette *et al.*, 1996, Henschman *et al.*, 2005), which results in altered downstream signalling pathways and hence the message is transduced from the extracellular environment to the intracellular area. For example, when an agonist binds the tyrosine kinase receptor, phosphorylation of tyrosine residues of the intracellular part of the receptor occurs and hence results in activation of signal transduction pathways; in receptors linked to ion channels it results in

opening of the ion channels allowing the movement of ions across the membrane down a concentration gradient (Jelacic *et al.*, 1999).

The two-state model of receptors suggests that a receptor exists in equilibrium between inactive (R) and active (R*) states (Black and Leff, 1983, Del Castillo and Katz, 1957) (see Fig 1-1). An agonist, which has higher affinity for the active form R* binds to it selectively. This removes the free active form from the equilibrium resulting in re-equilibration and a shift of the equilibrium to the right, creating more receptor in the active R* state, enhancing the physiological response. An inverse agonist has higher affinity for the receptor in the inactive R form and shifts the equilibrium to the inactive state, resulting in a negative physiological response.

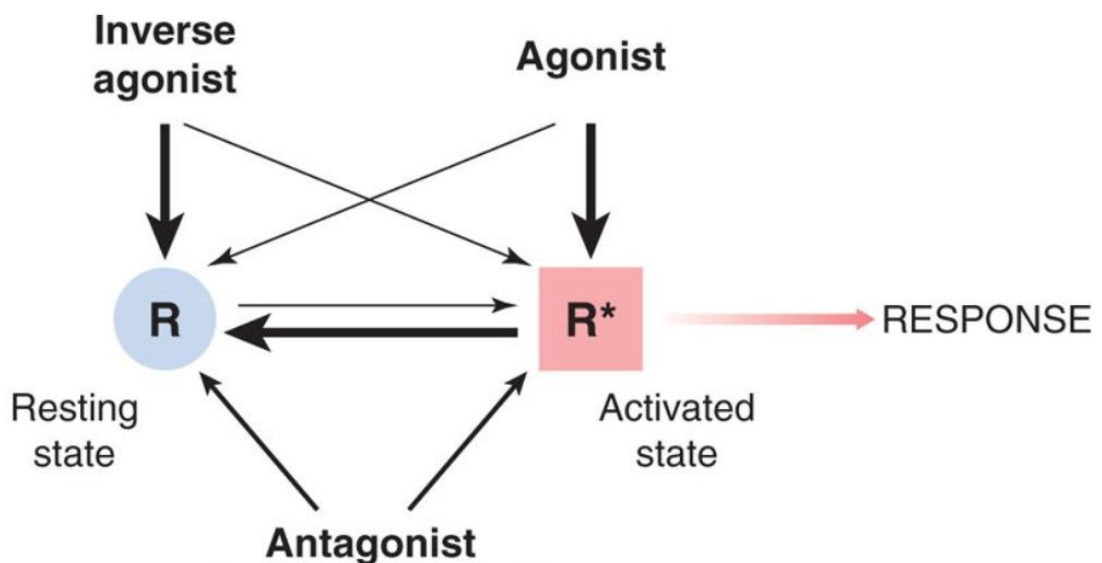


Figure 1-1: The two-state model of receptors.

Receptors exist in an inactive form (R) and an active form (R*). Inverse agonists selectively bind R, whereas agonists selectively bind R*. Pure antagonists bind both R and R* with no selectivity. Figure taken from Rang and Dale's Pharmacology, 6th Ed.

A pure antagonist has the same affinity for both inactive R and active R* states of the receptor so binding of an antagonist does not alter the equilibrium and so gives no direct response, as shown in Figure 1-1. It does, however, inhibit the

binding of an agonist or inverse agonist preventing them from having their effects

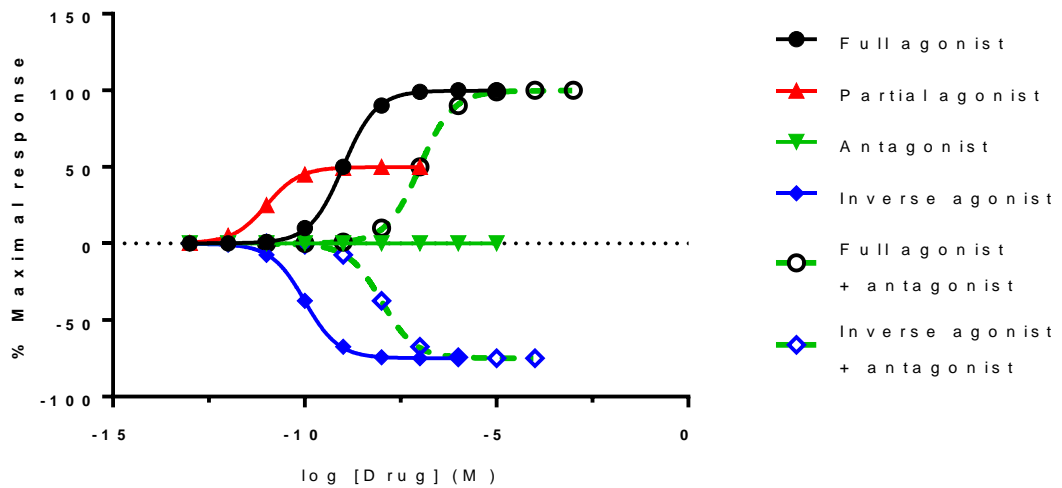


Figure 1-2: Example of dose response curve to different types of ligands.

A full agonist is able to produce a maximal response. Inverse agonists induced a negative response. Partial agonists produce a less than maximal response. Competitive antagonists have no effect, but do alter the ability of agonists to cause their effects.

A full agonist may need to bind to a small number of receptors as compared to partial agonist to produce a physiological response, whereas a partial agonist may not be able to elicit a maximal physiological response despite occupying all the receptors. Potency relates to the concentration of a drug required to produce a physiological response of a given intensity (x-axis), it is measured by the effective concentration of a drug giving 50% of its maximal response (EC_{50}). Efficacy describes the maximal size of a response elicited by a drug (y-axis), it is measured by the intrinsic activity (IA) of a drug in the specific system. A full agonist would have an IA of 1, whereas a partial agonist would have an IA of less than one. There is no relationship between potency and efficacy.

1.2 History of the sigma-2 binding site

Although it has been more than 40 years since sigma receptors were initially identified as a subclass of opioid receptors, the understanding of sigma receptors is still far from complete. Initial work on sigma receptors was directed on their role in the central nervous system, however subsequently it was shown that these receptors are abundantly distributed outside the central nervous system as well (Vilner *et al.*, 1995b).

Martin *et al.* initially suggested the term sigma-opioid receptor in 1976 to explain the psychomimetic effects seen with benzomorphan, N-allyl-normetazocine (SKF 10047) and its analogues. Martin *et al.* (Martin *et al.*, 1976) described the psychomimetic effects of SKF 10047 whilst working with morphine dependant and non-dependant chronic spinal dogs. Rather than causing analgesia, benzomorphans such as SKF 10047 and pentazocine caused psychomimetic effects. These receptors were suggested as novel opioid receptors in view of effects of SKF 10047 which could not be attributed to μ (morphine) receptors, κ (ketocyclazocine) receptors or δ receptors, and the fact that the effects were antagonized by naloxone, a universal opioid antagonist. Martin suggested SKF 10047 to be agonist at sigma opioid receptor, in order to cause these effects (Martin *et al.*, 1976). SKF 10047 was called an agonist because it caused tachycardia, tachypnea, mydriasis and raised body temperature, whereas μ receptor agonist resulted in bradycardia, low reparatory rate, hypothermia and miosis. Antagonists were agents that could block these responses.

Whilst trying to characterise the sigma-opioid receptor, Su discovered a binding site that was labelled by SKF 10047, a sigma-opioid ligand, but showed no affinity to naloxone (Su, 1982). This binding site was different from what Martin *et al.* had suggested, since the latter was sensitive to naloxone. Experiments with SKF 10047 were repeated again and it was found that the psychomimetic effects of SKF 10047 were not antagonized by naltrexone, another potent

analogue of naloxone, hence the binding site identified by Su was different to the sigma opioid receptor (Su *et al.*, 1988). Furthermore this binding site showed stereoselectivity for dextrorotatory benzomorphans such as (+) SKF 10047 and (+) pentazocine, which was not characteristic of an opioid receptor.

For some time the sigma receptor was confused with the phencyclidine (PCP) binding sites within the N-methyl-D-aspartate (NMDA) receptor (Mendelsohn *et al.*, 1985, Zukin *et al.*, 1984). However, in subsequent years further binding studies with specific ligands led to reclassification of these binding sites as unique entities unlike any other neurotransmitter or hormone binding protein (Quirion *et al.*, 1987, Tam, 1985). These receptors were later called “sigma receptors” distinguishing them from opioid receptors. Su also noted that none of the endogenous opioid ligands inhibited sigma receptor binding. Still no endogenous ligand for sigma receptors has been identified.

1.3 Sigma-2 binding site structure and function

Sigma receptors are classified in two main subtypes; sigma-1 and sigma-2, based on pharmacological and biochemical properties (Hellewell and Bowen, 1990, Quirion *et al.*, 1992). The subtypes differ mainly in their affinity for different drugs. The sigma-1 receptor has high affinity for the (+)-isomer of pentazocine and SKF 10047, whereas the sigma-2 binding site has high affinity for the (-)-stereoisomers (Bowen *et al.*, 1993, Hellewell *et al.*, 1994). Both subtypes also differ in distribution pattern, cellular localization and molecular weight (Itzhak, 1994, Torrence-Campbell and Bowen, 1996).

The sigma-1 receptor has been cloned from human placental choriocarcinoma cells (Kekuda *et al.*, 1996), human brain (Prasad *et al.*, 1998), guinea-pig liver (Hanner *et al.*, 1996), rat brain (Seth *et al.*, 1998) and mouse brain (Pan *et al.*, 1998). Recently, the crystal structure of the sigma-1 receptor has been solved.

It appears to exist as a homotrimer and contains one transmembrane domain. The crystal structure of the sigma-1 receptor is shown in Figure 1-3.

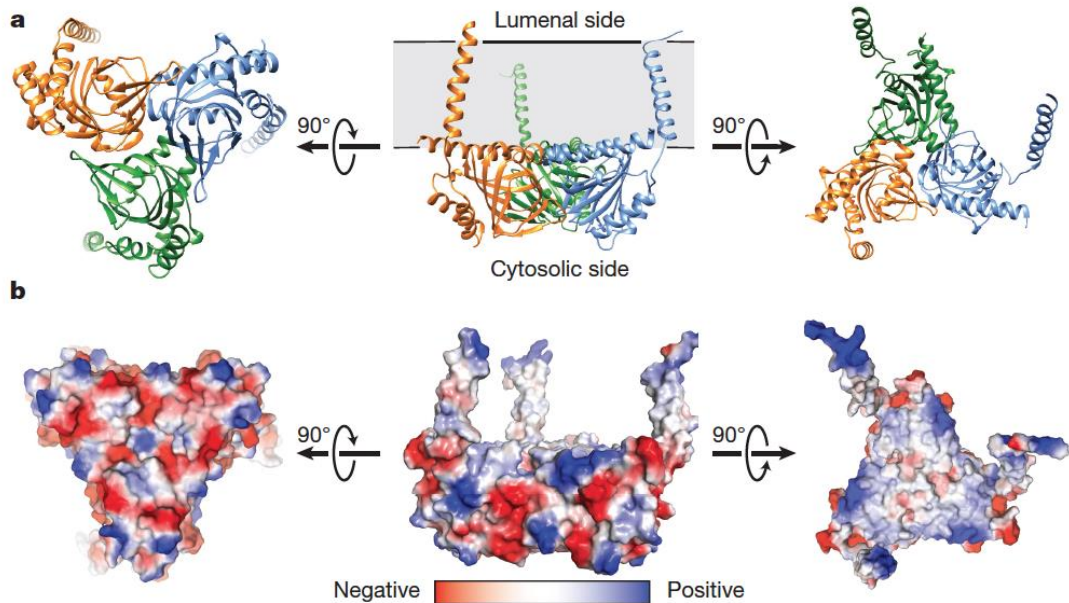


Figure 1-3: Crystal structure of the sigma-1 receptor

A, viewed perpendicular to the membrane plane, the sigma-1 receptor shows a triangle structure comprising three tightly associated protomers, each with a single transmembrane domain at the corner of the oligometric triangle. From the side, the receptor reveals a flat membrane-associated surface. B, Colouring by electrostatic potential reveals a polar cytosolic surface, and a non-polar membrane-interacting surface flanked by positive charges. Images taken from (Schmidt *et al.*, 2016).

The sigma-2 binding site is not yet cloned. The molecular size of sigma-2 binding site determined by photoaffinity labelling and sodium dodecyl sulphate (SDS) polyacrylamide gel electrophoresis is reported to be 18-21kDa (Hellewell and Bowen, 1990, Hellewell *et al.*, 1994). In order to visualize the sigma-2 binding site, radioligands have been used. Unfortunately, these ligands do not completely discriminate between sigma-1 and sigma-2 binding sites. However, some studies have suggest that these two receptors are usually co-localized (Bouchard and Quirion, 1997, McCann *et al.*, 1994), yet they may be present in different ratios (Leitner *et al.*, 1994). A proposal that the sigma-2 binding site is the progesterone receptor membrane component-1 (Xu *et al.*, 2011) has raised

fierce debate. Other research groups show they are different (Abate *et al.*, 2015a, Chu *et al.*, 2015, Hiranita, 2016, Pati *et al.*, 2016) while supporting data for co-identity from the original laboratory has also been published (Zeng *et al.*, 2016).

1.4 Sigma-2 binding site distribution and cellular proliferation

Sigma binding sites were initially discovered in the central nervous system. However, they are widely distributed in various tissues such as liver, kidney, endocrine and nervous system (Hellewell *et al.*, 1994, Heroux *et al.*, 1992). Sigma-2 binding sites are found in high density in liver and kidney (Hellewell *et al.*, 1994). In order to see if there was any relationship between sigma-2 binding site density and cellular proliferation Mach *et al.* conducted an important study in 1997. The author used a well-characterised *in vitro* mouse mammary adenocarcinoma, line 66, and showed that the sigma-2 binding site density was 10 times more in proliferating cells as compared to quiescent cells (Mach *et al.*, 1997). Since Mach *et al.* used a single cell line further studies are needed to see if sigma-2 binding site density could be a biomarker for proliferation.

In another important study, Al-Nabulsi *et al.* (Al-Nabulsi *et al.*, 1999) investigated other factors apart from cell proliferation, which might affect the expression of sigma-2 binding sites. The sigma-2 binding site density in proliferative cells of cell line 67 (aneuploidy mouse mammary adenocarcinomas) was found to be 8 times higher than in quiescent cells, showing similar results to those previously reported by Mach *et al.* in diploid cells. In cell line 9L, cells formed a plateau phase from division-death equilibrium, unlike cell line 66 cells, which formed plateau by forming quiescent population of cells. Sigma-2 binding site density was reduced in plateau phase and it was independent of other factors like cell-cell contact, depletion of nutrition or altered metabolism. Finally, when MCF7 cells were treated with tamoxifen, which is a cytostatic drug, a decrease in sigma-2 binding site density

was observed. Hence, it was concluded that sigma-2 binding site density was influenced by proliferation rate and not affected by other physiological or biological factors.

1.5 Sigma-2 binding sites and cancer

Cancer is characterised by uncontrolled cell growth and invasion and spread of cells from the site of origin to distant sites in the body. In 2000, Hanahan and Weinberg defined six hallmarks of cancer, which, according to them, were essential for carcinogenesis. These are shown in Figure 1-4. These hallmarks included acquiring growth signal autonomy, evasion of growth inhibitory signals, evasion of apoptosis, unlimited replicative potential, formation of new blood vessels and invasion and metastasis (Hanahan and Weinberg, 2000).

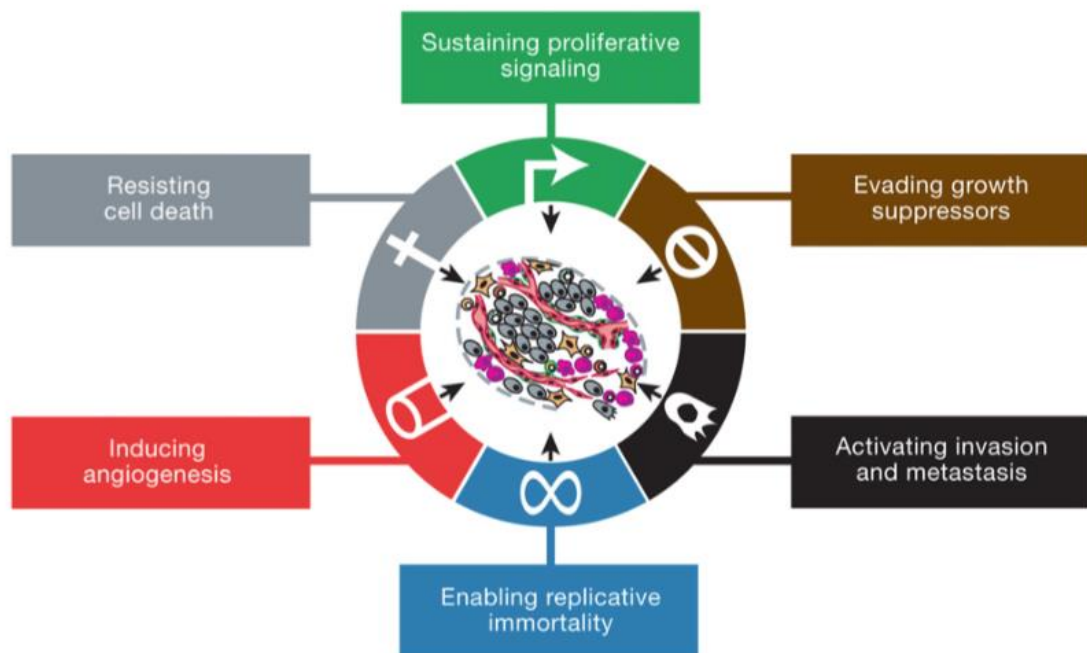


Figure 1-4: Hallmarks of cancer

Set of functional capabilities acquired by most of the cancer cells (Hanahan and Weinberg, 2000).

Most of the agents that can cause cancer would usually cause alteration to DNA sequence ranging from point mutations to large chromosomal changes,

like chromosomal deletion or translocation. The abnormalities in genetic material can be caused by either carcinogens (e.g., tobacco smoke, radiation, chemicals, or infectious agents) or by random mutations during cell replication. The incidence of cancer has increased because we are living longer and with increasing age there is an increased chance of accumulating mutations, which could lead to carcinogenesis.

In order to keep a check on the net number of cells, there are three important processes in place: First is cell proliferation, which includes both cell division and growth; second, programmed cell death or apoptosis; thirdly, cell differentiation. Any imbalance between cell growth, apoptosis or differentiation can lead to carcinogenesis. Two important gene groups that play pivotal roles in cell growth are oncogenes and tumour suppressor genes. Oncogenes (known as proto oncogenes in normal cells) have important roles in cell growth and hence a mutation of a proto-oncogene results in the up-regulation and increased production of proteins, driving cell division and growth (Vogt, 1993). Examples of oncogenes include the epidermal growth factor receptor, a tyrosine kinase receptor (Lurje and Lenz, 2009), the Myc gene, a transcription factor (Ruggero, 2009) and the GTPase, Ras (Bracquart *et al.*, 2009).

Tumour suppressor genes inhibit uncontrolled growth and multiplication. Hereditary syndromes that predispose individuals to cancer are caused by inheritance of germ line mutations of an allele and acquiring somatic mutations in a second allele later in life. This was first described by Knudson and is known as Knudson's two-hit hypothesis. It describes a strict definition of tumour suppressor genes: genes in which a germ line mutation predisposes an individual to cancer (Knudson, 1971). P53 was the first tumour suppressor gene to be identified and it is mutated in about 50% of human tumours (Hollstein *et al.*, 1991). P53 is at the heart of tumour suppressive mechanism and is also called "guardian of the genome". It holds the cell in the G1 phase of the cell cycle so that the damaged DNA can be repaired and can even initiate apoptosis if the DNA cannot be repaired (Zilfou and Lowe, 2009). Other examples of

mutations in tumour suppressor genes include adenomatous polyposis coli (APC), which, when mutated, leads to an increased risk of colorectal cancer, and PTEN (phosphatase and tensin homolog on chromosome 10), which can act both as lipid and protein phosphatase. PTEN dephosphorylates phosphatidylinositol-3, 4, 5 trisphosphate (PIP₃) to phosphatidylinositol 4, 5 bisphosphate (PIP₂), which antagonizes the PI-3 kinase pathway and inhibits cell proliferation (Chu and Tarnawski, 2004).

Apart from being distributed in various tissues, sigma-2 binding sites are overexpressed in many cancer cell lines. Malignant cells express much higher density as compared to non-malignant cells of the same tissue (Aydar *et al.*, 2004). In a study looking at sigma binding site expression in human brain tumours, Thomas *et al.* detected sigma receptors in 15 out of 16 cell lines examined. Very high densities of sigma-2 binding sites were found in brain metastasis from adenocarcinoma lung and in human neuroblastoma (Thomas *et al.*, 1990). Sigma-2 binding sites were expressed in higher density as compared to sigma-1 receptor in renal and colorectal carcinoma (Bem *et al.*, 1991). Similarly, sigma-2 binding sites are overexpressed 1.5 to 4 times in high grade urothelial cancer as compared to low grade cancers (Colabufo *et al.*, 2006). In bovine high-grade cancer of urinary bladder sigma-2 binding site is 25 to 44 times overexpressed whereas in low grade bladder cancers its only 3 to 5 folds overexpressed (Roperto *et al.*, 2010).

1.6 Sigma-2 binding sites and their role in non-invasive imaging of cancer

Sigma-2 binding site overexpression in various tumour cell lines and particularly in high grade tumours suggest that sigma receptor expression might be a biomarker of cellular proliferation and probably play an important role in tumour biology.

Given the fact that sigma 2 binding sites are found in high density in various cancer cell lines, the possibility of sigma ligands being used in diagnosis and treating cancer has been explored.

The development of radiotracers for cancer imaging has been explored for more than two decades. The sigma receptor binding radiotracers have higher affinity for proliferating cells when compared to inflamed tissue and, hence, could be more sensitive and specific in providing information about a tumour's proliferative status. Sigma ligands have been used in non-invasive imaging of the tumour using SPECT and PET.

The first SPECT ligand IDAB for sigma receptor was developed in 1991 by Michelot *et al.* to image malignant melanoma (Michelot *et al.*, 1993). For imaging purposes the compound was labelled with ^{123}I . When used in mice bearing murine B16 melanoma, it showed a high tumour to muscle ratio, hence a phase II trial was conducted in 110 patients diagnosed with malignant melanoma using ^{123}I -IDAB. The trial indicated that ^{123}I -IDAB was useful in diagnosis of malignant melanoma (sensitivity 81% and specificity 100%) (Michelot *et al.*, 1993). The same group carried out a follow up study for 48 patients diagnosed with malignant melanoma and showed that IDAB scintigraphy could be used for staging malignant melanoma (Rodot *et al.*, 1994). The results were not as encouraging when another study looked at IDAB scintigraphy in 26 patients with melanoma and non-small cell lung cancer: the sensitivity of the technique in melanoma was 64% and 22% for non-small cell lung cancer. Liver metastases from amelanotic melanoma were not detected (Everaert *et al.*, 1997).

For SPECT imaging the first sigma-2 specific SPECT ligands [(N-[2-((3'-N'propyl-[3,3,1]aza-bicyclononan-3 α -yl)(2''-methoxy-5-methyl-phenylcarbamate)(2-mercaptoethyl)amino)acetyl]-2-aminoethanethiolato] $^{99\text{m}}\text{Tc}$ -technetium (V) oxide, was reported in 2001 (Choi *et al.*, 2001, Mach *et al.*, 2001). The non-radioactive surrogate bound preferentially to sigma-2 binding

sites and showed very little affinity to sigma-1 receptors. Biodistribution was studied in mice bearing a mouse mammary adenocarcinoma (cell line 66). Stereoselectivity of binding was significantly better for one of the enantiomers and tumour to muscle ratios reached a peak at 4 hours post-administration. Treatment with haloperidol (a mixed sigma-1 and sigma-2 binding site ligand) reduced the uptake of tracer by 30% and at 1 hour the tumour site only contained the parent compound. It was postulated that breast tumours could be visualized provided a sigma-2 selective SPECT ligand was used, however increased uptake of the tracer in liver, kidney and bladder could potentially cause problems with interpreting the scan (Choi *et al.*, 2001, Mach *et al.*, 2001).

Another radioiodinated sigma-2 ligand, 5-iodo-2,3-dimethoxy-N-[2-(6,7-dimethoxy-3,4-dihydro-1H-isoquinolin-2-yl)-butyl]-benzamide, was developed by same authors and labelled with radioactive iodine (^{125}I and ^{123}I). The non-radioactive bromide had high selectivity for sigma-2 binding sites and bound with high affinity. Biodistribution in mice carrying EMT6 cell lines (mouse mammary tumour) showed that tumour to muscle ratio of 7 was reached 2 hours post-administration. Imaging hardly showed the tumour, suggesting that a high target to non-target ratio was required for successful microSPECT imaging (Hou *et al.*, 2006).

The tumour to muscle ratio is a scoring system developed for qualitative interpretation for PET imaging to grade the uptake in a tumour compared to adjacent normal tissue (Yeh *et al.*, 1996). Hirata *et al.* prepared an iodinated analogue of SA4503, which had equal affinity to both sigma-1 receptors and sigma-2 binding sites. Different tumour cell lines were tested. Biodistribution studies in nude mouse bearing A375 (human melanoma cell line) showed that the tumour to muscle ratio of 7 was reached 24 hours post-administration. Lower values were achieved with neuroblastoma (SK-N-SH), cervical carcinoma (ME180) and glioma (C6) cells. There was good correlation between concentration of iodinated ligand and sigma-2 binding site density suggesting

that SPECT could be used to determine sigma-2 binding site density (Hirata *et al.*, 2008).

Radioiodinated vesamicol was tried as well and was found to have the best tumour to muscle ratio in mice bearing human prostate tumour (DU-145) cells. Once again increased uptake of radioactivity by kidneys and liver limited the interpretation of the scan (Ogawa *et al.*, 2009).

Research on developing sigma labelled ligands for PET imaging started in 1990 with the aim of better understanding and mechanisms underlying movement disorders and mental health problems. Because of overexpression of sigma-2 binding sites in various tumour cell lines the research was also directed to see if such radiotracers could be used in diagnosing cancer with the help of PET.

Several ligands labelled with positron emitters were tested for imaging of sigma receptors in various tumour cell lines. One of the initial ligands with good results was ^{18}F -1-(3-Fluoropropyl)-4-(4-cyanophenoxy-methyl) piperidine (FPS). It had subnanomolar affinity for sigma-1 receptor. In nude mouse harbouring B16 melanoma tumour cells, the tracer achieved tumour/blood ratio of 124 and a tumour muscle ratio of greater than 7 at 4 hours post-administration (Waterhouse and Collier, 1997). After initial animal studies it was found to be safe in humans (Waterhouse *et al.*, 2003).

Radiotracers with high affinity for sigma-2 binding sites have also been developed. Cyclohexyl piperidine was labelled with ^{11}C and tested in animals. PB167 known to have high affinity for sigma-2 binding sites was labelled with methoxy group but unfortunately there was no difference in uptake between normal tissue and the tumour (Abate *et al.*, 2009, Colabufo *et al.*, 2005, Colabufo *et al.*, 2006). ^{11}C -PB28 has been trialled in healthy mice and was found to be not suitable for sigma-2 binding site imaging since it could not be blocked with unlabelled PB28 (Kassiou *et al.*, 2005).

Mach *et al.* prepared 4 ^{11}C labelled ligands with high affinity for the sigma-2 binding site and tested them in mice bearing EMT6 breast tumours. One of the radiotracer achieved tumour to muscle ratio of 3 at 30 minutes post administration (Tu *et al.*, 2005).

5- ^{76}Br -bromo-N(4-(3,4-dihydro-6,7-dimethoxy-isoquinolin-2(1H)-yl)butyl)-2,3-dimethoxybenzamide, a radiobrominated radiotracer with high affinity for sigma-2 binding sites, was tested with good results. In mice bearing EMT6 tumours, tumour to muscle ratio of 10 was achieved at 4 hours after administration. Prior administration of a non-radioactive sigma ligand significantly reduced the tumour to muscle ratio from 8.6 to 3.6 at 2 hours. This radiotracer could not be used to image liver due to its high uptake. However, it was found to be suitable to image tumours in lung, head and neck or lower abdomen (Rowland *et al.*, 2006).

Four benzamide analogues labelled with ^{18}F were also evaluated for tumour imaging. These compounds had higher affinity for sigma-2 binding sites. One of the compounds showed activity almost similar to radiobrominated compound (Tu *et al.*, 2007). ^{18}F -WC-59, a radiolabelled azabicyclononane with sub nanomolar affinity and high selectivity for sigma-2 binding sites produced tumour to muscle ratio of maximally 2.5 when used in EMT6 tumour-bearing mice (Chu *et al.*, 2009). In view of poor tumour to muscle ratio it could not be used in PET imaging.

Over a period of time sigma-2 binding site-selective PET ligands have been developed showing some range of activity and application in tumour imaging. Since sigma-2 binding sites are overexpressed in most of the tumours from various tissues, sigma-2 labelled PET ligands seem to be the obvious choice for further research in search of ideal ligands in PET imaging of tumours.

1.7 Sigma-2 binding sites and apoptosis in tumour cells

Apoptosis, or programme cell death, plays an important role in controlling the net number of cells and getting rid of damaged cells, and hence plays an important role in preventing carcinogenesis. Apoptosis can be initiated by extracellular signals, called “death factors” or intracellular changes due to damage to DNA, oxidative stress or calcium influx into the cytoplasm or released from the endoplasmic reticulum (Mattson and Chan, 2003).

Extracellular signals activate the extrinsic pathway whereas intracellular changes activate the intrinsic pathway. The extrinsic pathway is activated by death signals (TNF or Fas ligand). Binding of these ligands to death receptors results in a conformational change of the receptor, which leads to activation of adaptor proteins. Adaptor proteins cause aggregation of procaspase-8, a zymogen which is cleaved to form active caspase-8, which further activates the caspase cascade causing proteolysis and apoptosis (Wajant, 2002).

The intrinsic pathway is activated by cellular stress, which activates Bax protein. Bax undergoes a conformational change and inserts into the outer mitochondrial membrane. Important regulators are released from the intermembrane space (Almonte-Becerril *et al.*, 2010). Caspase-9 is activated which results in the caspase cascade and apoptosis.

The role of the sigma-2 binding site in regulation of cell proliferation and cell viability has been extensively studied and cytotoxic effects of sigma ligands observed both *in vivo* and *in vitro* (Vilner and Bowen, 1993, Vilner *et al.*, 1995a). Ligands with high affinity for the sigma-2 binding site exhibit cytotoxicity (Bowen *et al.*, 1995) whereas other ligands with affinity for sigma-1 receptors or ion channels do not induce these cytotoxic effects on the cells. Cytotoxic effects are dose dependant with higher doses leading to death occurring in a shorter time.

Sigma-2 binding site ligands induce death by apoptosis (Crawford and Bowen, 2002, Vilner *et al.*, 1995a).

Sigma-2 binding sites are thought to play an important role in cell survival and morphology (Guitart *et al.*, 2004, Vilner *et al.*, 1995a). It is believed that sigma-2 binding site agonists stop tumour cell proliferation by inducing apoptosis whereas sigma-2 binding site antagonists promote tumour survival (Waarde *et al.* 2010). Vilner *et al.*, whilst working with C6 glioma cells, found that sigma ligands affected the cell morphology and caused death by inhibiting cell division (Vilner and Bowen, 1993, Vilner *et al.*, 1995a). They showed a correlation between affinity of the drugs to the sigma-2 binding site and degree of inhibition of tumour cell growth. Kashiwage *et al.* showed that sigma-2 binding site ligands induced apoptosis by activating caspase-3, where sigma-1 receptor ligands did not have this effect (Kashiwagi *et al.*, 2007), although Spruce had previously shown that the effects of rimcazole, a mixed sigma-1 antagonist and sigma-2 agonist, on caspase-3 activation were reversed by the sigma-1 selective agonists SKF 10047 and (+) pentazocine (Spruce *et al.*, 2004).

By measuring the DNA fragmentation, annexin V and chromatin condensation, Hornick *et al.* showed that there was a correlation between apoptosis and affinities of sigma-2 binding site ligands (Hornick *et al.*, 2010). Sigma-2 ligands CB-64D and CB-184 caused inhibition of tumour cell growth and apoptosis in both drug sensitive tumour cell lines MCF7 and drug resistant tumour cell lines such as MCF7/Adr, SKBr3 and T47D (Brent *et al.*, 1996, Brent and Pang, 1995, Crawford and Bowen, 2002). Siramesine, a highly selective sigma-2 binding site ligand caused apoptosis in various tumour lines tested derived from breast, cervix, lung, prostate and connective tissue. It was particularly active against fibrosarcoma and breast carcinoma grafts in mice (Groth-Pedersen *et al.*, 2007, Ostefeld *et al.*, 2005).

The ability of sigma-2 ligands to induce apoptosis led to further investigation of downstream signalling pathways of sigma-2 binding sites. We know that

calcium plays a vital role in cytotoxicity and alteration in intracellular calcium levels can induce apoptosis in various cell lines (McConkey and Orrenius, 1996, Nicotera and Orrenius, 1998). The role of calcium in apoptosis is shown in Figure 1-5.

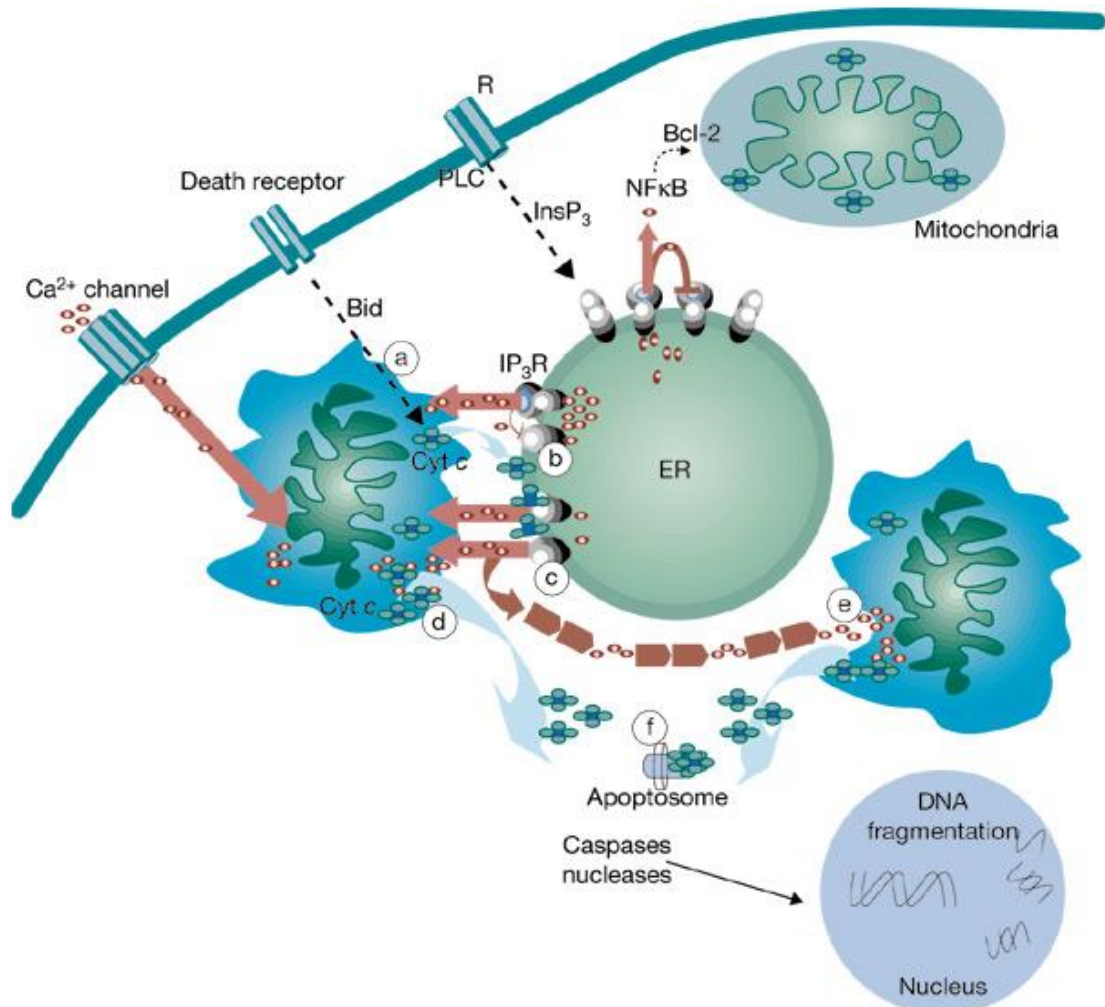


Figure 1-5: The role of calcium and cytochrome C in cellular apoptosis (Mattson and Chan, 2003).

Cytochrome C release from the mitochondria can be activated by an increase in cytoplasmic calcium, caused by either calcium entry through channels at the plasma membrane or via release from intracellular stores by $InsP_3$.

Experiments using sigma-2 ligands showed both transient increase in intracellular calcium, which returned to baseline in about 8 minutes and a latent and more sustained rise in calcium levels. It was suggested that the transient rise results from calcium release from the endoplasmic reticulum and the latent

rise is due to release of calcium from mitochondrial stores (Vilner and Bowen, 2000).

Caspase inhibitors were found to block apoptosis induced by DNA damaging agents in wild type MCF7 cells, caspase inhibitors had little or no effect on sigma-2 ligand-related apoptosis (Crawford and Bowen, 2002). The rise in intracellular calcium levels caused by sigma-2 binding site ligands is possibly the mechanism by which these ligands induce apoptosis.

1.8 Sigma-2 binding site ligands

Sigma receptors were initially classified as a subtype of opioid receptors based on their affinity for benzomorphans like SKF 10047. Further studies confirmed that opioid receptors had high affinity for (-) SKF 10047 and sigma receptors had high affinity for (+) SKF 10047, hence classified as a distinct class of receptors (Khazan *et al.*, 1984, Martin *et al.*, 1976, Vaupel, 1983, Wong *et al.*, 1988). Binding studies with [³H] DTG revealed two subtypes of sigma receptors and sigma-1 receptor having higher affinity for (+) SKF 10047 (Hellewell and Bowen, 1990, Hellewell *et al.*, 1994). In early 1990's many derivatives of piperidine, pyrrolidine, dialkylamine and trialkylamine were developed which could bind to sigma receptors with high affinity (Berardi *et al.*, 2009, Huang *et al.*, 2001a, Narayanan *et al.*, 2011, Newman *et al.*, 2001). As a result of improvement in binding assays, new ligands with higher affinity for the sigma-2 binding site were developed. Sigma-2 binding site ligands have been classified into four classes based on their structure.

1. 6,7-dimethoxytetrahydroisoquinoline derivatives,
2. Tropane related bicyclic structures,
3. Siramesine related indole derivatives and
4. Cyclohexylpiperazine analogues.

There is also a small group of ligands, which are structurally not related to any of the four classes.

1.8.1 6,7-dimethoxytetrahydroisoquinoline derivatives

Towards the late 1990's whilst developing new amides for dopamine receptors, a series of piperidine and pyrrolidine derivatives were found to have high affinity for sigma receptors (Huang *et al.*, 1998, Huang *et al.*, 2001b, Mach *et al.*, 2005, Mach *et al.*, 2001, Mach *et al.*, 2003). Further research was carried out to find ligands with high affinity for sigma-2 binding sites to be used in cancer imaging. A series of benzamides and carbamates were discovered which were found to have significantly high affinity for sigma-2 binding sites. A number of compounds from this family have been analysed to see if they could be used for PET imaging of cancer (Mach and Wheeler, 2009, Narayanan *et al.*, 2011, Zeng *et al.*, 2011). Some of the compounds from this family are shown in Table 1-1.

No	Name	Structure	sigma-1 K _i (nM)	sigma-2 K _i (nM)
1	yun179		>1000	25.8
2	yun201		189.1	21.1
3	yun204		1159	17.6
4	yun234		5484	12.4
5	yun236		2932	16.3
6	yun242		10412	13.3
7	yun243		3078	10.3
8			534	2.63

Table 1-1: Sigma-2 binding site-selective 6,7-Dimethoxytetrahydroisoquinoline analogue ligands

Adapted from (Huang *et al.*, 2014).

1.8.2 Tropane and Granatane derivatives

Since benzomorphan-based ligands had affinity for sigma receptors, this structure became the lead compound for further development of sigma ligands. Bowen *et al.* developed two of the well-known sigma-2 binding site ligands, CB-64 D and CB-184 (Bertha *et al.*, 1994, Bertha *et al.*, 1995, Bowen *et al.*, 1995). BIMU-1, another high affinity sigma-2 binding site ligand was used by many researchers to develop further sigma-2 binding site ligands.

A number of compounds from this family have been developed into fluorescent sigma-2 binding site ligands and used in tumour imaging and assessment of cancer cell proliferation (Chu *et al.*, 2009). Some of the compounds from this family with their affinities for both sigma-1 and sigma-2 binding site are shown in Table 1-2.

No	Name	Structure	sigma-1 K _i (nM)	sigma-2 K _i (nM)
1	BIMU-1		6300	32
2	(±)SM21		>1000	67.5
3	RHM-138		544	12.3
4	CB-64D		3063	16.5
5	CB-184		7436	13.5
6	ABN-1		92.5	10.5
7	yun245		2250	5.0
8	yun253		162.5	10.5

Table 1-2: Sigma-2 binding site-selective granatane or tropane analogue ligands

Adapted from (Huang *et al.*, 2014).

1.8.3 Indole derivatives

Indole is an aromatic heterocyclic organic compound with formula C_8H_7N . It has a bicyclic ring fused to a five membered nitrogen containing a pyrrole ring. Siramesine, an indole derivative (Moltzen *et al.*, 1995, Perregaard *et al.*, 1995, Soby *et al.*, 2002) and one of the best known sigma-2 binding site ligands, was initially developed for treatment of anxiety and depression. Siramesine has been extensively studied and found to induce apoptosis in cancer cell lines both *in vitro* and *in vivo* (Jonhede *et al.*, 2010, Ostenfeld *et al.*, 2005). A number of siramesine analogues were derived by modifying the spiropiperidine structure. Some of these compound have been investigated in PET imaging. Some of the compounds from this family are shown in Table 1-3.

No	Name	Structure	sigma-1 K _i (nM)	sigma-2 K _i (nM)
1	Siramesine		17	0.12
2			290	1.8
3			5.5	0.3
4			150	0.58
5			180	2.6
6			23	1.1
7			53	0.9
8			5.7	0.21

Table 1-3: Sigma-2 binding site-selective indole analogue ligands
Adapted from (Huang *et al.*, 2014).

1.8.4 Cyclohexylpiperazine derivatives

Cyclohexylpiperazine and cyclohexylpiperadines are the most extensively studied analogues for sigma receptors (Berardi *et al.*, 2009, Huang *et al.*, 1998, Huang *et al.*, 2001a, Mir *et al.*, 2012). Derivatives in this group are usually non-selective for sigma receptors. PB28 is one of the most widely reported sigma-2 binding site ligands, which shows 40-fold selectivity for the sigma-2 binding site. Some of the compounds are shown in Table 1-4.

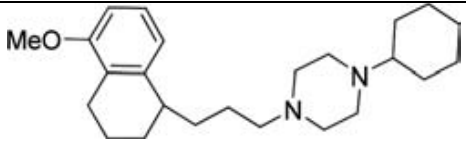
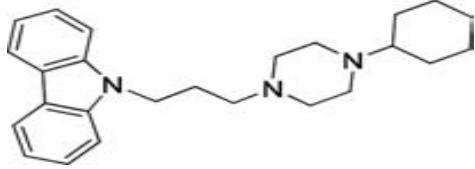
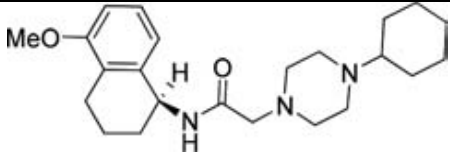
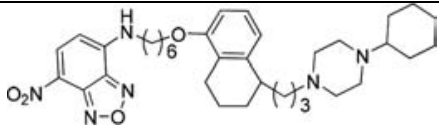
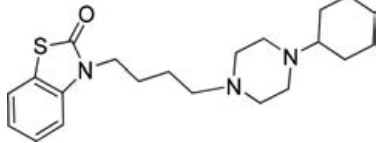
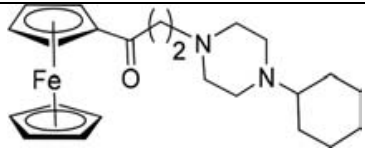
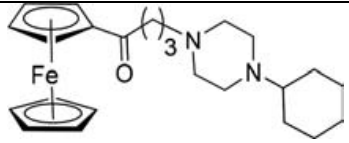
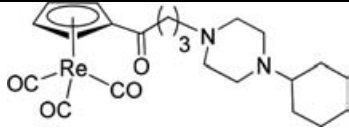
No	Name	Structure	sigma-1 K _i (nM)	sigma-2 K _i (nM)
1	PB28		13.6	0.34
2	F281		3450	12.6
3			94.6	5.92
4			78.7	10.8
5			4.1	0.3
6			158	20.5
7			4162	43.6
8			808	64.4

Table 1-4: Sigma-2 binding site-selective cyclohexylpiperazine analogue ligands.

Adapted from (Huang *et al.*, 2014).

1.8.5 Miscellaneous compounds with high affinity for sigma-2 binding sites

In addition to the compounds mentioned above, there are some more sigma-2 selective ligands, which are structurally unrelated to any of the four groups discussed earlier. It is interesting to note that some of these compounds have very simple structures and yet have very high affinity and selectivity for sigma-2 binding sites as shown in Table1-5.

No	Name	Structure	sigma-1 K _i (nM)	sigma-2 K _i (nM)
1	yun202		69.1	4.8
2	yun209		1499	25.1
3	yun210		231	10
4	yun212		534	2.63
5	yun250		809	75.0
6	yun251		751	26.3
7			10320	26.8
8			>10000	39

Table 1-5: Sigma-2 binding site-selective ligands - miscellaneous structures

Adapted from (Huang *et al.*, 2014).

1.9 The Sigma-2 binding site ligand pharmacophore

As mentioned in the above section, a number of high-affinity sigma-2 binding site ligands have been developed, but still the exact binding requirement for sigma-2 binding sites has not been described. One of the main hurdles is probably the fact that the sigma-2 binding site has not been cloned yet. Several models for binding of ligands to the sigma-2 binding site have been proposed and each is based on a limited set of ligands. One such model was proposed by Huang *et al.* (Huang *et al.*, 1998) based on phenylacetamides, a series of non-selective ligands. This model proposed that hydrophobic and bulky substituents on aromatic ring of phenylacetamides were more favourable for sigma-2 binding.

Cratteri *et al.* proposed a sigma-2 binding site pharmacophore based on tropane derivatives. According to this model, there was a shorter distance between the primary and secondary hydrophobic binding domains and a longer distance between the hydrogen bond donor and primary hydrophobic binding pocket as compared to the sigma-1 receptor pharmacophore (Cratteri *et al.*, 2004). Glennon *et al.* proposed a pharmacophore based on binding properties of piperidines, piperazines, long chain amines and long chain trialkylamines. According to Glennon *et al.*, for a ligand to bind to sigma-2 binding site, it should have an amine site and two hydrophobic sites (Glennon, 2005). This group also conducted a 3D-QSAR study on PB28 and related cyclohexylpiperazines (Abate *et al.*, 2009). A more recent binding model was proposed by Laurini *et al.* This binding model was based on 19 benzoxazolone derivatives (Laurini *et al.*, 2010). According to this model, the sigma-2 binding site consists of an ionisable atom (PI), a hydrogen bond acceptor group (HBA), a hydrophobic aromatic site (HYAr), a hydrophobic aliphatic site (HYAl) and a generic hydrophobic site (HTY). HYAl was required for high sigma-2 affinity. Based on the structures of sigma-2 ligands, Huang *et al.* proposed a hypothetical sigma-2 binding model as shown in Figure 1-6.



Figure 1-6: Hypothetical sigma-2 binding site binding model

This sigma-2 binding model consists of an electrostatic or hydrogen bond, a large hydrophobic binding pocket, a small hydrophobic binding pocket and an additional hydrophobic binding site (Huang *et al.*, 2014).

Huang *et al.* (Huang *et al.*, 2014) also summarised the binding profile of the sigma-2 binding site ligands as follows:

Ligands with high affinity for sigma-2 binding sites contain a basic nitrogen and a hydrophobic moiety. Additional hydrophobic moieties are not needed but it increases sigma-2 binding site affinity and selectivity. A bulky hydrophobic moiety increases sigma-2 binding site binding.

The basic nitrogen may be quaternised in physiological conditions to interact with a carboxylic group of the receptor and a secondary nitrogen, which is four or more carbon units apart; this may increase sigma-2 binding site binding (Glennon, 2005).

1.10 Sigma-2 binding sites and lipid rafts

Until the molecular identity of the sigma-2 binding site is established, our ability to determine its subcellular location and trafficking around the cell are severely hindered. Some attempts have been made in determining some characteristics.

Using liver extracts, Torrence-Campbell and Bowen showed that sigma-2 binding sites were resistant to solubilisation with detergents like 3-[(3-cholamidopropyl) dimethylammonio]-1-propanesulfonate (CHAPS) or Triton X-100, suggesting they are located in lipid rafts (Torrence-Campbell and Bowen, 1996). Sucrose gradient purification and co-localisation with flotillin-2 further confirmed the association with these lipid rafts (Gebreselassie and Bowen, 2004).

According to fluid mosaic model proposed by Singer and Nicholson, the cell membrane is composed of a phospholipid bilayer and membrane proteins, which give structure to the membrane (Singer and Nicholson, 1972). The plasma membrane contains micro domains, called lipid rafts, which are enriched with cholesterol, sphingolipids such as sphingomyelin and glycosylphosphatidylinositol (GPI)-linked proteins (Brown and London, 1998, Brown and London, 2000, Dobrowsky, 2000, Edidin, 2003, Simons and Ikonen, 1997). Lipid rafts can incorporate the cholesterol binding protein called caveolin and form specialised structure called caveolae (Brown and London, 1998, Dobrowsky, 2000). Lipid raft domains are resistant to solubilisation by detergents such as Triton X-100 and CHAPS and hence can be isolated using sucrose density gradient centrifugation techniques. Lipid rafts are believed to play a number of important roles such as cell signalling, membrane trafficking, molecular sorting and cell signal transduction of receptors (Brown and Rose, 1992, Dobrowsky, 2000, Fiedler *et al.*, 1993, Ikonen, 2001, Nguyen and Hildreth, 2000, Oliferenko *et al.*, 1999, Palestini *et al.*, 2000, Rodgers and Rose, 1996, Veri *et al.*, 2001, von Haller *et al.*, 2001). Lipid rafts are also involved in cellular differentiation and programmed cell death (apoptosis) (Galbiati *et al.*, 2001, Zhang *et al.*, 2010). The distribution of the lipid raft over the cell membrane differs depending on the cell type, for example lipid rafts are more abundant on somal and axonal membranes than on dendritic membranes (Suzuki, 2002). Sphingolipid metabolism has been shown to be involved in cell growth (Kolesnick and Kronke, 1998). Bowen *et al.* had demonstrated that treatment of breast cancer cell lines and neuroblastoma cell resulted in increase in ceramide and

sphingosylphosphorylcholine, with concomitant decrease in sphingomyelin (Bowen, 2001, Crawford *et al.*, 2002).

The fact that sigma-2 binding sites are overexpressed in tumour cell lines and also plays important role in cell growth and proliferation suggests that it can induce sphingolipid-dependant apoptosis.

These findings would place the sigma-2 binding site in the inner leaflet of the plasma membrane.

Using a different approach, Zeng *et al.*, used fluorescently labelled sigma-2 ligands and monitored their location (Zeng *et al.*, 2011). The first, SW107, co-localised with the plasma membrane marker FM 1-43FX, whereas the location of the second, K05-138, was less clear, colocalising with markers for the mitochondria, lysosomes, endoplasmic reticulum, and possibly, plasma membrane. Such differences could be accounted for by agents stimulating trafficking of the receptor, or the drugs in isolation.

1.11 Sigma-2 binding sites and PGRMC1

PGRMC1 (progesterone receptor membrane component 1) is a heme-binding protein, related to cytoplasmic cytochrome b5 domain. Its molecular weight ranges between 22 and 28kDa (Cahill, 2007, Peluso *et al.*, 2012a, Peluso *et al.*, 2012b). PGRMC1 is overexpressed in certain cancers like colorectal, breast, thyroid and lung (Rohe *et al.*, 2009), and is required for cancer growth, proliferation and metastasis (Ahmed *et al.*, 2010). AG-205, an antagonist of PGRMC1 inhibits ERK1/2 pathway and hence reduces cancer cell proliferation. Due to similarities between PGRMC1 and the sigma-2 binding site, Mach *et al.* conducted experiments and showed that WC-21, a fluorescent highly selective sigma-2 ligand, cross-linked with a protein that showed sequence homology with PGRMC1, and also that cells with increased PGRMC1 expression had high

sigma-2 binding, while cells with decreased PGRMC1 levels showed reduced sigma-2 binding. Based on these conclusions, they suggested that the sigma-2 binding site was likely to be PGRMC1 (Xu *et al.*, 2011). They also managed to show that anti-PGRMC1 antibody and SW120 (a fluorescent sigma-2 ligand) labelled the same intracellular sites under confocal microscopy.

Despite these above findings, several questions remain to be answered. For example, the molecular weight of the sigma-2 binding site is around 21.5kDa (Hellewell *et al.*, 1994, Wheeler *et al.*, 2000) whereas PGRMC1 has a molecular weight of 22 to 28kDa (Cahill, 2007, Peluso *et al.*, 2012a, Peluso *et al.*, 2012b), PGRMC1 ligands do not seem to bind the sigma-2 binding site and similarly sigma-2 binding site ligands do not seem to bind to PGRMC1. PGRMC1 can bind to p450 but sigma-2 binding sites do not (Rohe *et al.*, 2009).

It has also been found that inhibition of PGRMC1 by AG-205 reduced tumour proliferation whereas inhibition of the sigma-2 binding site by antagonists stimulated tumour proliferation and activation of the sigma-2 binding site by agonists caused apoptosis (Jonhede *et al.*, 2010, van Waarde *et al.*, 2010). It is worth mentioning that the definitions of agonist and antagonist in this context are not clear and not universally accepted.

1.12 Aim of my thesis

The proposed pharmacophore of the sigma-2 binding site has been based on original opioid receptor ligands and further developed after identification of agents like DTG, which often contain more than 1 nitrogen and have complex aromatic ring structures. A number of studies looking for structure-activity relationships between ligands and the sigma-2 binding site have been carried out earlier (Ablordeppey *et al.*, 2000, Ablordeppey *et al.*, 2002, Glennon, 2005, Glennon *et al.*, 1994, Glennon *et al.*, 1991a, Glennon *et al.*, 1991b, Glennon *et al.*, 1991c). Almost all the studies looked at complex structures and therefore

did not come up with simple sigma-2 ligands. Earlier work from this laboratory (Brimson, 2010) has shown that ligands with much more simple structures had high affinity for the sigma-1 receptor and were more selective than some commercially available ligands. In this thesis, I have assessed the affinity of these same simple ligands for the sigma-2 binding site in order to reduce the complexity of the sigma-2 binding site pharmacophore. In addition, I have used these simple drugs alongside commercially available drugs to understand the pharmacology of the sigma-2 binding site. Furthermore based on the activity of ligands I have tried to define agonist and antagonist.

I also wished to determine whether the source of the tumour cell being treated would affect the outcome of sigma-2 agonist treatment. To this end, I have screened a number of cell lines from a number of different sources. All but one (MCF7) also contained sigma-1 receptors, restricting my attempts to determine this outcome. During these studies, I have also established a novel protocol for assessing sigma-1 receptor and sigma-2 binding site content in cell lines and tissues.

Chapter 2. MATERIALS & METHODS

2.1 General Materials

General laboratory chemicals were purchased from Sigma Aldrich Company Ltd (Dorset UK). Tissue culture media, trypsin and Foetal Bovine Serum (FBS) were purchased from Gibco. Ninety six-well plates and tissue culture flasks were purchased from Fisher Scientific (Loughborough, Leicestershire, UK)

2.2 Tissue Culture

A range of cancer cell lines were used in these studies. These include oesophageal: OE21, OE33 and FLO-1; breast: MCF7 and MDA-MB-468; colorectal: Caco-2, SW480, HT-29 and HCT 116; human embryonic kidney: 293; and lung: A549. MCF7 cells were chosen as they are reported to not express sigma-1 receptors (Vilner et al., 1995b), whereas MDA-MB-468 cells, which are also a breast cancer cell line have been widely used to study the sigma-1 receptor (Spruce et al., 2004) (Brimson, 2010). Other cell lines were used as their sigma-1 and sigma-2 status was unknown or required verifying. They were tested in order to seek out cell lines that lacked sigma-2 binding sites and could, therefore, be used as negative controls for later studies.

A549, MDA-MB-468, 293, MCF7, FLO-1 and HCT 116 cells were grown in Dulbecco Modified Eagle's minimum essential medium (DMEM),(Gibco, #41965). SW480 cells were grown Leibovitz's L-15 medium (Gibco, #11415), Caco-2 cells were grown in minimum essential medium (Gibco, #32360), HT-29 cells were grown in McCoys's 5a medium (Gibco, #26600). OE21 and OE33 were grown in RPMI 1640 medium (Gibco, #21875). All of the above growth media were supplemented with 1% L-glutamine and 10% heat inactivated FBS (Gibco, #10500). The cells were incubated at 37°C in a humidified air and 5% CO₂ atmosphere. All the cell lines used in these studies were adherent, as such, they were propagated in monolayers.

2.3 Cell propagation and storage

Handling of cells was performed in a Class II biological safety cabinet, which had been switched on at least 15 minutes prior to use. All surfaces were wiped clean with a solution consisting of 70% ethanol in water and allowed to air dry. Single-use pipettes and tissue culture consumables were handled in this clean environment using aseptic technique. Cell morphology and confluency were observed using an inverted phase contrast microscope (Olympus CK2-TR).

When cells reached 80% confluency, they were harvested using 0.25% w/v trypsin 0.91mM EDTA (Gibco, #25200) (typically, 5ml was used for a 175cm² tissue culture flask) and incubated at 37°C until the cells had detached from the flask. An equal volume of pre-warmed medium containing 1% L-glutamine and 10% FBS was added before transferring to new tissue culture flasks containing required volume of tissue culture medium. The FBS in the medium acted as a trypsin inhibitor. In practice, cells were routinely split once a week, with a split ratio of 1:5 or 1:10, depending on the growth characteristics of each cell line and in line with the suppliers. Medium was exchanged after 3 and 6 days.



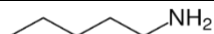
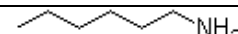
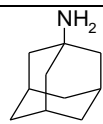
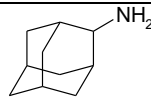
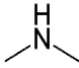
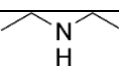
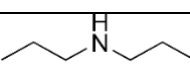
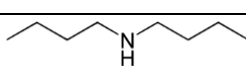
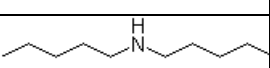
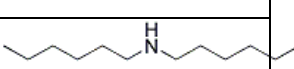
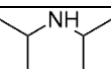
When freezing the cells down for storage, the trypsinized cells were transferred to a sterile centrifuge tube and centrifuged at 500g for 1 minute. The pellet was resuspended in freezing mixture (90% DMSO and 10% culture medium) and transferred to 2ml cryogenic vials. The cells were chilled slowly to 4°C before being placed at -20°C overnight. The following day the vials were transferred to -80°C ultra freezer for long-term storage.

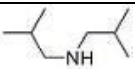
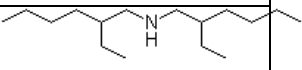
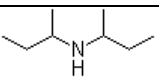
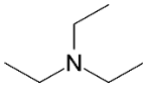
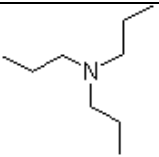
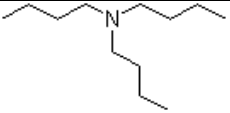
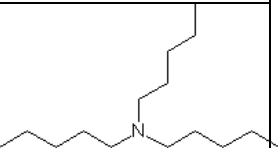
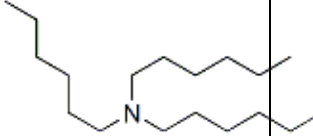
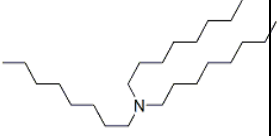
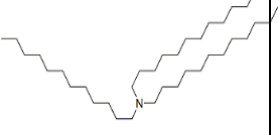
When thawing the cells, the vials were taken from -80°C freezer and placed into a 37°C water bath to thaw rapidly. Once thawed the contents of the vials were transferred to a tissue culture flask containing growth medium, pre-warmed to 37°C in humidified air incubator with 5% CO₂. The flasks were incubated overnight and the following day the medium was changed to remove all cells

that failed to adhere to the flask; this also allowed much of the DMSO to be removed from the culture medium. Cells were then allowed to grow to 80% confluency, harvested and again grown to 80% confluency before being used in experiments.

2.4 General Ligand preparation

The simple amines were purchased from Sigma Aldrich (Dorset UK), Fluka (Sigma-Aldrich, Dorset, UK) or Arcos Organics (Fisher Scientific, Loughborough, UK) as either Hydrochloride Salts (HCl) or as a free base

Name	Salt/Base	Vender	Chemical formula	Structure
Primary amines				
Propylammonium	Free base	Fluka	C ₃ H ₉ N	
Butylammonium	Free base	Fluka	C ₄ H ₁₁ N	
Pentylammonium	Free base	Fluka	C ₅ H ₁₃ N	
Hexylammonium	Free base	Fluka	C ₆ H ₁₅ N	
Branched-chain Primary amines				
1-Adamantly ammonium	Free base	Sigma Aldrich	C ₁₀ H ₁₇ N	
2-Adamantly ammonium	HCl•	Sigma Aldrich	C ₁₀ H ₁₇ N	
Secondary amines				
Dimethylammonium	HCl•	Sigma Aldrich	C ₂ H ₇ N	
Diethylammonium	HCl•	Sigma Aldrich	C ₄ H ₁₁ N	
Dipropylammonium	HCl•	Sigma Aldrich	C ₆ H ₁₅ N	
Dibutylammonium	Free base	Sigma Aldrich	C ₈ H ₁₉ N	
Dipentylammonium	Free base	Sigma Aldrich	C ₁₀ H ₂₃ N	
Dihexylammonium	Free base	Sigma Aldrich	C ₁₂ H ₂₇ N	
Branched chain Secondary amines				
Diisopropyl ammonium	Free base	Sigma Aldrich	C ₆ H ₁₅ N	

Diisobutylammonium	HCl•	Sigma Aldrich	C ₈ H ₁₉ N	
Bis-2-(ethyl)hexyl ammonium	Free base	Sigma Aldrich	C ₁₆ H ₃₅ N	
Di-sec-butyl ammonium	Free base	Sigma Aldrich	C ₈ H ₁₉ N	
Tertiary amines				
Trimethylammonium	HCl•	Fluka	C ₃ H ₉ N	
Triethylammonium	HCl•	Fluka	C ₆ H ₁₅ N	
Tripropylammonium	HCl•	Sigma Aldrich	C ₉ H ₂₁ N	
Tributylammonium	HCl•	Fluka	C ₁₂ H ₂₇ N	
Tripentylammonium	Free base	Sigma Aldrich	C ₁₅ H ₃₃ N	
Trihexylammonium	Free base	Sigma Aldrich	C ₁₈ H ₃₉ H	
Trioctylammonium	Free base	Sigma Aldrich	C ₂₄ H ₅₁ N	
Tridodecylammonium	Free base	Sigma Aldrich	C ₃₆ H ₇₅ N	

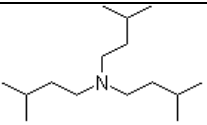
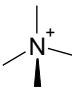
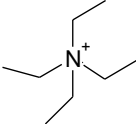
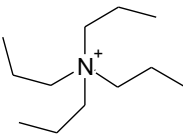
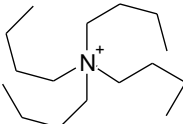
Branched-chain tertiary amines				
Triisopentyl ammonium	Free base	Fluka	C ₁₅ H ₃₃ N	
Quaternary amines				
Tetramethyl ammonium	HCl•	Acros Organic s	C ₄ H ₁₂ N	
Tetraethylammonium	HCl•	Sigma Aldrich	C ₈ H ₂₀ N	
Tetrapropyl ammonium	HCl•	Acros Organic s	C ₁₂ H ₂₈ N	
Tetrabutylammonium	HCl•	Sigma Aldrich	C ₁₆ H ₃₆ N	

Table 2-1: Simple amine structure, salt and where it was purchased.

The free base amines were made soluble in water by making HCl salt. 5ml of free base amine was dissolved in 15ml of ether, and hydrochloric acid (HCl) was added slowly until the mixture turned acidic, measured using universal indicator paper (Sigma-Aldrich, Dorset UK). The formed solid was filtered and the remaining solvent was removed under vacuum. If the solid did not come out of solution the solvents were removed under vacuum.

2.5 General Radioligand binding

Cells were harvested prior to the experiments using 0.25% trypsin 1mM EDTA and stored at -20°C. On the day of experimentation, cells were thawed and

resuspended in Tris-buffered saline (TBS) (50mM Tris HCl pH 8.5). The cells were sonicated using six 5 second pulses separated by a 5 second pause using a sonicating probe. The output was adjusted to permit cavitation of the suspension, optimising cell disruption. Membranes were harvested by centrifugation at 4°C and 2000g for 15 minute. The supernatant was discarded and the pellet was resuspended in TBS. Assays were performed at room temperature in 4ml polystyrene tubes.

2.5.1 Saturation binding assays

2.5.2 Pentazocine

[³H] (+) Pentazocine was prepared at a concentration of 1024nM (approximately, exact concentration was determined by counting a sample and using specific activity calculations for each experiment). Serial 1:1 dilutions were prepared to give concentrations of approximately (see above) 512, 256, 128, 64, 32 and 16nM. These concentrations were selected as they bracket the K_d of (+) pentazocine previously published for the sigma-1 receptor (17nM) (Brimson et al., 2011). Ten μ l were added to the tubes, with a final volume of 100 μ l consisting of membranes (exact amount of protein was calculated for individual experiments using the “Bradford” assay as explained later in this chapter), and, where appropriate, 10 μ l of 10mM haloperidol to determine non-specific binding. The amount of protein added was optimized for each cell line to permit a high signal-to-noise ratio while preventing ligand depletion. In order to standardize this, conditions were chosen where no more than 10% of the radioligand was bound to the membranes. Assays were permitted to incubate at room temperature for 4 hours (time required to reach equilibrium) before the separation of bound from free ligand. After equilibration, the membranes were harvested using a vacuum filtration manifold (Millipore) through GF/C glass fibre filters, washing two times with 3ml ice-cold wash buffer (10mM Tris HCl 150mM NaCl, pH 7.4). The glass fibre filter containing the cell membranes bound to the radioligand were placed in scintillation vials with 2ml of scintillant (Optiphase,

Fisher Scientific). The glass fibre filters were allowed to soak overnight before counting in a Perkin Elmer Liquid scintillation analyzer Tricarb 2800TR (5 minute counts).

2.5.3 DTG

[³H] DTG was prepared at a concentration of 2056nM approximately (exact concentration was determined by counting a sample and using specific activity calculations for each experiment). Serial 1:1 dilutions were prepared to give concentrations of approximately (see above) 1024, 512, 256, 128, 64, 32 and 16nM. These concentrations were selected as they bracket the K_d of DTG previously published for the sigma-1 receptor and sigma-2 binding site (36nM and 40nM, respectively) (Lever et al., 2006). Ten μ l was added to each tube, with a final volume of 100 μ l consisting of membranes, and, where appropriate, 10 μ l of 10mM haloperidol to determine non-specific binding. Assays were permitted to incubate at room temperature for 4 hours before the separation of bound from free ligand. After equilibration the membranes were harvested using a vacuum filtration manifold (Millipore) through GF/C glass fibre filters, washing two times with 3ml ice-cold wash buffer. The glass fibre filter containing the cell membranes bound to the radioligand were placed in scintillation vials with 2ml of scintillant. The glass fibre filters were allowed to soak overnight before counting in a Perkin Elmer Liquid scintillation analyzer Tricarb 2800TR (5 minute counts).

2.6 Competition binding assay

Radioligands were diluted in TBS to 500nM and 10 μ l were added to the tubes giving final assay concentrations of approximately 50nM (exact concentration was determined by scintillation counting for each experiment). The unlabeled, competing ligand was prepared at 10 times the required concentration, and 10 μ l was added to the tube. Initial tests were performed using a single high concentration of competing ligand (1mM where possible). Those ligands that

showed significant binding were then tested more rigorously using a range of concentrations permitting 0-100% reduction of radioligand binding in order to determine a pK_i. The volume was made to 50µl TBS, before adding 50µl of cell membranes to make a final volume of 100µl. The assay was allowed to equilibrate for at least 4 hours at room temperature. After equilibration, the cell membranes were harvested using a vacuum filtration manifold and processed as above.

2.7 Protein measurement

Protein amounts were determined using BioRad Protein Dye Reagent, based on Coomassie Brilliant Blue G250. Bovine serum albumin (BSA) was dissolved in water and eight dilutions of BSA (ranging from 0-400µg/ml) were prepared as protein standard. Ten µl of the standard and sample solution was added in duplicates to a 96-well plate. 100µl of Protein Dye Reagent (prepared by diluting 1 part Dye Reagent Concentrate with 4 parts distilled water) was added to all the wells. Following an incubation of 10 minutes the absorbance was measured at 595nm (Bradford, 1976) .

2.8 MTS cell proliferation assay

The cells were harvested with 0.25% trypsin and 1mM EDTA and centrifuged at 240g for 5 minutes. The pellet was washed in fresh DMEM containing 10% FCS, cells were counted and seeded into each well of a 96 well plate and allowed to adhere overnight. The drugs were added on day 2 and the cells incubated overnight (10X concentration and 10µl into 90µl of DMEM to give 1X in the well). Initial screens were performed using a single high concentration of ligand (1mM where possible). Those ligands that showed significant reduction of metabolic

activity were then tested more rigorously using a range of concentrations permitting 0-100% reduction of metabolic activity in order to determine a pIC_{50} . The day after drug addition the metabolic activity was measured using the CellTiter 96® AQueous Non-Radioactive Cell Proliferation Assay (MTS) (Promega Southampton UK). Metabolically active cells converted 3-(4,5dimethylthiazol-2-yl)-5-(3-carboxymethoxyphenyl)-2-(4-sulfophenyl)-2H-terazolium (MTS) into soluble formazan, and absorbance (490nm) was measured at 0, 1, 2 and 3 hours. The amount of formazan produced is directly proportional to the number of metabolically active cells in the well. Linear regression was performed to determine the rate of growth under each condition. To determine % inhibition, the absorbance of drug-treated wells was compared with control wells (vehicle only, 100%) and wells containing no cells (0%). IC_{50} values were calculated using non-linear regression (GraphPad Prism, version 7.0 for Macintosh).

2.9 Fura-2 Calcium measurement

On the day of experimentation, cells were harvested with 0.25% trypsin 1mM EDTA and centrifuged at 240g for 5 minutes. The pellet was resuspended in Krebs'-like buffer containing 115mM NaCl, 5mM KCl, 1mM NaH_2PO_4 , 0.5mM $MgSO_4$, 11mM glucose, 1.36mM $CaCl_2$, 0.1% BSA, 50mM Tris (note that Tris and not 4-(2-hydroxyethyl)-1-piperzineethanesulfonic acid (HEPES) was used to buffer the cells as HEPES has sigma-1 receptor affinity (of approximately 10mM, (Brimson et al., 2011) pH 7.4. Approximately 20 million cells were resuspended in 2ml of buffer. The cells were loaded with 5 μ M cell permeable Fura-2-acetoxymethyl ester (Fura-2-AM) (Invitrogen, UK) (5mM stock, in DMSO) and incubated at room temperature for 45 minutes. Loading at room temperature rather than 37°C reduced the cellular compartmentalization of the Fura-2 resulting in better cytoplasmic loading of the cells (Roe et al., 1990). The cells were then harvested by centrifugation at 240g for 5 minutes and washed in warmed Krebs'-like buffer three times before being made up to 1

million cells per ml and incubated at room temperature for a further 30 minutes to allow the acetoxymethyl groups to be removed by cellular esterases resulting in free Fura-2 in the cells. The cells were then kept in suspension in the dark at room temperature before use in calcium measurements. Two ml of Fura-2 loaded cells were placed in a cuvette with a magnetic stirring bar and placed into the fluorometer, (Perkin Elmer luminescence spectrometer LS-50B) and were maintained at 37°C. The cells were excited at 340nm and 380nm and emissions were recorded at 510nm. Fura-2 undergoes an excitation shift between 335nm (calcium free) and 363nm (calcium saturated) whilst the emission wavelength remains unchanged. This can be visualized by scanning the excitation wavelength between 300nm and 400nm and recording the emission at 510nm.

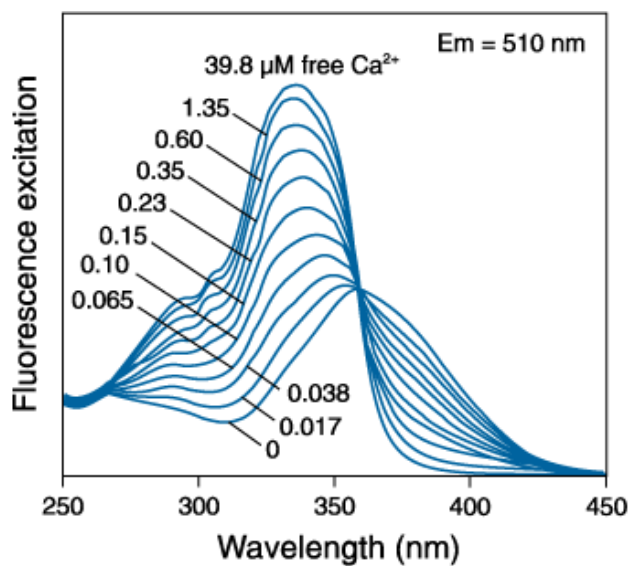


Figure 2-1: Fluorescence excitation spectra of Fura-2

Multiple solutions containing between 0 and 39.8 μ M free $[Ca^{2+}]$, scanned between 250nm and 450nm and emission (Em) read at 510nm. Data obtained from Invitrogen.

The largest dynamic range for $[Ca^{2+}]$ dependent fluorescent signals is obtained by using the ratio of fluorescence emitted at 510nm after excitation at 340nm and 380nm. The affinity of Fura-2 for calcium (K_d 225nM) permits this dye to measure cytoplasmic calcium at physiologically relevant concentrations. At low concentrations of dye, taking 340/380nm ratios allows accurate measurements

of intracellular calcium and allows for differences in dye loading, cell thickness and other problems that can effect calcium measurements.

Upon introduction of the cells to the fluorometer, cells were given 30 seconds to establish a baseline calcium level prior to the addition of drug. Drugs were made up at 100 times concentration and pH balanced to 7.4 before 20µl was injected into the cuvette resulting in 1 x concentration in the cuvette. At the end of each individual experiment 20µl of 1mg/ml digitonin was added to the cuvette to permeabilise the cells allowing calcium to flood the dye giving a maximum fluorescence, followed by 60µl of 0.5M EDTA pH 8.5 to chelate the calcium giving a minimum fluorescence. These values were then used to calculate the cytosolic calcium concentration of the cells, using the (Grynkiewicz et al., 1985) equation.

$$[Ca^{2+}]_i = K_d (R - R_{min}) / (R - R_{max}).$$

Where the K_d for Fura-2 is 225nM, R is the ratio of emissions recorded at 340nm and 380nm, R_{min} is the minimum ratio of emissions recorded at 340nm and 380nm after the addition of EDTA chelating the calcium, and R_{max} is the maximum ratio emissions recorded at 340nm and 380nm after the addition of digitonin causing the Fura-2 to be saturated with calcium. Unloaded cells were used to check autofluorescence and drug fluorescence. The data were then transferred into GraphPad Prism for graphical representation.

2.10 Data analysis

Saturation data analysis was analysed using GraphPad Prism (version 7.0 for Macintosh) non-linear regression analysis to fit saturation curves and calculate maximal radioligand binding and dissociation constants.

$$\text{Equation: } S = B_{max} \cdot [L] / K_d + [L]$$

Where S is the Specific binding, [L] is the concentration of free radioligand, B_{max} is the total number of receptors expressed in the same units as S (i.e. sites/cell, cpm or fmol/mg protein) and K_d is the equilibrium dissociation constant expressed in the same units as [L] (usually nM).

Non-linear regression was performed, rather than the traditional Scatchard plots due to the fact that transforming the data to a linear form distorts the experimental error, whilst linear regression assumes that the scatter around the line follows the Gaussian distribution and that the standard error around X is the same for every point, this is not true for the transformed data, and there are much larger errors associated at the low concentrations of bound ligand, and therefore they have undue influence over the slope of the regression line resulting in a K_d and B_{max} further from the true value than using non-linear regression.

One-way ANOVA was performed for all saturation curves. Data obtained from the highest concentration of ligand was used as a comparator. F and p values are given for each curve.

Competition binding data was analysed using GraphPad Prism non-linear curve fitting software in one of the two ways.

The equation used to fit competition binding data in Chapter 4 was the sigmoidal dose response (variable slope) model.

Equation: $Y = \text{Bottom} + (\text{Top} - \text{Bottom}) / 1 + (10^{((\text{LogIC}_{50} - X) \cdot \text{Hillslope}))}$

Where X is the logarithm of the concentration of competing ligand, Y is the response (i.e. Counts per minute or % specific radio ligand binding) and the Hill slope is the slope factor, a number that describes the steepness of the curve. A one site competitive binding curve that follows the law of mass action will have a slope of -1 (negative as the slope goes down). The IC_{50} is dependent on the K_i of the ligand for the receptor, but also dependent on the concentration of radio labelled drug used in the assay (i.e. increasing the radiolabelled drug concentration will change the IC_{50} whilst the K_i remains the same).

Competition assays performed in chapter 3 were analysed differently. The ligands here (DTG and (+) pentazocine) bind each site with a Hill slope of unity. [³H] DTG binds both sigma-1 and sigma-2 sites with equal affinity, whereas (+) pentazocine binds sigma-1 receptors with much higher affinity than the sigma-2 binding site. In these assays a two-site fit was used. Affinities are known for each ligand, so it is the proportion of high and low affinity sites for (+) pentazocine that are being determined using the following equations.

$$\log EC_{50Lo} = \log(10^{\log KiLo} * (1 + HotNM/HotKdNMLo))$$

$$\log EC_{50Hi} = \log(10^{\log KiHi} * (1 + HotNM/HotKdNMHi))$$

$$Span = Top - Bottom$$

$$Part1 = FractionHi * Span / (1 + 10^{(X - LogEC50Hi)})$$

$$Part2 = (1 - FractionHi) * Span / (1 + 10^{(X - LogEC50Lo)})$$

$$Y = Bottom + Part1 + Part2$$

Computer-assisted data analysis, therefore, permitted me to determine the proportion of sites with high and low affinity for (+) pentazocine.

The unpaired two-tailed Student's t-test was only performed when comparing two sets of data pairwise. Gaussian distribution and sphericity were assumed in all cases. Values for K_d , K_i , K_{50} , EC_{50} and IC_{50} were transformed to pK_d , pK_i , pK_{50} , pEC_{50} and pIC_{50} before any statistical manipulation was attempted, as these are not normally distributed otherwise. A p values < 0.05 is considered statistically significant.

Unpaired, two-tailed one-way ANOVA was performed when comparing more than two sets of data. When comparing "all means" with each other, Tukey *post hoc* analyses were performed when necessary. When data sets were compared against a "control" group only, Bonferroni *post hoc* analyses were performed when necessary. Gaussian distribution and sphericity were assumed in all cases. Values for K_d , K_i , K_{50} , EC_{50} and IC_{50} were transformed to pK_d , pK_i , pK_{50} ,

pEC_{50} and pIC_{50} before any statistical manipulation was attempted, as these are not normally distributed otherwise. An adjusted p value < 0.05 is considered statistically significant.

Two-way ANOVA was performed for the competition binding curves. Data for each cell line (row factor) was compared with that obtained for MCF7 between the concentrations of 10nM and 10 μ M (column factor). Those with $p < 0.05$ (following the Bonferroni adjustment for multiple comparisons) were deemed significantly different to MCF7 data points. An adjusted p value < 0.05 is considered statistically significant.

In order to give a more true representation of the drugs affinity for the receptor, the IC_{50} was converted to a K_i value using the Cheng Prusoff equation (Cheng and Prusoff, 1973).

$$\text{Equation: } K_i = IC_{50} / (1 + ([\text{Radioligand}] / K_d))$$

The K_i value is derived from the IC_{50} which is on a log scale, therefore it does not make sense to present mean K_i values \pm standard error of the mean (SEM) as the error is not symmetrical around the mean. The K_i was also converted into pK_i ($-\log K_i$), which is normally distributed therefore the SEM is symmetrical about the mean pK_i .

MTS assays were read using a Versamax plate reader, and the data collected using Softmax Pro software. Data were analysed as described for ligand binding to sigma-2 receptors above, using competition binding data with a sigmoidal dose response (variable slope) model.

$$\text{Equation: } Y = \text{Bottom} + (\text{Top} - \text{Bottom}) / 1 + (10^{((\text{Log}IC_{50} - X) \cdot \text{Hillslope})})$$

Linear regression was performed using the least squares (ordinary) fit. Data were unweighted. The equation of best fit is presented, along with R^2 , F and p values.

**Chapter 3. CHARACTERISATION OF SIGMA-1
RECEPTORS AND SIGMA-2 BINDING SITES IN
HUMAN CANCER CELL LINES**

3.1 Background

Sigma receptors were initially described as novel opioid receptors but later they were found to be a distinct class of receptors due to their ability to bind to different drugs. Pharmacological studies have characterised two subtypes: sigma-1 and sigma-2. These subtypes differ in their ability to bind to different drugs. Sigma receptors were initially identified in central nervous system and since then extensive work has been done to delineate their physiological roles and potential clinical uses (Bowen, 2000, Debonnel, 1993, Matsumoto et al., 2003, Maurice et al., 2001, Novakova et al., 1998)

Sigma-1 receptors have been identified and cloned (Abate et al., 2010, Hanner et al., 1996, Kekuda et al., 1996, Mei and Pasternak, 2001) whereas the existence of the sigma-2 binding site has only been proven pharmacologically (Guitart et al., 2004). Photoaffinity studies have revealed molecular weight of sigma-1 receptor to be 25kDa and 18-21kDa for sigma-2 binding site (Hellewell and Bowen, 1990, Hellewell et al., 1994). In addition to the central nervous system, sigma receptors are also found in high density in endocrine, immune, reproductive tissues (Wolfe et al., 1989), liver and kidney (Hellewell et al., 1994).

Endogenous ligands for sigma receptors have not been identified, however steroids hormones, sphingolipid-derived amines and N,N-dimethyltryptamine (DMT) were investigated to see if they could be potential endogenous ligands (van Waarde et al., 2010). Both subtypes, in particular sigma-2 binding sites are overexpressed in rapidly dividing normal cells and in tumour cell lines derived from various tissues (Vilner et al., 1995a). These included lung, breast, prostate, melanoma glioma and neuroblastoma. In small cell lung cancers the sigma-2 binding sites are overexpressed up to 6-fold and similarly the plasma levels were significantly elevated in patients with non-small cell lung cancer. It has been concluded that the sigma-2 binding site is a potential tumour and serum biomarker and could be used as a therapeutic target for lung cancer (Mir et al.,

2012). Expression of sigma-1 receptors and sigma-2 binding sites in various human tumour cell lines is show in Table 3-1

Cell Line	Origin	Radioligand	B _{max} (fmol/mg protein or %)
A375	Melanoma	³ H-(+) pentazocine	34
A375	Melanoma	³ H-DTG (+1μM DEX)	3403
BE(2)-C	Neuroblastoma	³ H-(+) pentazocine	2980
LNCa.FGG	Prostate cancer	³ H-(+) pentazocine	1196
LNCa.FGG	Prostate cancer	³ H-DTG (+1μM DEX)	727
MCF7	Breast adenocarcinoma	³ H-(+) pentazocine	0
MCF7	Breast cancer	³ H-DTG (+1μM DEX)	2071
NCI-H727	Lung carcinoid	³ H-(+) pentazocine	26
NCI-H727	Lung carcinoid	³ H-DTG (+1μM DEX)	2835
SK-N-SH	Neuroblastoma	³ H-(+) pentazocine	975
SK-N-SH	Neuroblastoma	³ H-DTG (+1μM DEX)	944
T47D	Breast cancer	³ H-(+) pentazocine	108
T47D	Breast cancer	³ H-DTG (+1μM DEX)	1221
Th-P1	Leukaemia	³ H-(+) pentazocine	1411
Th-P1	Leukaemia	³ H-DTG (+1μM DEX)	491
U-138MG	Glioblastoma	³ H-(+) pentazocine	1115
U-138MG	Glioblastoma	³ H-DTG (+1μM DEX)	3136

Table 3-1: Expression of sigma receptors in human cancer cell lines. Sigma-1 and sigma-2 binding site expression in various cancer cell lines. DEX = dextromethorphan, adapted from (van Waarde et al., 2010).

Sigma-1 receptors have been well studied and several functions have been described, which include: modulation and synthesis of dopamine and acetylcholine (Booth and Baldessarini, 1991, Patrick et al., 1993), modulation of

NMDA-stimulated neurotransmitter release (Gonzalez-Alvear and Werling, 1995, Monnet et al., 1996), modulation of opioid analgesia (King et al., 1997) and neuroprotective and anti-amnesic activity (Maurice and Lockhart, 1997). Sigma-2 binding sites are mainly involved in regulation of cell proliferation and viability (Bowen, 2000). The cytotoxicity of sigma-2 binding site ligands was confirmed *in vitro* using both neuronal and non neuronal cell lines (Vilner and Bowen, 1993, Vilner et al., 1995a). Exposure to sigma-2 binding site ligands resulted in assumption of spherical shape, detachment from surface followed by cell death. These effects are dose dependent hence with higher doses the changes and cell death occurs quicker. The mode of cell death is apoptotic (Crawford and Bowen, 2002, Vilner et al., 1995a).

The main purpose of this chapter was to determine the level of expression of sigma-1 receptor and sigma-2 binding site in different human cell lines (oesophageal: OE21, OE33 and FLO-1, breast: MCF7, MDA-MB-468, colorectal: Caco-2, SW480, HT-29 and HCT 116, human embryonic kidney cells: 293 and lung: A549. By determining which cells express which proteins, I could then attempt to distinguish which protein plays a role in particular biochemical events and determine whether sigma-1 and sigma-2 proteins could potentially act additively, synergistically or in opposition to each other.

3.2 Expression of sigma-1 receptor

Saturation binding experiments were carried out in order to calculate the number of sigma-1 receptors expressed on the cancer cell lines (B_{max}) and equilibrium dissociation constant (K_d) of [3H] (+) pentazocine. Non-specific binding was carried out in the presence of 1mM haloperidol. Specific binding was calculated by subtracting the non-specific binding from total [3H] (+) pentazocine binding. B_{max} and K_d were calculated using nonlinear regression software (GraphPad Prism, California).

3.3 Oesophageal cancer cell lines (FLO-1, OE21 and OE33)

Saturation binding experiments were carried out to determine B_{max} and K_d of [3H] (+) pentazocine binding to cell membranes from three oesophageal cancer cell lines: FLO-1, OE21 and OE33.

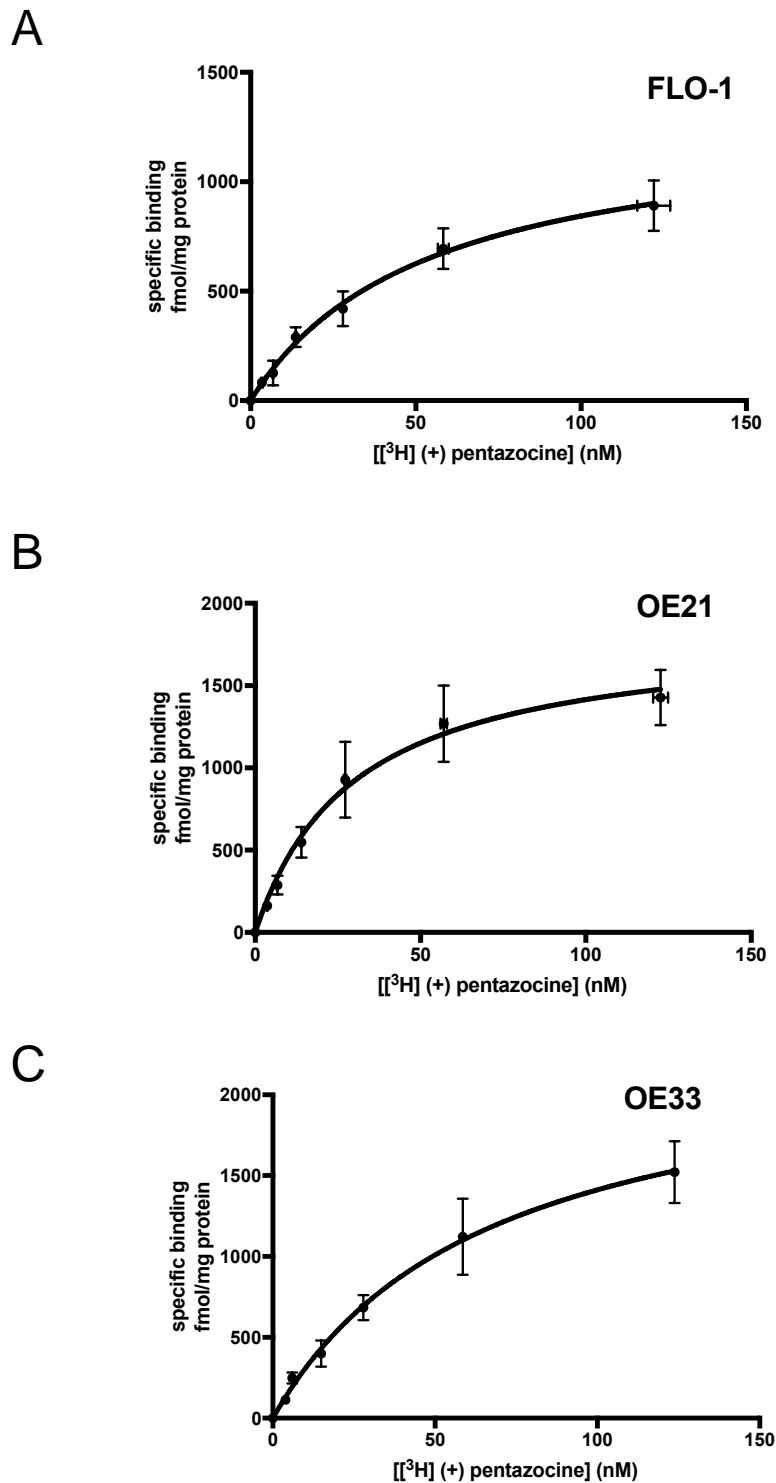


Figure 3-1: Saturation binding of [³H] (+) pentazocine to oesophageal cancer cell lines (A: FLO-1, B: OE21 and C: OE33).

Saturation binding curve for [³H] (+) pentazocine to oesophageal cancer cell lines. Non-specific binding was determined in the presence of 1mM haloperidol. Figure represents mean \pm SEM from 3-5 independent experiments. One-way ANOVA, using the highest concentration of ligand as comparator, shows a strong concentration-dependant increase in ligand binding: A (FLO-1) $[F(6,13) =$

24.6, $p < 0.0001$]; B (OE21) [$F(5,30) = 11.0$, $p < 0.0001$]; C (OE33) [$F(6,14) = 20.7$, $p < 0.0001$].

All three oesophageal cancer cell lines expressed binding sites for [^3H] (+) pentazocine. The mean $pK_d \pm \text{SEM}$ of [^3H] (+) pentazocine for the sigma-1 receptor expressed in FLO-1, OE21 and OE33 cells was determined as 7.38 ± 0.05 , 7.43 ± 0.12 and 7.15 ± 0.07 . The B_{max} was determined as 1100 ± 100 , 2250 ± 150 and $2400 \pm 300 \text{fMol/mg}$ protein respectively. Data were calculated from 3-5 independent saturation binding experiments.

3.4 Breast cancer cell lines (MCF7, MDA-MB-468)

Saturation binding experiments were carried out to determine B_{max} and K_d of [^3H] (+) pentazocine to cell membranes from two breast cancer cell lines: MDA-MB-468 and MCF7. Figure 3-2 shows saturation binding curve for [^3H] (+) pentazocine in membranes prepared by sonicating breast cancer cell lines. B_{max} and K_d were calculated using GraphPad Prism.

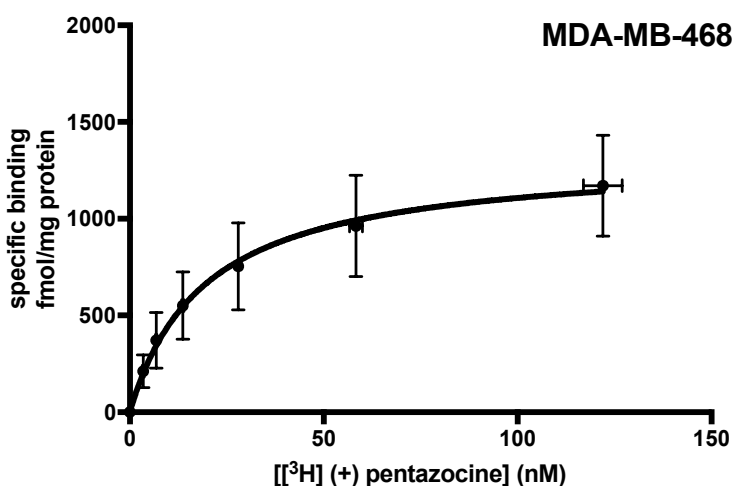


Figure 3-2: Saturation binding of [^3H] (+) pentazocine to MDA-MB-468 cells
Saturation binding curve for [^3H] (+) pentazocine to membranes prepared from MDA-MB-468 breast cancer cells. Non-specific binding was determined in the presence of 1mM haloperidol. Figure represents mean \pm SEM from 3 independent experiments. One-way ANOVA, using the highest concentration of ligand as comparator, shows a strong concentration-dependant increase in ligand binding: [$F(6,14) = 4.9$, $p = 0.0065$]

MCF7 showed no specific binding site for [³H] (+) pentazocine. The mean $pK_d \pm$ SEM of [³H] (+) pentazocine for the sigma-1 receptor expressed in MDA-MB-468 was 7.65 ± 0.13 and the B_{max} was found to be 1700 ± 150 fMol/mg protein. Data were calculated from 3 independent saturation experiments.

3.5 Colorectal cancer cell lines (Caco-2, HCT 116, HT-29 and SW480)

Saturation binding experiments were carried out to determine B_{max} and K_d of [³H] (+) pentazocine for four colorectal cancer cell lines: Caco-2, HCT 116, HT-29 and SW480. Figure 3-3 shows saturation binding curve for [³H] (+) pentazocine to membranes prepared by sonicating colorectal cancer cell lines. B_{max} and K_d were calculated using GraphPad Prism.

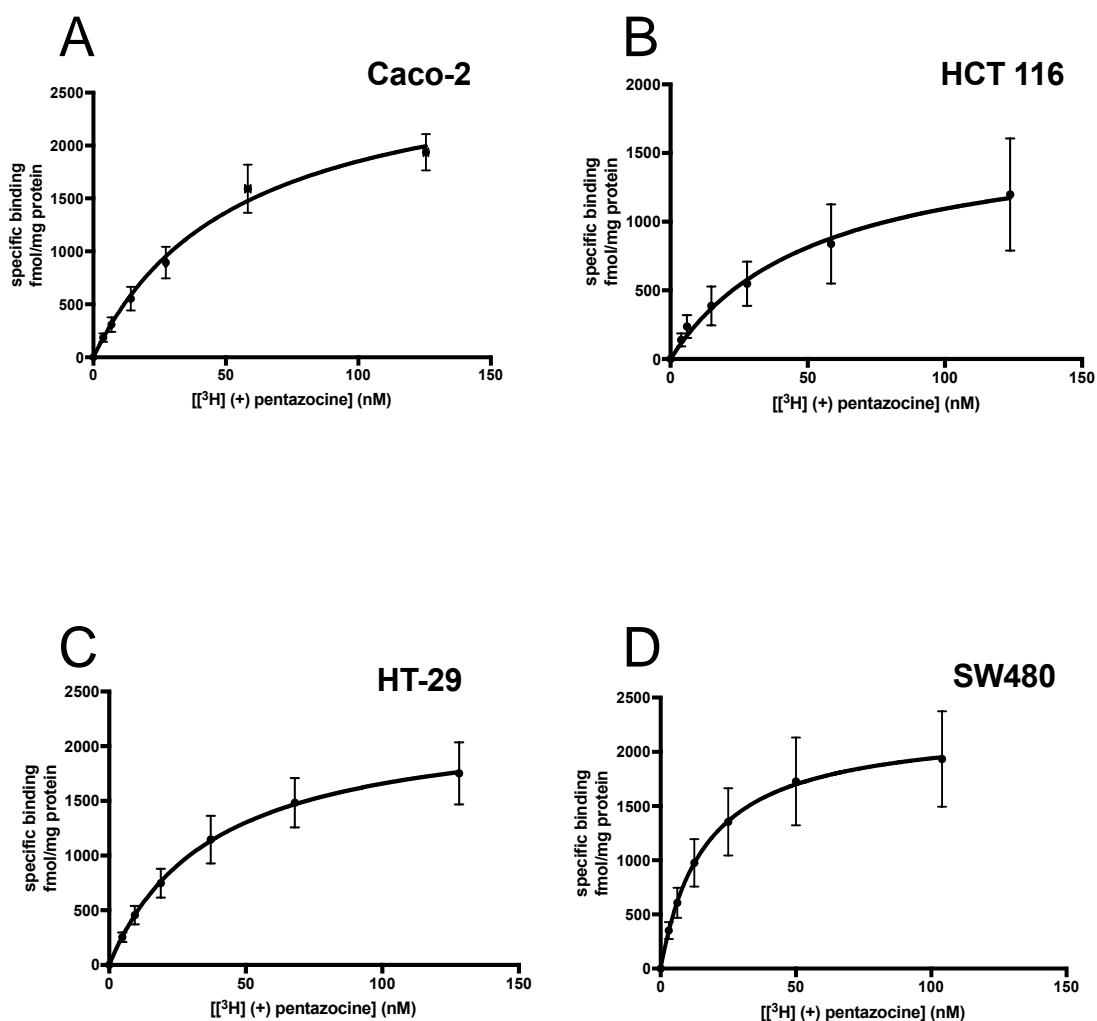


Figure 3-3: Saturation binding of [³H] (+) pentazocine to colorectal cancer cell lines (A: Caco-2, B: HCT 116, C: HT-29 and D: SW480)

Saturation binding curve for [³H] (+) pentazocine to membranes prepared from colorectal cancer cell lines. Non-specific binding was determined in the presence of 1mM haloperidol. Figure represents mean \pm SEM from 3 independent experiments. One-way ANOVA, using the highest concentration of ligand as comparator, shows a strong concentration-dependant increase in ligand binding: A (Caco-2) [F(6,27) = 30.1, $p < 0.0001$]; B (HCT 116) [F(6,14) = 4.1, $p = 0.015$]; C (HT-29) [F(6,14) = 14.4, $p < 0.0001$]; D (SW480) [F(6,14) = 6.86, $p = 0.0015$].

The mean $pK_d \pm$ SEM of [³H] (+) pentazocine for the sigma-1 receptor expressed on Caco-2, HCT 116, HT-29 and SW480 cells was determined as 7.40 ± 0.07 , 7.28 ± 0.04 , 7.41 ± 0.04 and 7.78 ± 0.00 , the B_{max} was determined as 2400 ± 50 , 1700 ± 600 , 2250 ± 300 and 2250 ± 500 fmol/mg protein respectively. Data were calculated from 3 independent saturation experiments.

3.6 Human embryonic kidney cell line (293)

Saturation binding experiments were carried out to determine B_{\max} and K_d of [^3H] (+) pentazocine for 293 cells. Figure 3-4 shows saturation binding curve for [^3H] (+) pentazocine to membranes prepared by sonicating colorectal cancer cell lines. B_{\max} and K_d were calculated using GraphPad Prism.

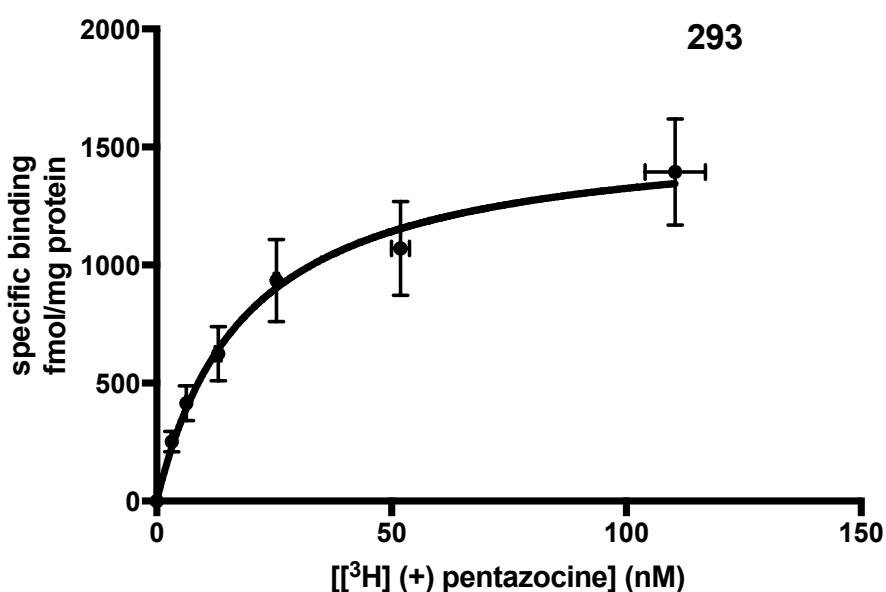


Figure 3-4: Saturation binding of [^3H] (+) pentazocine to 293 cells

Saturation binding curve for [^3H] (+) pentazocine to membranes prepared from 293 cells. Non-specific binding was determined in the presence of 1mM haloperidol. Data were calculated from 3 independent saturation experiments. One-way ANOVA, using the highest concentration of ligand as comparator, shows a strong concentration-dependant increase in ligand binding: [$F(6,14) = 12.0, p < 0.0001$].

The mean $pK_d \pm \text{SEM}$ of [^3H] (+) pentazocine for the sigma-1 receptor expressed in 293 cells was 7.63 ± 0.08 and the B_{\max} was found to be $1600 \pm 250\text{fMol/mg}$ protein. Data were calculated from 3 independent saturation experiments.

3.7 Lung cancer cell line (A549)

Saturation binding experiments were carried out to determine B_{\max} and K_d of [^3H] (+) pentazocine for A549 cells. Figure 3-5 shows saturation binding curve for [^3H] (+) pentazocine in membranes prepared by sonicating lung cancer cell lines.

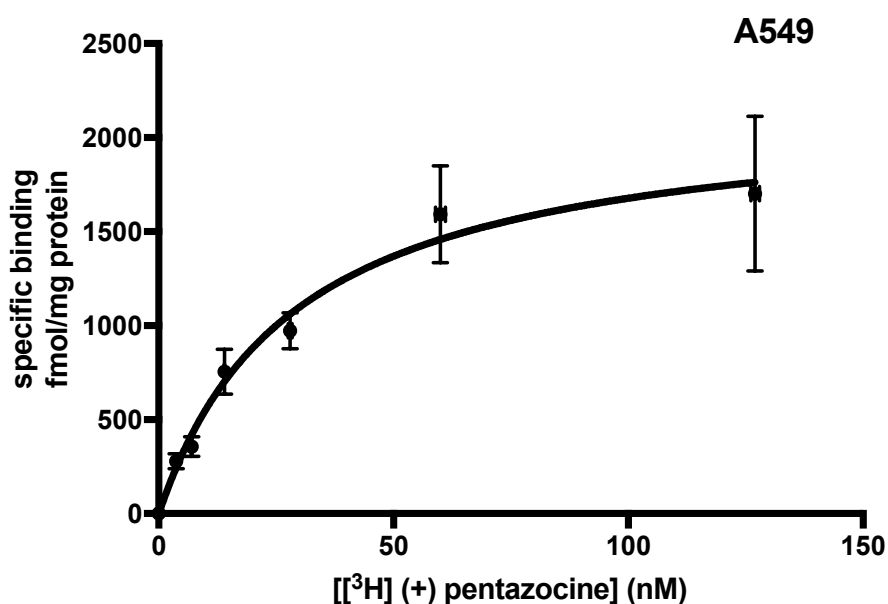


Figure 3-5: Saturation binding of [^3H] (+) pentazocine to A549 cells

Saturation binding curve for [^3H] (+) pentazocine to membranes prepared from A549 cells. Non-specific binding was determined in the presence of 1mM haloperidol. Data were calculated from 3 independent saturation experiments. One-way ANOVA, using the highest concentration of ligand as comparator, shows a strong concentration-dependant increase in ligand binding: [$F(6,33) = 13.9, p < 0.0001$].

The mean $pK_d \pm \text{SEM}$ of [^3H] (+) pentazocine for the sigma-1 receptor expressed in A549 cells was 7.6 ± 0.09 and the B_{\max} was found to be 1300 ± 150 fmol/mg protein. Data were calculated from 3 independent saturation experiments.

Table 3-2 shows a summary of the findings from all cell lines studied.

Origin	Cell Line	$B_{max} \pm SEM$ fMol/mg protein	$pK_d \pm SEM$	R^2
Oesophagus	FLO-1	1100 \pm 100	7.38 \pm 0.05	0.9
	OE21	2250 \pm 150	7.43 \pm 0.12	0.9
	OE33	2400 \pm 300	7.15 \pm 0.07	0.9
Breast	MCF7	No binding		
	MDA-MB-468	1700 \pm 150	7.6 \pm 0.13	0.9
Colorectal	Caco-2	2400 \pm 50	7.40 \pm 0.07	0.9
	HCT 116	1700 \pm 600	7.28 \pm 0.04	0.9
	HT-29	2250 \pm 300	7.41 \pm 0.04	0.9
	SW480	2250 \pm 500	7.78 \pm 0.00	0.9
Human embryonic kidney	293	1600 \pm 250	7.63 \pm 0.08	0.9
Lung	A549	1300 \pm 150	7.60 \pm 0.09	0.9

Table 3-2: Binding parameters of sigma-1 receptors in various human tumour cell lines.

Sigma-1 binding was carried out as described in chapter 2 “Materials and Methods”. [3H] (+) pentazocine concentration was varied in 6 concentrations over a range of 4-128nM. Apart from the MCF7 cell line, all the cell lines expressed sigma-1 receptors. Unpaired 1-way ANOVA, followed by *post hoc* Tukey (“all means”) comparison, with p value adjusted for multiple comparisons, shows a significant difference in B_{max} values: [F(10,29) = 3.52, p = 0.0039]. MCF7 cells expressed significantly fewer sigma-1 receptors than all other cell lines, p < 0.022 for all cases. All other comparisons show no significant difference between B_{max} values. Unpaired 1-way ANOVA, followed by *post hoc* Tukey (“all means”) comparison, with p value adjusted for multiple comparisons, shows a significant difference in pK_d values: [F(9,28) = 3.60, p = 0.0044]. The pK_d for OE33 cells was found significantly different to SW480 (p = 0.015) and

A549 ($p = 0.017$) cells. All other comparisons show no significant difference between pK_d values.

3.8 Measurement of pan-sigma binding

The standard protocol used for determining sigma-2 binding site presence and number relies on [3 H]-DTG. DTG is a pan-sigma ligand, binding both sigma-1 (K_i 35.5nM) and sigma-2 (K_i 39.9nM) (Lever et al., 2006) sites with equal affinity. As most binding assays have been performed in tissues or cell lines containing sigma-1 receptors, it has become standard to determine sigma-2 binding in the presence of either (+) pentazocine or dexrallorphan (Chu et al., 2015, Vilner et al., 1995b). This protocol, while fully integrated into the sigma receptor researcher's toolkit, is seriously flawed. I will explain why:

(+) pentazocine and dexrallorphan are not specific for the sigma-1 receptor. (+) pentazocine has a range of published affinities between 1.6nM (Xu et al., 2015) and 17nM (Brimson et al., 2011, Vilner and Bowen, 2000) for the sigma-1 receptor. Its affinity for sigma-2 binding sites is between 728nM (Xu et al., 2015) and 6.6 μ M (Vilner and Bowen, 2000).

(+) Pentazocine binds with a Hill slope of one and so from these data, one can model a saturation binding isotherm. This will show the relative binding of (+) pentazocine to sigma-1 and sigma-2 binding sites at different concentrations as shown in Figure 3-6.

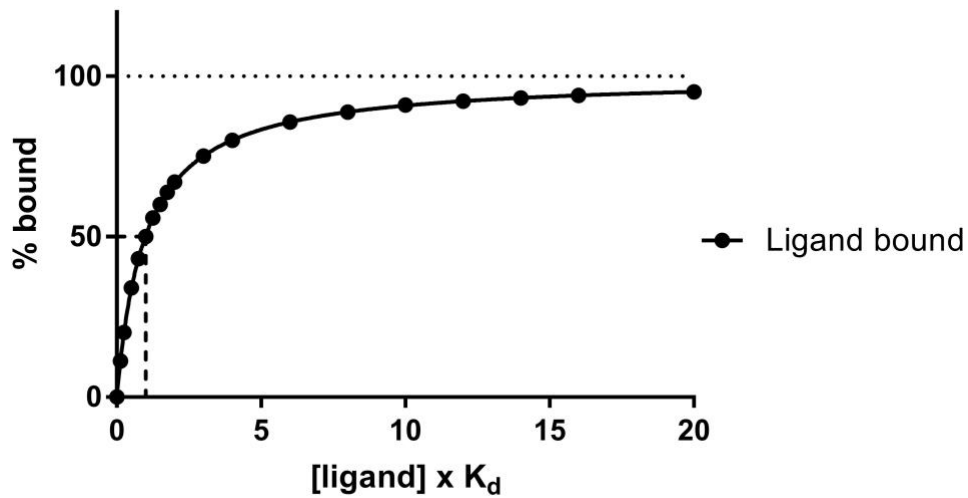


Figure 3-6: Binding profile of a ligand.

Figure showing the binding profile of a ligand with Hill slope of unity. The K_d , at which 50% of the receptors are bound, and 100% binding, which the rectangular hyperbola approaches but never reaches are shown.

If one draws the best (greatest difference between sigma-1 (1.6nM) and sigma-2 (6600nM)) affinities and worst (least difference between sigma-1 (17nM) and sigma-2 (728nM)) case scenarios for (+) pentazocine, and compares the “masking” described at concentrations used (100nM and 1 μ M) it is clear that data can be easily misinterpreted (Figure 3-7).

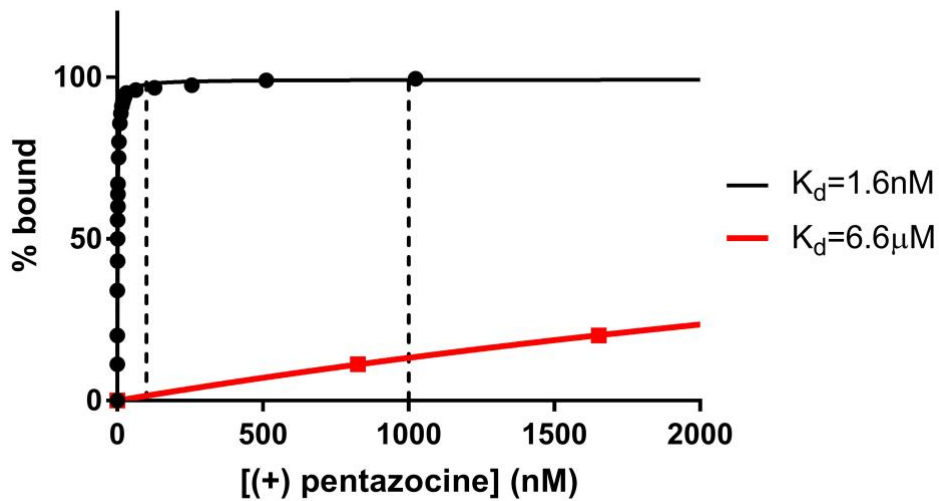


Figure 3-7: Binding profile of sigma receptors in the best case scenario

Figure shows the calculated binding of pentazocine to receptors with affinity of 1.6nM (highest reported affinity for sigma-1 receptors) and 6.6µM (lowest claimed affinity for sigma-2 binding site). Dotted lines show commonly used concentrations of (+) pentazocine.

From the data in Figure 3-7, one can calculate that, in the absence of competing agents, 100nM (+) pentazocine would bind 97.8% of sigma-1 receptors and 1.49% of sigma-2 binding sites whereas 1µM (+) pentazocine would bind 99.1% of sigma-1 receptors and 13.2% of sigma-2 binding sites. This is the “best case” scenario.

The worst case scenario is shown in Figure 3-8. One can calculate that, in the absence of competing agents, 100nM (+) pentazocine would bind 85.4% of sigma-1 receptors and 12.2% of sigma-2 binding sites whereas 1µM (+) pentazocine would bind 98.0% of sigma-1 receptors and 58.1% of sigma-2 binding sites.

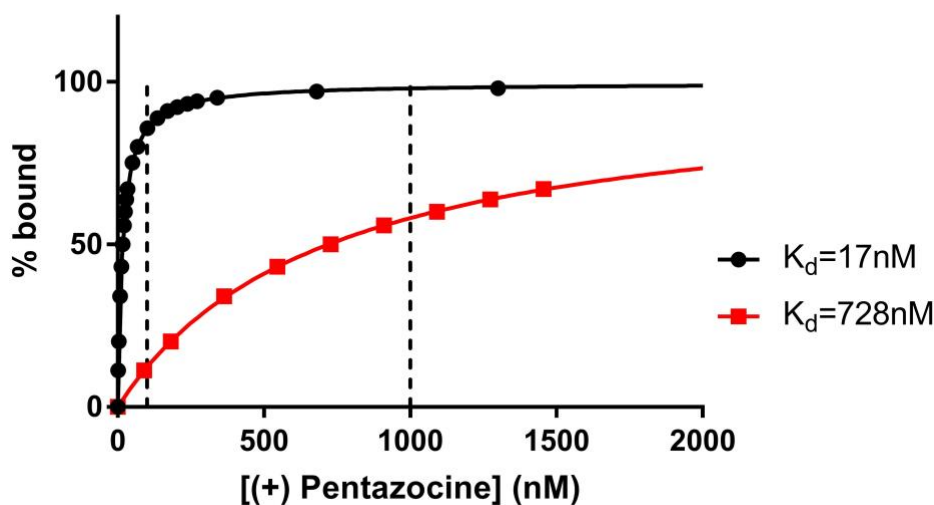


Figure 3-8: Binding profile of sigma receptors in the worst case scenario.

Figure showing the worst case scenario of calculated binding of (+) pentazocine to receptors with affinity of 17nM (lowest reported affinity for sigma-1 receptors) and 728nM (highest claimed affinity for sigma-2 binding site). Dotted lines show commonly used concentrations of (+) pentazocine.

From these numbers alone, it is clear that the accepted protocol for sigma-2 binding site characterisation should not be used.

Furthermore, when the addition of a second drug that binds both sites non-selectively, matters are further complicated. Simplified curves were drawn based on DTG competing at the sigma-1 receptor and at the sigma-2 binding site in isolation. It was acknowledged that the situation was more complex as binding and release of each drug to one target (e.g. sigma-1 receptor) would have an impact on second target (e.g. sigma-2 binding site). Using a calculation based on Cheng and Prusoff (Cheng and Prusoff, 1973) the inhibition of binding of a ligand based on the affinities and concentration of each ligand could be determined.

$$f_i = \frac{I}{1 + K_i(1 + L_T/K_d)}$$

Where:

- f_i fraction inhibition
- I added unlabelled drug
- K_i affinity of inhibitor
- LT total labelled drug added
- K_d affinity of labelled drug

In the scenarios below “labelled” will be used for (+) pentazocine, as its concentration remains constant, and “unlabelled” will be used for DTG (actually the radioligand), as its concentrations are varied in a saturation assay.

Modelling the dissociation of (+) pentazocine at 100nM with affinities of 1.6nM and 17nM with a range of DTG concentrations 0 – 256nM with an affinity of 35.5nM for the sigma-1 receptor (Lever et al., 2006) shows how DTG will compete with (+) pentazocine at the sigma-1 receptor with increasing effect, meaning that each point will have different amounts of DTG bound .

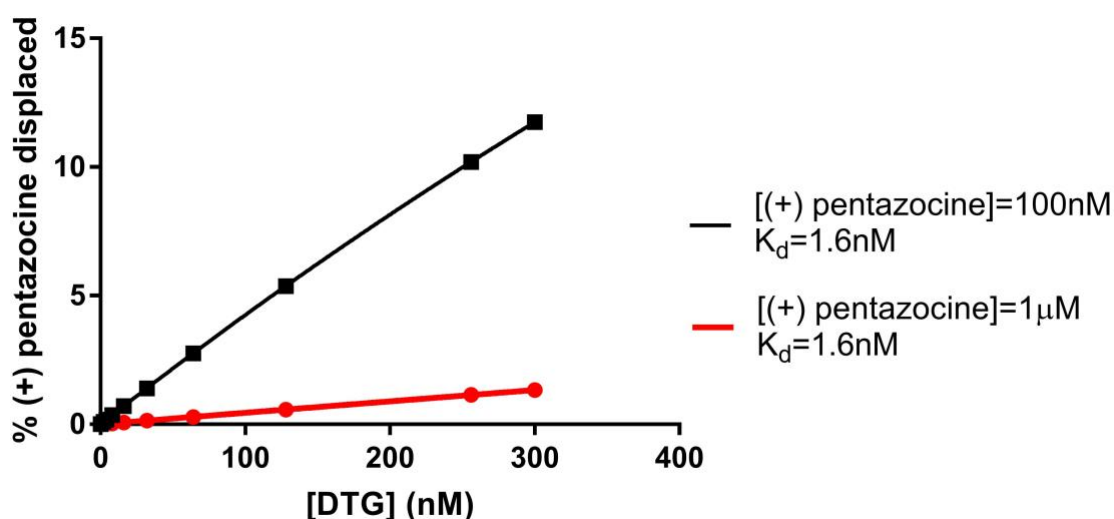


Figure 3-9: Percentage change in (+) pentazocine displacement with increasing DTG concentration.

Figure showing the percentage of (+) pentazocine displaced from the sigma-1 receptor as DTG concentration increases to prepare a saturation binding curve. Data are modelled for the two commonly used concentrations of (+) pentazocine (100nM and 1µM) and an affinity of (+) pentazocine for the sigma-1 receptor of 1.6nM.

Figure 3-9 shows that DTG can readily displace a significant percentage of (+) pentazocine from this receptor, even with the higher affinity estimate for (+) pentazocine used.

When the lower affinity of (+) pentazocine (17nM) is substituted into these calculations, the effects of DTG on (+) pentazocine binding, and hence the amount of DTG (tritiated signal in a binding assay) increases further as shown in Figure 3-10.

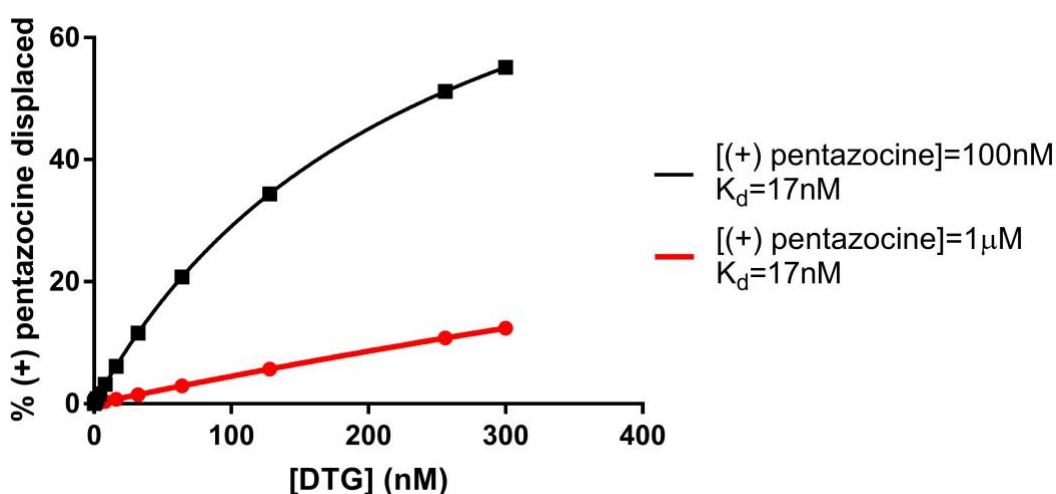


Figure 3-10: (+) Pentazocine displacement with increasing DTG concentration

Figure showing the percentage of (+) pentazocine displaced from the sigma-1 receptor as DTG concentration increases to prepare a saturation binding curve. Data are modelled for the two commonly used concentrations of (+) pentazocine (100nM and 1µM) and an affinity of (+) pentazocine for the sigma-1 receptor of 17nM.

DTG will readily displace the (+) pentazocine bound to the sigma-2 binding sites, with modelled data for (+) pentazocine concentrations of 100nM and 1µM and affinities of 738nM and 6.6µM shown below in Figure 3-11.

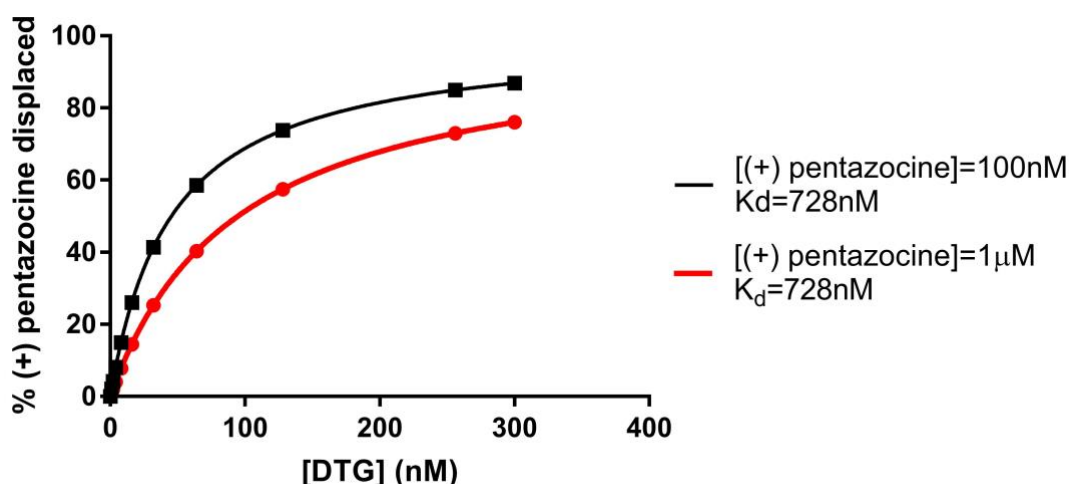


Figure 3-11: Percentage displacement of (+) pentazocine with increasing DTG concentration.

Figure showing the percentage of (+) pentazocine displaced from the sigma-2 binding site as DTG concentration increases to prepare a saturation binding curve. Data are modelled for the two commonly used concentrations of (+) pentazocine (100nM and 1µM) and an affinity of (+) pentazocine for the sigma-2 binding site of 728nM.

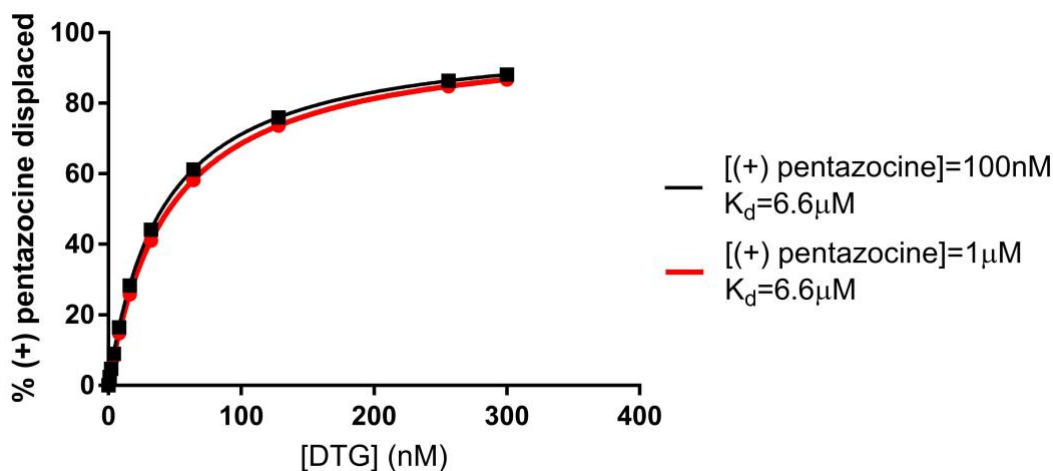


Figure 3-12: Displacement of (+) pentazocine from sigma-2 binding site with increasing concentration of DTG.

Figure showing the percentage of (+) pentazocine displaced from the sigma-2 binding site as DTG concentration increases to prepare a saturation binding curve. Data are modelled for the two commonly used concentrations of (+) pentazocine (100nM and 1µM) and an affinity of (+) pentazocine for the sigma-2 binding site of 6.6µM.

Calculations with dexrallorphan yield similar data.

Since the affinity of dexrallorphan for the sigma-2 binding site has not been defined, the only data point found (Hellewell and Bowen, 1990) for this ligand, was used, which was obtained using [³H] DTG and [³H] (+)-3-(3-hydroxyphenyl)-N-(1-propyl)piperidine (PPP) in PC-12 cells. This appears to be the only paper in which the binding of dexrallorphan to sigma-2 sites is reported and the only time PC-12 cells have been used to study sigma-2 sites. Both these issues raise concern. In this paper, dexrallorphan is described as displacing less than 30% of [³H] DTG or [³H] PPP when used at 5µM. As a similar statement regarding other drugs showing less than 30% displacement at 10µM is made elsewhere, The affinity was estimated based on 30% displacement of 5nM DTG, with an affinity of 23.7nM and 3nM PPP with an affinity of 86.3nM.

Entering these values into the above equation gives K_{30} (as only 30% was displaced) values for dexrallorphan of between 6550nM (calculated using PPP) and 18760nM (calculated using DTG). From a rectangular binding isotherm, 30% binding corresponds to a concentration 42% of the K_i . This estimates the K_i of dexrallorphan for the sigma-2 binding site of 15µM and 44.7µM.

Taking these values, one can then estimate the binding of dexrallorphan to sigma-2 binding sites and determine how much will bind under experimental conditions.

Modelling rectangular hyperbolae with these affinities shows that 1µM dexrallorphan will bind between 6.3% (taking an affinity of 15µM) and 2.2% (taking an affinity of 44.7µM) of the sigma-2 binding sites.

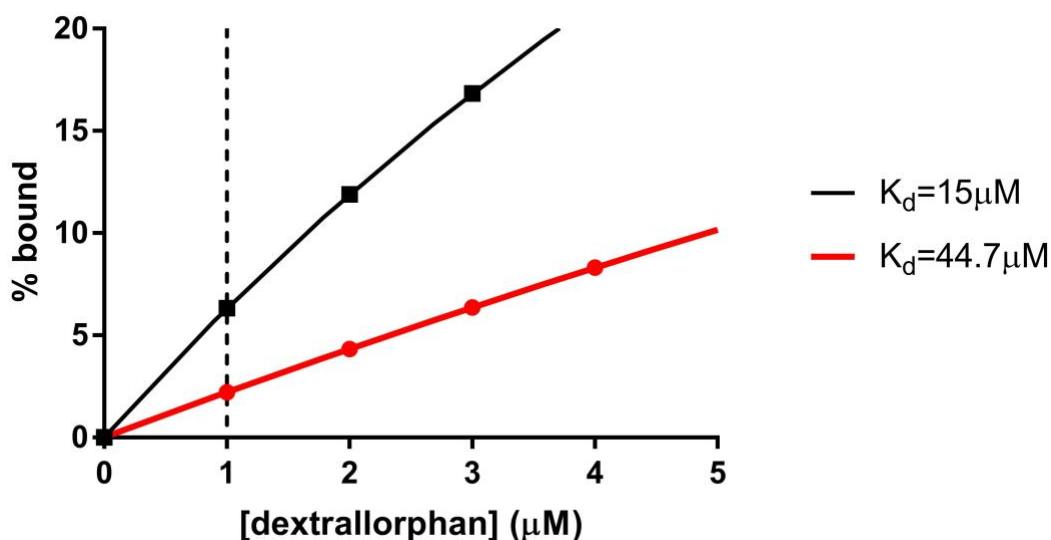


Figure 3-13: Calculated binding dextrallorphan to sigma-2 sites.

Figure showing the calculated binding of dextrallorphan to sigma-2 sites with affinity of 15µM (highest calculated affinity for sigma-2 binding sites using PPP data) and 44.7µM (highest calculated affinity for sigma-2 binding site using DTG data). Dotted line shows the commonly used concentration of dextrallorphan.

The only published affinity of dextrallorphan for the sigma-1 receptor shows a K_i of 16.1nM (Hellewell and Bowen, 1990) A second paper (Largent et al., 1987) gives an IC_{50} (163nM) along with K_d (30nM) and concentration (1-2nM) of the ligand ($[^3H]$ PPP) binding assays were performed using. From this, we can calculate a K_i of 153-158nM. I will model data using these two affinities (16.1nM and 155nM) in order to estimate binding achieved when the “masking” protocol is used.

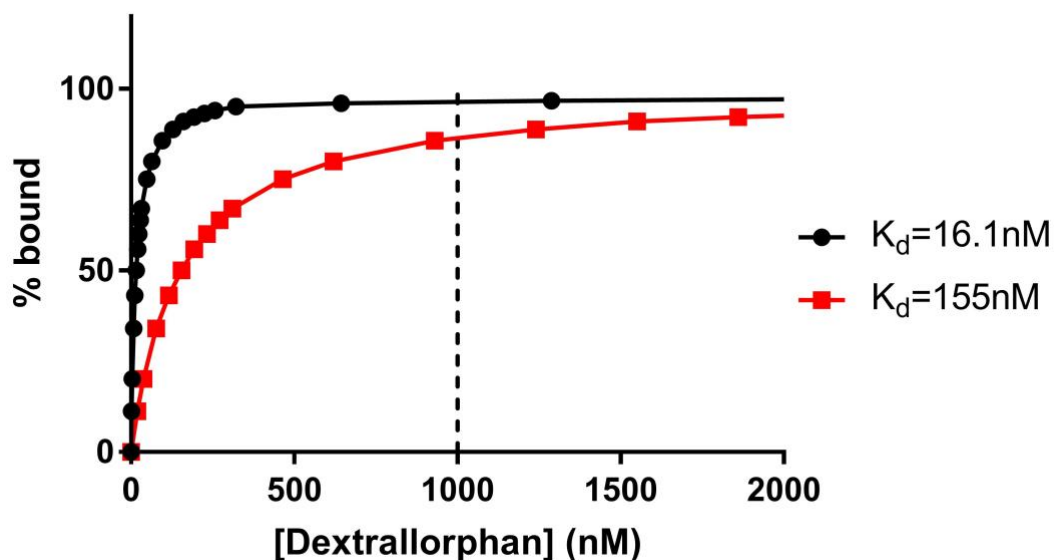


Figure 3-14: Binding of dextrallorphan at two different affinities.

Calculated binding of dextrallorphan to receptors with affinity of 16.1nM (highest affinity for sigma-1 receptor) and 155nM (lowest calculated affinity for sigma-1 receptor). Dotted line shows the commonly used concentration of dextrallorphan.

Using these calculations, 1 μM dextrallorphan binds 97.8% (using 16.1nM affinity) or 86.3% (using 155nM affinity) of the sigma-1 receptors present as shown in Figure 3-14.

Modelling the dissociation of dextrallorphan at 1 μM with affinities of 16.1 μM and 155 μM with a range of DTG concentrations 0 – 256nM with an affinity of 39.9nM for the sigma-1 receptor (Lever et al., 2006) shows how DTG will compete with dextrallorphan at the sigma-1 receptor with increasing effect, meaning that each point will have different amounts of DTG bound.

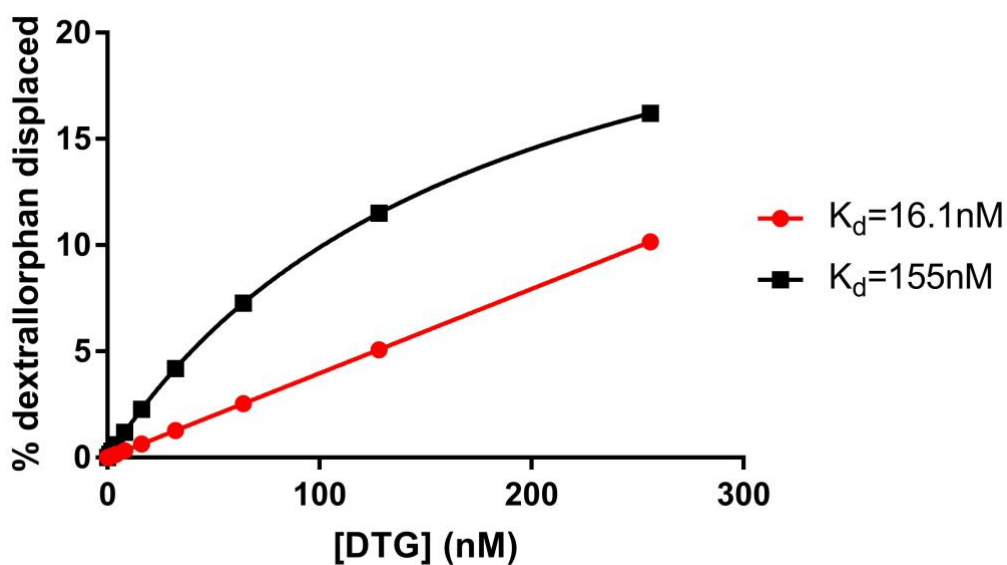


Figure 3-15: Displacement of dextrallorphan with increasing concentration of DTG.

Figure showing the percentage of dextrallorphan ($1 \mu\text{M}$) displaced from the sigma-1 receptor as DTG concentration increases to prepare a saturation binding curve. Data are modelled for the two reported affinities of dextrallorphan for the sigma-1 receptor.

DTG readily displaces dextrallorphan from the sigma-2 binding site as shown in Figure 3-16

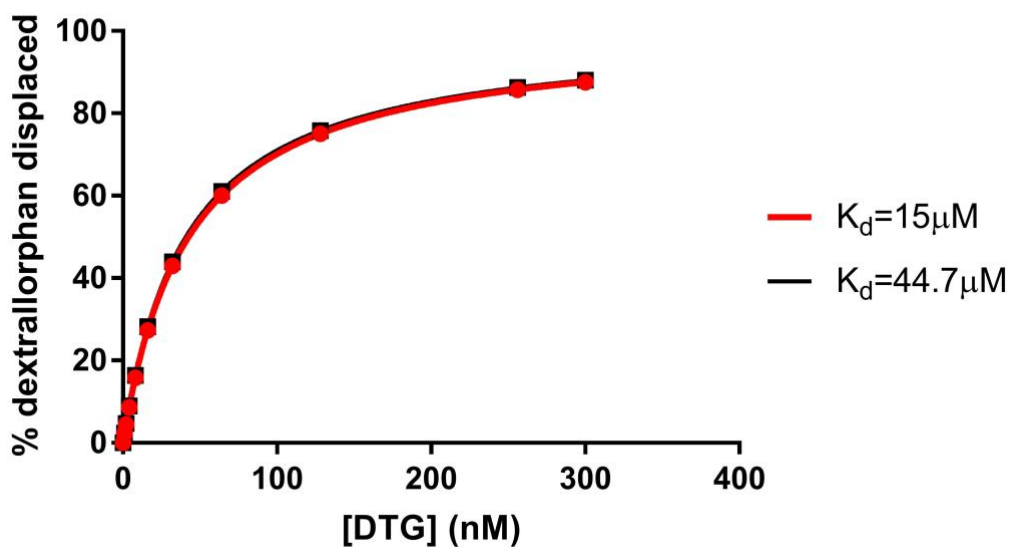


Figure 3-16: Percentage displacement of dexrallorphan with increasing DTG concentration.

Figure showing the percentage of dexrallorphan ($1 \mu\text{M}$) displaced from the sigma-2 binding site as DTG concentration increases to prepare a saturation binding curve. Data are modelled for the two reported affinities of dexrallorphan for the sigma-2 binding site.

From the above data, it is clear that none of the masking protocols widely accepted should be used. Summary of these findings are tabulated below (Table 3-3, 3-4, 3-5, 3-6).

(+) Pentazocine concentration (μM)	sigma-1 affinity (nM)	% sigma-1 binding	sigma-2 affinity (nM)	% sigma-2 binding
0.1	1.6	97.8	6,600	1.49
0.1	17	85.4	728	12.2
1	1.6	99.1	6,600	13.2
1	17	98.0	728	58.1

Table 3-3: Summary of range of (+) pentazocine binding to sigma binding sites.

Table summarising the range of calculated binding of (+) pentazocine to sigma-1 and sigma-2 sites under standard conditions used.

Dextrallorphan concentration (μM)	sigma-1 affinity (nM)	% sigma-1 binding	sigma-2 affinity (nM)	% sigma-2 binding
1	16.1	97.8	15,000	6.3
1	155	86.3	44,700	2.2

Table 3-4: Summary of range of dextrallorphan to sigma binding sites.

Table summarising the range of calculated binding of dextrallorphan to sigma-1 and sigma-2 sites under standard conditions used.

Addition of DTG will compete with the binding of (+) pentazocine and dextrallorphan to both sigma-1 and sigma-2 sites. When performing saturation binding curves, it is common to use concentrations in excess of 200nM. The table below shows calculated displacement of (+) pentazocine and dextrallorphan at 256nM DTG from the sigma-1 and sigma-2 sites.

Masking agent	Concentration (μM)	sigma-1 affinity (nM)	% displacement
(+) Pentazocine	0.1	1.6	10.1
	0.1	17	51.2
(+) Pentazocine	1	1.6	1.1
	1	17	10.8
Dextrallorphan	1	16.1	10.2
	1	155	16.2

Table 3-5: Displacement of (+) pentazocine or dextrallorphan by DTG.

Table showing the percent displacement of (+) pentazocine or dextrallorphan from the sigma-1 receptor by 256nM DTG.

Masking agent	Concentration (μM)	sigma-2 affinity (μM)	% displacement
(+) Pentazocine	0.1	0.728	84.9
	0.1	6.6	86.3
(+) Pentazocine	1	0.728	73.0
	1	6.6	84.8
Dextrallorphan	1	15	85.7
	1	44.7	86.2

Table 3-6: Displacement of (+) pentazocine or dextrallorphan by DTG (256nM).

Table showing the percent displacement of (+) pentazocine or dextrallorphan from the sigma-2 binding site by 256nM DTG.

The data above shows several reasons why the masking protocol is seriously flawed.

In the case of (+) pentazocine, 100nM (and an affinity of 17nM, the value obtained in our laboratory) would only bind 85.4% of the sigma-1 receptors, even in the absence of DTG. As DTG is added, up to 51.2% would be

competed out at a concentration of 256nM DTG. This is the equivalent of 43.7% of the sigma-1 receptors being bound by [³H] DTG.

The use of 1µM (+) pentazocine would decrease the effects of DTG, with only 10.8% of the sigma-1 receptors being bound by the radioligand at 256nM. At this concentration of (+) pentazocine (1µM) however, 58.1% (assuming an affinity of 728nM) of the sigma-2 binding sites would be bound by (+) pentazocine and only 73.0% of these would be released upon addition of 256nM DTG.

Dextrallorphan fares little better. Whilst it does bind few sigma-2 binding sites – fewer than 6.3% at the standard concentration of 1µM (assuming an affinity of 15µM, based on a single published observation), it may mask only 86.3% of the sigma-1 receptors (using the affinity of 155nM). Again, addition of DTG at 256nM will release and bind to some 16.2% of these sigma-1 sites.

It is for these reasons that the experiments were performed using DTG in the absence of any masking agent. Furthermore, the exclusive use of the masking protocol when determining the presence of sigma-2 binding sites may explain why no cell line has been found to lack sigma-2 binding sites. The description above could show a signal equivalent to 27% of the sigma-1 receptors with dextrallorphan and up to 58% with 100nM (+) pentazocine.

Saturation and competition binding experiments were carried out in order to calculate the number of sigma-2 binding sites expressed on the cancer cell lines (B_{max}) and equilibrium dissociation constant (K_d) of [³H] DTG. Non-specific binding was carried out in the presence of 1mM Haloperidol. B_{max} and K_d were calculated using nonlinear regression software (GraphPad Prism, California).

3.9 Oesophageal cancer cell lines (OE21, OE33 and FLO-1)

Saturation binding experiments were carried out to determine B_{\max} and K_d of [^3H] DTG for three oesophageal cancer cell lines: FLO-1, OE21 and OE33. Figure 3-17 shows saturation binding curve for [^3H] DTG in membranes prepared by sonicating oesophageal cancer cell lines. B_{\max} and K_d were calculated using GraphPad Prism.

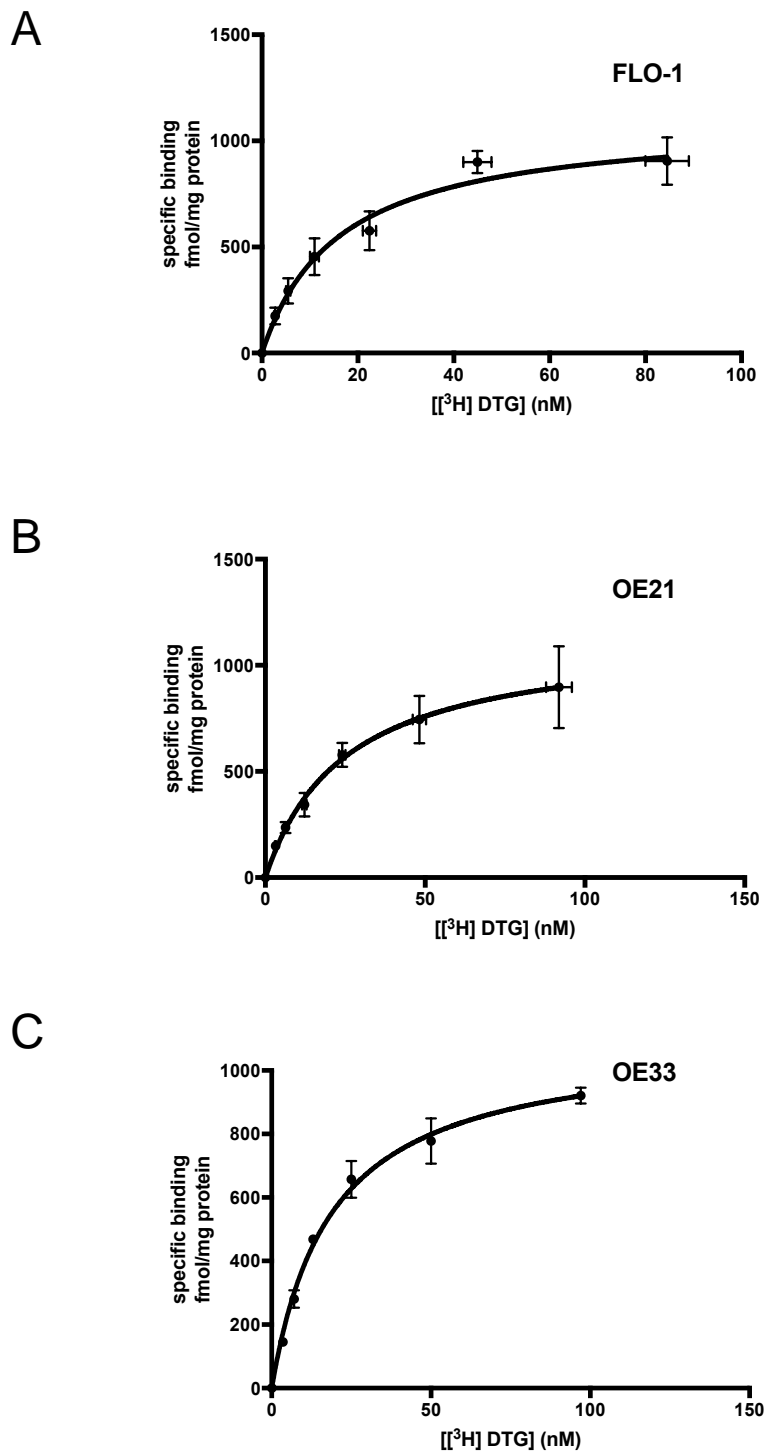


Figure 3-17: Saturation binding of [³H] DTG in oesophageal cancer cell lines (A: FLO-1, B: OE21 and C: OE33).

Saturation binding curve for [³H] DTG to membranes prepared from oesophageal cancer cell lines. Non-specific binding was determined in the presence of 1mM haloperidol. Figure represents mean \pm SEM from 3 independent experiments. One-way ANOVA, using the highest concentration of ligand as comparator, shows a strong concentration-dependant increase in

ligand binding: A (FLO-1) [F(6,13) = 20.0, $p < 0.0001$]; B (OE21) [F(6,14) = 10.1, $p = 0.0002$]; C (OE33) [F(6,14) = 79.8, $p < 0.0001$].

The mean $pK_d \pm SEM$ of [3H] DTG for pan-sigma binding in FLO-1, OE21 and OE33 was 7.79 ± 0.12 , 7.64 ± 0.15 and 7.72 ± 0.02 . The B_{max} was found to be 1050 ± 100 , 1400 ± 350 and 1100 ± 50 fMol/mg protein. Data were calculated from 3 independent experiments.

3.10 Breast cancer cell lines (MCF7, MDA-MB-468)

Saturation binding experiments were carried out to determine B_{max} and K_d of [3H] DTG for two breast cancer cell lines: MDA-MB-468 and MCF7. Figure 3-18 shows saturation-binding curve for [3H] DTG in membranes prepared by sonicating MCF7 and MDA-MB-468 cell line. B_{max} and K_d were calculated using GraphPad Prism.

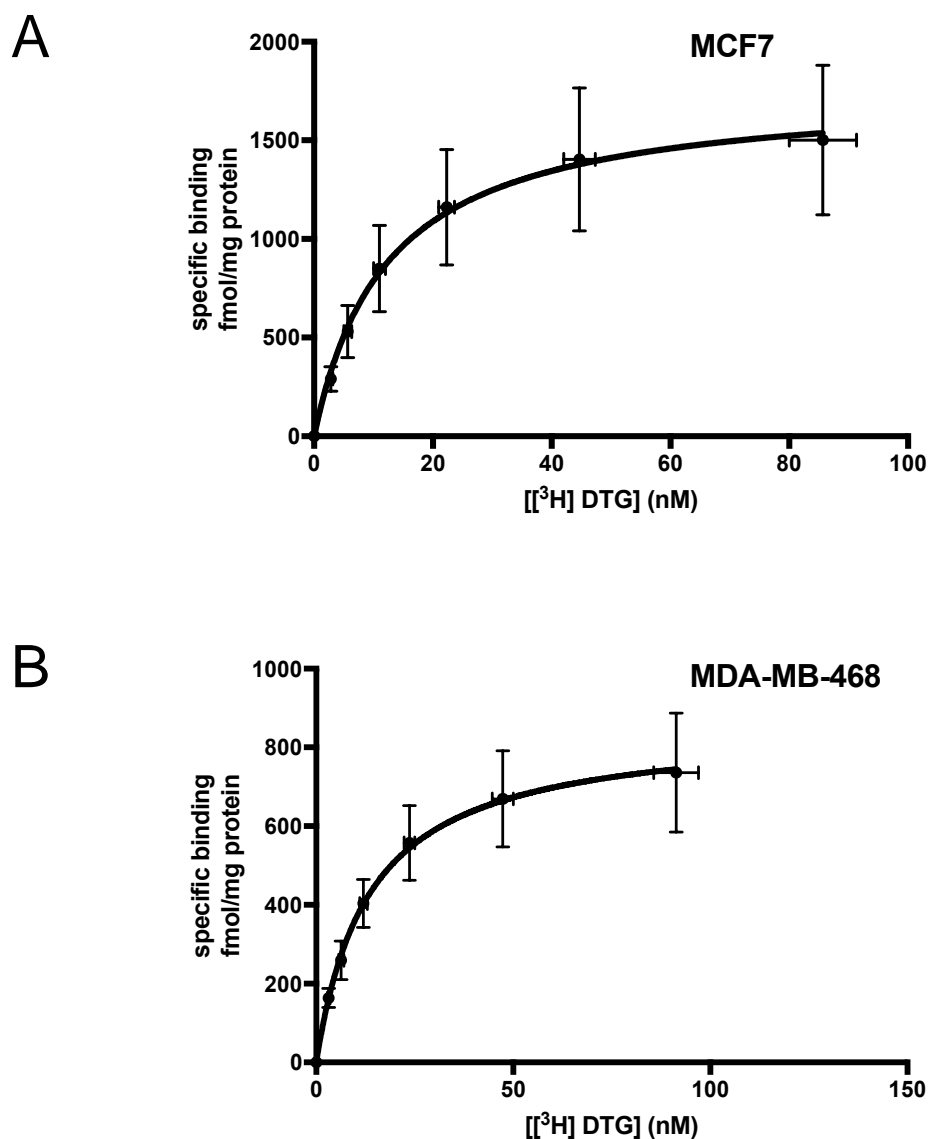


Figure 3-18: Saturation binding of [³H] DTG in breast cancer cell lines (A: MCF7, B: MDA-MB-468)

Saturation binding curve for [³H] DTG in breast cancer cell lines. Non-specific binding was determined in the presence of 1mM haloperidol. Figure represents mean \pm SEM from 3 independent experiments. One-way ANOVA, using the highest concentration of ligand as comparator, shows a strong concentration-dependant increase in ligand binding: A (MCF7) [F(6,14) = 5.32, p = 0.0048]; B (MDA-MB-468) [F(6,14) = 9.71, p = 0.0003].

The mean $pK_d \pm$ SEM of [³H] DTG for pan-sigma binding in MCF7 and MDA-MB-468 was 7.92 ± 0.03 and 7.88 ± 0.01 , respectively. The B_{max} was found to be 2050 ± 100 and 850 ± 200 fMol/mg protein. This is a representative of 3 independent saturation experiments.

3.11 Colorectal cancer cell lines (Caco-2, SW480, HT-29 and HCT 116).

Saturation binding experiments were carried out to determine B_{\max} and K_d of [^3H] DTG for four colorectal cancer cell lines: Caco-2, HCT 116, HT-29 and SW480. Figure 3-19 shows saturation binding curve for [^3H] DTG in membranes prepared by sonicating colorectal cancer cell lines. B_{\max} and K_d were calculated using GraphPad Prism.

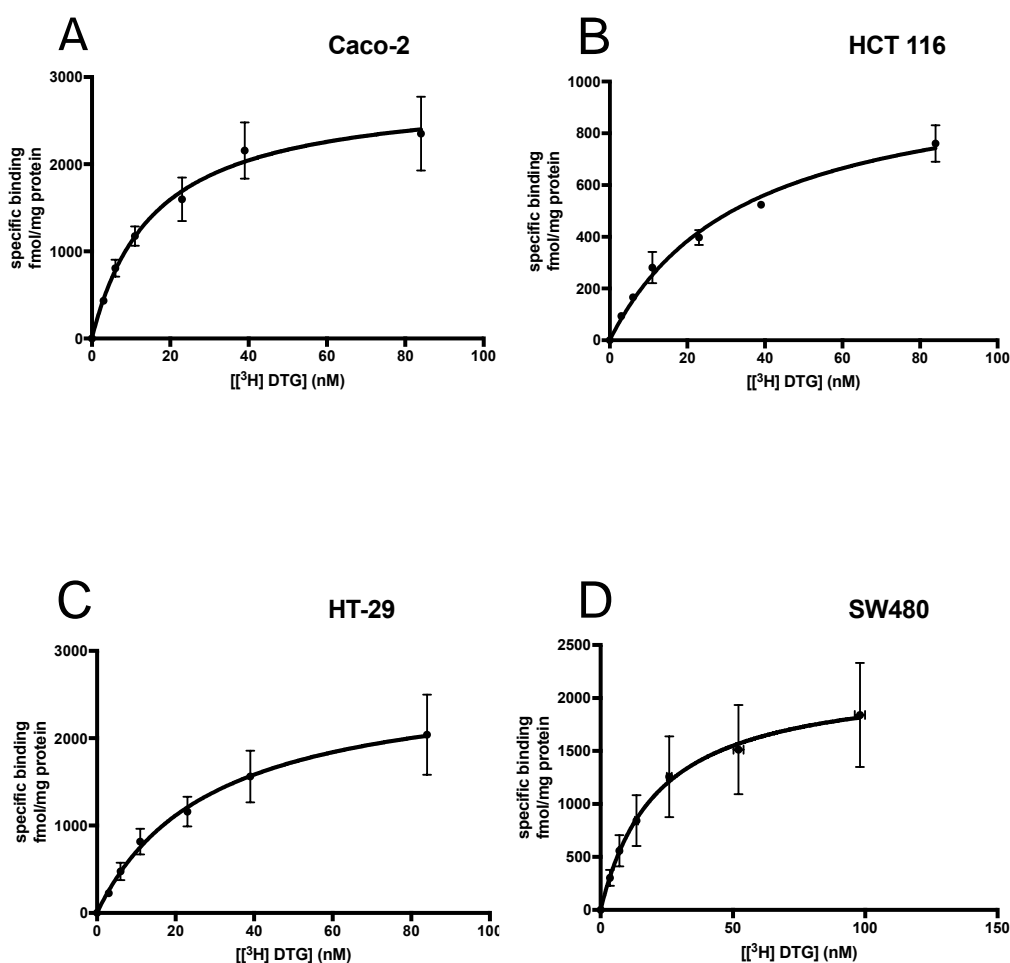


Figure 3-19: Saturation binding of [³H] DTG to colorectal cancer cell lines (A: Caco-2, B: HCT 116, C: HT-29 and D: SW480)

Saturation binding curve for [³H] DTG to membranes prepared from colorectal cancer cell lines. Non-specific binding was determined in the presence of 1mM haloperidol. Figure represents mean \pm SEM from 3 independent experiments. One-way ANOVA, using the highest concentration of ligand as comparator, shows a strong concentration-dependant increase in ligand binding: A (Caco-2) [F(6,14) = 14.4, $p < 0.0001$]; B (HCT 116) [F(6,13) = 49.9, $p < 0.0001$]; C (HT-29) [F(6,14) = 10.5, $p = 0.0002$]; D (SW480) [F(6,28) = 4.8, $p = 0.0018$].

The mean $pK_d \pm$ SEM of [³H] DTG for pan-sigma binding in Caco-2, HCT 116,

HT-29 and SW480 cells was found to be 7.28 ± 0.07 , 7.48 ± 0.05 , 7.55 ± 0.06 and 7.65 ± 0.03 . The B_{max} was determined 2750 ± 450 , 1050 ± 100 , 2750 ± 650 and 1700 ± 100 fMol/mg protein. This is a representative of 3 independent saturation experiments.

3.12 Human embryonic kidney cell line (293)

Saturation binding experiments were carried out to determine B_{\max} and K_d of [^3H] DTG for 293 cells. Figure 3-20 shows saturation binding curve for [^3H] DTG in membranes prepared in membranes prepared by sonicating colorectal cancer cell lines. B_{\max} and K_d were calculated using GraphPad Prism.

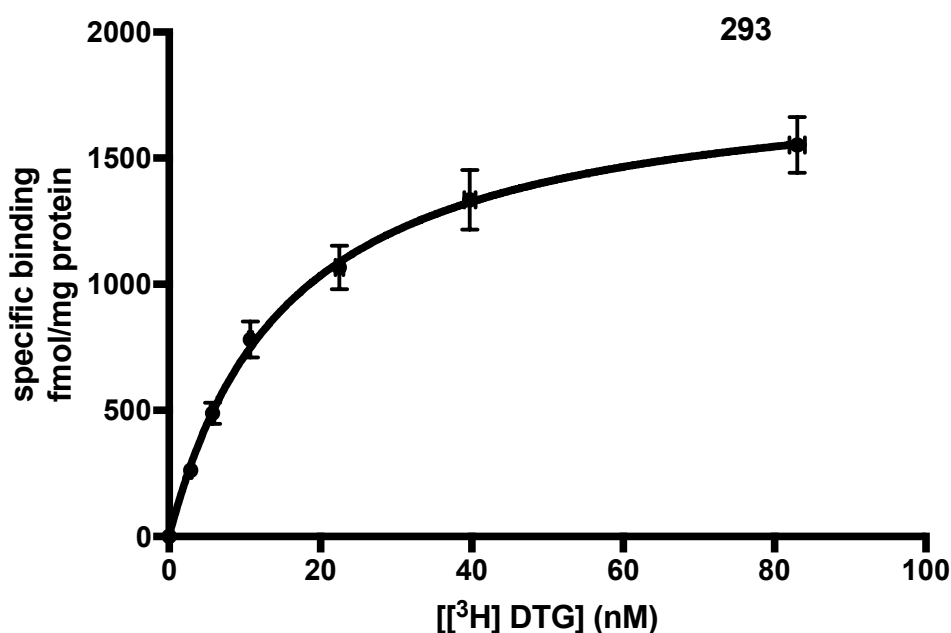


Figure 3-20: Saturation binding of [^3H] DTG to 293 cells

Saturation binding curve for [^3H] DTG to membranes prepared from 293 cells. Non-specific binding was determined in the presence of 1mM haloperidol. Figure represents mean \pm SEM from 3 independent experiments. One-way ANOVA, using the highest concentration of ligand as comparator, shows a strong concentration-dependant increase in ligand binding: [F(6,21) = 55.4, $p < 0.0001$].

The mean $pK_d \pm$ SEM of [^3H] DTG for pan-sigma binding in 293 cells was 7.81 ± 0.05 and the B_{\max} was found to be 1700 ± 100 fMol/mg protein. This is a representative of 3 independent saturation experiments.

3.13 Lung cancer cell line (A549).

Saturation binding experiments were carried out to determine B_{\max} and K_d of [^3H] DTG for A549 cells. Figure 3-21 shows saturation binding curve for [^3H]

DTG in membranes prepared by sonicating colorectal cancer cell lines. B_{\max} and K_d were calculated using GraphPad Prism.

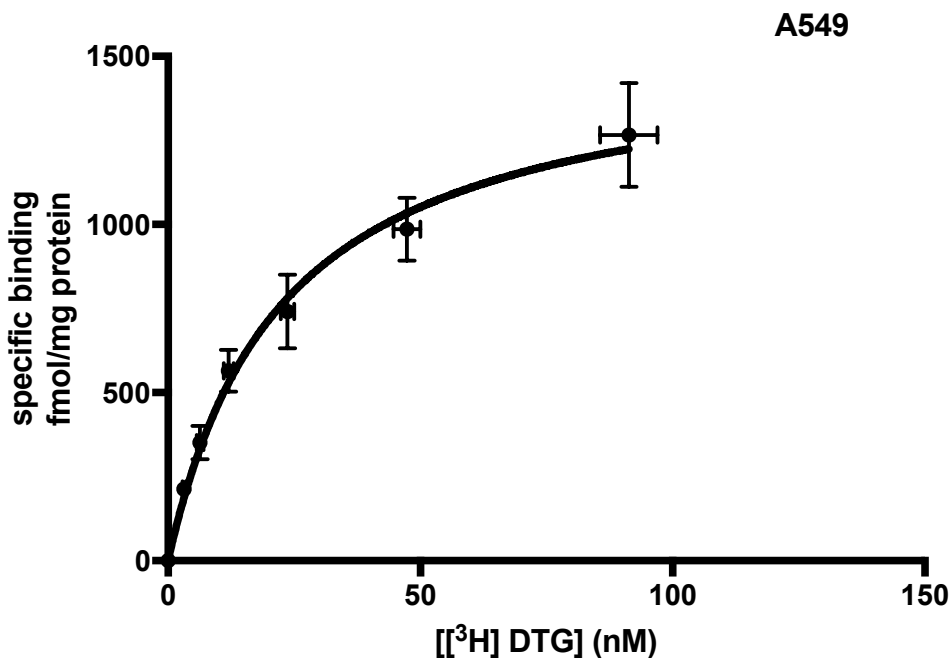


Figure 3-21: Saturation binding of [³H] DTG in A549

Saturation binding curve for [³H] DTG to membranes prepared from A549 cells. Non-specific binding was determined in the presence of 1mM haloperidol. Figure represents mean \pm SEM from 3 independent experiments. One-way ANOVA, using the highest concentration of ligand as comparator, shows a strong concentration-dependant increase in ligand binding: [F(6,14) = 26.8, $p < 0.0001$].

The mean $pK_d \pm$ SEM of [³H] DTG for pan-sigma binding in A549 was 7.64 ± 0.07 . The B_{\max} was found to be 1550 ± 150 fmol/mg protein. Data were calculated from 3 independent saturation experiments.

In order to determine the relative ratio of sigma-1 receptors to sigma-2 binding sites, one should be able to subtract the B_{\max} of (+) pentazocine (sigma-1 receptors) from the DTG binding (pan-sigma ligand, binding to both sigma-1 receptors and sigma-2 binding sites).

Origin	Cell Line	Sigma-1 B_{max} fMol/mg protein	PanSigma-2 B_{max} fMol/mg protein	Calculated sigma-2 B_{max}
Oesophagus	FLO-1	1100	1050	-50
	OE21	2250	1400	-850
	OE33	2400	1100	-1300
Breast	MCF7	No binding	2050	2050
	MDA- MB-468	1700	850	-850
Colorectal	Caco-2	2400	2750	350
	HCT 116	1700	1050	-650
	HT-29	2250	2750	550
	SW480	2250	1700	-550
Human embryonic kidney	293	1600	1700	100
Lung	A549	1300	1550	250

Table 3-7: Calculation of sigma-2 binding site density.

It is clear that (+) pentazocine binding was higher in most cases, indicating this simple calculation was inappropriate. Therefore a second series of experiments were performed to calculate an accurate ratio of sigma-1 to sigma-2 sites.

3.14 Competition binding

In order to calculate sigma-2 binding site density in cancer cell lines from various tissues I carried out competition binding of [³H] DTG and (+) pentazocine in these cell lines.

3.14.1 Oesophageal cancer cell lines

Competition binding experiments were carried out to determine the proportion of sigma-1 receptors to sigma-2 binding sites in three oesophageal cancer cell lines: FLO-1, OE21 and OE33. Figure 3-22 shows competition binding curves in membranes prepared by sonicating oesophageal cancer cell lines.

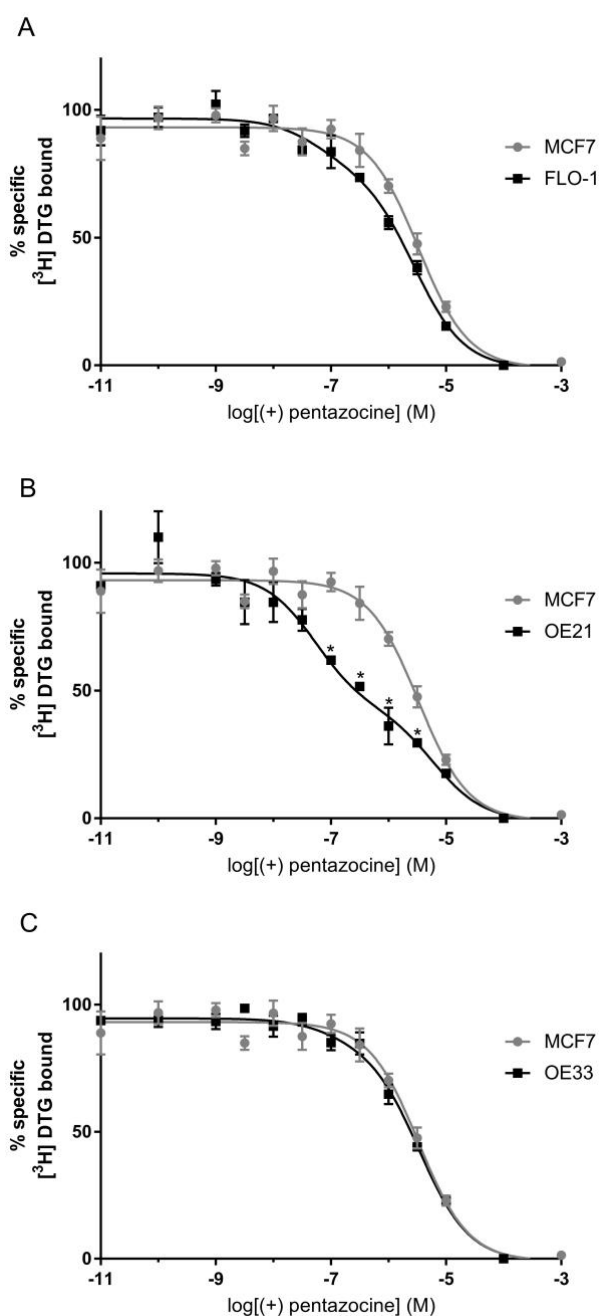


Figure 3-22: Competition binding between [³H] DTG and (+) pentazocine in oesophageal cancer cell lines.

Data represented as percent specific binding of [³H] DTG in presence of increasing concentration of (+) pentazocine. A: FLO-1, B: OE21 and C: OE33 cell lines. Figure represents mean \pm SEM from 3-5 independent experiments. MCF7 data are shown to highlight the binding profile of a pure sigma-2 population. Two-way ANOVA, comparing the effects of cell line and concentration of (+) pentazocine (between 10nM and 10 μ M), was performed. All 10 cell lines were compared pair-wise with MCF7 cells only. The concentration of (+) pentazocine had a major effect [$F(6,207) = 655, p < 0.0001$],

contributing to 84% of the variation; cell type also had an effect [$F(10, 207) = 35.1, p < 0.0001$]. * signifies data point significantly different to MCF7 results at that data point.

The percentage of sigma-1 binding sites in FLO-1, OE21 and OE33 was found to be 29, 49 and 12%, respectively and sigma-2 binding sites was found to contribute 71, 51 and 88%.

3.14.2 Breast cancer cell lines

Competition binding experiments were carried out to determine the proportion of sigma-1 receptors to sigma-2 binding sites in two breast cancer cell lines: MCF7 and MDA-MB-468. Figure 3-23 shows competition binding curves in membranes prepared by sonicating breast cancer cell lines.

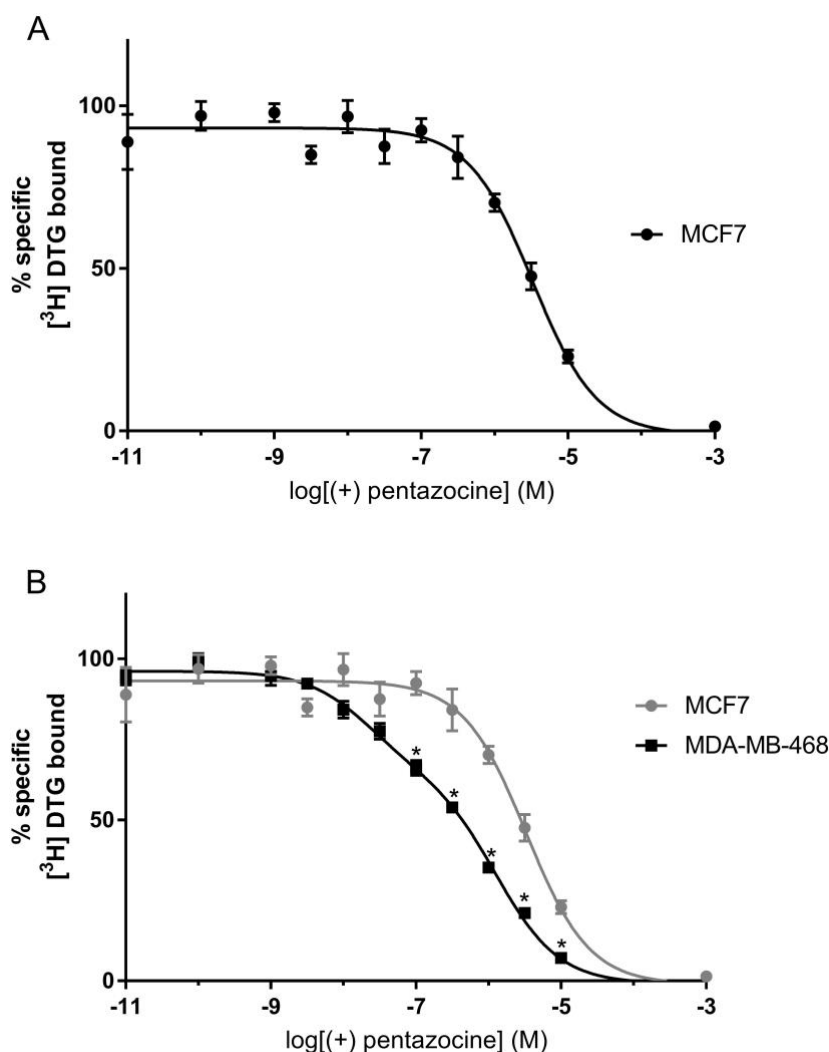


Figure 3-23: Competition binding between [3H] DTG and (+) pentazocine in breast cancer cell lines.

Data represented as percent specific binding of [3H] DTG in presence of increasing concentration of (+) pentazocine A: MCF7, B: MDA-MDA-468 cell lines. Figure represents mean \pm SEM from 3-5 independent experiments. MCF7 data are shown to highlight the binding profile of a pure sigma-2 population. Two-way ANOVA, comparing the effects of cell line and concentration of (+) pentazocine (between 10nM and 10 μ M), was performed. All 10 cell lines were compared pair-wise with MCF7 cells only. The concentration of (+) pentazocine had a major effect [$F(6,207) = 655$, $p < 0.0001$], contributing to 84% of the variation; cell type also had an effect [$F(10, 207) = 35.1$, $p < 0.0001$]. * signifies data point significantly different to MCF7 results at that data point.

The percentage of sigma-1 binding sites for MDA-MB-468 cells was found to be 36% and sigma-2 was 64%. There was no sigma-1 expression in the case of MCF7 cells.

3.14.3 Colorectal cancer cell line

Competition binding experiments were carried out to determine the proportion of sigma-1 receptors to sigma-2 binding sites in four colorectal cancer cell lines: Caco-2, HCT 116, HT-29 and SW480 cells. Figure 3-24 shows competition binding curves in membranes prepared by sonicating colorectal cancer cell lines.

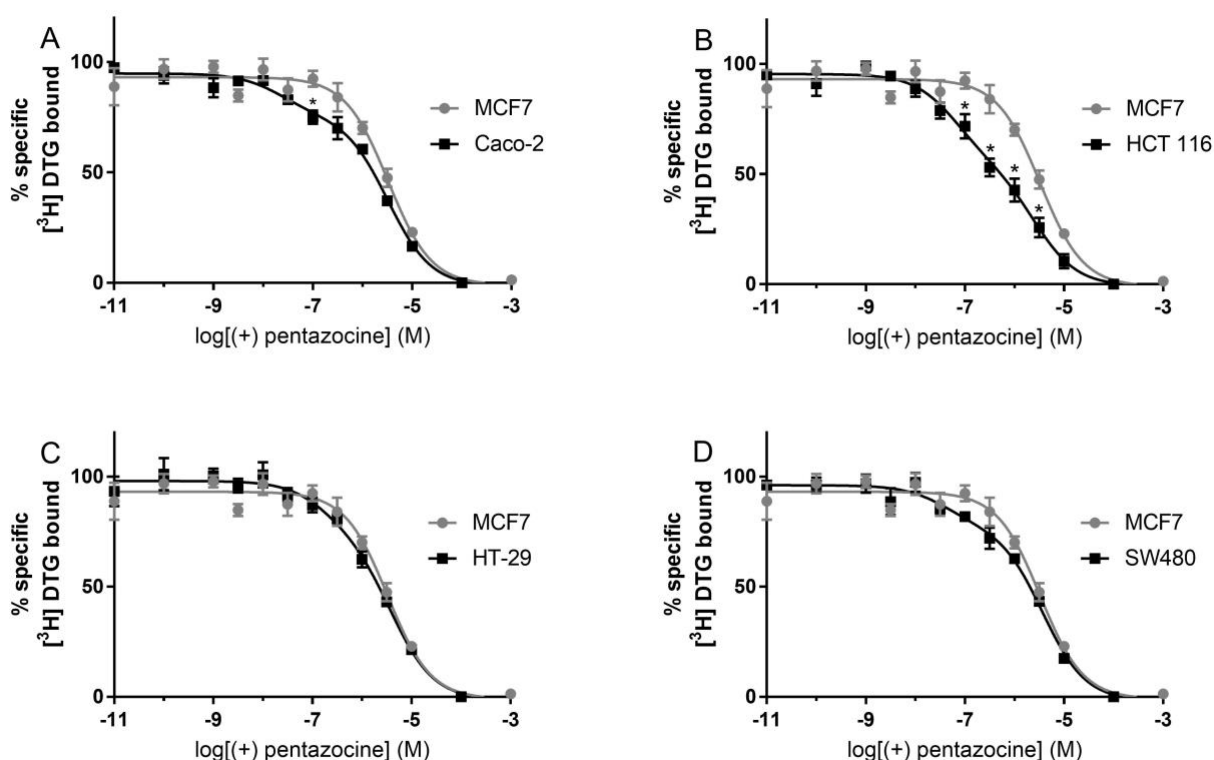


Figure 3-24: Competition binding between (+) pentazocine and [³H] DTG in colorectal cancer cell lines.

Data represented as percent specific binding of [³H] DTG in presence of increasing concentration of (+) pentazocine A: Caco-2, B: HCT 116 C: HT-29 and D: SW480 cell lines. Figure represents mean \pm SEM from 3-5 independent experiments. MCF7 data are shown to highlight the binding profile of a pure sigma-2 population. Two-way ANOVA, comparing the effects of cell line and concentration of (+) pentazocine (between 10nM and 10 μ M), was performed. All 10 cell lines were compared pair-wise with MCF7 cells only. The concentration of (+) pentazocine had a major effect [$F(6,207) = 655, p < 0.0001$], contributing to 84% of the variation; cell type also had an effect [$F(10, 207) = 35.1, p < 0.0001$]. * signifies data point significantly different to MCF7 results at that data point

The percentage of sigma-1 binding sites in Caco-2, HCT 116, HT-29 and SW480 was found to be 20, 40, 23 and 19%, respectively. Sigma-2 binding sites contributed 80, 60, 77 and 81%, respectively.

3.14.4 Human embryonic kidney (293) and lung cancer (A549) cell lines.

Competition binding experiments were carried out to determine the proportion of sigma-1 receptors to sigma-2 binding sites in human embryonic kidney and lung cancer cell lines: 293 and A549 cells. Figure 3-25 shows competition binding curves in membranes prepared by sonicating 293 and A549 cell lines.

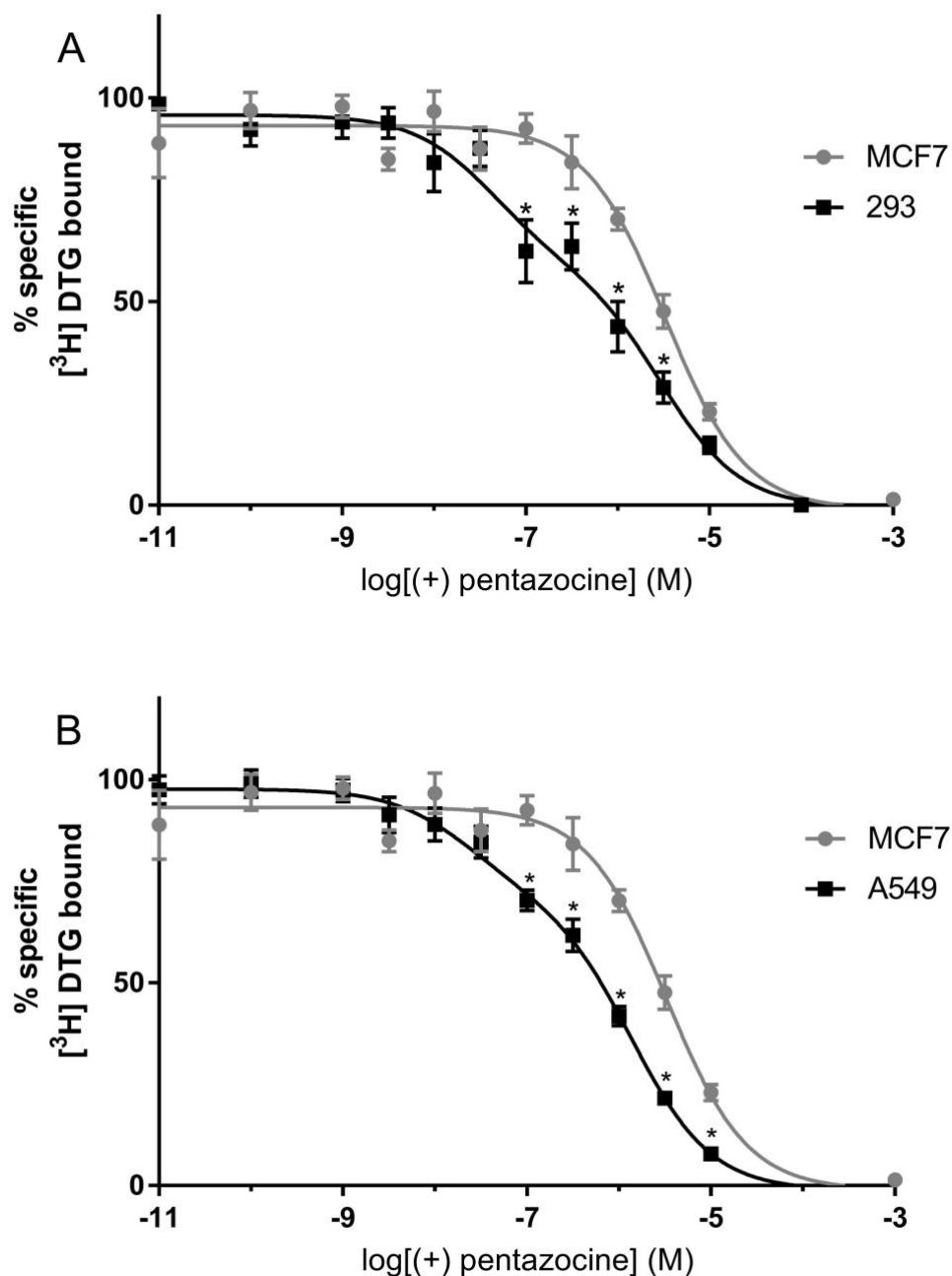


Figure 3-25: Competition binding of (+) pentazocine and [³H] DTG in human embryonic and lung cancer cell lines.

Data represented as percent specific binding of DTG in presence of increasing concentration of (+) pentazocine. A: 293, B: A549 cell lines. Figure represents mean \pm SEM from 3 independent experiments. MCF7 data are shown to highlight the binding profile of a pure sigma-2 population. Two-way ANOVA, comparing the effects of cell line and concentration of (+) pentazocine (between 10nM and 10 μ M), was performed. All 10 cell lines were compared pair-wise with MCF7 cells only. The concentration of (+) pentazocine had a major effect [$F(6,207) = 655, p < 0.0001$], contributing to 84% of the variation; cell type also

had an effect [$F(10, 207) = 35.1, p < 0.0001$]. * signifies data point significantly different to MCF7 results at that data point.

The percentage of sigma-1 sites in 293 and A549 was found to be 40 and 29%, respectively. Sigma-2 binding sites contributed 60 and 71%, respectively.

Figure 3-26 shows a summary of the relative ratio of sigma-1 receptors in all of the cancer cell lines tested.

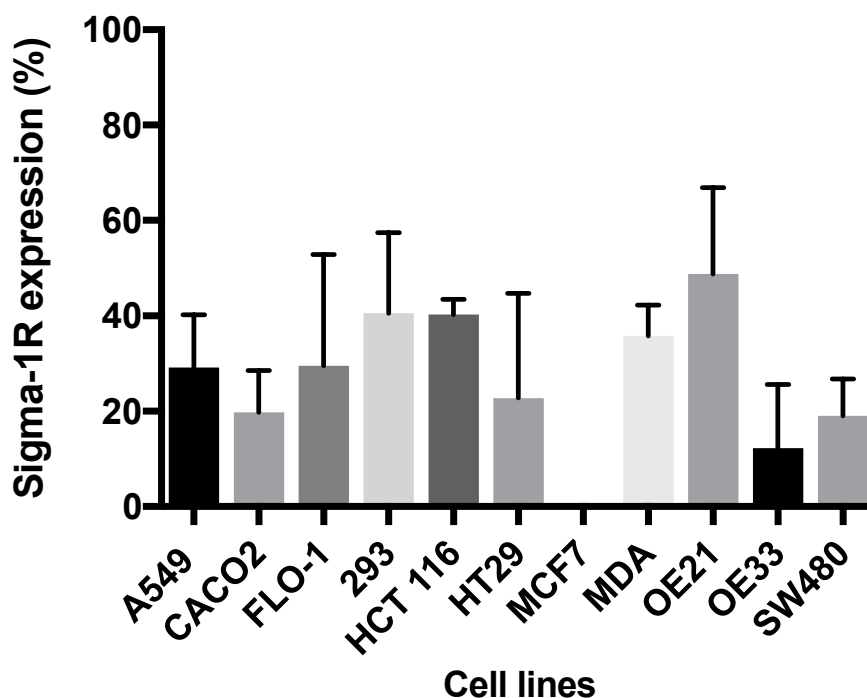


Figure 3-26: Summary of the relative ratio of sigma-1 and sigma-2 binding sites in a range of cells.

The graph shows the contribution of sigma-1 receptors as a percentage of all sigma binding sites, as determined by competition binding assays. Data represents mean \pm SEM from 3-5 independent experiments. Unpaired 1-way ANOVA, followed by *post hoc* Tukey (“all means”) comparison, with p value adjusted for multiple comparisons, shows a significant difference in % sigma-1 receptor expression values: [$F(10,32) = 5.47, p = 0.0001$]. MCF7 cells express a significantly lower % sigma-1 receptors than: 293 cells ($p = 0.015$); HCT 116 cells ($p = 0.0022$); MDA-MB-468 cells ($p = 0.031$); and OE21 cells ($p = 0.0005$). OE33 cells express a significantly lower % sigma-1 receptors than: OE21 cells ($p = 0.0027$); and HCT 116 cells ($p = 0.0141$). OE21 cells express a significantly higher % sigma-1 receptors than: Caco-2 cells ($p = 0.040$); FLO-1 cells ($p = 0.0313$); and SW480 cells ($p = 0.0428$). All other comparisons show no significant difference.

Concentration of sigma-2 binding site was determined by subtracting sigma-1 receptor density from pan-sigma binding site density as show in table 3-14 below.

Origin	Cell Line	DTG B _{max} fMol/mg protein	Sigma-1 binding site %	Sigma-1 receptor fMol/mg protein	Sigma-2 binding site %	Sigma-2 binding site fMol/mg protein
Oesophagus	FLO-1	1050	29	305	71	745
	OE21	1400	49	685	51	715
	OE33	1100	12	130	88	970
Breast	MCF7	2050	0	0	100	2050
	MDA- MB-468	850	36	305	64	545
Colorectal	Caco-2	2750	20	550	80	2200
	HCT 116	1050	40	420	60	630
	HT-29	2750	23	630	77	2120
	SW480	1700	19	325	81	1375
Human embryonic kidney	293	1700	40	680	60	1020
Lung	A549	1550	29	450	71	1100

Table 3-8: Calculation of sigma-1 and sigma-2 binding sites based on competition binding assay.

3.15 Discussion

In this chapter, it was shown that tumour cell lines from various tissues express both sigma-1 receptors and sigma-2 binding sites. Most cell lines express both sigma-1 receptors and sigma-2 binding sites. This finding is consistent with previous studies done to quantify these receptors in various tumour cell lines. MCF7 cell lines only expressed sigma-2 binding sites and failed to show any specific binding to [³H] (+) pentazocine, which is again consistent with previous findings (Vilner et al., 1995b).

These calculations now bring into question the previously accepted method of calculating sigma-2 levels in cell lines (DTG in the presence of pentazocine or dextrallorphan). These calculations show clearly that the number of sigma-2 binding sites have been greatly overestimated in nearly all previous publications in this field, as its likely that, if present, sigma-1 receptors will have also been bound by radioligand. Only time will tell if these findings can be published and whether fellow experimenters in the field will take heed.

In order to address this failing, an alternative approach was taken. Sigma-1 B_{max} ((+) pentazocine) and pan-sigma levels (DTG) were determined to calculate sigma-1 and sigma-2 levels. This calculation has led to several cell lines having negative levels of sigma-2 sites, as the B_{max} from DTG binding was lower than that of (+) pentazocine levels. Other groups have performed sigma-2 binding assays using increasing DTG concentrations in the presence of (+) pentazocine or dextrallorphan. This method can skew data, as (+) pentazocine and dextrallorphan have appreciable affinities for sigma-2 sites. While the concentrations of these ligands would not appreciably compete with high concentrations of DTG for the sigma-2 site, calculations show that they would also impact on the [³H] DTG binding at low concentrations.

This is not the only error caused by such an approach. Radioligand binding is one of the few assays performed where concentrations of materials are

determined solely by either counting the amount of radiochemical present or measuring the volume of liquid removed. Radioligands are prepared and shipped with specific activity values provided. Should these be erroneous or subject to chemical breakdown of the radioligand, permitting radioactive material to be present which is not the ligand will lead to incorrect values being determined. Tritium exchange is common with some chemicals, where the radioactive component of the ligand exchanges protons with some other material, including water. This would permit tritiated water to contribute to the radioactive signal without contributing to the binding.

Secondly, whilst quality control of manufacture is not in question with commercial suppliers of radioligands, many ligands are provided in volatile solvents. Removal of a fixed amount of liquid from a “fresh” bottle may contain much less radioligand than after several months’ storage and use when a bottle has been opened many times and solvent evaporation can be significant from a small initial volume.

It was not found necessary to compare the density of sigma-1 and sigma-2 binding sites – they do appear, after all, to be very different proteins. However, the scientific field has grouped these targets together and frequently performs such comparisons. This is seen in countless publications. The currently favoured method appears flawed. Initial attempts to use an alternative protocol ((+) pentazocine B_{max} for sigma-1 receptors and DTG B_{max} for all sigma receptors followed by simple arithmetic) failed.

At this point, it was considered whether the presence of sigma-2 sites in (+) pentazocine quantification of sigma-1 receptors was also a problem.

In “worst case” scenario, where the affinity of pentazocine for the sigma-2 binding site is 728nM, approximately 12.2% of the sigma-2 sites are occupied at a concentration of 100nM. There is no need to consider the higher

concentration (1 μ M), as this would not be used when performing saturation binding analyses.

Binding assays with [3 H] (+) pentazocine used up to 128nM, at which concentration 15.1% of the sigma-2 binding sites would be occupied.

Could this explain why the (+) pentazocine saturation data overestimate sigma-1 receptor number? During the masking protocol, the lifespans of the ligand-protein complex for unlabelled (+) pentazocine and dextralorphan are unimportant, as it is their effects under equilibrium that one is interested in. The proportion of sites occupied is all that matters. In such binding assays, the lifespan of the radioligand-target is important, as, at the end of the assay bound is separated from free by rapid washing and filtering. As the equilibrium constant K_d equals K_{off}/K_{on} (the K_{off} rate, or dissociation rate divided by K_{on} , the association rate) there is a direct relationship between K_d and K_{off} . I do not have and cannot calculate the K_{on} for (+) pentazocine to both the sigma-1 receptor and sigma-2 site; I will assume, for the sake of this discussion, they are similar. K_{off} for sigma-2 would then be 728/17 of that for sigma-1 receptor (relative K_d values). The dissociation rate for pentazocine for the sigma-2 site would be 43 times faster than for the sigma-1 site.

Association rate constants (K_{on}) are commonly in the range of 10^5 - 10^6 $M^{-1} \cdot s^{-1}$. Using these values to plot the dissociation rate, expressed as $t_{1/2}$ (half time = $\ln(2)/K_{off}$), one can see that as K_d increases, the half-life decreases (Figure 3-27)

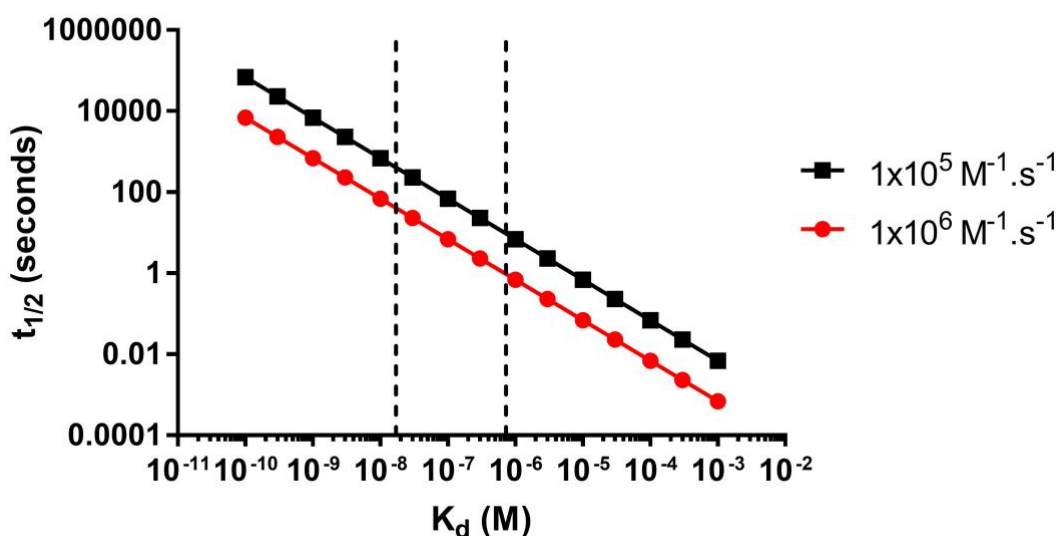


Figure 3-27: Relationship between K_d and off rate.

Figure showing relationship between K_d and half time of dissociation. Plots are presented for K_{on} of 10^5 and $10^6 \text{ M}^{-1} \cdot \text{s}^{-1}$. Dotted lines represent the highest affinity of (+) pentazocine for the sigma-2 binding site (728nM) and the lowest affinity of (+) pentazocine for the sigma-1 receptor (17nM). The graph is plotted using a log scale, but values are presented in standard format to aid comprehension.

From the above graph, we can see that for (+) pentazocine binding to the sigma-1 receptor the half-life of dissociation is between 41 and 408 seconds, using K_{on} of 10^6 and $10^5 \text{ M}^{-1} \cdot \text{s}^{-1}$, respectively. Taking the smallest value would mean that after 41 seconds half of the (+) pentazocine would have dissociated from the receptor. For (+) pentazocine binding to the sigma-2 binding site the half-life of dissociation is between 0.95 and 9.5 seconds, using K_{on} of 10^6 and $10^5 \text{ M}^{-1} \cdot \text{s}^{-1}$, respectively. Typically, binding assay wash protocols are complete in under 5 seconds.

In such a scenario, the dissociation from the sigma-1 receptor would be negligible whereas that to the sigma-2 would be either complete ($t_{1/2}$ 0.95 s) or significant ($t_{1/2}$ 9.5 s). As there was no evidence of pentazocine binding to MCF7 cells which have no sigma-1 receptors yet an abundance of sigma-2 binding sites, it would appear that, whilst one should consider the possibility,

[³H] (+) pentazocine binding to sigma-2 sites does not appear to cause an artefactual signal.

Using solely [³H] DTG to obtain a pan-sigma B_{max} and (+) pentazocine competition to obtain a ratio of sigma-1 to sigma-2 sites is the best approach if direct comparisons are needed. Computer assisted data analysis (e.g. GraphPad Prism, as used here) is sufficiently developed to determine the presence of relatively small proportions of one receptor or the other. By using the protocol used here, we can be confident that a direct ratio is well defined and reliable.

The presence of sigma-2 binding sites in all tumour cell lines considered here and other publications (van Waarde et al., 2010, Vilner et al., 1995b) (although see the caveat above), and its higher levels than in non-cancer cells does suggest it is a useful target both for tumour imaging as well as possible targeted therapy against such tumours. Till date no one has been able to find a cell line which does not possess sigma-2 binding sites and it is overcome by the use of the sigma-1–specific ligand (+) pentazocine which can be used to selectively bind sigma-1 receptors at the concentrations used in radioligand binding competition assays.

It has been confirmed and verified that MCF7 cells do not express sigma-1 receptors and these cells remain the only cells routinely used which lack sigma-1 receptors allows their use in drug discovery to search out sigma-2 binding site ligands in the absence of interference from sigma-1 receptor binding. The use of (+) pentazocine in cells containing sigma-1 receptors and DTG in cells lacking sigma-1 receptors now allows me to use these protocols in considering the affinities of a range of potential ligands at these two sites. Furthermore, it was possible to determine the effects of sigma-2 ligands on the biology of cells without the interference of sigma-1 receptors. This will be the target of the following two chapters: MCF7 cells will be used to determine the affinity and cytotoxicity of a range of novel compounds identified as having a graded affinity

and range of effects on cells through sigma-1 receptors; these will be compared with established ligands known to have effects through the sigma-2 binding site. A549 and MDA-MB-468 cell lines were also used since they contain both sigma-1 receptors and sigma-2 binding sites in order to determine whether the effects through these two proteins can be determined as being additive, synergistic or antagonistic towards each other.

One further problem does arise: Direct comparison of [³H] (+) pentazocine binding and the calculated number of sigma-1 receptors from [³H] DTG competition binding assays do not correlate well (Table 3-9).

Origin	Cell Line	Determined B _{max} fMol/mg protein	Calculated B _{max} Sigma-1 receptor, fMol/mg protein
Oesophagus	FLO-1	1100	305
	OE21	2250	685
	OE33	2400	130
Breast	MCF7	0	0
	MDA-MB-468	1700	305
Colorectal	Caco-2	2400	550
	HCT 116	1700	420
	HT-29	2250	630
	SW480	2250	325
Human embryonic kidney	293	1600	680
Lung	A549	1300	450

Table 3-9: Calculation of sigma-1 and sigma-2 binding sites based on competition binding assay.

Table showing the experimentally derived B_{max} of sigma-1 receptors in a range of cancer cell lines from [³H] (+) pentazocine saturation binding assays alongside the calculated B_{max} from [³H] DTG saturation and (+) pentazocine competition assays.

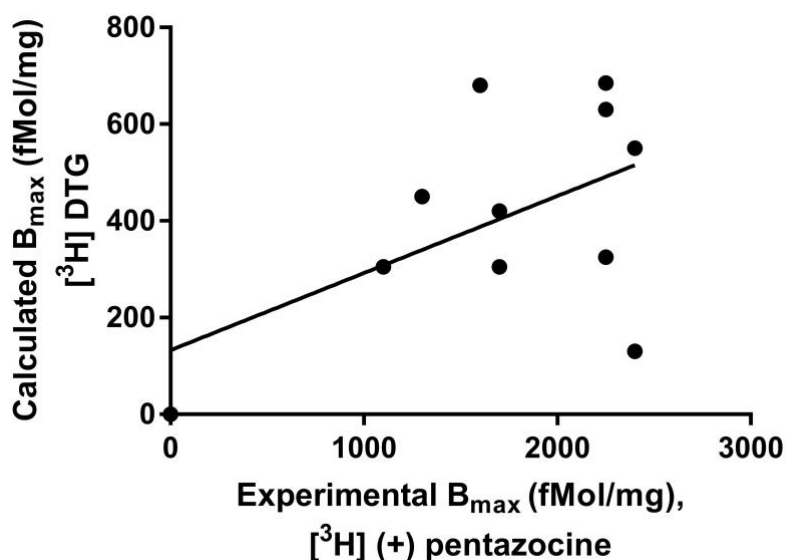


Figure 3-28: Comparison of sigma-1 B_{max} calculated by two methods.

Figure comparing experimentally derived B_{max} of sigma-1 receptors in a range of cancer cell lines from [3H] (+) pentazocine saturation binding assays alongside the calculated B_{max} from [3H] DTG saturation and (+) pentazocine competition assays. Linear regression shows the line $y = 0.1594x + 132.6$, $R^2 = 0.27$ [$F(1,9) = 3.38$, $p = 0.099$].

From the above table and figure, it is clear that there are other issues, which require resolving. There is little correlation between sigma-1 receptor densities calculated by the two methods. This would suggest that, while [3H] DTG competition with (+) pentazocine is a good method for calculating relative proportions of sigma-1 receptors to sigma-2 binding sites, the two-step nature of calculating a B_{max} indirectly may introduce additional errors. Comparing my internal data, with pK_d [3H] DTG (this chapter) 7.92 and K_i DTG (Chapter 4) 8.0 (both determined using MCF7 cells) would suggest that the [3H] DTG used in my studies is comparable in affinity to the unlabeled DTG and has neither degraded nor contains significant levels of contaminants.

However, the affinity of [3H] (+) pentazocine for the sigma-1 receptor in this study (pK_d 7.15 – 7.78, this chapter) is also similar to that previously found in several previous studies (Brimson et al., 2011, Spruce et al., 2004), and the affinity of (+) pentazocine for the sigma-2 binding site (355nM, Chapter 4) is higher than previously described (Vilner and Bowen, 2000, Xu et al., 2015).

This suggests that all reagents used are active and performing as should be expected. An alternative suggestion could be that [³H] (+) pentazocine is binding sites not recognised by [³H] DTG. By removing one artefact have I introduced another?

**Chapter 4. AFFINITY OF AMMONIUM SALTS AND
SIGMA-2 LIGANDS TO THE SIGMA-2 BINDING SITE.**

4.1 Background

Sigma receptors were initially described in 1976 as a subtype of opioid receptors based on the effects produced by SKF 10047 which could not be attributed to μ (morphine), κ (ketocyclazocin), or δ receptors (Martin *et al.*, 1976) and hence called it sigma opioid receptor. In 1982 Su, whilst working with [^3H] SKF 10047, managed to characterise a protein with nanomolar affinity (Su, 1982). This protein was different from the sigma opioid receptor identified by Martin *et al.*, in 1976, as it had no affinity for naloxone, an opioid antagonist and showed stereoselectivity for dextrorotatory benzomorphans, which is opposite to other opioid receptors. Su proposed that it was a distinct class of receptor, different from other opioid receptors and called it the sigma binding site (Su, 1982).

Classification of sigma receptors led to research and synthesis of compounds and they were screened for binding affinities for sigma-1 and sigma-2 binding sites. Initially many piperazine, piperidine dialkylamine and trialkylamine derivative were synthesized and shown to bind with high affinity to sigma-1 and sigma-2 binding sites (Berardi *et al.*, 2009, Huang *et al.*, 1998, Huang *et al.*, 2001a, Narayanan *et al.*, 2011, Newman *et al.*, 2001). With subsequent improvement in binding assays, more selective ligands towards both subtypes of sigma binding sites became available. Sigma-2 binding site ligands can be classified in four classes based on their structure (Huang *et al.*, 2014).

1. 6,7-dimethoxytetrahydroisoquinoline derivatives,
2. Tropane related bicyclic structures,
3. Siramesine related indole derivatives and
4. Cyclohexylpiperazine analogues.

There is also a small group of ligands, which are structurally not related to any of the four classes.

Despite extensive research and development of high affinity sigma-2 binding site ligands, the pharmacophore model for sigma-2 binding site is still not available. One of the main reasons for not having a pharmacophore is probably because the sigma-2 binding site is not cloned and also the fact that there is diverse range of molecules that bind to sigma-2 binding site. There are several binding models available for the sigma-2 binding site, each based on a limited number of sigma-2 ligands. One of the models is proposed by Glennon (Glennon, 2005), based on his work with piperidines, piperazine, long chain dialkylamines and long chain trialkylamines. According to this model, for a ligand to fit sigma-2 binding site binding pocket, compounds should possess an amine site and two hydrophobic sites. One of the hydrophobic site being phenyl group and five carbon units away from the amine and the other hydrophobic site four carbon units away from amine site as shown in Figure 4-1.

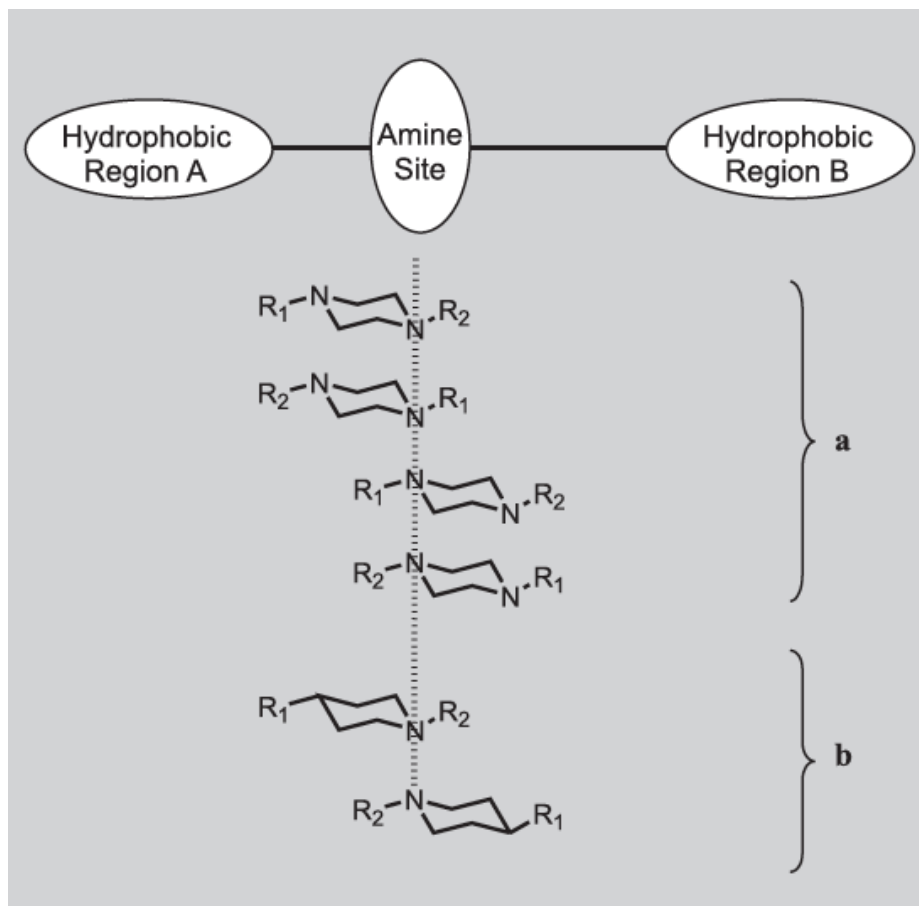


Figure 4-1: Hypothetical sigma-2 binding site pharmacophore.

The sigma-2 binding site pocket consists of an amine binding site and two hydrophobic sites. Hydrophobic region A is situated at a distance of four carbon atoms whereas hydrophobic region B seems to accommodate a phenyl group at a distance of five carbon atom away from amine (Glennon 2005).

It has been previously suggested that ligands with phenylpropylamine-based structures are more likely to result in high-affinity sigma-2 selective ligands (Maeda et al., 2002). However, molecules based on simple ammonium salts have not been investigated as yet. The purpose of this section of my thesis was to investigate the affinity of ammonium salts and to compare it with commercially available sigma-2 ligands. The ammonium salts differ from commonly used sigma-2 ligands, which often contains more than one nitrogen and have complex aromatic ring structures. I have used MCF7 cells as they have been identified to only have sigma-2 binding sites and lack sigma-1

receptors (Vilner et al., 1995b). Since sigma-1 and sigma-2 are different proteins, using MCF7 cells would exclude the effects of sigma-1 receptors.

4.2 Saturation [³H] DTG binding in MCF7 cells

Saturation binding experiments were carried out to determine B_{max} and K_d of [³H] DTG for breast cancer cell line MCF7. Figure 4-2 shows saturation-binding curve for [³H] DTG in membranes prepared by sonicating MCF7 cell line. B_{max} and K_d were calculated using nonlinear regression software (GraphPad Prism, California).

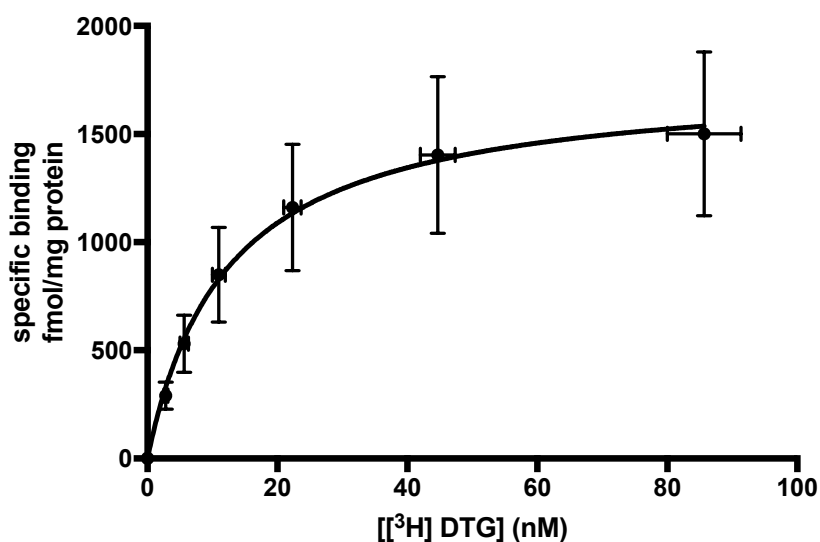


Figure 4-2: Saturation binding of [³H] DTG in MCF7 cells

The mean $pK_d \pm SEM$ of [³H] DTG for the sigma-2 binding site in MCF7 cells was 7.92 ± 0.03 and the B_{max} was found to be 2050 ± 100 fMol/mg protein. Non-specific binding was determined in the presence of 1mM haloperidol. Figure represents mean \pm SEM from 3 independent experiments. One-way ANOVA, using the highest concentration of ligand as comparator, shows a strong concentration-dependant increase in ligand binding [$F(6,14) = 5.32$, $p = 0.0048$]. Data previously shown in Figure 3-18.

4.3 Simple straight chain ammonium salts

The primary ammonium salt consists of single nitrogen and a single carbon chain. There have been a number of previous studies looking at structural relationship between sigma receptor ligands and their affinity to sigma receptors (Ablordeppey et al., 2000, Glennon et al., 1991c). The importance of nitrogen atom for sigma receptors ligands has been shown for the phenylalkylpiperidines and phenylalkylpiperzines (Ablordeppey et al., 2000), however no one has looked at simple molecules as the ammonium salts discussed in this chapter.

4.4 Primary ammonium salt affinity for the sigma-2 binding site

The primary ammonium salts consist of a single carbon and a single carbon chain. The affinity of primary ammonium salts for sigma-2 binding site was calculated using radioligand binding. In order to visualise the affinities for the sigma-2 binding site more clearly with symmetrical errors, the K_i values obtained from the competition binding curves were converted into pK_i values ($-\log_{10}K_i$) shown in Figure 4-3.

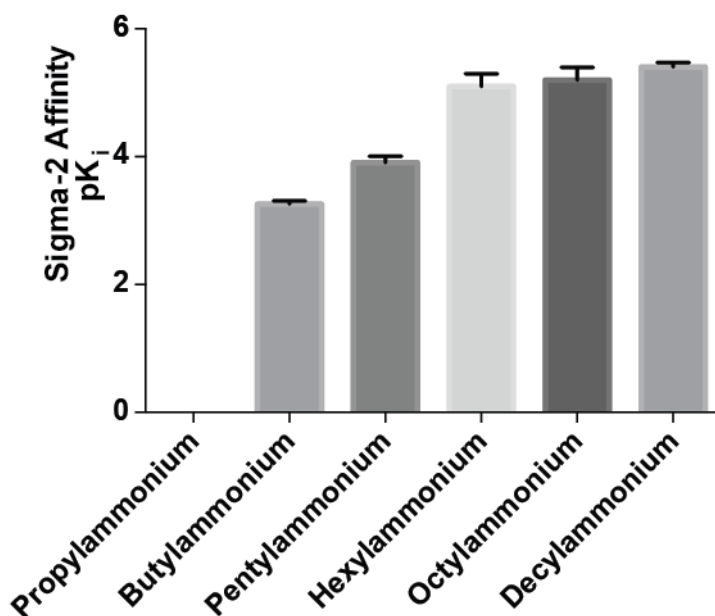


Figure 4-3 Summary of primary ammonium salt binding to the sigma-2 binding site.

The affinities of the primary ammonium salts for the sigma-2 binding site (pK_i ± SEM) were: butylammonium 3.26 ± 0.05; pentylammonium 3.9 ± 0.1; hexylammonium 5.1 ± 0.2; octylammonium 5.2 ± 0.2 and decylammonium 5.2 ± 0.2. Error bars represent SEM from 3-5 independent experiments. Unpaired 1-way ANOVA, followed by *post hoc* Tukey (“all means”) comparison, with p value adjusted for multiple comparisons, shows a significant difference in affinities [F(4,15) = 45.5, p < 0.0001]. Propylammonium is excluded from statistical analysis, as I was unable to obtain a value, due to low affinity. Butylammonium has significantly lower affinity than all others (p ≤ 0.038). Pentylammonium has significantly lower affinity than the remaining ammonium salts (p ≤ 0.0002). The affinities of hexylammonium, octylammonium and decylammonium are not significantly different from each other.

Of the primary amines tested, all except propylammonium were found to bind to sigma-2 binding sites. A trend was observed between carbon chain length and affinity for sigma-2 binding site. There was a slight increase in affinity for the sigma-2 binding site in the primary ammonium salts as the carbon chain length increases from 4 to 6, peaking at pK_i 5.1 for hexylammonium. Since the affinity did not increase any further with increase in carbon chain length I did not investigate primary ammonium salts beyond decylammonium.

4.5 Secondary ammonium salt affinity for the sigma-2 binding site

The secondary ammonium salts consist of single nitrogen and two carbon chains. Dimethylammonium has been shown to interfere with cell growth and has a toxic effect on tumour cells (Guest and Varma, 1991). The mechanism by which dimethylammonium causes these effects has not been investigated. The affinity of secondary ammonium salts to sigma-2 binding site was determined by radiolabelled competition binding assay. In order to visualize the affinities for sigma-2 binding site more clearly, K_i values obtained from competition binding curves were converted into pK_i values. The pK_i values (\pm SEM) are shown in Figure 4-4.

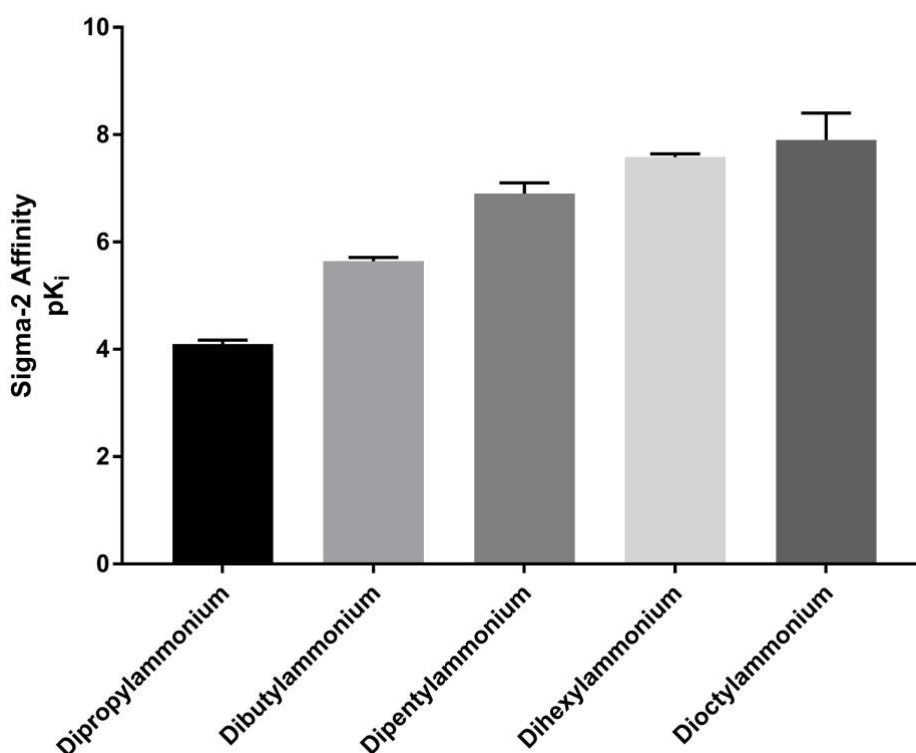


Figure 4-4: Summary of Secondary ammonium salt binding to the sigma-2 binding site

The affinities of the secondary ammonium salts for the sigma-2 binding site (pK_i ± SEM) were: dipropylammonium 4.10 ± 0.07; dibutylammonium 5.64 ± 0.07; dipentylammonium 6.9 ± 0.2; dihexylammonium 7.58 ± 0.06 and dioctylammonium 7.9 ± 0.5. Error bars represent SEM from 3-5 independent experiments. Unpaired 1-way ANOVA, followed by *post hoc* Tukey (“all means”) comparison, with p value adjusted for multiple comparisons, shows a significant difference in affinities [F(4,15) = 40.2, p < 0.0001]. Dipropylammonium has significantly lower affinity than all others (p < 0.004). Dibutylammonium has significantly lower affinity than the remaining ammonium salts (p < 0.02). The affinities of dipentylammonium, dihexylammonium and dioctylammonium are not significantly different from each other.

A similar trend was observed with secondary ammonium salts. As the chain length increased, so did the affinity peaking at pK_i of 7.9 for dioctylammonium. There was an increase in affinity for the sigma-2 binding site as the carbon chain length increases from 3 to 6; however the increase was not large enough to warrant continuing investigating longer chain lengths ammonium salts in this series.

4.6 Tertiary ammonium salt affinity for the sigma-2 binding site

The tertiary ammonium salts discussed in this section consist of single central nitrogen and three straight carbon chains. The preliminary data showed that the triethylammonium has sigma-2 binding site affinity therefore the tertiary ammonium salts series from trimethylammonium with three single carbons to tridodecylammonium with twelve carbons were investigated. The affinity for the tertiary ammonium salts was investigated using radioligand binding competition assays. In order to visualise the affinities for the sigma-2 binding site more clearly, K_i values obtained from the competition binding curves were converted into pK_i values. The pK_i (\pm SEM) values are represented in Figure 4-5.

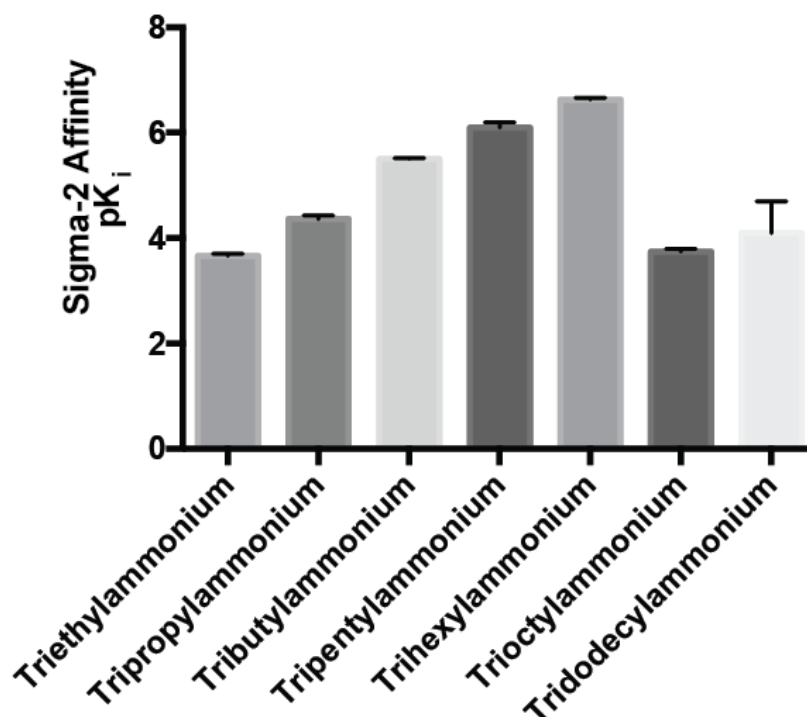


Figure 4-5: Summary of tertiary ammonium salts binding to the sigma-2 binding site.

The mean $pK_i \pm$ SEM values for tertiary ammonium salts were: triethylammonium 3.66 ± 0.04 ; tripropylammonium 4.36 ± 0.07 ; tributylammonium 5.5 ± 0.2 ; tripentylammonium 6.1 ± 0.1 ; trihexylammonium 6.63 ± 0.03 ; trioctylammonium 3.74 ± 0.06 and tridodecylammonium 4.1 ± 0.6 . Error bars represent SEM from 3-5 independent experiments. Unpaired 1-way ANOVA, followed by *post hoc* Tukey (“all means”) comparison, with *p* value adjusted for multiple comparisons, shows a significant difference in affinities [$F(6,21) = 23.8$, $p < 0.0001$]. Triethylammonium, tripropylammonium, trioctylammonium and tridodecylammonium have significantly lower affinity than tributylammonium, tripentylammonium and trihexylammonium ($p \leq 0.049$). Tributylammonium has significantly lower affinity than trihexylammonium ($p = 0.049$). No other comparison show significant differences.

On assessing the affinities of tertiary ammonium salts, the same trend persists. Increasing the length of the alkyl group resulted in increased affinity. The affinity peaked at pK_i 6.63 for trihexylammonium and further increased in the chain length resulted in rapid decline in the affinity. Introduction of branched chain alkyl groups showed no reproducible pattern: triisopropylammonium had lower affinity than tripropylammonium, triisobutylammonium had same affinity as tributylammonium, and triisopentylammonium showed slightly better affinity

than tripentylammonium. There was a decrease in affinity from six to the twelve carbon long chain (tridodecylammonium pK_i 4.1 ± 0.6) therefore no ammonium salts were tested with carbon chains longer than twelve.

4.7 Quaternary ammonium salt affinity for the sigma-2 binding site

The quaternary ammonium salts discussed in this section consist of a single positive nitrogen and 4 straight carbon chains. A series of quaternary ammonium salts from one carbon to four carbons in chain length was tested for sigma-2 binding site affinity using radioligand competition assays. In order to visualise the affinities for sigma-2 binding site more clearly, K_i values obtained from the competition binding were converted into pK_i values shown in Figure 4-6

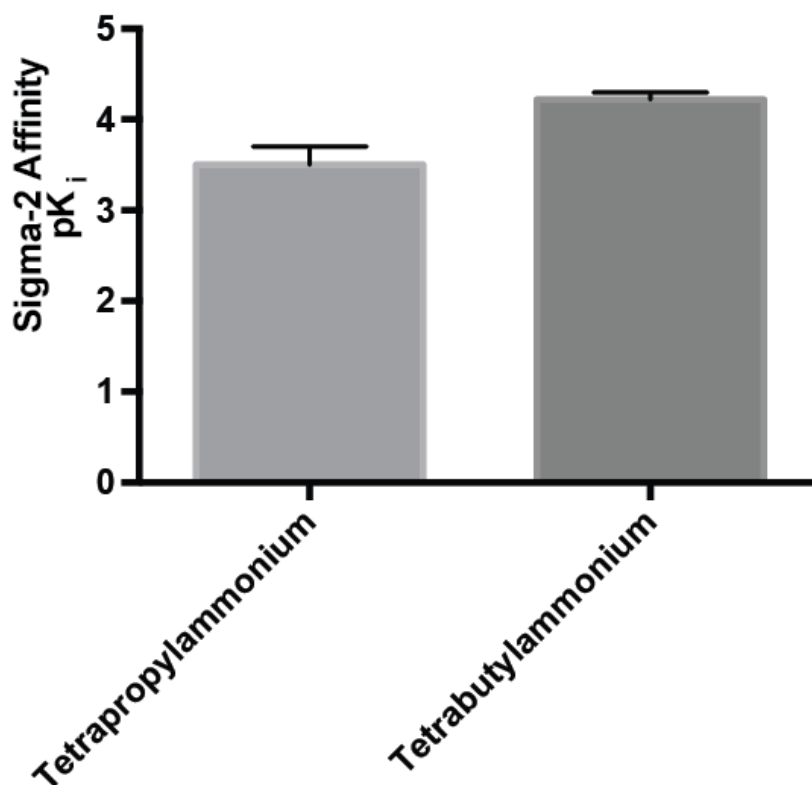


Figure 4-6: Summary of quaternary ammonium salt binding to the sigma-2 binding site

The mean $pK_i \pm SEM$ values for quaternary ammonium salts were: tetrapropylammonium 3.5 ± 0.2 and tetrabutylammonium 4.22 ± 0.08 . Error bars represent SEM from 3-5 independent experiments. Unpaired student's t-test shows that the affinity of tetrabutylammonium is significantly higher than tetrapropylammonium ($p = 0.016$).

Tetramethylammonium and tetraethylammonium had no affinity within the range tested. Quaternary ammonium salts showed only little affinity for the sigma-2 binding site and there was little increase in affinity as the carbon chain length increased, therefore no larger quaternary amines were tested for sigma-2 binding site affinity.

4.8 Simple branched chain ammonium salts

In an earlier section of this chapter I identified 4 high affinity sigma-2 binding site ligands, dipentylammonium, dihexylammonium, dioctylammonium and dicyclohexylammonium. In order to try to find higher affinity ligands I moved on to investigate branched chain ammonium salts. The branched chain ammonium

salts remain simple ammonium salts, and are the simplest variation on that could alter the affinity for the sigma-2 binding site.

4.9 Primary branched chain ammonium salt affinity for sigma-2 binding site affinity

Despite the straight chain primary ammonium salts having low affinity for the sigma-2 binding site, the branched chain primary ammonium salts were investigated for their affinities for sigma-2 binding site. The affinities of 1-adamantylammonium and 2-adamantylammonium were assessed using radioligand competition binding and the K_i values obtained from the competition binding were converted to pK_i as shown in the Figure 4-7.

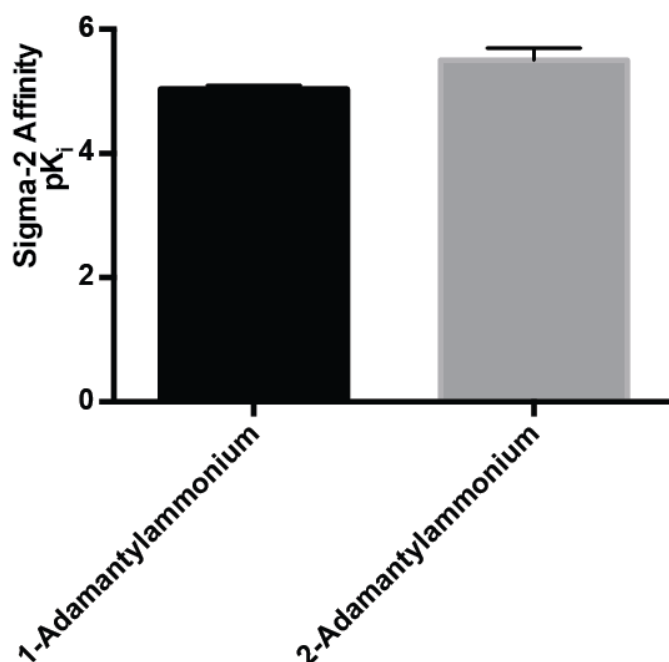


Figure 4-7: Summary of simple primary branched chain primary ammonium salt binding to the sigma-2 binding site.

The affinities of these agents for the sigma-2 binding site ($pK_i \pm$ SEM) were: 1-adamantylammonium 5.04 ± 0.05 and 2-adamantylammonium 5.5 ± 0.2 . Error bars represent SEM from 3-5 independent experiments. Unpaired student's t-test shows that the affinities of 1-adamantylammonium and 2-adamantylammonium are not significantly different from each other ($p = 0.067$).

Unlike simple straight chain ammonium salts, branched chain ammonium salts had very low affinity for sigma-2 binding site. The affinity of 1-adamantylammonium for the sigma-2 binding site was pK_i 5.04 and 2-adamantylammonium was pK_i 5.5. No other primary branched chain ammonium salts were assessed for binding to sigma-2 binding site.

4.10 Secondary branched chain ammonium salt affinity for the sigma-2 binding site

In order to assess the structure activity relationship of the simple ammonium salts with the sigma-2 binding site, some simple branched ammonium salts that were of similar chain length to the straight chain ammonium salts with high affinity for the sigma-2 binding site, were tested for the sigma-2 binding site affinity using [3H] DTG in the radioligand binding competition assay. In order to compare the affinities of the simple branched chain ammonium salts K_i values obtained were converted to pK_i , as shown in the Figure 4-8.

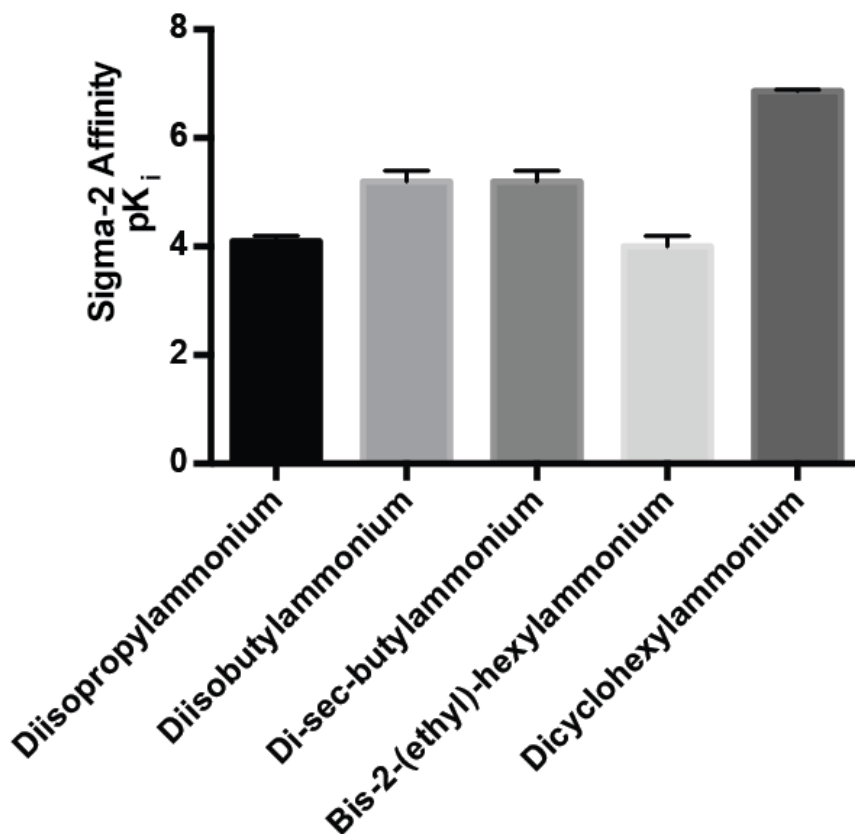


Figure 4-8: Summary of the simple secondary branched chain ammonium salts to the sigma-2 binding site

The affinities ($pK_i \pm \text{SEM}$) of the secondary branched ammonium salts for the sigma-2 binding site were: diisopropylammonium 4.1 ± 0.1 ; diisobutylammonium 5.2 ± 0.2 ; di-sec-butylammonium 5.2 ± 0.2 ; bis-2-(ethyl)hexylammonium 4.0 ± 0.2 and dicyclohexylammonium 6.86 ± 0.03 . Error bars represent SEM from 3-5 independent experiments. Unpaired 1-way ANOVA, followed by *post hoc* Tukey (“all means”) comparison, with p value adjusted for multiple comparisons, shows a significant difference in affinities [$F(4,15) = 50.8, p < 0.0001$]. All comparisons showed highly significant differences ($p < 0.002$), except diisopropylammonium compared with bis-2-(ethyl)hexylammonium, and diisobutylammonium compared with di-sec-butylammonium, which are not significantly different from each other.

Of the simple branched secondary amines tested dicyclohexylammonium had the highest affinity with a pK_i of 6.86. Compared to simple straight chain secondary ammonium salts the simple branched ammonium salts were found to have low affinities and I could not see a trend of increasing affinity with increasing chain length.

4.11 Tertiary branched chain ammonium salt affinity for the sigma-2 binding site

The simple straight chain tertiary ammonium salts with carbon chain length between five and six carbons had the highest affinity for the sigma-2 binding site, therefore triisopentylammonium (being the longest simple branched chain ammonium salt commercially available) was tested for sigma-2 binding site affinity using [³H] DTG in the radioligand binding competition assay. In order to compare the affinities of the simple branched chain ammonium salts K_i values obtained were converted to pK_i , as shown in the Figure 4-9.

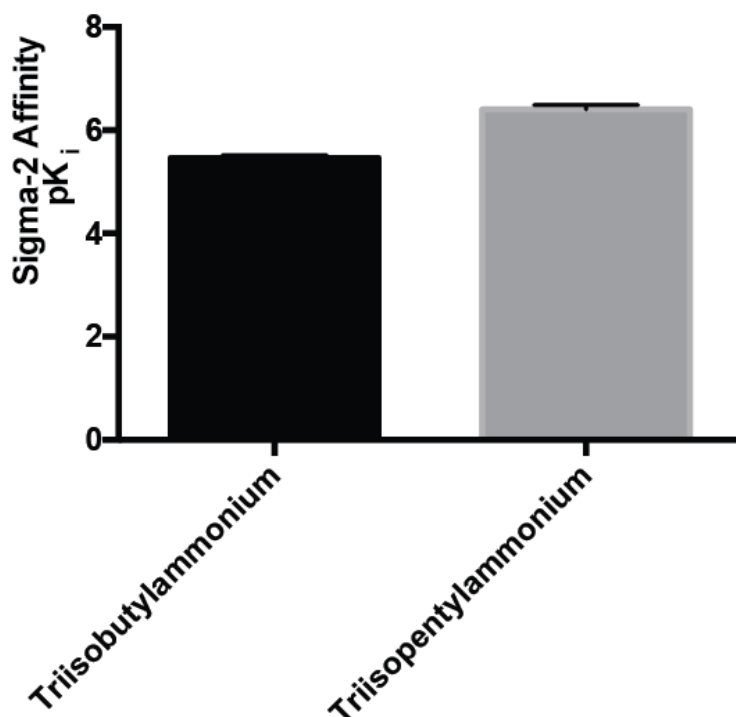


Figure 4-9: Summary of the simple tertiary branched chain ammonium salts to the sigma-2 binding site.

The affinities ($pK_i \pm$ SEM) of the tertiary branched ammonium salts for the sigma-2 binding site were: triisobutylammonium 5.46 ± 0.06 and triisopentylammonium 6.40 ± 0.09 . Error bars represent SEM from 3-5 independent experiments. Unpaired student's t-test shows that triisopentylammonium has significantly higher affinity than triisobutylammonium ($p = 0.0001$).

The affinity of tertiary branched chain ammonium salts was somewhat similar to simple straight chain tertiary ammonium salts. Triisopentylammonium had the highest affinity for sigma-2 binding site with pK_i of 6.40.

4.12 Sigma-2 ligands affinity for the sigma-2 binding site

In order to compare the affinities of the various commercially available sigma-1 receptor and sigma-2 binding site ligands, these were also considered and tested for sigma-2 binding site affinity using [^3H] DTG in the radioligand binding competition assay. In order to compare the affinities of these ligands K_i values obtained were converted to pK_i as shown in Figure 4-10.

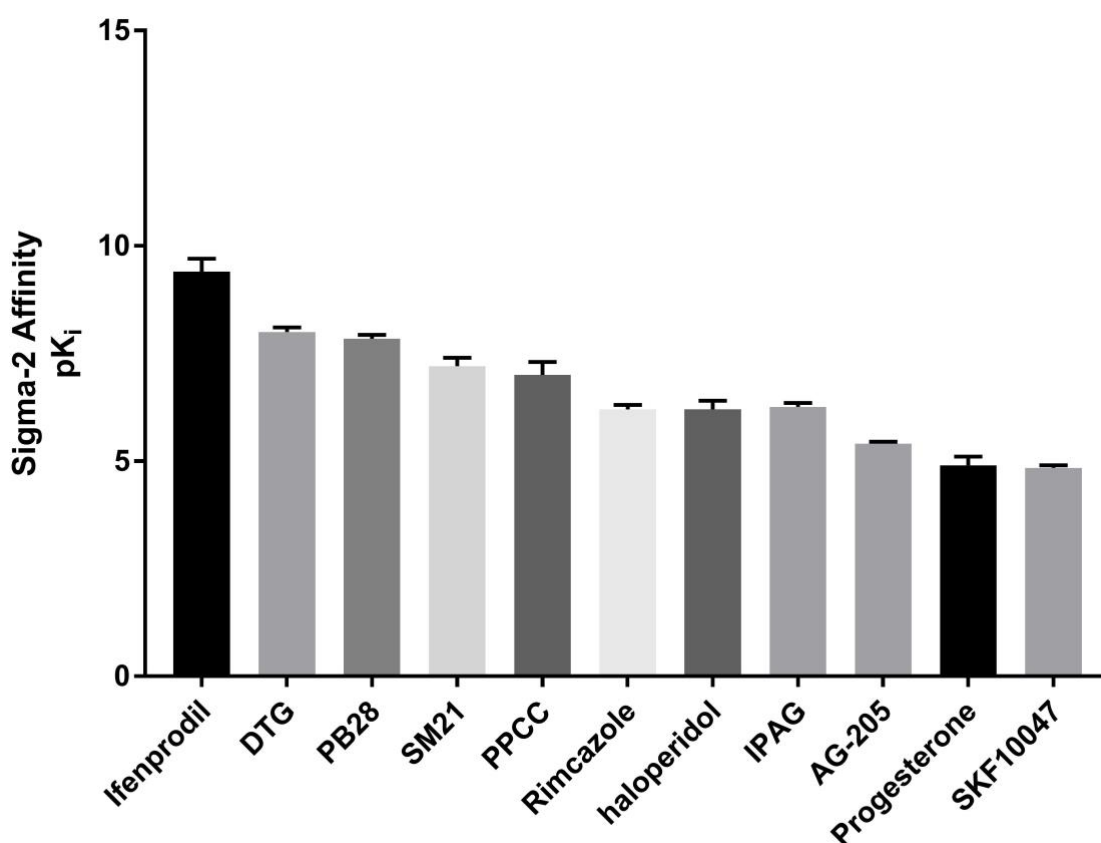


Figure 4-10: Summary of affinity of sigma-2 ligands to the sigma-2 binding site

The affinities (pK_i ± SEM) of the sigma-2 ligands were: ifenprodil 9.4 ± 0.3; DTG 8.0 ± 0.1; PB28 7.84 ± 0.09; SM21 7.2 ± 0.2; PPCC 7.0 ± 0.3; rimcazole 6.2 ± 0.1; haloperidol 6.2 ± 0.2; IPAG 6.16 ± 0.09; AG-205 5.4 ± 0.05; progesterone 4.9 ± 0.2 and SKF 10047 4.84 ± 0.06. Error bars represent SEM from 3-5 independent experiments. Unpaired 1-way ANOVA, followed by *post hoc* Tukey (“all means”) comparison, with p value adjusted for multiple comparisons, shows a significant difference in affinities [F(10,33) = 63.3, p < 0.0001]. Ifenprodil binds with significantly higher affinity than all other agents (p < 0.001). DTG binds with significantly higher affinity to other reagents (p ≤ 0.013) except PB28 and SM21 (ns). PB28 and SM21 bind with significantly higher affinity to the remaining drugs (p < 0.025), except each other and PPCC (ns). PPCC binds with significantly higher affinity than AG-205, progesterone and SKF 10047 (p < 0.0001). Rimcazole, haloperidol and IPAG bind with significantly higher affinity than progesterone and SKF 10047 (p ≤ 0.0005). All other comparisons show no significant differences.

Amongst commercially available sigma-2 binding site ligands, ifenprodil had the highest affinity (pK_i 9.4) and SKF 10047 had the lowest affinity (pK_i 4.84).

4.13 Discussion

4.13.1 Primary ammonium salts

These ammonium salts are different from previously known ligands in their simplicity and they have never been tested before. Eight primary ammonium salts were tested for sigma-2 binding site affinity. A trend was seen in affinity of primary ammonium salts, the affinity increased as the chain length increased, peaking at pK_i of 5.1 for hexylammonium. Any further increase in chain length did not increase the affinity. The primary ammonium salts 1-adamantylammonium and 2-adamantylammonium are more complex in structure than the other primary ammonium salts tested. Both the salts showed similar binding affinities and had slightly low affinity for sigma-2 binding site as shown in Table 4-1.

Ammonium salt	Sigma-2 binding site affinity (pK _i) *	nH
Propylammonium	<3	-
Butylammonium	3.26	0.86 ± 0.09
Pentylammonium	3.9	1.0 ± 0.1
Hexylammonium	5.1	0.72 ± 0.04
Octylammonium	5.2	0.9 ± 0.2
Decylammonium	5.2	0.92 ± 0.06
1-adamantylammonium	5.04	0.73 ± 0.03
2-adamantylammonium	5.5	0.8 ± 0.2

Table 4-1: Affinity of primary ammonium salts for the sigma-2 binding site.

* SEM removed for clarity; these values can be found earlier in this chapter. Unpaired 1-way ANOVA, with p value adjusted for multiple comparisons, shows no significant difference in Hill slope values [F(6,21) = 0.71, p = 0.64]. Propylammonium was excluded from this analysis.

4.13.2 Secondary ammonium salts

Twelve secondary amines were tested in [³H] DTG competition assay ranging from dimethylammonium with 2 single carbon chains to dioctylammonium with 2 eight-carbon chains. There was increased affinity with addition of carbon to the chain until eight-carbon chain long dioctylammonium, which had a pK_i of 7.9 (Table 4-2).

Adding side branches to the chains of these simple ammonium salts altered their affinity for the sigma-2 binding site. The most significant change in affinity for the sigma-2 binding site was observed with bis-2(ethyl)hexylammonium, by adding an ethyl group (C₂H₅) to the 2nd carbon along each of the carbon chains of dihexylammonium resulted in a 300-fold reduction of affinity as shown in Table 4-2.

Ammonium salt	Sigma-2 binding site affinity (pK _i) *	nH
Dimethylammonium	<3	-
Diethylammonium	<3	-
Dipropylammonium	4.10	0.8 ± 0.1
Diisopropylammonium	4.1	0.75 ± 0.09
Dibutylammonium	5.64	0.6 ± 0.1
Diisobutylammonium	5.2	0.78 ± 0.05
Di-sec-butylammonium	5.2	0.8 ± 0.1
Dipentylammonium	6.9	0.67 ± 0.04
Dihexylammonium	7.58	0.68 ± 0.06
Dicyclohexylammonium	6.86	0.72 ± 0.07
Bis-2-(ethyl)Hexylammonium	4.0	0.65 ± 0.04
Diocetylammonium	7.9	0.6 ± 0.2

Table 4-2: Affinity of secondary ammonium salts for the sigma-2 binding site.

* SEM removed for clarity; these values can be found earlier in this chapter. Unpaired 1-way ANOVA, with p value adjusted for multiple comparisons, shows no significant difference in Hill slope values [$F(9,30) = 0.64$, $p = 0.76$]. Dimethylammonium and diethylammonium were excluded from this analysis.

4.13.3 Tertiary and quaternary ammonium salts.

When I looked at the affinities of tertiary ammonium salts several trends were the same. Increase in the length of alkyl group resulted in increased affinity. Increasing the chain length further resulted in a rapid decline in affinity. Introduction of branched chain alkyl groups showed no reproducible pattern. Triisopropylammonium had lower affinity than tripropylammonium,

triisobutylammonium had the same affinity as tributylammonium whereas triisopentylammonium showed slightly higher affinity than tripentylammonium as shown below in Table 4-3.

Ammonium salt	Sigma-2 binding site affinity (pK _i) *	nH
Trimethylammonium	<3	-
Triethylammonium	3.66	0.88 ± 0.02
Ethyldiisopropylammonium	4.44	0.70 ± 0.02
Tripentylammonium	4.36	0.93 ± 0.07
Triisopropylammonium	<3	-
Tributylammonium	5.5	0.68 ± 0.05
Triisobutylammonium	5.46	0.7 ± 0.2
Tripentylammonium	6.1	0.8 ± 0.2
Triisopentylammonium	6.4	0.73 ± 0.05
Trihexylammonium	6.63	0.7 ± 0.1
Trioctylammonium	3.74	1.1 ± 0.1
Tridodecylammonium	4.1	0.7 ± 0.2

Table 4-3: Affinity of tertiary ammonium salts for the sigma-2 binding site.

* SEM removed for clarity; these values can be found earlier in this chapter. Unpaired 1-way ANOVA, with p value adjusted for multiple comparisons, shows no significant difference in Hill slope values [F(9,30) = 1.32, p = 0.27]. Trimethylammonium and triisopropylammonium were excluded from this analysis.

Four quaternary ammonium salts were tested, all of which had low affinities for the sigma-2 binding site. Tetrabutylammonium had the highest affinity, with pK_i 4.22, and since there was no increase in the affinity with increase in carbon

chain length, no further quaternary amines were tested for sigma-2 binding site affinity.

4.13.4 Commercially available sigma ligands

Several commercially available sigma ligands were tested for affinity for sigma-2 binding site. Ifendprodil had the highest affinity with pK_i 9.4. (+) Pentazocine, the classical sigma-1 receptor ligand, bound as well but with lower affinity as shown in the Table 4-4

Compound name	Sigma-2 binding site affinity (pKi) *	nH
Pentazocine	6.45	0.73 ± 0.06
Haloperidol	6.2	1.1 ± 0.2
DTG	8.0	0.6 ± 0.1
Rimcazole	6.2	0.7 ± 0.1
Progesterone	4.9	0.7 ± 0.2
IPAG	6.16	0.7 ± 0.1
RU-486	<3	-
Ifenprodil	9.4	0.5 ± 0.1
PPCC	7.0	0.58 ± 0.08
SM21	7.2	0.63 ± 0.03
SKF10047	4.84	0.94 ± 0.04
AG-205	5.40	1.06 ± 0.03
Spermidine	<3	-
Spermine	<3	-

Table 4-4: Affinity of commercially available sigma ligands for the sigma-2 binding site.

* SEM removed for clarity; these values can be found earlier in this chapter. Unpaired 1-way ANOVA, followed by *post hoc* Tukey (“all means”) comparison, with p value adjusted for multiple comparisons, shows a significant difference in Hill slope values [F(10,33) = 3.22, p = 0.0054]. The Hill slope for ifenprodil was significantly lower than haloperidol (p = 0.019) and AG-205 (p = 0.036). All other comparisons show no significant differences.

4.14 Summary

Simple ammonium salts show graded response in affinities for sigma-2 binding site. Straight chain primary, secondary and tertiary ammonium salts have sigma-2 binding affinity, which increase as the carbon chain length between 4 and 6 carbons. Any further increase in the number of carbons has no effect on the affinity. Decylammonium, dioctylammonium and trihexylammonium were found to have the highest affinities of primary, secondary and tertiary ammonium salts for sigma-2 binding site.

It is also shown that branched chain ammonium salts have lower affinity for the sigma-2 binding site. Two branched chain ammonium salts, bis-2-(ethyl)hexylammonium and triisopentylammonium particularly stood out. Although the affinity of most of the ammonium salts was low compared to known sigma-2 ligands, some of the salts had affinities comparable to commercially available sigma-2 ligands. *In vitro* results suggest that two ammonium salts had affinity for the sigma-2 binding site comparable to commercial sigma-2 binding site ligands: dihexylammonium, with pK_i 7.58 and dioctylammonium, with pK_i 7.9. In the next chapter, it will be investigated if they have activity *in vivo*.

**Chapter 5. BIOLOGICAL ACTIVITY OF SIGMA-2
BINDING SITE LIGANDS**

5.1 Background

Determining structure-activity relationships for receptors is routinely performed by medicinal chemists. Much of this is an academic activity, as the information discovered may not inform the requirements of drugs turning into medicines. This is particularly the case when drug targets are not on the cell surface. In the case of the sigma-2 binding site, while its identity is not known, its location is (Peluso et al., 2009). As an intracellular protein, structural requirements have to be balanced with bioavailability and cell membrane permeability.

Functional assays to determine whether a drug is binding its target bring together the determination of whether a drug reaches its target and then whether it has an effect.

In the case of the sigma-2 binding site, few functional assays are routinely used:

5.1.1 Effects on electrically stimulated bladder

Kinney *et al.* have previously used electrically stimulated guinea pig ileum to study the effects of sigma-2 ligands, with correlations between affinity and effect being present (Kinney et al., 1995). Colabufo *et al.* also used this assay, although the presence of many other receptors that could interfere with data interpretation was acknowledged (Colabufo et al., 2003). As most interest in sigma-2 ligands concerns their effects on tumour growth and development, more recent assays have focused on their effects on cell growth and proliferation.

5.1.2 MTS cell “viability” assays.

The MTS (or older MTT/XTT) assay merely records cellular metabolic activity. As such, it is used to measure cell number (Tan et al., 2013), toxicity of drugs (Spruce et al., 2004), even in bacteria (Belanger et al., 2011) to name a few. It is not specific in any way and is subject to interference by reducing agents

(Bernas and Dobrucki, 2002, Chakrabarti et al., 2000, Collier and Pritsos, 2003, Ulukaya et al., 2004). In order to test the effects of sigma-2 ligands, a fixed number of cells are seeded into wells and, following prolonged incubation with the test drugs, metabolic activity is then assessed. The read-out requires interpretation as quiescent cells (non-dividing cells in G₀) will appear the same as cells blocked in the cell cycle or dead cells. This is an important distinction as bacteriostatic drugs (agents that stop bacteria from dividing while present, but will then allow them to restart their growth once the drug is removed or metabolised) have very different roles to bactericidal drugs (these kill the bacteria). Likewise in oncology, drugs that prevent tumours from growing are useful as in many cases the immune system will be able to destroy the tumour if its growth is retarded (Zitvogel et al., 2008). The MTS assay also does not distinguish between why a population of cells has a reduced signal. This is important when looking at experimental drugs causing cell death. The differences between death by apoptosis or necrosis are great.

5.1.3 Lactate dehydrogenase (LDH) assays

These assays measure the release of LDH from a cell. LDH is present in most cell types and can leak out when the cell membrane becomes damaged. By the time the plasma membrane becomes permeable to this large protein (140 kDa) it has passed the point of no return and is inviable. It does not distinguish between necrosis and late-stage apoptosis (Chan et al., 2013). This event is more closely linked to the death of a cell than MTS metabolism. As the LDH assay can be used to measure cell death, Colabufo and colleagues (Colabufo et al., 2009b) have discriminated between antiproliferative effects of agents (using an assay like MTS) with that of cytotoxicity. In this respect, one should be able to distinguish between cytotoxic and cytostatic effects of drugs. Data from 2009 does show differences between doses required of some sigma-2 ligands to cause cytotoxicity and have antiproliferative effects. Unfortunately as the assays were performed 24 and 48 hours after drug treatment, it is possible that these differences were due to the protocols used and not necessarily separation of effects. Others outside the field of sigma-2 signalling have

compared the two assays in greater detail (Smith et al., 2011). Due to its simplicity, the MTS assay is by far the most widely accepted assay used.

Cell death occurs via two major routes: apoptosis and necrosis (Criddle et al., 2007). Apoptosis, or programmed cell death, is an ordered series of events and occurs naturally during development of the foetus – a key example is the development of individual fingers as the interdigital cells undergo apoptosis, revealing five digits from what was a single paddle (Suzanne and Steller, 2013). When a cell undergoes apoptosis, the cell shrinks, the plasma membrane flips, exposing phosphatidylserine to the extracellular environment, DNA is lysed into a characteristic ladder and small subcellular packages are created, allowing the dead cell contents to be phagocytosed by neighbours. Necrosis usually occurs as a consequence of insult – physical damage to cells, treatment with harsh chemicals or toxins. Cells swell and the contents are released, causing damage to neighbouring cells.

Apoptosis requires the activation of a series of biochemical events. This includes a pulse of calcium which precedes activation of a series of caspase protease enzymes (Tantral et al., 2004), leading to the study of calcium homeostasis (Vilner and Bowen, 2000) and use of caspase-3 assays to determine the activity of sigma-2 ligands (Zeng et al., 2014).

5.1.4 Calcium homeostasis

Spruce *et al.* have previously studied calcium regulation following treatment of sigma-1 receptors (Spruce et al., 2004). These studies were preceded by studies comparing the effects of sigma ligands acting through sigma-1 receptors and sigma-2 binding sites. Vilner and Bowen (1999) showed that the ligands used activated calcium release from intracellular stores, as they were abolished if cells were pretreated with the endoplasmic/sarcoplasmic reticulum

calcium ATPase poison thapsigargin (Vilner and Bowen, 2000). Thapsigargin acts by preventing uptake into this pool allowing for calcium stores to be depleted, as these stores are leaky. The role of extracellular calcium was downplayed, as its removal, while affecting the calcium response to KCl, only affected the calcium response to one of the sigma ligands tested. Vilner and Bowen claimed there was a correlation between affinity of a ligand for the sigma-2 binding site and its ability to cause a calcium response. I have reproduced a figure of this correlation. I remain unconvinced that the correlation is valuable information.

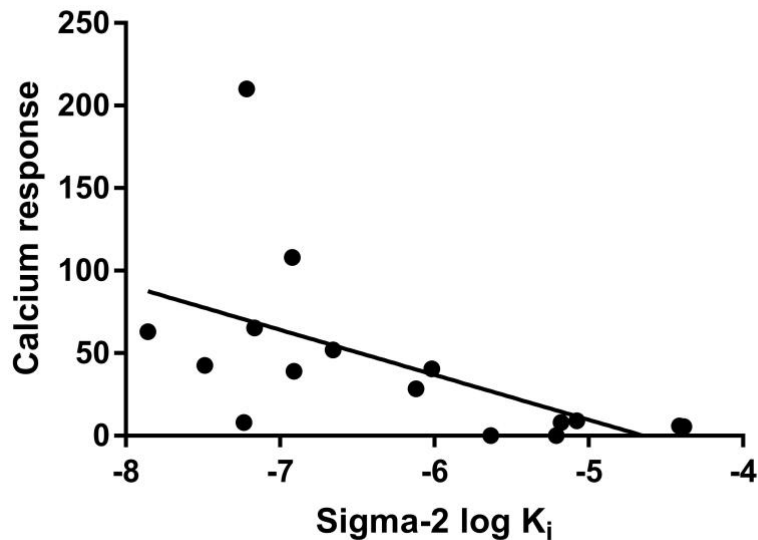


Figure 5-1: Correlation between affinity for the sigma-2 binding site and calcium response

Correlation of calcium response at a fixed concentration of ligand (100 μ M) and affinity for the sigma-2 binding site, data taken from Vilner and Bowen (Vilner and Bowen, 2000). Linear regression shows the line $y = -27.26x - 126.6$, $R^2 = 0.322$ [$F(1,14) = 6.65$, $p = 0.022$].

5.1.5 Caspase activation assays

Caspases are calcium-activated proteases. Caspase-3 cleaves the specific peptide sequence DVED, allowing assays to be developed in which a fluorophore (for example rhodamine) is quenched by positioning the peptide such that until cleaved the rhodamine does not fluoresce (Zeng et al., 2014). This is one of the few routinely used assays that distinguishes between death by apoptosis (positive result) and necrosis (negative result).

I have used two of the above methods, the MTS assay to determine which agents decrease metabolic activity and have revisited the calcium response data in order to determine whether a correlation does exist. By comparing the affinity, EC_{50} for reduction in metabolic activity and size of calcium response, I hope to shed more light on distinguishing agonists from antagonists, and propose if partial agonists exist in this system.

5.2 Results

5.2.1 Effects of ammonium salts on cellular proliferation

The ability of the amines and several previously characterised sigma ligands to affect proliferation of MCF7 cells was determined. MCF7 cells were used as they had previously (Vilner et al., 1995b) and currently (this study) been identified as having sigma-2 binding sites but lacking sigma-1 receptors. While sigma-1 and sigma-2 are believed to be proteins with different characteristics, localisation and properties, many ligands have cross-reactivity. Using MCF7 cells devoid of sigma-1 receptors means that the effects of this protein are excluded, helping clarify the role of sigma-2 binding sites in cell death and the effects of these compounds on the sigma-2 binding sites without interference from the sigma-1 receptor.

From binding data, we see that most of the simple primary, secondary, tertiary and, to a lesser extent, quaternary amines bind the sigma-2 binding site. In order to determine their biological activity, the standard assay used was to look at their effects on metabolic activity. I have done this in MCF7 cells as these cells lack sigma-1 receptors, which would confound my data.

Ammonium salt	Sigma-2 binding site affinity (pK _i) *	nH *	pIC ₅₀ MCF7	% Inhibition of 100μM rimcazole	clogD (pH 7.4)
Propylammonium	<3	-	-	0.5 ± 0.5	-2.45
Butylammonium	3.26	0.86	-	0	-2.12
Pentylammonium	3.9	1.0	-	0.3 ± 0.3	-1.34
Hexylammonium	5.1	0.72	-	0	-1.02
Octylammonium	5.2	0.9	3.13 ± 0.03	0	-0.07
Decyl Ammonium	5.41	0.92	4.06 ± 0.08	4.0 ± 0.6	1.07
1-adamantyl Ammonium	5.0	0.73	-	0.5 ± 0.3	-0.37
2-adamantyl Ammonium	5.5	0.8	-	0.8 ± 0.5	-0.61

Table 5-1: Primary ammonium salts characteristics

Table showing characteristics of ammonium salts. Mean ± SEM were calculated from 3-5 individual experiments. * SEM removed for clarity; these values can be found in Chapter 4. Unpaired 1-way ANOVA, followed by post hoc Tukey (“all means”) comparison, with p value adjusted for multiple comparisons, shows a significant difference in the ability to reverse the effects of rimcazole [F(4,15) = 11.8, p = 0.0002]. Decylammonium shows a greater ability to reverse the effects of rimcazole than all other agents tested (p < 0.0015). All other comparisons show no significant difference. Butylammonium, hexylammonium and octylammonium were excluded from these comparisons.

Of the primary amines tested, while all above propylammonium bound the sigma-2 binding site *in vitro*, only octylammonium and decylammonium salts inhibited growth of MCF7 cells. This identified them as agonists at the sigma-2 binding site. That other amines were without effect did not indicate they were antagonists. An antagonist, by definition has no effect alone but blocks the effects of an agonist in that system. In order to determine whether these agents were antagonists, MCF7 cells were pretreated with the potential antagonist (1mM) prior to addition of 100 μ M rimcazole, a known agonist that inhibits MCF7 proliferation. A sub-maximal dose of rimcazole was used in order to make the assay sensitive to inhibition whilst allowing for any unexpected potentiation to also be observed. With one exception (decylammonium), none of the agents tested reversed the growth inhibition induced by rimcazole. This could suggest that the sigma-2 binding site is not on the cell surface, and access requires compounds to either be transported to the site or diffuse through membranes. More so, it suggests these compounds are unable to access the sigma-2 site in living cells. Decylammonium reversed the rimcazole effects but only slightly.

5.2.2 Physicochemical properties of primary ammonium salts

In order to explain these findings, the physicochemical properties of these sigma-2 binding site ligands were considered. When comparing the octanol:water partition coefficient at pH 7.4 (presented as a calculated log D at pH 7.4 or clogD (7.4) from the ACD calculation present on the chemspider.com website), a trend appeared. Increasing the chain length increased the proportion of material partitioning into the organic layer. It was only those materials which partitioned equally or more towards the octanol layer that showed biological activity. Comparing the acid dissociation constant (pK_a) values of these materials, the amine group is dominant, giving the molecules a pK_a of over 10, indicating they would exist in a protonated form at neutral pH values. In contrast to the straight-chained decylammonium, the more complex structures of 1- and 2-adamantylammonium (which still contained 10 carbons), were unable to alter metabolic activity of MCF7 cells. One may be able to

explain this by the reduction in the clogD (7.4) caused by the crown-like structure of these adamantylammonium compounds, as compared to the straight-chained decylammonium compound.

It was decided to use logD , not logP in all the observations. LogP is concerned with the partition coefficient of the uncharged molecule. LogD , is the partition coefficient of all species at the defined pH, which was used as 7.4 – the pH of the plasma and generally accepted as the pH of the “extracellular space”. logD tells us what proportion of these molecules would partition into an aqueous phase and what proportion into octanol. If a molecule would evenly separate into both, there would be 50% in octanol, 50% in water 50/50 gives 1 and $\text{log}1 = 0$, so anything with a negative logD would favour partitioning to the water, anything with logD greater than 1 favours octanol). As we believe the sigma-2 binding site to be intracellular, a high octanol:water solubility ratio would be favoured. Progesterone would seem a reasonable benchmark and has a clogD of 3.72. (as this is a log scale, there would be $10^{3.72}$ - 5200 times more progesterone in the octanol than in the water).

Ammonium salt	Sigma-2 binding site affinity (pK _i) *	nH *	pIC ₅₀ MCF7	% Inhibition of 100μM rimcazole	clogD (pH 7.4)
Dimethylammonium	<3	-	-	0	-3.18
Diethylammonium	<3	-	-	0.3 ± 0.3	-2.21
Dipropylammonium	4.10	0.8	-	1.0 ± 0.6	-1.25
Diisopropylammonium	4.1	0.75	-	0.8 ± 0.5	-1.45
Dibutylammonium	5.64	0.6	-	0.8 ± 0.8	-0.43
Diisobutylammonium	5.2	0.78	-	0.5 ± 0.3	-0.61
Di-sec butylammonium	5.2	0.8	-	0.3 ± 0.3	-0.62
Dipentylammonium	6.9	0.67	-	0	0.65
Dihexylammonium	7.58	0.68	3.40 ± 0.07	0.3 ± 0.3	1.38
Dicyclohexylammonium	6.86	0.72	3.75 ± 0.02	0.8 ± 0.3	0.62
Bis-2-ethylhexyl ammonium	4.0	0.65	-	0	3.38
Diocetyl ammonium	7.9	0.6	4.44 ± 0.08	30 ± 6	3.88

Table 5-2: Secondary ammonium salts characteristics.

Table showing characteristics of secondary ammonium salts. Mean ± SEM were calculated from 3-5 individual experiments. * SEM removed for clarity; these values can be found in Chapter 4. Unpaired 1-way ANOVA, followed by post hoc Tukey (“all means”) comparison, with p value adjusted for multiple comparisons, shows a significant difference in the ability to reverse the effects of rimcazole [F(8,27) = 22.9, p < 0.0001]. Dioctylammonium shows a greater ability to reverse the effects of rimcazole than all other agents tested (p < 0.0001). All other comparisons show no significant difference.

Dimethylammonium, dipentylammonium and bis-2-(ethyl)hexylammonium were excluded from these comparisons.

5.2.3 Physicochemical properties of secondary ammonium salts

A similar trend was observed with secondary ammonium salts. As chain length increased, so did affinity, peaking at just above 10nM (dioctylammonium, pK_i 7.9). Dialkylammonium salts with fewer than six carbons per chain did not affect metabolic activity of MCF7 cells either by reducing activity or reversing the effects of rimcazole. As with the primary ammonium salts, the $clogD$ (7.4) increases with chain length. While the $clogD$ (7.4) of dipentylammonium (0.65) is greater than that of the active octylammonium ($clogD$ (7.4) -0.07), this too was inactive. Dihexylammonium and dicyclohexylammonium were both active, reducing metabolic activity to similar extents with similar pIC_{50} values. The compound with highest affinity for the sigma-2 binding site was also most effective in reducing metabolic activity. Dioctylammonium was found to have a pK_i of 7.9 and pIC_{50} of 4.44. Strangely, it was also the only secondary ammonium salt to (partially) reverse the effects of rimcazole.

Introduction of branched side chains had differing effects: no difference was observed when comparing dipropylammonium with diisopropylammonium. The affinities of diisobutylammonium and di-sec-butylammonium were marginally lower than that for dibutylammonium, whereas the difference between dihexylammonium and dicyclohexylammonium was moderate, but these salts showed approximately 1000-fold higher affinity than bis-2-(ethyl)hexylammonium. The lack of biological effect of bis-2-(ethyl)hexylammonium, despite such subtle differences, may have been due to the low affinity of this potential ligand. Positive $clogD$ (7.4) values again appear to be necessary for these compounds to be active.

Ammonium salt	Sigma-2 binding site affinity (pK _i) *	nH *	pIC ₅₀ MCF7	% Inhibition of 100µM rimcazole	clogD (pH 7.4)
Trimethylammonium	<3	-	-	0	-2.14
Triethylammonium	3.66	0.88	-	1.0 ± 0.4	-1.18
Ethyldiisopropyl ammonium	4.44	0.70	-	0.8 ± 0.5	-0.55
Tripropylammonium	4.36	0.93	-	0.3 ± 0.3	0.52
Triisopropyl ammonium	<3	-	-	0	-0.18
Tributylammonium	5.5	0.68	-	0	1.69
Triisobutyl ammonium	5.46	0.7	-	0.3 ± 0.3	2.03
Tripentylammonium	6.1	0.8	-	0.3 ± 0.3	3.73
Triisopentyl ammonium	6.4	0.73	-	0	2.68
Trihexylammonium	6.63	0.7	3.9 ± 0.2	14 ± 3	4.85
Trioctylammonium	3.74	1.1	-	0	8.10
Tridodecyl ammonium	4.1	0.7	-	2.6 ± 0.7	14.50

Table 5-3: Characteristics of tertiary ammonium salts.

Table showing characteristics of tertiary ammonium salts. Mean ± SEM were calculated from 3-5 individual experiments. * SEM removed for clarity; these values can be found in Chapter 4. Unpaired 1-way ANOVA, followed by post hoc Tukey (“all means”) comparison, with p value adjusted for multiple comparisons, shows a significant difference in the ability to reverse the effects of rimcazole [$F(6,21) = 17.4$, $p < 0.0001$]. Trihexylammonium shows a greater ability to reverse the effects of rimcazole than all other agents tested ($p < 0.0001$). All other comparisons show no significant difference.

Trimethylammonium, triisopropylammonium, tributylammonium, triisopentylammonium and trioctylammonium were excluded from these comparisons.

5.2.4 Physicochemical properties of tertiary ammonium salts

When I looked at the effects of tertiary ammonium salts, several trends were the same. Increasing the length of the alkyl groups increased affinity. In this case, trihexylammonium had peak affinity (pK_i 6.63). Increasing chain length further caused a rapid decline. Trihexylammonium was also the only tertiary ammonium salt that reduced metabolic activity, albeit with a low pIC_{50} (3.9). Introduction of branched chain alkyl groups showed no reproducible pattern: triisopropylammonium had lower affinity than tripropylammonium, triisobutylammonium had the same affinity as tributylammonium whereas triisopentylammonium showed a slightly higher affinity than tripentylammonium.

When looking at the ability of these compounds to alter the effects of rimcazole, again, the agent that reduced metabolic activity was the only one that reversed the effects of rimcazole, albeit modestly. Trihexylammonium (1mM) reversed rimcazole's effects by 14%. The $clogD$ (7.4) values for tripropylammonium and larger salts were positive, albeit some being very high. It is worth reminding ourselves that a $clogD$ (7.4) of 5 means an octanol:water partition coefficient of 100,000:1, indicating that 99.999% of such a material would reside in the octanol phase at pH 7.4.

Ammonium salt	Sigma-2 binding site affinity (pK _i) *	nH	pIC ₅₀ MCF7	% Inhibition of 100µM rimcazole	clogD (pH 7.4)
Tetramethylammonium	<3	-	-	0.3 ± 0.3	-3.15
Tetraethylammonium	<3	-	-	1.0 ± 0.4	-2.79
Tetrapropylammonium	3.5	0.7 ± 0.01	-	0.3 ± 0.3	-1.77
Tetrabutylammonium	4.2	0.8 ± 0.03	-	1.8 ± 0.8	-0.64

Table 5-4: Characteristic of quaternary ammonium salts.

Table showing characteristics of quaternary salts. Mean ± SEM were calculated from 3-5 individual experiments. * SEM removed for clarity; these values can be found in Chapter 4. Unpaired 1-way ANOVA, with p value adjusted for multiple comparisons, shows no significant difference in the ability to reverse the effects of rimcazole [$F(3,12) = 2.08$, $p = 0.156$].

5.2.5 Physicochemical properties of quaternary salts

Quaternary ammonium salts had little effect on the sigma-2 binding sites and did not reverse the effects of rimcazole. On considering the clogD (7.4) of the compounds tested, they all have negative values, indicating low solubility in octanol and hence are unlikely to gain access to the interior of the cell.

5.2.6 Physicochemical properties of commercial ligands

Several commercial ligands for the sigma-1 receptor or sigma-2 binding site were also considered. (+) Pentazocine, the classical sigma-1 ligand, did bind the sigma-2 binding site with low affinity (pK_i 6.45) and was found to reduce metabolic activity in MCF7 cells, albeit with pIC₅₀ of 3.8. Haloperidol, DTG, progesterone, IPAG, PPCC and SKF 10,047 bound but do not affect metabolic activity. Ifenprodil, SM21 and AG-205 bound and reduced metabolic activity, suggesting these are agonists at the sigma-2 binding site. Haloperidol, progesterone, PPCC and AG-205 were able to reverse the effects of rimcazole to varying degrees. Spermine and spermidine are naturally occurring agents

with similar structures to secondary ammonium salts; these were also considered. They were of particularly low affinity and did not alter metabolic activity of MCF7 cells either in the absence or presence of rimcazole. With the exception of spermine and spermidine, these agents all show clogD (7.4) values between 0 and 5. Mifepristone (RU-486), the progesterone receptor antagonist was tested. It showed little affinity for the sigma-2 binding site.

Ligand	Sigma-2 binding site affinity (pK _i) *	nH *	pIC ₅₀ MCF7	% Inhibition of 100μM rimcazole	clogD (pH 7.4)
(+) Pentazocine	6.45	0.73	3.80 ± 0.00	1.5 ± 0.3	2.26
Haloperidol	6.2	1.1	-	10.9 ± 0.9	2.65
DTG	8.0	0.6	-	2.5 ± 0.9	2.31
Rimcazole	6.2	0.7	4.47 ± 0.07	-	2.63
Progesterone	4.9	0.7	-	12 ± 3	3.72
IPAG	6.16	0.7	-	0.8 ± 0.5	2.74
RU-486	<3	-	-	80 ± 9 [#] Precipitation	5.16
Ifenprodil	9.4	0.5	3.6 ± 0.1	2.8 ± 0.8	1.66
PPCC	7.0	0.58	-	34 ± 6	2.17
SM21	7.2	0.63	4.0 ± 0.2	0	1.19
SKF10047	4.84	0.94	-	0.8 ± 0.5	2.16
AG-205	5.40	1.06	3.38 ± 0.03	29 ± 4	2.46
Spermidine	<3	-	-	0.3 ± 0.3	-5.91
Spermine	<3	-	-	0.3 ± 0.3	-6.78

Table 5-5: characteristics of commercially available sigma-1 and sigma-2 binding site ligands.

Table showing characteristics of commercially available sigma-1 and sigma-2 ligands. Mean ± SEM were calculated from 3-5 individual experiments. [#] indicates precipitation during the assay, leading to spurious results. * SEM removed for clarity; these values can be found in Chapter 4. Unpaired 1-way ANOVA, followed by post hoc Tukey (“all means”) comparison, with p value adjusted for multiple comparisons, shows a significant difference in the ability to reverse the effects of rimcazole [F(10,33) = 25.1, p < 0.0001]. PPCC and AG-205 show a greater ability to reverse the effects of rimcazole than all other agents tested (p < 0.001), except each other (p = 0.92). All other comparisons show no significant difference. RU-486 and SM21 were excluded from these comparisons.

Data on the effects of rimcazole on metabolic activity appears to be confounded by precipitation of RU-486 during the time required for its effects to be seen. The MTS assay relies on a conversion of the colourless tetrazolium to coloured formazan. However, microscopic analysis showed the presence of colourless crystals present and, presumably, interference with the colorimetric analysis by diffracting light in the plate reader. As we have seen with the ammonium salts, very few agents reduced metabolic activity of MCF7 cells. Notable exceptions are the archetypal sigma-2 agonist ifenprodil and the PGRMC1 ligand, AG-205. My results here are in stark contrast to (Abate et al., 2015a) who found no affinity for or effect through the sigma-2 binding site. Ifenprodil has little effect on rimcazole-mediated reduction in metabolic activity, but AG-205 greatly reverses these effects, suggesting it may be a partial agonist as it causes an effect, but also reverses the effects of a fellow agonist. Three of these agents showed antagonist activity with no effect by themselves, whilst significantly reversing rimcazole-mediated reduction in metabolic activity. Haloperidol and progesterone show modest reversal, whereas PPCC gave the best profile to be described as an antagonist: it did not affect metabolic activity alone, but significantly protected the cells from the effects of rimcazole.

5.2.7 Effects of ligands on intracellular calcium

The pathways involved in reducing metabolic activity frequently require a pulse of calcium to initiate apoptosis, as is seen with activation of the sigma-1 receptor. Indeed, Vilner and Bowen have proposed that sigma-2 affinity is (weakly) correlated to the ability of ligands to mobilise calcium from intracellular stores (Vilner and Bowen, 2000). In order to further analyse such a potential correlation, I compared the ability of sigma-2 ligands to affect metabolic activity with their ability to mobilise calcium. To determine this, the ability of a select number of compounds to elicit a calcium response in MCF7 cells pre-loaded with Fura-2 ratiometric dye was considered. All drugs were tested to determine whether they, like rimcazole, fluoresced causing an artefact. Rimcazole (Figure

5-2) showed a dramatic increase in ratiometric signal and so cannot be used in these assays. This has previously been reported (Brimson et al., 2011).

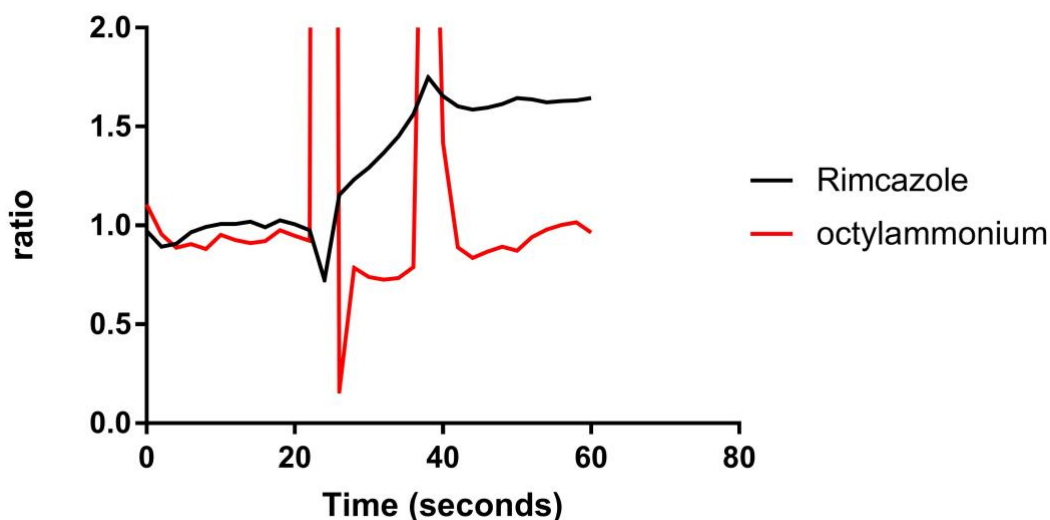


Figure 5-2: Change in fluorescence following addition of rimcazole and octylammonium.

Figure showing change in fluorescence following addition of rimcazole (1mM) or octylammonium (1mM) to KLB containing no fluorophore. Ratio refers to fluorescence emitted at 520 nm after excitation at 340nm and 380 nm. Artefacts are introduced at 22 and 36 seconds due to the opening of the light-tight chamber required for the introduction of the drugs at 30 seconds.

In order to determine if sigma-2 ligands do elicit a calcium response as part of their mechanism to decrease metabolic activity and lead to cell death by apoptosis, each active agent was tested to see if it was able to produce a calcium response. Equally, several commercial ligands, described as both agonists and antagonists, were tested.

The primary ammonium salts octylammonium and decylammonium both produced a calcium response, although the response to decylammonium was much larger than that to octylammonium, which, while small did reproducibly produce a response (Figure 5-3).

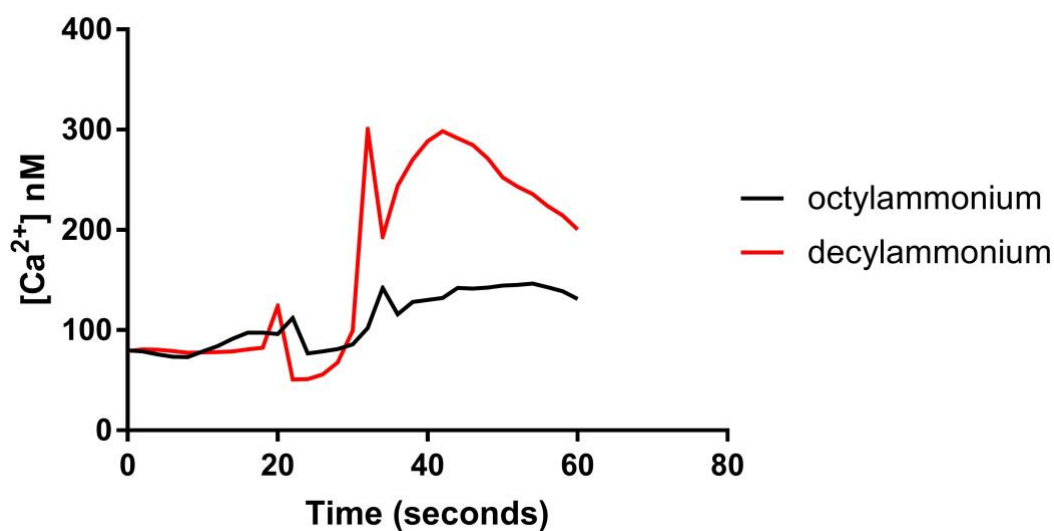


Figure 5-3: Effects of octylammonium and decylammonium on intracellular calcium.

Calculated intracellular calcium concentration following the introduction of octylammonium or decylammonium (1mM) in MCF7 cells preloaded with Fura-2 dye. Artefacts are introduced at 20 and 34 seconds due to the opening of the light-tight chamber required for the introduction of the drugs at 30 seconds.

Dihexylammonium produced a similar response as that seen with decylammonium. In contrast, treatment with trihexylammonium caused a fall in intracellular calcium (Figure 5-4). Unfortunately, due to time constraints, I was unable to pursue this observation, which remains a single experiment.

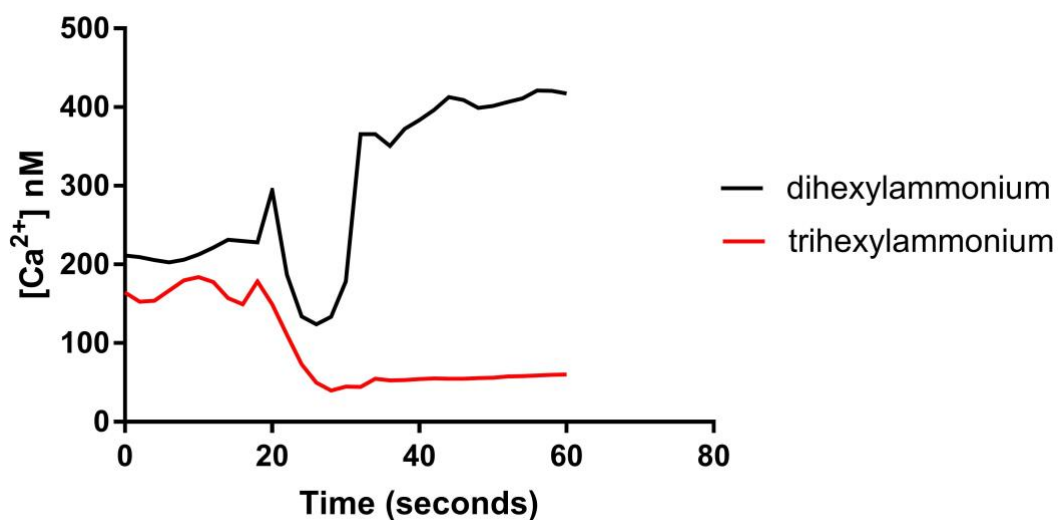


Figure 5-4: Effects of dihexylammonium and trihexylammonium on intracellular calcium.

Calculated intracellular calcium concentration following the introduction of dihexylammonium or trihexylammonium (1mM) in MC7 cells preloaded with Fura-2 dye. Artefacts are introduced at 20 and 34 seconds due to the opening of the light-tight chamber required for the introduction of the drugs at 30 seconds.

A second agent which appeared to lower intracellular calcium was AG-205 (Figure 5-6). Addition caused a dose-dependent decline in the signal. This could be considered surprising as AG-205 was found to promote a decrease in metabolic activity.

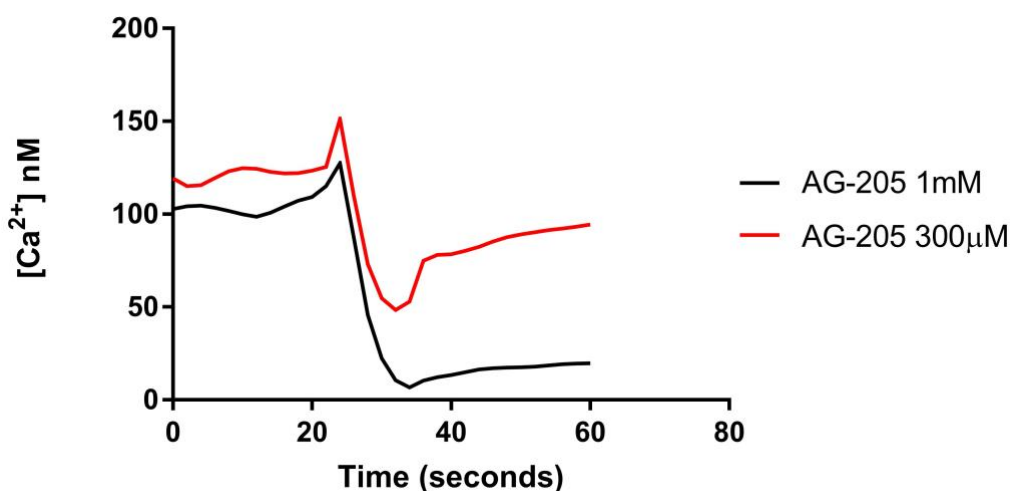


Figure 5-5: Effects of AG-205 on intracellular calcium.

Calculated intracellular calcium concentration following the introduction of AG-205 (1mM or 300 μ M) in MCF7 cells preloaded with Fura-2 dye. Artefacts are introduced at 22 and 36 seconds due to the opening of the light-tight chamber required for the introduction of the drugs at 30 seconds.

Whether this apparent reduction in intracellular calcium was real was brought into question when the fluorescence of AG-205 alone was monitored: as with rimcazole, AG-205 appeared to interfere with the Fura-2 based assay. A small change in ratio observed in Figure 5-6 may account for this finding. All other drugs tested (apart from rimcazole, see above and trihexylammonium, not tested) did not interfere with the ratiometric signal.

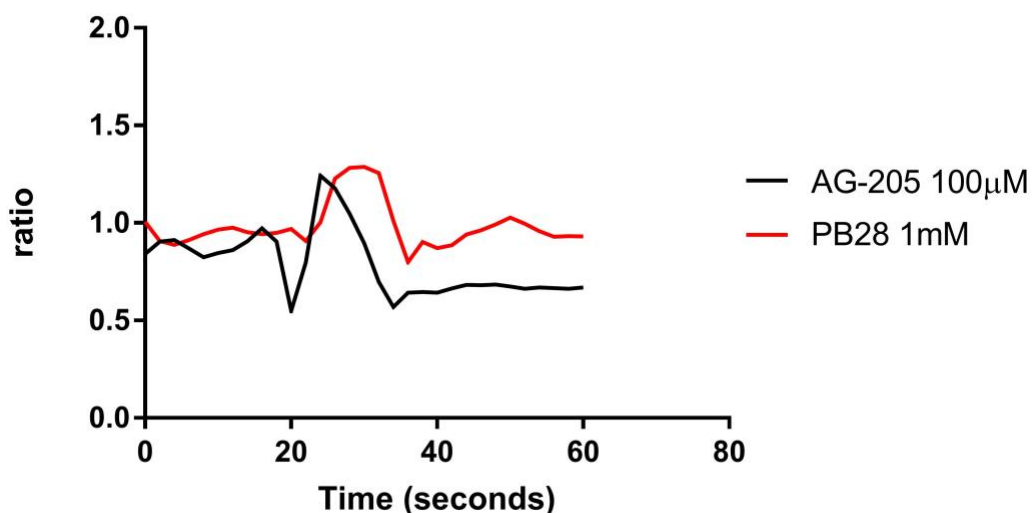


Figure 5-6: Effects of AG-205 and PB28 on Fura-2's ratiometric signal

Figure showing change in fluorescence following addition of PB28 (1mM) or AG-205 (100µM) to KLB containing no fluorophore. Ratio refers to fluorescence emitted at 520 nm after excitation at 340nm and 380 nm. Artefacts are introduced at 20 and 36 seconds due to the opening of the light-tight chamber required for the introduction of the drugs at 30 seconds.

The small decrease in ratiometric signal was initially missed, permitting many experiments to be performed with AG-205. Clearly, such data requires careful analysis and are readily prone to overanalysis.

Of the commercial ligands tested, (+) pentazocine caused only a small response, whereas progesterone was more effective (Figure 5-7). The progesterone response looked slower than that of others. This may be due to the drug first precipitating then going into solution as it becomes diluted.

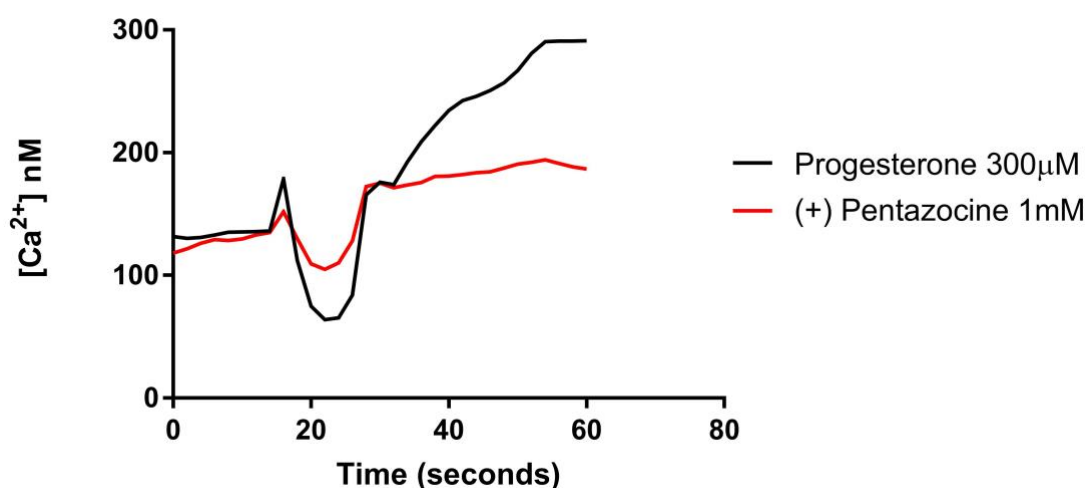


Figure 5-7: Effects of progesterone and (+) pentazocine on intracellular calcium.

Calculated intracellular calcium concentration following the introduction of progesterone (300µM) or (+) pentazocine (1mM) in MCF7 cells preloaded with Fura-2 dye. Artefacts are introduced at 16 and 32 seconds due to the opening of the light-tight chamber required for the introduction of the drugs at 30 seconds. Precipitation was observed with higher concentrations of progesterone and may have also caused the delayed response observed at the dose shown above.

Higher concentrations of progesterone caused a large dip in the signal which recovered more slowly (Figure 5-8). It is assumed that this was due to precipitation followed by the progesterone slowly redissolving.

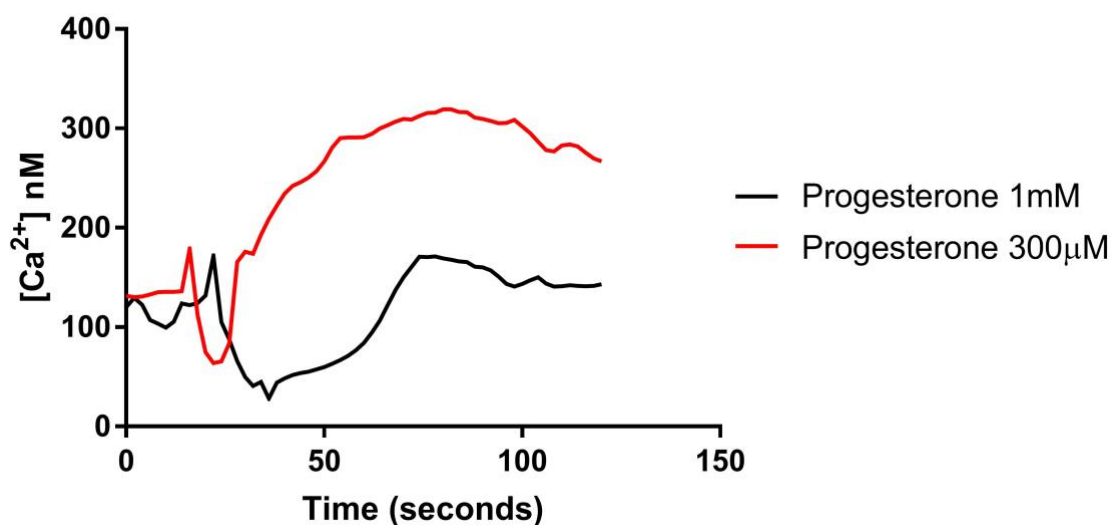


Figure 5-8: Effects of Progesterone on intracellular calcium.

Calculated intracellular calcium concentration following the introduction of progesterone (300µM or 1mM) in MCF7 cells preloaded with Fura-2 dye. Artefacts are introduced at 16/22 and 32/36 seconds due to the opening of the light-tight chamber required for the introduction of the drugs at 30 seconds. Note the longer time scale on the x-axis.

PB28 gave a robust calcium signal, whereas SM21 appeared to give a very small response indeed (Figure 5-9), routinely raising calcium levels by 30nM.

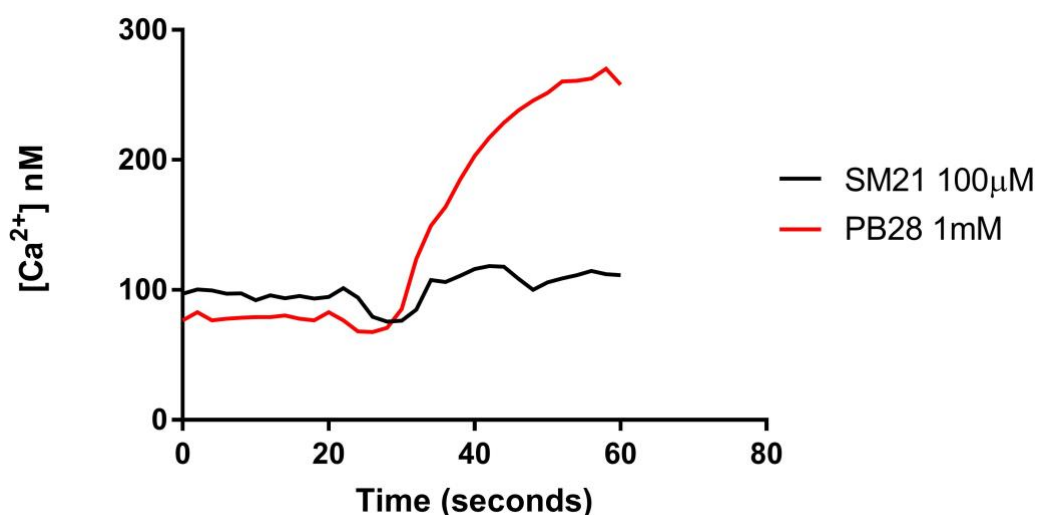


Figure 5-9: Effects of SM21 and PB28 on intracellular calcium

Calculated intracellular calcium concentration following the introduction of PB28 (1mM) or SM21 (100µM) in MCF7 cells preloaded with Fura-2 dye. Artefacts are introduced at 20 and 34 seconds due to the opening of the light-tight chamber required for the introduction of the drugs at 30 seconds. Precipitation

was observed with higher concentrations of progesterone and may have also caused the delayed response observed at the dose shown above.

Both ifenprodil and haloperidol caused increases in intracellular calcium, although haloperidol appeared more efficacious raising calcium by 220nM compared to 130nM (Figure 5-10).

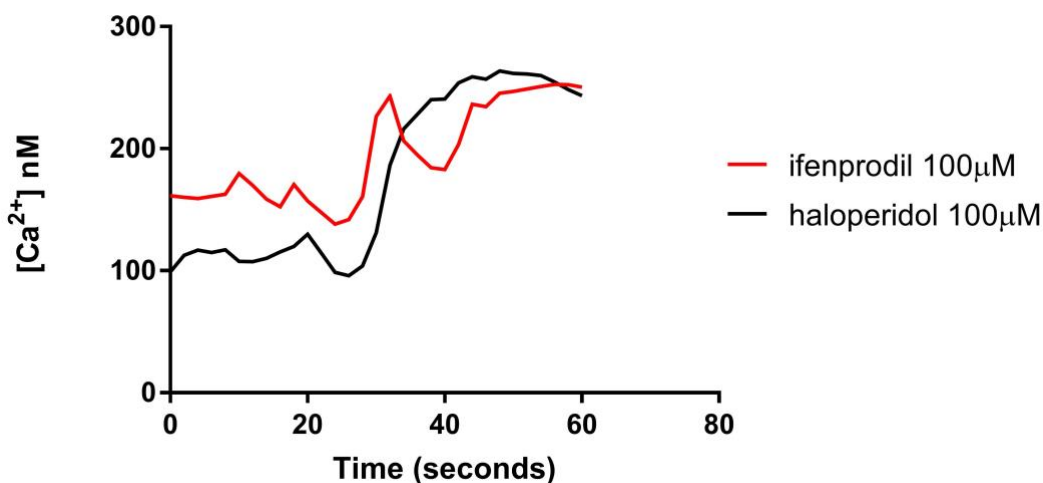


Figure 5-10: Effects of ifenprodil and haloperidol on intracellular calcium.

Calculated intracellular calcium concentration following the introduction of ifenprodil (100µM) or haloperidol (100µM) in MCF7 cells preloaded with Fura-2 dye. Artefacts are introduced at 20 and 34 seconds due to the opening of the light-tight chamber required for the introduction of the drugs at 30 seconds.

The above results comparing pIC₅₀ at the sigma-2 binding site and calcium responses in MCF cells are summarised below (Table 5-6 and Figure 5-11: pIC₅₀ and calcium response in MCF7 cells with sigma-2 binding site ligands. From my experiments, while limited, it is clear that there is no correlation between pIC₅₀ of an agent acting through sigma-2 binding sites and their ability to mobilise calcium. It should also be noted that two agents (haloperidol and progesterone) did not cause a decrease in metabolic activity yet were able to produce a robust calcium response; these cannot be shown on the graph. It is noteworthy that PB28 has previously been found not to drive a calcium response (Cassano et al., 2006).

Ligand	pIC₅₀ *	Calcium response (nM), mean ± SEM	n
Octylammonium (1mM)	3.13	130 ± 40	5
Decylammonium (1mM)	4.06	330 ± 180	3
Dihexylammonium (1mM)	3.40	210 ± 30	3
Dicyclohexylammonium (1mM)	4.06	0	1
Dioctylammonium (1mM)	4.44	Precipitation seen	1
Trihexylammonium (1mM)	3.9	-100	1
AG-205 (1mM-100µM)	3.4	See text	
Haloperidol (100µM)	No effect	220 ± 120	3
Ifenprodil (100µM)	3.6	130 ± 50	3
PB28 (100µM)	3.55	140 ± 30	3
(+) Pentazocine (1mM)	3.8	80 ± 30	3
Progesterone (300µM)	No effect	160 ± 110 (range)	2
Rimcazole	4.47	Unable to test	
SM21 (100µM)	4.0	33 ± 8	3

Table 5-6: Summary of pIC₅₀ and calcium response to sigma-2 binding site ligands

Compilation of pIC₅₀ and calcium response to the noted concentration of ligand in MCF7 cells. n values are also shown for calcium response experiments. * SEM removed for clarity; these values can be found earlier in this chapter. Unpaired 1-way ANOVA, with p value adjusted for multiple comparisons, shows

no significant difference in the ability to elicit a calcium response [$F(8,19) = 1.17$, $p = 0.369$].

These ammonium salts have been tested before on MDA-MB-468 cells at lower doses and were found to have no effect on calcium or metabolic activity.

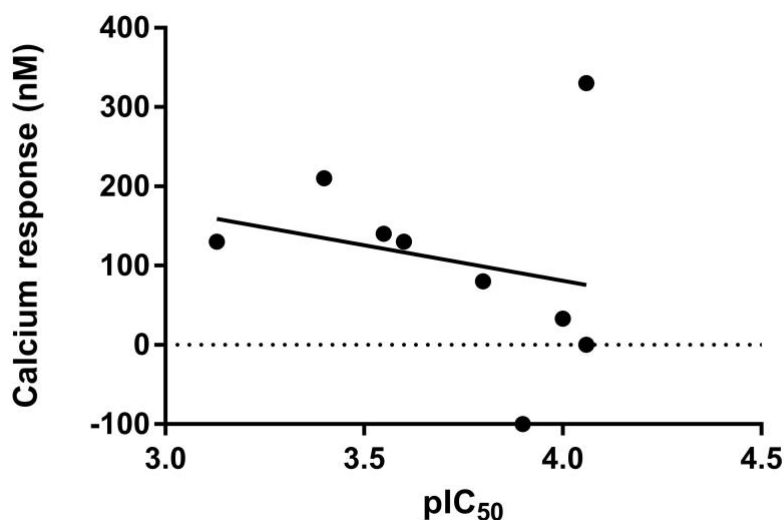


Figure 5-11: pIC₅₀ and calcium response in MCF7 cells with sigma-2 binding site ligands.

Comparison of pIC₅₀ for reduction in metabolic activity of sigma-2 ligands with the size of calcium response in MCF7 cells. Linear regression shows the line $y = -89.74x + 439.9$, $R^2 = 0.055$ [$F(1,7) = 0.41$, $p = 0.54$], indicating no significant correlation between pIC₅₀ and maximum calcium response.

5.2.8 Is there evidence for sigma-1 receptor and sigma-2 binding site cross talk?

The presence of sigma-2 binding sites on all tumour cell lines tested so far, along with similar findings with sigma-1 receptors, which have been found in all but one cell line (MCF7) led me to then test whether the ligands described, which often bind to both sigma-1 and sigma-2 sites would act additively, synergistically or in opposition. Those found to reduce metabolic activity in MCF7 cells were, therefore, tested in A549 and MDA-MB-468 cells. These cells contain a mixture of sigma-1 receptors and sigma-2 binding sites (Chapter 3).

Ligand	sigma-1 receptor affinity (pK _i) *	sigma-2 binding site affinity (pK _i) #	pIC ₅₀ MCF7 \$	pIC ₅₀ MDA- MB-468	pIC ₅₀ A549
Octylammonium	6.1	5.2	3.13	<4*	3.9 ± 0.06
Decylammonium	6.5	5.4	4.06	<4*	4.7 ± 0.09
Dihexylammonium	6.8	7.5	3.40	<4*	3.6 ± 0.12
Dicyclohexyl Ammonium	5.8	6.8	3.75	3.9 ± 0.1	2.9 ± 0.09
Diethylammonium	n.d.	7.9	4.44	5.0 ± 0.2	4.9 ± 0.00
Trihexylammonium	8.1	6.6	3.9	<4*	4.2 ± 0.2
(+) Pentazocine	8.5	6.4	3.80	3.8 ± 0.1	3.8 ± 0.13
Rimcazole	6.2	6.2	4.47	4.4 ± 0.2*	4.7 ± 0.15
Ifenprodil	n.d.	9.4	3.6	4.3 ± 0.3	3.9 ± 0.04
SM21	n.d.	7.2	4.0	3.9 ± 0.04	3.9 ± 0.18
AG-205	n.d.	5.4	3.38	3.8 ± 0.10	3.7 ± 0.2
PB28	n.d.	7.8	3.55	3.9 ± 0.03	4.0 ± 0.07

Table 5-7: Summary of sigma-1 receptor and sigma-2 binding affinities and pIC₅₀ values for inhibition of metabolic activities in MCF7, MDA-MB-468 and A549 cells

Table of sigma-1 receptor and sigma-2 binding affinities and pIC₅₀ values for inhibition of metabolic activities in MCF7, MDA-MB-468 and A549 cells. Values represent mean ± SEM values where n=3-8 independent values. * data taken from (Brimson, 2010), *, #, \$ SEM removed for clarity; these values can be found in *Brimson (2010), #Chapter 4 and \$earlier in this chapter, respectively. n.d., not determined. Unpaired student's t-test shows that octylammonium and decylammonium are significantly more potent against A549 cells over MCF7 cells (p = 0.0001, p = 0.0018 respectively). Unpaired 1-way ANOVA, followed by post hoc Tukey ("all means") comparison (where appropriate), with p value adjusted for multiple comparisons, shows dicyclohexylammonium is significantly

more potent [$F(2,9) = 47.2$, $p < 0.0001$] against A549 cells over MCF7 ($p < 0.0001$) and MDA-MB-468 cells ($p < 0.0001$). Dioctylammonium [$F(2,9) = 5.77$, $p = 0.024$] is significantly more potent against MCF7 cells over A549 ($p = 0.027$). PB28 [$F(2,9) = 10.6$, $p = 0.0043$] is significantly more potent against MCF7 cells over both MDA-MB-468 cells ($p = 0.019$) and A549 cells ($p = 0.0045$).

From the above table, it is clear that the presence of sigma-1 receptors did not affect the potency of these ligands. This was the case for those found by Brimson (Brimson, 2010) to be agonists (all ammonium salts shown, (+) pentazocine) or antagonists (rimcazole) at the sigma-1 receptor. No further analyses were undertaken.

5.3 Discussion

5.3.1 Definition of agonist and antagonist at the Sigma-2 binding site

I have shown that these simple primary, secondary, tertiary and quaternary ammonium salts show graded affinity for the sigma-2 binding site. These experiments were performed using membranes from sonicated MCF7 cells. Returning to the intact cell scenario, many compounds with affinity for the sigma-2 binding site had no effect on metabolic activity. Does this make them antagonists? No, despite a recent paper in this area claiming this to be the case (Zeng et al., 2014). For these agents to be classified as antagonists, they must hinder an agonist from performing its functions. This was not the case with these agents.

In any emerging field, it is often the early adopters who are permitted to define particular parameters. The sigma-2 binding site has been proven of interest to mostly those in the area of oncology, yet sigma-2 ligands have also been found to affect behaviour. Sigma-2 ligands that induce neck dystonia (a marked deviation in head angle) when injected into the red nucleus in one hemisphere of experimental animals have been defined as agonists. In such assays, antagonists are able to reverse the effects of agonists (Ghelardini et al., 2000).

In oncology, an agonist has been defined as a ligand that reduces cellular activity (determined using MTS) – often assumed synonymous with cell death. The mechanism or mechanisms underlying death are unclear. Activation of a calcium response is occasionally seen coupled with activation of caspase-3. At other times, no calcium response has been observed. The defining of an antagonist has been less clear. Some papers appear to avoid the conflict, merely describing all agents as “ligands” (Abate et al., 2011). Unfortunately, Zeng *et al.* have tried to redefine agonists, partial agonists and antagonists merely by their “cytotoxic effects” – using the MTS procedure. Using a single dose of agent, any agent causing over 90% death after 24 hours was defined a full agonist (Zeng et al., 2014). Death of 10-90% of cells was caused by partial agonists. Less than 10% death was effected by antagonists. To date (21/01/17) this paper has been cited 10 times. This highly flawed approach unfortunately undermines the area.

Others correctly describe agents that are cytotoxic (or those reducing metabolic activity) as agonists, their effects being reversed by antagonists (Abate et al., 2012, Colabufo et al., 2004).

Of course, using different tissue and different assays can give different results. A classic example would that of tamoxifen, which acts as an antagonist in the breast, but a partial agonist in the uterus (Dowsett and Howell, 2002). Closer to home, sigma-1 receptor antagonists also show differences, with their effects on tumour cell line (producing a large calcium response and causing cell death) and cerebellar granule cells (no calcium response, very limited cell death) being the reason for the hope that they can act as tumour specific anticancer drugs (Spruce et al., 2004).

The effects of decylammonium, while only slight, could suggest that it was acting as a partial agonist at the sigma-2 binding site. While it was capable of causing a reduction in metabolic activity, it was also able to partially reverse the

effects of rimcazole in the same assay. The affinities of the adamantylammonium compounds for the sigma-2 binding site were comparable with the more simple structure of decylammonium, but the crown-like structures have a lower logD, perhaps making them too lipid insoluble to access the interior of the cell.

When comparing the effects of the secondary ammonium salts, once again affinity increased with increasing size of the side chains. Introduction of a second alkyl group has increased affinity by over 100-fold: the highest affinity of a primary ammonium salt (decylammonium) had a pK_i 5.4, in comparison dioctylammonium had a pK_i of 7.9. A branched chain compound (bis-2-ethylhexylammonium) bound with much lower affinity and did not affect metabolism of MCF7 cells. This was highly surprising, as branched chains are important in the distinction of agonists and antagonists at the sigma-1 receptor (Brimson, 2010). While bis-2-(ethyl)hexylammonium also showed reduced activity for the sigma-1 receptor when compared with dioctylammonium, it was able to reduce metabolic activity in MDA-MB-468 cells and reduce growth of MAC 13 mouse adenocarcinoma cells transplanted into NMRI mice *in vivo* (Brimson, 2010).

Dioctylammonium gave some strange results: in my studies, it was the most effective at reducing metabolic activity, yet also partially reversed the effects of rimcazole. Reasons for this are unclear. The concept of a partial agonist is difficult to comprehend with respect to the sigma-2 binding site as its molecular identity remains shrouded. It is noted that this phenomenon was also seen with decylammonium.

Trihexylammonium also gave somewhat confusing data. While it was capable of reducing metabolic activity when used alone, it was also able to partially reverse the effects of rimcazole. Furthermore, trihexylammonium appeared to lower resting calcium levels in these cells (although this was $n=1$), suggesting that there may be more than one pathway involved. The previously published

data showing that rimcazole drives a calcium signal (Spruce et al., 2004) has to be ignored as it has also been shown to give a false positive signal in Fura-2 based assays (Brimson et al., 2011). Further information could be obtained for rimcazole, AG-205 and trihexylammonium by using a calcium sensor with different spectral qualities. The Fura-2 method has several advantages, two being that it is well understood and the ratiometric calculation allows intracellular calcium concentration to be determined. Many other dyes are available, so comparing the absorbance spectra for rimcazole, AG-205 and trihexylammonium with the properties of commercially available calcium dyes should allow further experimentation on these compounds.

Ligand	Sigma-2 binding site affinity (pK _i) *	nH *	pIC ₅₀ MCF7 §	IC ₅₀ /K _i
Octylammonium	5.2	0.9	3.13	118
Decylammonium	5.41	0.92	4.06	22.4
Dihexylammonium	7.58	0.68	3.40	15100
Dicyclohexylammonium	6.86	0.72	3.75	1290
Diethylammonium	7.9	0.6	4.44	2670
Trihexylammonium	6.63	0.7	3.9	538
(+) Pentazocine	6.45	0.73	3.80	446
Rimcazole	6.2	0.7	4.47	53.8
Ifenprodil	9.4	0.5	3.6	628000
SM21	7.2	0.63	4.0	1590
AG-205	5.40	1.06	3.38	105
PB28	7.84	0.5	3.55	19500

Table 5-8: Summary of characteristics of sigma-2 binding site ligands

Table highlighting the affinity of ligands for the sigma-2 binding site, the Hill slope of binding and the pIC₅₀ for reduction in metabolic activity. The ratio of IC₅₀/K_i has also been calculated. *, § SEM removed for clarity; these values can be found in * Chapter 4 or § earlier in this chapter.

On comparing IC₅₀ values with K_i values, it was clear that all dose-response curves lie well to the right of the binding curves. Normally, this would be considered “impossible”. In many cases above, one would have to assume that over 99% of receptors have to be occupied before an effect is seen. This has been described before. Using a less-well characterised sigma ligand (¹¹C-SA4503) and uptake assays opposed to ligand binding, Rybczynska *et al.* showed sigma ligands were required at concentrations approximately 100-fold

higher to prevent proliferation as was required to prevent uptake (Rybczynska et al., 2008). A number of explanations are possible. I shall discuss the most plausible here:

Ifenprodil has previously been described as both a sigma-2 agonist (Ishima and Hashimoto, 2012) and antagonist (Shin et al., 2007) as well as binding sigma-1 and NMDA receptors (Ishima and Hashimoto, 2012); (Hashimoto and London, 1995). Both NMDA receptors (North et al., 2010) and alpha-2 receptors (Vazquez et al., 1999) have been found in MCF7 cells.

My data showed that spermine was without effect in our assays. Spermine is reported to cause cell death by activation of the NMDA receptor, an effect reversed by ifenprodil and a non-competitive NMDA receptor antagonist, MK-801 (de Vera et al., 2008). However, the effects of a range of sigma-2 ligands was not affected by MK-801 in MCF7 cells (Brent and Pang, 1995). This would suggest that these receptors are not involved in my observations regarding the sigma-2 binding site.

AG-205 has been used to argue whether the sigma-2 binding site is the PGRMC1, showing both moderate affinity (10 μ M displacing 70-90% [¹²⁵I]-RHM-4 binding in mouse mammary 66 and HeLa cells (Xu et al., 2011) as well as low affinity >10,000nM, (Abate et al., 2015b) binding to sigma-2 binding sites. The picture from this study further clouded the matter, AG-205 binding with an affinity of 4 μ M, aligning more closely with data from (Xu et al., 2011).

SM21 has previously been described as a sigma-2 binding site antagonist using a behavioural assay, reversing the effects of DTG (Ghelardini et al., 2000). The complex nature of these assays and the clear difference in outcomes working on a target in non-cancerous cells means no parallels or correlation can be drawn at this time. SM21 had previously been shown not to bind sigma-1 receptors or 5HT₃ and 5HT₄ receptors (Mach et al., 1999). As expected (due to its similarity to the muscarinic receptor antagonist atropine), it does bind

muscarinic receptors with K_i 174nM (Gualtieri et al., 1994). No other information regarding its selectivity seems available. From these data, it is unlikely that the effects of SM21 can be ascribed to any other receptor, but it remains possible.

Little is known about PB28. It is described as a mixed sigma-1/sigma-2 ligand (Berardi et al., 1996), specifically a mixed sigma-2 agonist/sigma-1 antagonist (Colabufo et al., 2004) that does not effect calcium release, but indeed blocks inositol 1,4,5-trisphosphate and calcium-induced calcium release (Cassano et al., 2006). PB28 has also been shown to block P-glycoprotein (Colabufo et al., 2009a). Binding of tritiated PB28 to MCF7 cells could be completely abolished by DTG and haloperidol at low doses (Colabufo et al., 2008) suggesting some level of selectivity of PB28 binding to the sigma-2 site. Interestingly, homologous competition assays with unlabelled PB28 showed a low Hill slope. Using PB28 and related ligands, Pati *et al.* (Pati et al., 2017) have proposed the mechanism of action in cytotoxicity relates to mitochondrial superoxide production.

Taking these issues together, one can argue that the only common known factor is the presence of sigma-2 binding sites in MCF7 cells. The explanation regarding comparisons between equilibrium binding to membranes and *in vivo* metabolic activity needs to be addressed.

5.3.2 Correlation between Hill slope and agonistic behaviour

Until the molecular identity of the sigma-2 binding site is established, it is difficult to determine whether differences in Hill slopes for these agents is significant. The classic comparison of high- and low-affinity binding of agonists to heterotrimeric G-protein coupled receptors which only recognise antagonists with a single affinity has been suggested for the sigma-1 receptor (Brimson et al., 2011). In this case, agonists binding with the same affinity, whereas antagonists expose a GTP-sensitive high-affinity state of the receptor. An explanation behind this observation awaits discovery.

A range of Hill slopes was identified when binding was considered, ranging from 0.5 (ifenprodil, the agent with the largest discrepancy between pIC_{50} and pK_i : 628,000 fold) to AG-205 (nH 1.06, pIC_{50}/pK_i 105). On plotting nH against $\log(IC_{50}/K_i)$, a negative correlation appeared to exist, although one can accept that the data are from a relatively small group (12 data points) – the lower the Hill slope, the greater the difference between binding affinity and inhibition of metabolic activity. While I have taken the time to consider Hill slopes, no previous publication has done so, so I am unable to add further data points to determine how representative my data are. A parallel is drawn with the sigma-1 receptor. Although much work had been done previously, it was this lab (Brimson et al., 2011) who first showed that sigma-1 receptors bound agonists with a Hill slope of unity, whereas the anticancer antagonists showed low and high affinity states. The high affinity state in that case was GTP-sensitive, suggesting that the sigma-1 receptor is G-protein coupled. Brimson further showed that the anti-cancer properties of antagonists could be related to the Hill slope and difference between high and low affinity states – the greater the difference, the more effective as an anticancer drug. Although the sigma-1 receptor and sigma-2 binding site are believed to be very different on a molecular level, one can speculate that a similar process could be taking place here. This correlation between Hill slope and IC_{50}/K_i was only discovered following completion of access to the laboratory, so I am unable to pursue this observation. Hence, I would propose: further testing of other compounds believed to reduce metabolic activity through the sigma-2 binding site and a more detailed study of the Hill slopes of binding using many more concentrations of the cytotoxic drugs. The competition curves would need to be repeated in the absence and presence of GTP and suramin (Brimson et al., 2011) to see if the Hill slope reverted to unity upon their addition. Should binding be sensitive to GTP, I would advise the use of bacterial toxins known to interact directly with heterotrimeric G-proteins: pertussis toxin to disrupt coupling to G_i (Hausdorff et al., 1990) cholera toxin to disrupt coupling to G_s

(Sidhu et al., 1998) removing high-affinity, GTP-sensitive binding to receptors coupling through these receptors.

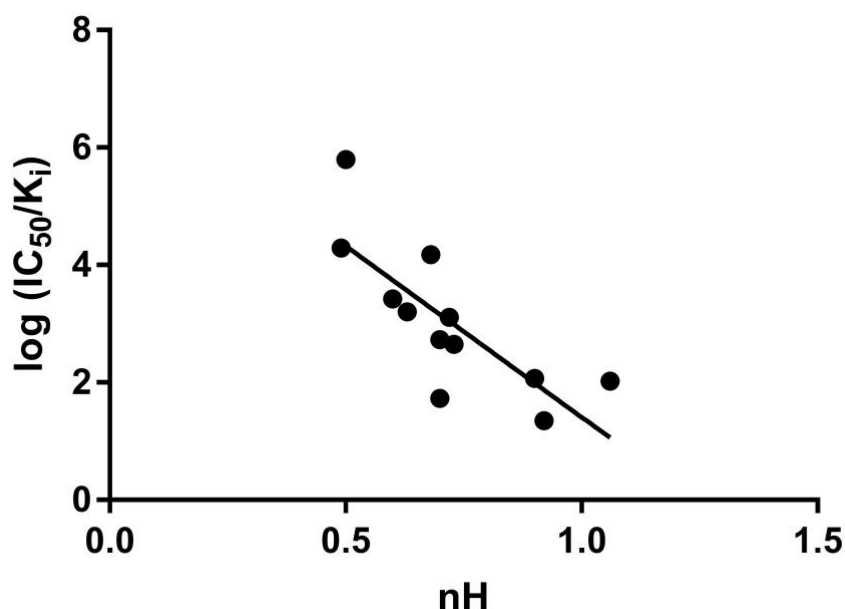


Figure 5-12: Relationship between Hill slope (nH) and log (IC₅₀/K_i) in MCF7 cells.

Comparison of the Hill slope (nH) for binding of ligands to the sigma-2 binding site and the log of discrepancy between binding K_i and dose required to inhibit metabolic activity by 50% in MCF7 cells. Linear regression shows the line $y = -5.8x + 7.2$, $R^2 = 0.61$ [$F(1,10) = 15.7$, $p = 0.0027$], indicating a statistically significant correlation.

Whilst such a correlation is familiar with GPCRs, the pEC₅₀ is to the left of the pK_i, and we attribute the lower Hill slope to the agonist showing greater selectivity for the active form of the receptor. In this case, the opposite is true – the lower the Hill slope, the greater the relative concentration over the affinity is required. Further work must be undertaken in order to determine whether this is a coincidence or meaningful correlation.

One possible explanation is that agents are able to drive receptors into a new conformation. The low affinity state could exist for a few seconds or less but be part of the drive for reduced metabolic activity/cell death/apoptosis. This could then switch to a high affinity state which is what is seen in equilibrium binding assays. This scenario is seen with the nicotinic receptor. Heidmann *et al.* have

shown that ligand affinity for the nAChR can increase 10,000-fold in less than a minute, as the receptor transitions from a low affinity active form to a high affinity desensitised form through an intermediate affinity (Heidmann et al., 1983). Several similar studies with different combinations of nAChR components show that desensitisation and recovery rates vary greatly (Quick and Lester, 2002). Other ligand-gated receptors show similar properties, including GABA(A) receptors (Chang et al., 2002) and, possibly, the 5-HT₃ receptor (Sepulveda et al., 1991). Interestingly, this final paper shows a much smaller discrepancy between binding and EC₅₀ for a partial agonist.

It is proposed that phosphorylation plays a part in nAChR desensitisation, as with many other receptors, including G-protein coupled (Tobin, 2008) and tyrosine kinase receptors (Yamamoto et al., 2014). My experimental design (preparing washed membranes) would have greatly diluted, if not removed, ATP and hence would suggest that sigma-2 binding sites are not phosphorylated during the protocol used.

In order to determine whether such a change from low to high affinity could occur with the sigma-2 binding site at this time would be problematic. I could propose looking at time courses of binding association and dissociation of sigma-2 ligands (the 12 above would be a good starting point, especially as ifenprodil is in clinical trials (Ifenprodil tartrate treatment of adolescents with post-traumatic stress disorder: a double blind placebo controlled trial. NCT01896388)).

If one could observe a step which would suggest a switching from low to high affinity one could speculate this to be plausible. However, as the sigma-2 binding site is intracellular and there are several unknowns I would advise such assays to be undertaken once the target's identity has been verified. Even then, this may be difficult as the low affinity, active state may be very short-lived and there is no suggestion that the protein would have channel-like activity.

Measuring potential conformational changes could be impossible, especially with the lack of tools available.

A second factor to consider is whether there is a physiological reason for such a switch. Moving to a high-affinity, desensitised state would “encourage” agonist binding to this state, mopping up ligand, and reducing the opportunity for an accidental activation caused by binding to active receptors which would then drive cell death.

5.3.3 Do Sigma-2 ligands meet Lipinski’s rule of Five

A further factor to consider which can explain the discrepancy between binding affinities and the IC₅₀ for inhibition of metabolic activity as the cellular localisation of the sigma-2 binding site. Using antibodies prepared against the PGRMC1 receptor, showed it was present in the nucleus, cytoplasm and at the segments of the plasma membrane (Peluso et al., 2009). Earlier work has described it as predominantly nuclear (Engmann et al., 2011). Fluorescent labelling of novel sigma-2 binding site ligands showed they are internalised via an active, endocytic pathway. In contrast to the work obtained with antibodies, Zeng *et al.* showed that sigma-2 ligands were concentrated in the mitochondria, endoplasmic reticulum, lysosomes and plasma membranes (Zeng et al., 2011, Zeng et al., 2007). Using a similar approach, Abate *et al.* (2010) showed fluorescent analogues of PB28 were endocytosed to the endoplasmic reticulum and lysosome (Abate et al., 2010). Of course, with such an approach it is easy to envision user-introduced artefacts. The presence of a ligand does not necessarily determine the presence of the binding partner. Equally, such drugs may alter the processing and location of their targets. More traditional approaches, including sub-cellular fractionation have been tried. Using this approach, Gebreselassie and Bowen (2004) proposed the sigma-2 binding site was located in the membrane lipid rafts (Gebreselassie and Bowen, 2004).

These factors would suggest that the sigma-2 binding site is not readily available to ligands approaching the cell. Although quite varied and unclear, all the locations mentioned above are intracellular, possibly nuclear, indicating that the ligand will have to traverse the plasma membrane to gain access and bind. In order to assess what barriers these compounds may have to overcome, I have considered their physicochemical natures.

Such a scenario was famously assessed by Chris Lipinski, working at Pfizer. His assessment of physicochemical properties of drugs and whether they were orally active allowed him to propose that predictions can be made as to the relative success of future drugs in such a setting. Lipinski's "rule of 5" states that "poor absorption or permeation is more likely when there are more than 5 H-bond donors, 10 H-bond acceptors, the molecular weight is greater than 500 and the calculated logP (the calculated logarithm of the partition coefficient between n-octanol and water) is greater than 5" (Lipinski et al., 2001). Whilst I am not considering the oral absorption of these drugs, these guidelines also help guide whether such materials will enter cells *in vitro*. Analysis of these compounds should also determine whether they meet all 5 of Lipinski's "rules".

One consideration for access to the interior of the cell is how charged molecules pass through the membrane. Classical understanding is that they would not be able to traverse the hydrophobic region comprising the tails of phospholipids. Many organic cation and anion transporters (OCT and OATs) exist. These merely permit a route for such molecules to traverse down a concentration gradient across the membrane (Girardin, 2006).

However, the membrane distribution of charged amines has been known for some time not to follow that expected from the octanol:water distribution coefficient. Indeed, charged amines have a surprisingly high membrane affinity (Austin et al., 1995). Austin *et al.* also showed that amlodipine, an L-type calcium channel blocker that is a primary amine, had vastly different membrane:aqueous distribution than octanol:water. As such, this charged

molecule is able to act on the L-type calcium channel at a site embedded in the membrane (Tang et al., 2014). It is possible that the alkyl tail of these ammonium salts aligns with the hydrophobic tails of the phospholipids and the positively charged head interacts with the negatively charged phosphate groups of the phospholipids (Austin et al., 1995). Such interactions are not possible with the uncharged octanol. Whether this would lock the ammonium salts into a single conformation in the plasma membrane and inhibit transfer is unclear.

Further predictions regarding these compounds can be achieved. Their likeliness of crossing the blood brain barrier, again despite being charged, appears high. Clark has highlighted 5 'rules of thumb' regarding such permeation predictions (Clark, 2003):

1. Sum of N + O < 5
2. $\text{clogP} - (\text{N} + \text{O}) > 0$
3. Polar surface area (PSA) < 60-70 Å²
4. MW < 450
5. $1 < \log D < 3$

Clark also says that a +1 charge favours access of drugs to the brain, but that $\text{pK}_a > 10$ does not. This second factor would exclude most of the compounds discussed here (Clark, 2003, Fischer et al., 1998).

Ligand	clogD (pH 7.4)	MW*	logP	Hydrogen bond donors/ acceptors	pK _a	Charge at pH 7.4	PSA
Propylammonium	-2.45	95.6	0.40	1/1	10.7	+1	26
Butylammonium	-2.12	109.6	0.93	1/1	10.8	+1	26
Pentylammonium	-1.34	123.7	1.46	1/1	10.6	+1	26
Hexylammonium	-1.02	137.7	1.99	1/1	10.2	+1	26
Octylammonium	-0.07	165.7	3.06	1/1	10.2	+1	27.6
Decylammonium	1.07	193.7	4.12	1/1	10.6	+1	27.6
1-adamantyl ammonium	-0.37	187.7	2.22	1/1	10.7	+1	26
2-adamantyl ammonium	-0.61	187.2		1/1	10.5	+1	26
Dimethyl ammonium	-3.18	81.6	-0.43	1/1	10.5	+1	12
Diethylammonium	-2.21	109.6	0.63	1/1	10.5	+1	12
Dipropylammonium	-1.25	137.7	1.70	1/1	10.7	+1	12
Diisopropyl ammonium	-1.45	137.7	1.33	1/1	10.7	+1	12
Dibutylammonium	-0.43	165.7	2.76	1/1	10.7	+1	12
Diisobutyl ammonium	-0.61	165.7	2.39	1/1	11.0	+1	12
Di sec butyl ammonium	-0.62	165.7	2.39	1/1	10.9	+1	12
Dipentyl ammonium	0.65	193.8	3.82	1/1	10.7	+1	12
Dihexyl Ammonium	1.38	221.8	4.88	1/1	10.7	+1	12
Dicyclohexyl ammonium	0.62	217.8	3.69	1/1	11.1	+1	12
Bis-2-ethylhexyl ammonium	3.38	277.9	6.64	1/1	11.1	+1	12
Diocetylammmonium	3.88	277.9	7.01	1/1	10.7	+1	12
Trimethyl ammonium	-2.14	95.6	0.06	0/1	9.5	+1	3.2

Triethyl ammonium	-1.18	137.7	1.66	0/1	10.2	+1	3.2
Ethyl-diisopropyl ammonium	-0.55	165.7	2.35	0/1	10.7	+1	3.2
Tripropyl ammonium	0.52	179.8	3.25	0/1	10.8	+1	3.2
Triisopropyl ammonium	-0.18	179.8	2.70	0/1	11.0	+1	3.2
Tributyl ammonium	1.69	221.8	4.84	0/1	10.8	+1	3.2
Triisobutyl ammonium	2.03	220.8	4.29	0/1	11.5	+1	3.2
Tripentyl ammonium	3.73	263.9	6.44	0/1	10.8	+1	3.2
Triisopentyl ammonium	2.68	263.9	5.89	0/1	10.9	+1	3.2
Trihexyl ammonium	4.85	306.0	8.03	0/1	10.8	+1	3.2
Tri-octyl ammonium	8.10	390.1	11.22	0/1	10.8	+1	3.2
Tridodecyl ammonium	14.50	558.5	17.60	0/1	10.8	+1	3.2
Tetramethyl ammonium	-3.15	109.6	-2.89	0/1	-	+1	0
Tetraethyl ammonium	-2.79	165.7	-3.17	0/1	-	+1	0
Tetrapropyl ammonium	-1.77	221.9	-2.64	0/1	-	+1	0
Tetrabutyl ammonium	-0.64	278	-1.72	0/1	-	+1	0
(+) Pentazocine	2.26	285.4	4.53	1/2	9.5, 10.4	+0.99	23.5
Haloperidol	2.65	375.9	3.01	1/3	8.0, 13.9	+0.82	40.5
DTG	2.31	239.3	3.77	2/3	10.6	+1	50.4
Rimcazole	2.63	321.5	5.10	1/3	4.0, 9.8	+1	20.2
Progesterone	3.72	314.5	4.04	0/2	-	0	34.1

IPAG	2.74	395.3	5.42	3/3	-1.41, 10.61	+1	50.4
RU-486	5.16	429.6	4.95	1/3	4.8, 12.8	0	40.5
Ifenprodil	1.66	325.4	4.25	2/3	9.0, 9.6, 14.0	+0.97	43.7
PPCC	2.17	379.5	2.90	1/4	8.7, 14.0	+0.95	249
SM21	1.19	337.8	3.64	0/4	9.3	+0.99	38.8
SKF 10047	2.16	257.2	3.46	½	9.3, 10.3	+0.99	23.5
AG-205	2.46	455.0	5.39	0/7	8.0, 8.6, 12.4, 14.5	+1.74	92.4
Spermidine	-5.91	145.2	-0.84	5/3	8.1, 10.0, 10.6	+2.84	64.1
Spermine	-6.78	202.3	-0.96	6/4	7.8, 8.4, 10.3,1 0.8	+3.73	76.1

Table 5-9: Physicochemical properties of all the ligands

Table showing a range of physicochemical properties of the ligands tested in this thesis. * MW of hydrochloride salt, where appropriate. Values are obtained using ACD from chemspider.com and chemicalize.com. Values in **italic bold** are outside Lipinski's rules.

The pK_a values of all the simple amines is above 10. This would mean that these compounds are protonated and hence positively charged at all times under physiological conditions. Looking at the calculated log of the

octanol:water partition coefficient (clogD), most of the compounds tested have clogD values below 5. Although I present logP (partition coefficient of the uncharged species) as well as clogD, I have chosen to focus on clogD, as this is more appropriate to consider when most compounds are highly charged. As can be seen in Table 5-9, most of the compounds tested meet Lipinski's rule of 5. A group of tertiary ammonium salts have logP greater than 5, with the corresponding clogD of the highest ammonium salts also exceeding 5. Several highly prized laboratory tools (rimcazole, IPAG and AG-205) also possess logP values over 5. As these materials also possess a positive charge at pH 7.4, their clogD values are all well below 5.

One may consider that access to the sigma-2 binding site may then, be the barrier to inhibiting cellular metabolism. In comparing $\log (IC_{50}/K_i)$ with clogD there is clearly no correlation, and so this explanation can be dismissed (Table 5-10 and figure 5-13).

Compound	clogD	IC ₅₀ /K _i
Octylammonium	-0.07	118
Decylammonium	1.07	22.4
Dihexylammonium	1.38	15100
Dicyclohexylammonium	0.62	1290
Diocetylammmonium	3.88	2670
Trihexylammonium	4.85	538
(+) Pentazocine	2.26	446
Rimcazole	2.63	53.8
Ifenprodil	1.66	628000
SM21	1.19	1590
AG-205	2.46	105
PB28	3.6	19500

Table 5-10: log (IC₅₀/K_i) and clogD of sigma-2 binding site ligands.

Table showing the showing clogD and ratio between IC₅₀ in MTS assays and K_i of binding to membranes of MCF7 cells of a range of sigma-2 ligands.

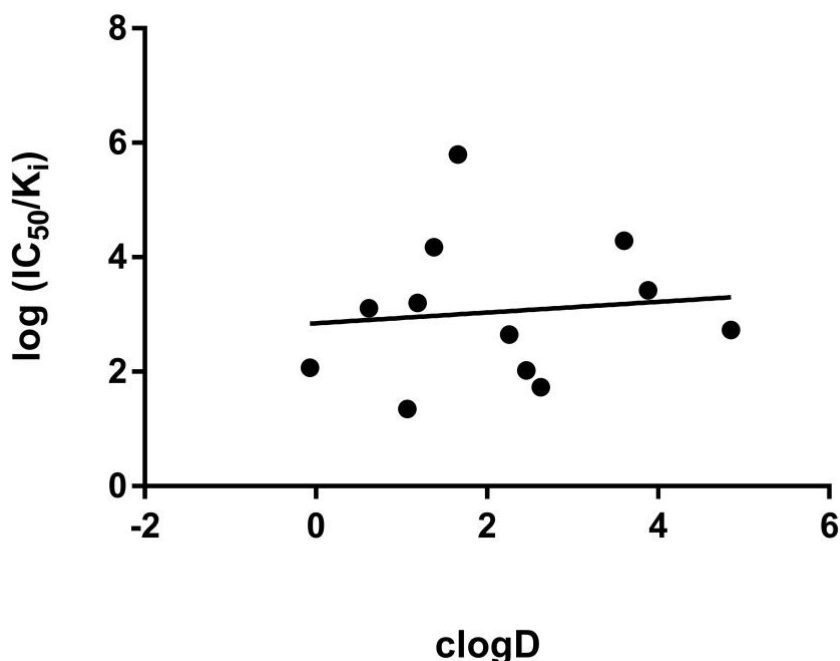


Figure 5-13: log (IC₅₀/K_i) and clogD of sigma-2 binding site ligands.

Plot showing lack of correlation between clogD and log of ratio between IC₅₀ in MTS assays and K_i of binding to membranes of MCF7 cells. Linear regression shows the line $y = 0.094x + 2.8$, $R^2 = 0.012$ [$F(1,10) = 0.12$, $p = 0.74$], indicating no correlation.

PB28, another sigma-2 binding site ligand, has been used as a lead compound in identifying clinically useful compounds. PB28 was considered too lipophilic, with clogD (7.4) 3.99, logP 5.05, for development as a positron emission tomography (PET) or single photon emission computed tomography (SPECT) agent, being described as “abundantly out of the range that was considered optimal”, which is estimated as being around log D (7.4) 2.0-2.5. (Abate et al., 2011).

In summary, I have characterised a series of novel sigma-2 ligands as well as several previously identified commercial ligands. Some of these appeared to reduce cellular proliferation in MCF7 cells; I believe these effects were mediated by the sigma-2 binding site. Several of these compounds also affected intracellular calcium concentration. There appeared to be no or little correlation between the ability of a compound to elicit a calcium response and its ability to reduce metabolic activity of a cell. Likewise, there was no

correlation between a sigma-2 ligand's ability to access the cell interior and cause a reduction in metabolic activity.

In this respect, my attempts to determine and identify agonists at the sigma-2 binding site have been unsuccessful. Without knowing the molecular identity of the sigma-2 binding site such molecules may prove difficult to characterise. A recent publication suggests that CM572 is a partial agonist. It is described as a cytotoxic agent that mobilises calcium, is selectively toxic towards cancer cell lines and partially reverses the effects of the sigma-2 agonist, CB-64D (Nicholson et al., 2015). I, too, have observed agonists that are effective at reducing metabolic activity also partially reverse the effects of rimcazole. The mechanism may be specific, or related to how much organic cations are able to enter the cell. The reduction observed may be competition on cell entry rather than effects at the binding site.

More importantly, there does appear to be a correlation between the Hill slope of binding of a ligand and its ability to reduce metabolic activity. Equally, the decreased Hill slope of binding correlates well with the discrepancy between the K_i of binding and the IC_{50} in MTS assays. This discrepancy, while frequently noted, has not previously been explained. I propose that agonists at the sigma-2 binding site are able to drive a response when binding to a low-affinity state of the binding site and then cause desensitisation of the receptor. This desensitised state of the receptor possesses a much higher affinity than the active state and explains the discrepancy previously observed.

Chapter 6. Discussion

The debate regarding the identity of the sigma-2 binding site continues, with most focus on whether or not it is the progesterone receptor membrane component-1. This controversy will be soon resolved and interested parties can continue studying the regulation and therapeutic uses of this site. Levels of the sigma-2 binding site do seem related to proliferative status of a cell and so all tumours appear to express this protein (with some reservation, as some systems may have been mis-labelled as possessing sigma-2 binding sites when, in fact, they have merely seen “unmasked” sigma-1 receptors, discussed in chapter 3). The use of sigma-2 ligands in imaging looks likely to become a reality, with several successful animal models. Indeed, while no data have yet been published on the completed phase 1 clinical trials NCT00968656, recruitment for further phase 1 trials has already started (NCT02762110 NCT02284919, to determine whether such tools should join the battery of agents in the imaging and treatment of cancers.

The effects of certain ligands on cancer cells causing reduced cell proliferation and apoptosis should also continue to be studied. The results shown here confirm that the binding pocket for ligands/agonists is far more simple than previously described. Earlier findings were, perhaps, starting from a point where complex drugs were being tested for other receptors (e.g., sigma-1) which were then found to also act at the sigma-2 binding site.

These results will have a positive effect on the sigma-2 field in several ways:

6.1 Correct designation of sigma-1 and sigma-2 levels in cells and tissue.

The use of masking agents (pentazocine and dexrallorphan) and cells expressing sigma-1 receptors must be reconsidered. It is shown clearly that protocols using a pan sigma radioligand (DTG) and cells or tissue expressing both sigma-1 receptors and sigma-2 binding sites presents many issues the researchers cannot address or compensate for. Whiles the use of [³H] (+)

pentazocine for sigma-1 studies appears safe due to its low affinity for the sigma-2 binding site, sigma-2 binding assays must be revised. It can be recommended to use [³H] DTG and cells or tissues lacking sigma-1 receptors (as is used here, with MCF7 cells verified as lacking sigma-1 receptors). Equally, the development and use of novel sigma-2-selective fluorescent or radioligands would be satisfactory once characterised. The use of [³H] DTG in competition assays with selective sigma-1 or sigma-2 ligands would also be a recommended means by which total sigma B_{\max} and proportion of sigma-1: sigma-2 sites can be determined. This may (and does in my hands) result in different determinations of sigma-1 receptor density, which may be important. However, it appears that many researchers are interested in the relative ratios of these sites in cells and tissue, as such it appears to be a more transparent and direct assessment of this. Also, the use of a single radioligand to characterise both sites removes the problems caused by artefacts introduced when working with two drugs with unknown contaminants or levels of chemical decay, as described by Lazareno and Birdsall (Lazareno and Birdsall, 2000) By using [³H] (+) pentazocine and [³H] DTG to characterise, then compare, the two sigma sites two sets of independent errors are introduced. As Segal's Law states, "A man with a watch knows the time, a man with two is never sure".

6.2 Identification of simple, high-affinity ligands.

Having redefined the manner in which sigma-2 binding sites should be characterised, it was then shown that simple ammonium salts show a structure-affinity relationship, with increasing alkyl chain length affecting affinity for primary, secondary and tertiary ammonium salts. The affinities of the highest affinity ammonium salts was not dissimilar to that of many commercial ligands used in sigma-2 studies in this thesis and many publications.

It is, however, in the characterisation of the pharmacological effects of sigma-2 ligands that I wish to focus here. Several key observations and hypotheses that will aid research in this area.

6.3 Biologically active drugs have a low Hill slope

Firstly, the Hill slope of the binding of agents that were effective in decreasing cellular metabolic activity was low. This observation should now be further assessed. Do these findings suggest that the sigma-2 binding site has more than one affinity state for cytotoxic ligands. Are these high affinity states sensitive to the addition of GTP, which would suggest that the sigma-2 binding site is coupled through G-proteins. My findings are based on a relatively small number of drugs tested. Large-scale tests would be required before such an observation could be used in predicting whether a sigma-2 ligand is an agonist (causing cytotoxicity) or antagonist (preventing the effects of an agonist). Should my prediction hold up, high-throughput screening of compounds becomes a possibility: looking for agents with low Hill slopes to identify active drugs.

6.4 Sigma-2 activity is not related to calcium or lipophilicity

It has previously been proposed that a correlation exists between the ability of sigma-2 ligands to drive a calcium response. Whilst the original data showed only a very weak correlation, my results would strongly argue against this. Equally, as the sigma-2 binding site is believed to be located inside the cell, access may require passage through the plasma membrane. I have shown that there is no correlation between the lipophilicity of a compound and its ability to drive a biological effect.

6.5 Desensitisation of sigma-2 binding sites raises the affinity.

A further observation on the effects of these drugs affecting metabolic activity, is the possibility that sigma-2 binding sites have an active and desensitised state. Previous publication in this field have not explained how and why the EC_{50} for any biological effect through this binding site is much higher than the affinity for the site. One such explanation described it necessary to occupy

99 % of the sigma-2 binding sites before a biological effect is observed (Rybczynska et al., 2008). This is contrary to pharmacological understanding, yet remains a commonly held belief. Taking the corollary from ligand-gated ion channels, I propose that an agonist binds to a low-affinity state of the receptor which causes a biological effect. This receptor then undergoes desensitisation to a high-affinity state, which is the one observed when equilibrium competition binding assays are performed. Returning to point 3 above, there was also a strong correlation between low Hill slope for binding and the discrepancy between binding K_i and EC_{50} for reducing metabolic activity. In the case of ligand-gated ion channels, this desensitisation step occurs very rapidly (on the millisecond or second level). Testing for such a step with the sigma-2 binding protein will require far more advanced tools than we have at the moment. Such a concept can be revisited once the molecular identity of sigma-2 binding sites has been established. I am unaware that desensitised receptors of any other class show a shift to a high affinity than active receptors. One very provocative question can then be raised: is the sigma-2 binding site a ligand-gated ion channel?

Reference List

- ABATE, C., ELENEWSKI, J., NISO, M., BERARDI, F., COLABUFO, N. A., AZZARITI, A., PERRONE, R. & GLENNON, R. A. 2010. Interaction of the sigma(2) receptor ligand PB28 with the human nucleosome: computational and experimental probes of interaction with the H2A/H2B dimer. *ChemMedChem*, 5, 268-73.
- ABATE, C., FERORELLI, S., NISO, M., LOVICARIO, C., INFANTINO, V., CONVERTINI, P., PERRONE, R. & BERARDI, F. 2012. 2-Aminopyridine derivatives as potential sigma(2) receptor antagonists. *ChemMedChem*, 7, 1847-57.
- ABATE, C., MOSIER, P. D., BERARDI, F. & GLENNON, R. A. 2009. A structure-affinity and comparative molecular field analysis of sigma-2 (sigma2) receptor ligands. *Cent Nerv Syst Agents Med Chem*, 9, 246-57.
- ABATE, C., NISO, M., INFANTINO, V., MENGA, A. & BERARDI, F. 2015a. Elements in support of the 'non-identity' of the PGRMC1 protein with the sigma2 receptor. *Eur J Pharmacol*, 758, 16-23.
- ABATE, C., NISO, M., LACIVITA, E., MOSIER, P. D., TOSCANO, A. & PERRONE, R. 2011. Analogues of sigma receptor ligand 1-cyclohexyl-4-[3-(5-methoxy-1,2,3,4-tetrahydronaphthalen-1-yl)propyl]piperazine (PB28) with added polar functionality and reduced lipophilicity for potential use as positron emission tomography radiotracers. *J Med Chem*, 54, 1022-32.
- ABATE, C., PATI, M. L., CONTINO, M., COLABUFO, N. A., PERRONE, R., NISO, M. & BERARDI, F. 2015b. From mixed sigma-2 receptor/P-glycoprotein targeting agents to selective P-glycoprotein modulators: small structural changes address the mechanism of interaction at the efflux pump. *Eur J Med Chem*, 89, 606-15.
- ABLORDEPPEY, S. Y., FISCHER, J. B. & GLENNON, R. A. 2000. Is a nitrogen atom an important pharmacophoric element in sigma ligand binding? *Bioorg Med Chem*, 8, 2105-11.
- ABLORDEPPEY, S. Y., FISCHER, J. B., LAW, H. & GLENNON, R. A. 2002. Probing the proposed phenyl-A region of the sigma-1 receptor. *Bioorg Med Chem*, 10, 2759-65.
- AHMED, I. S., ROHE, H. J., TWIST, K. E., MATTINGLY, M. N. & CRAVEN, R. J. 2010. Progesterone receptor membrane component 1 (Pgrmc1): a heme-1 domain protein that promotes tumorigenesis and is inhibited by a small molecule. *J Pharmacol Exp Ther*, 333, 564-73.
- AL-NABULSI, I., MACH, R. H., WANG, L. M., WALLEN, C. A., KENG, P. C., STEN, K., CHILDERS, S. R. & WHEELER, K. T. 1999. Effect of ploidy, recruitment, environmental factors, and tamoxifen treatment on the expression of sigma-2 receptors in proliferating and quiescent tumour cells. *Br J Cancer*, 81, 925-33.
- ALMONTE-BECERRIL, M., NAVARRO-GARCIA, F., GONZALEZ-ROBLES, A., VEGA-LOPEZ, M. A., LAVALLE, C. & KOURI, J. B. 2010. Cell death of chondrocytes is a combination between apoptosis and autophagy during

- the pathogenesis of Osteoarthritis within an experimental model. *Apoptosis*, 15, 631-8.
- AUSTIN, R. P., DAVIS, A. M. & MANNERS, C. N. 1995. Partitioning of ionizing molecules between aqueous buffers and phospholipid vesicles. *J Pharm Sci*, 84, 1180-3.
- AYDAR, E., PALMER, C. P. & DJAMGOZ, M. B. 2004. Sigma receptors and cancer: possible involvement of ion channels. *Cancer Res*, 64, 5029-35.
- BELANGER, P. A., BEAUDIN, J. & ROY, S. 2011. High-throughput screening of microbial adaptation to environmental stress. *J Microbiol Methods*, 85, 92-7.
- BEM, W. T., THOMAS, G. E., MAMONE, J. Y., HOMAN, S. M., LEVY, B. K., JOHNSON, F. E. & COSCIA, C. J. 1991. Overexpression of sigma receptors in nonneural human tumors. *Cancer Res*, 51, 6558-62.
- BERARDI, F., ABATE, C., FERORELLI, S., COLABUFO, N. A. & PERRONE, R. 2009. 1-Cyclohexylpiperazine and 3,3-dimethylpiperidine derivatives as sigma-1 (sigma1) and sigma-2 (sigma2) receptor ligands: a review. *Cent Nerv Syst Agents Med Chem*, 9, 205-19.
- BERARDI, F., COLABUFO, N. A., GIUDICE, G., PERRONE, R., TORTORELLA, V., GOVONI, S. & LUCCHI, L. 1996. New sigma and 5-HT_{1A} receptor ligands: omega-(tetralin-1-yl)-n-alkylamine derivatives. *J Med Chem*, 39, 176-82.
- BERNAS, T. & DOBRUCKI, J. 2002. Mitochondrial and nonmitochondrial reduction of MTT: interaction of MTT with TMRE, JC-1, and NAO mitochondrial fluorescent probes. *Cytometry*, 47, 236-42.
- BERTHA, C. M., MATTSON, M. V., FLIPPEN-ANDERSON, J. L., ROTHMAN, R. B., XU, H., CHA, X. Y., BECKETTS, K. & RICE, K. C. 1994. A marked change of receptor affinity of the 2-methyl-5-(3-hydroxyphenyl)morphans upon attachment of an (E)-8-benzylidene moiety: synthesis and evaluation of a new class of sigma receptor ligands. *J Med Chem*, 37, 3163-70.
- BERTHA, C. M., VILNER, B. J., MATTSON, M. V., BOWEN, W. D., BECKETTS, K., XU, H., ROTHMAN, R. B., FLIPPEN-ANDERSON, J. L. & RICE, K. C. 1995. (E)-8-benzylidene derivatives of 2-methyl-5-(3-hydroxyphenyl)morphans: highly selective ligands for the sigma 2 receptor subtype. *J Med Chem*, 38, 4776-85.
- BLACK, J. W. & LEFF, P. 1983. Operational models of pharmacological agonism. *Proc R Soc Lond B Biol Sci*, 220, 141-62.
- BOOTH, R. G. & BALDESSARINI, R. J. 1991. (+)-6,7-benzomorphan sigma ligands stimulate dopamine synthesis in rat corpus striatum tissue. *Brain Res*, 557, 349-52.
- BOUCHARD, P. & QUIRION, R. 1997. [³H]1,3-di(2-tolyl)guanidine and [³H](+)pentazocine binding sites in the rat brain: autoradiographic visualization of the putative sigma1 and sigma2 receptor subtypes. *Neuroscience*, 76, 467-77.
- BOWEN, W. D. 2000. Sigma receptors: recent advances and new clinical potentials. *Pharm Acta Helv*, 74, 211-8.
- BOWEN, W. D. 2001. Sigma receptors and iboga alkaloids. *Alkaloids Chem Biol*, 56, 173-91.

- BOWEN, W. D., BERTHA, C. M., VILNER, B. J. & RICE, K. C. 1995. CB-64D and CB-184: ligands with high sigma 2 receptor affinity and subtype selectivity. *Eur J Pharmacol*, 278, 257-60.
- BOWEN, W. D., TOLENTINO, P. J., KIRSCHNER, B. N., VARGHESE, P., DE COSTA, B. R. & RICE, K. C. 1993. Sigma receptors and signal transduction: negative modulation of signaling through phosphoinositide-linked receptor systems. *NIDA Res Monogr*, 133, 69-93.
- BRACQUART, D., COUSIN, C., CONTREPAS, A. & NGUYEN, G. 2009. [The prorenin receptor]. *J Soc Biol*, 203, 303-10.
- BRADFORD, M. M. 1976. A rapid and sensitive method for the quantitation of microgram quantities of protein utilizing the principle of protein-dye binding. *Anal Biochem*, 72, 248-54.
- BRENT, P. J., PANG, G., LITTLE, G., DOSEN, P. J. & VAN HELDEN, D. F. 1996. The sigma receptor ligand, reduced haloperidol, induces apoptosis and increases intracellular-free calcium levels $[Ca^{2+}]_i$ in colon and mammary adenocarcinoma cells. *Biochem Biophys Res Commun*, 219, 219-26.
- BRENT, P. J. & PANG, G. T. 1995. Sigma binding site ligands inhibit cell proliferation in mammary and colon carcinoma cell lines and melanoma cells in culture. *Eur J Pharmacol*, 278, 151-60.
- BRIMSON, J. M. 2010. *The pharmacology of the sigma-1 receptor*. Doctor of Philosophy (PhD), University of Bath.
- BRIMSON, J. M., BROWN, C. A. & SAFRANY, S. T. 2011. Antagonists show GTP-sensitive high-affinity binding to the sigma-1 receptor. *Br J Pharmacol*, 164, 772-80.
- BROWN, D. A. & LONDON, E. 1998. Functions of lipid rafts in biological membranes. *Annu Rev Cell Dev Biol*, 14, 111-36.
- BROWN, D. A. & LONDON, E. 2000. Structure and function of sphingolipid- and cholesterol-rich membrane rafts. *J Biol Chem*, 275, 17221-4.
- BROWN, D. A. & ROSE, J. K. 1992. Sorting of GPI-anchored proteins to glycolipid-enriched membrane subdomains during transport to the apical cell surface. *Cell*, 68, 533-44.
- CAHILL, M. A. 2007. Progesterone receptor membrane component 1: an integrative review. *J Steroid Biochem Mol Biol*, 105, 16-36.
- CASSANO, G., GASPARRE, G., CONTINO, M., NISO, M., BERARDI, F., PERRONE, R. & COLABUFO, N. A. 2006. The sigma-2 receptor agonist PB28 inhibits calcium release from the endoplasmic reticulum of SK-N-SH neuroblastoma cells. *Cell Calcium*, 40, 23-8.
- CHAKRABARTI, R., KUNDU, S., KUMAR, S. & CHAKRABARTI, R. 2000. Vitamin A as an enzyme that catalyzes the reduction of MTT to formazan by vitamin C. *J Cell Biochem*, 80, 133-8.
- CHAN, F. K., MORIWAKI, K. & DE ROSA, M. J. 2013. Detection of necrosis by release of lactate dehydrogenase activity. *Methods Mol Biol*, 979, 65-70.
- CHANG, Y., GHANSAH, E., CHEN, Y., YE, J. & WEISS, D. S. 2002. Desensitization mechanism of GABA receptors revealed by single oocyte binding and receptor function. *J Neurosci*, 22, 7982-90.
- CHENG, Y. & PRUSOFF, W. H. 1973. Relationship between the inhibition constant (K_1) and the concentration of inhibitor which causes 50 per cent

- inhibition (I50) of an enzymatic reaction. *Biochem Pharmacol*, 22, 3099-108.
- CHOI, S. R., YANG, B., PLOSSL, K., CHUMPRADIT, S., WEY, S. P., ACTON, P. D., WHEELER, K., MACH, R. H. & KUNG, H. F. 2001. Development of a Tc-99m labeled sigma-2 receptor-specific ligand as a potential breast tumor imaging agent. *Nucl Med Biol*, 28, 657-66.
- CHU, E. C. & TARNAWSKI, A. S. 2004. PTEN regulatory functions in tumor suppression and cell biology. *Med Sci Monit*, 10, RA235-41.
- CHU, U. B., MAVLYUTOV, T. A., CHU, M. L., YANG, H., SCHULMAN, A., MESANGEAU, C., MCCURDY, C. R., GUO, L. W. & RUOHO, A. E. 2015. The Sigma-2 Receptor and Progesterone Receptor Membrane Component 1 are Different Binding Sites Derived From Independent Genes. *EBioMedicine*, 2, 1806-13.
- CHU, W., XU, J., ZHOU, D., ZHANG, F., JONES, L. A., WHEELER, K. T. & MACH, R. H. 2009. New N-substituted 9-azabicyclo[3.3.1]nonan-3alpha-yl phenylcarbamate analogs as sigma2 receptor ligands: synthesis, in vitro characterization, and evaluation as PET imaging and chemosensitization agents. *Bioorg Med Chem*, 17, 1222-31.
- CLARK, D. E. 2003. In silico prediction of blood-brain barrier permeation. *Drug Discov Today*, 8, 927-33.
- COLABUFO, N. A., ABATE, C., CONTINO, M., INGLESE, C., FERORELLI, S., BERARDI, F. & PERRONE, R. 2008. Tritium radiolabelling of PB28, a potent sigma-2 receptor ligand: pharmacokinetic and pharmacodynamic characterization. *Bioorg Med Chem Lett*, 18, 2183-7.
- COLABUFO, N. A., BERARDI, F., CONTINO, M., FAZIO, F., MATARRESE, M., MORESCO, R. M., NISO, M., PERRONE, R. & TORTORELLA, V. 2005. Distribution of sigma receptors in EMT-6 cells: preliminary biological evaluation of PB167 and potential for in-vivo PET. *J Pharm Pharmacol*, 57, 1453-9.
- COLABUFO, N. A., BERARDI, F., CONTINO, M., FERORELLI, S., NISO, M., PERRONE, R., PAGLIARULO, A., SAPONARO, P. & PAGLIARULO, V. 2006. Correlation between sigma2 receptor protein expression and histopathologic grade in human bladder cancer. *Cancer Lett*, 237, 83-8.
- COLABUFO, N. A., BERARDI, F., CONTINO, M., NISO, M., ABATE, C., PERRONE, R. & TORTORELLA, V. 2004. Antiproliferative and cytotoxic effects of some sigma2 agonists and sigma1 antagonists in tumour cell lines. *Naunyn Schmiedebergs Arch Pharmacol*, 370, 106-13.
- COLABUFO, N. A., BERARDI, F., CONTINO, M., PERRONE, R. & TORTORELLA, V. 2003. A new method for evaluating sigma(2) ligand activity in the isolated guinea-pig bladder. *Naunyn Schmiedebergs Arch Pharmacol*, 368, 106-12.
- COLABUFO, N. A., BERARDI, F., PERRONE, M. G., CANTORE, M., CONTINO, M., INGLESE, C., NISO, M. & PERRONE, R. 2009a. Multi-drug-resistance-reverting agents: 2-aryloxazole and 2-arylthiazole derivatives as potent BCRP or MRP1 inhibitors. *ChemMedChem*, 4, 188-95.
- COLABUFO, N. A., CONTINO, M., INGLESE, C., NISO, M., PERRONE, R., ROPERTO, S. & ROPERTO, F. 2009b. In vitro and ex vivo

- characterization of sigma-1 and sigma-2 receptors: agonists and antagonists in biological assays. *Cent Nerv Syst Agents Med Chem*, 9, 161-71.
- COLLIER, A. C. & PRITSOS, C. A. 2003. The mitochondrial uncoupler dicumarol disrupts the MTT assay. *Biochem Pharmacol*, 66, 281-7.
- COUETTE, B., FAGART, J., JALAGUIER, S., LOMBES, M., SOUQUE, A. & RAFESTIN-OBLIN, M. E. 1996. Ligand-induced conformational change in the human mineralocorticoid receptor occurs within its hetero-oligomeric structure. *Biochem J*, 315 (Pt 2), 421-7.
- CRATTERI, P., ROMANELLI, M. N., CRUCIANI, G., BONACCINI, C. & MELANI, F. 2004. GRIND-derived pharmacophore model for a series of alpha-tropanyl derivative ligands of the sigma-2 receptor. *J Comput Aided Mol Des*, 18, 361-74.
- CRAWFORD, K. W. & BOWEN, W. D. 2002. Sigma-2 receptor agonists activate a novel apoptotic pathway and potentiate antineoplastic drugs in breast tumor cell lines. *Cancer Res*, 62, 313-22.
- CRAWFORD, K. W., COOP, A. & BOWEN, W. D. 2002. sigma(2) Receptors regulate changes in sphingolipid levels in breast tumor cells. *Eur J Pharmacol*, 443, 207-9.
- CRIDDLE, D. N., GERASIMENKO, J. V., BAUMGARTNER, H. K., JAFFAR, M., VORONINA, S., SUTTON, R., PETERSEN, O. H. & GERASIMENKO, O. V. 2007. Calcium signalling and pancreatic cell death: apoptosis or necrosis? *Cell Death Differ*, 14, 1285-94.
- DE VERA, N., MARTINEZ, E. & SANFELIU, C. 2008. Spermine induces cell death in cultured human embryonic cerebral cortical neurons through N-methyl-D-aspartate receptor activation. *J Neurosci Res*, 86, 861-72.
- DEBONNEL, G. 1993. Current hypotheses on sigma receptors and their physiological role: possible implications in psychiatry. *J Psychiatry Neurosci*, 18, 157-72.
- DEL CASTILLO, J. & KATZ, B. 1957. Interaction at end-plate receptors between different choline derivatives. *Proc R Soc Lond B Biol Sci*, 146, 369-81.
- DOBROWSKY, R. T. 2000. Sphingolipid signalling domains floating on rafts or buried in caves? *Cell Signal*, 12, 81-90.
- DOWSETT, M. & HOWELL, A. 2002. Breast cancer: aromatase inhibitors take on tamoxifen. *Nat Med*, 8, 1341-4.
- EDIDIN, M. 2003. The state of lipid rafts: from model membranes to cells. *Annu Rev Biophys Biomol Struct*, 32, 257-83.
- ENGMANN, L., ROMAK, J., NULSEN, J., BENADIVA, C. & PELUSO, J. 2011. In vitro viability and secretory capacity of human luteinized granulosa cells after gonadotropin-releasing hormone agonist trigger of oocyte maturation. *Fertil Steril*, 96, 198-202.
- EVERAERT, H., FLAMEN, P., FRANKEN, P. R., VERHAEGHE, W. & BOSSUYT, A. 1997. Sigma-receptor imaging by means of I123-IDAB scintigraphy: clinical application in melanoma and non-small cell lung cancer. *Anticancer Res*, 17, 1577-82.

- FIEDLER, K., KOBAYASHI, T., KURZCHALIA, T. V. & SIMONS, K. 1993. Glycosphingolipid-enriched, detergent-insoluble complexes in protein sorting in epithelial cells. *Biochemistry*, 32, 6365-73.
- FISCHER, H., GOTTSCHLICH, R. & SEELIG, A. 1998. Blood-brain barrier permeation: molecular parameters governing passive diffusion. *J Membr Biol*, 165, 201-11.
- GALBIATI, F., RAZANI, B. & LISANTI, M. P. 2001. Emerging themes in lipid rafts and caveolae. *Cell*, 106, 403-11.
- GEBRESELASSIE, D. & BOWEN, W. D. 2004. Sigma-2 receptors are specifically localized to lipid rafts in rat liver membranes. *Eur J Pharmacol*, 493, 19-28.
- GHELARDINI, C., GALEOTTI, N. & BARTOLINI, A. 2000. Pharmacological identification of SM-21, the novel sigma(2) antagonist. *Pharmacol Biochem Behav*, 67, 659-62.
- GIRARDIN, F. 2006. Membrane transporter proteins: a challenge for CNS drug development. *Dialogues Clin Neurosci*, 8, 311-21.
- GLENNON, R. A. 2005. Pharmacophore identification for sigma-1 (sigma1) receptor binding: application of the "deconstruction-reconstruction-elaboration" approach. *Mini Rev Med Chem*, 5, 927-40.
- GLENNON, R. A., ABLORDEPPEY, S. Y., ISMAIEL, A. M., EL-ASHMAWY, M. B., FISCHER, J. B. & HOWIE, K. B. 1994. Structural features important for sigma 1 receptor binding. *J Med Chem*, 37, 1214-9.
- GLENNON, R. A., ISMAIEL, A. M., SMITH, J. D., YOUSIF, M., EL-ASHMAWY, M., HERNDON, J. L., FISCHER, J. B., HOWIE, K. J. & SERVER, A. C. 1991a. Binding of substituted and conformationally restricted derivatives of N-(3-phenyl-n-propyl)-1-phenyl-2-aminopropane at sigma-receptors. *J Med Chem*, 34, 1855-9.
- GLENNON, R. A., SMITH, J. D., ISMAIEL, A. M., EL-ASHMAWY, M., BATTAGLIA, G. & FISCHER, J. B. 1991b. Identification and exploitation of the sigma-opiate pharmacophore. *J Med Chem*, 34, 1094-8.
- GLENNON, R. A., YOUSIF, M. Y., ISMAIEL, A. M., EL-ASHMAWY, M. B., HERNDON, J. L., FISCHER, J. B., SERVER, A. C. & HOWIE, K. J. 1991c. Novel 1-phenylpiperazine and 4-phenylpiperidine derivatives as high-affinity sigma ligands. *J Med Chem*, 34, 3360-5.
- GONZALEZ-ALVEAR, G. M. & WERLING, L. L. 1995. Sigma receptor regulation of norepinephrine release from rat hippocampal slices. *Brain Res*, 673, 61-9.
- GROTH-PEDERSEN, L., OSTENFELD, M. S., HOYER-HANSEN, M., NYLANDSTED, J. & JAATTELA, M. 2007. Vincristine induces dramatic lysosomal changes and sensitizes cancer cells to lysosome-destabilizing siramesine. *Cancer Res*, 67, 2217-25.
- GRYNKIEWICZ, G., POENIE, M. & TSIEN, R. Y. 1985. A new generation of Ca²⁺ indicators with greatly improved fluorescence properties. *J Biol Chem*, 260, 3440-50.
- GUALTIERI, F., BOTTALICO, C., CALANDRELLA, A., DEI, S., GIOVANNONI, M. P., MEALLI, S., ROMANELLI, M. N., SCAPECCHI, S., TEODORI, E., GALEOTTI, N. & ET AL. 1994. Presynaptic cholinergic modulators as potent cognition enhancers and analgesic drugs. 2. 2-Phenoxy-, 2-

- (phenylthio)-, and 2-(phenylamino)alkanoic acid esters. *J Med Chem*, 37, 1712-9.
- GUEST, I. & VARMA, D. R. 1991. Developmental toxicity of methylamines in mice. *Journal of Toxicology and Environmental Health, Part A Current Issues*, 32, 319-330.
- GUITART, X., CODONY, X. & MONROY, X. 2004. Sigma receptors: biology and therapeutic potential. *Psychopharmacology (Berl)*, 174, 301-19.
- HAGA, T. 2013. Molecular properties of muscarinic acetylcholine receptors. *Proc Jpn Acad Ser B Phys Biol Sci*, 89, 226-56.
- HANAHAH, D. & WEINBERG, R. A. 2000. The hallmarks of cancer. *Cell*, 100, 57-70.
- HANNER, M., MOEBIUS, F. F., FLANDORFER, A., KNAUS, H. G., STRIESSNIG, J., KEMPNER, E. & GLOSSMANN, H. 1996. Purification, molecular cloning, and expression of the mammalian sigma1-binding site. *Proc Natl Acad Sci U S A*, 93, 8072-7.
- HASHIMOTO, K. & LONDON, E. D. 1995. Interactions of erythro-ifenprodil, threo-ifenprodil, erythro-iodoifenprodil, and eliprodil with subtypes of sigma receptors. *Eur J Pharmacol*, 273, 307-10.
- HAUSDORFF, W. P., HNATOWICH, M., O'DOWD, B. F., CARON, M. G. & LEFKOWITZ, R. J. 1990. A mutation of the beta 2-adrenergic receptor impairs agonist activation of adenylyl cyclase without affecting high affinity agonist binding. Distinct molecular determinants of the receptor are involved in physical coupling to and functional activation of Gs. *J Biol Chem*, 265, 1388-93.
- HEIDMANN, T., OSWALD, R. E. & CHANGEUX, J. P. 1983. Multiple sites of action for noncompetitive blockers on acetylcholine receptor rich membrane fragments from torpedo marmorata. *Biochemistry*, 22, 3112-27.
- HELLEWELL, S. B. & BOWEN, W. D. 1990. A sigma-like binding site in rat pheochromocytoma (PC12) cells: decreased affinity for (+)-benzomorphans and lower molecular weight suggest a different sigma receptor form from that of guinea pig brain. *Brain Res*, 527, 244-53.
- HELLEWELL, S. B., BRUCE, A., FEINSTEIN, G., ORRINGER, J., WILLIAMS, W. & BOWEN, W. D. 1994. Rat liver and kidney contain high densities of sigma 1 and sigma 2 receptors: characterization by ligand binding and photoaffinity labeling. *Eur J Pharmacol*, 268, 9-18.
- HENCHMAN, R. H., WANG, H. L., SINE, S. M., TAYLOR, P. & MCCAMMON, J. A. 2005. Ligand-induced conformational change in the alpha7 nicotinic receptor ligand binding domain. *Biophys J*, 88, 2564-76.
- HEROUX, J. A., TAM, S. W. & DE SOUZA, E. B. 1992. Autoradiographic identification and characterization of sigma receptors in guinea pig brain using [3H]1(cyclopropylmethyl)-4-(2'-(4''-fluorophenyl)-2'-oxoethyl) piperidine ([3H]DuP 734), a novel sigma receptor ligand. *Brain Res*, 598, 76-86.
- HIRANITA, T. 2016. Identification of the Sigma-2 Receptor: Distinct from the Progesterone Receptor Membrane Component 1 (PGRMC1). *J Alcohol Drug Depend*, 4.

- HIRATA, M., MORI, T., UMEDA, T., ABE, T., YAMAMOTO, T. & OHMOMO, Y. 2008. Evaluation of radioiodinated 1-[2-(3,4-Dimethoxyphenyl)ethyl]-4-(2-iodophenylpropyl)piperazine as a tumor diagnostic agent with functional sigma receptor imaging by single photon emission computed tomography. *Biol Pharm Bull*, 31, 879-83.
- HOLLSTEIN, M., SIDRANSKY, D., VOGELSTEIN, B. & HARRIS, C. C. 1991. p53 mutations in human cancers. *Science*, 253, 49-53.
- HORNICK, J. R., XU, J., VANGVERAVONG, S., TU, Z., MITCHEM, J. B., SPITZER, D., GOEDEGEBUURE, P., MACH, R. H. & HAWKINS, W. G. 2010. The novel sigma-2 receptor ligand SW43 stabilizes pancreas cancer progression in combination with gemcitabine. *Mol Cancer*, 9, 298.
- HOU, C., TU, Z., MACH, R., KUNG, H. F. & KUNG, M. P. 2006. Characterization of a novel iodinated sigma-2 receptor ligand as a cell proliferation marker. *Nucl Med Biol*, 33, 203-9.
- HUANG, Y., HAMMOND, P. S., WHIRRETT, B. R., KUHNER, R. J., WU, L., CHILDERS, S. R. & MACH, R. H. 1998. Synthesis and quantitative structure-activity relationships of N-(1-benzylpiperidin-4-yl)phenylacetamides and related analogues as potent and selective sigma1 receptor ligands. *J Med Chem*, 41, 2361-70.
- HUANG, Y., LUEDTKE, R. R., FREEMAN, R. A., WU, L. & MACH, R. H. 2001a. Synthesis and structure-activity relationships of naphthamides as dopamine D3 receptor ligands. *J Med Chem*, 44, 1815-26.
- HUANG, Y., LUEDTKE, R. R., FREEMAN, R. A., WU, L. & MACH, R. H. 2001b. Synthesis of 2-(2,3-dimethoxyphenyl)-4-(aminomethyl)imidazole analogues and their binding affinities for dopamine D(2) and D(3) receptors. *Bioorg Med Chem*, 9, 3113-22.
- HUANG, Y. S., LU, H. L., ZHANG, L. J. & WU, Z. 2014. Sigma-2 receptor ligands and their perspectives in cancer diagnosis and therapy. *Med Res Rev*, 34, 532-66.
- IKONEN, E. 2001. Roles of lipid rafts in membrane transport. *Curr Opin Cell Biol*, 13, 470-7.
- ISHIMA, T. & HASHIMOTO, K. 2012. Potentiation of nerve growth factor-induced neurite outgrowth in PC12 cells by ifenprodil: the role of sigma-1 and IP3 receptors. *PLoS One*, 7, e37989.
- ITZHAK, Y. 1994. Modulation of the PCP/NMDA receptor complex and sigma binding sites by psychostimulants. *Neurotoxicol Teratol*, 16, 363-8.
- JELACIC, T. M., SIMS, S. M. & CLAPHAM, D. E. 1999. Functional expression and characterization of G-protein-gated inwardly rectifying K⁺ channels containing GIRK3. *J Membr Biol*, 169, 123-9.
- JOHNSON, E. F., PALMER, C. N., GRIFFIN, K. J. & HSU, M. H. 1996. Role of the peroxisome proliferator-activated receptor in cytochrome P450 4A gene regulation. *FASEB J*, 10, 1241-8.
- JONHEDE, S., PETERSEN, A., ZETTERBERG, M. & KARLSSON, J. O. 2010. Acute effects of the sigma-2 receptor agonist siramesine on lysosomal and extra-lysosomal proteolytic systems in lens epithelial cells. *Mol Vis*, 16, 819-27.
- KASHIWAGI, H., MCDUNN, J. E., SIMON, P. O., JR., GOEDEGEBUURE, P. S., XU, J., JONES, L., CHANG, K., JOHNSTON, F., TRINKAUS, K.,

- HOTCHKISS, R. S., MACH, R. H. & HAWKINS, W. G. 2007. Selective sigma-2 ligands preferentially bind to pancreatic adenocarcinomas: applications in diagnostic imaging and therapy. *Mol Cancer*, 6, 48.
- KASSIOU, M., DANNALS, R. F., LIU, X., WONG, D. F., RAVERT, H. T. & SCHEFFEL, U. A. 2005. Synthesis and in vivo evaluation of a new PET radioligand for studying sigma-2 receptors. *Bioorg Med Chem*, 13, 3623-6.
- KEKUDA, R., PRASAD, P. D., FEI, Y. J., LEIBACH, F. H. & GANAPATHY, V. 1996. Cloning and functional expression of the human type 1 sigma receptor (hSigmaR1). *Biochem Biophys Res Commun*, 229, 553-8.
- KHAZAN, N., YOUNG, G. A., EL-FAKANY, E. E., HONG, O. & CALLIGARO, D. 1984. Sigma receptors mediated the psychotomimetic effects of N-allylnormetazocine (SKF-10,047), but not its opioid agonistic-antagonistic properties. *Neuropharmacology*, 23, 983-7.
- KING, M., PAN, Y. X., MEI, J., CHANG, A., XU, J. & PASTERNAK, G. W. 1997. Enhanced kappa-opioid receptor-mediated analgesia by antisense targeting the sigma1 receptor. *Eur J Pharmacol*, 331, R5-6.
- KINNEY, G. G., HARRIS, E. W., RAY, R. & HUDZIK, T. J. 1995. sigma2 Site-mediated inhibition of electrically evoked guinea pig ileum longitudinal muscle/myenteric plexus contractions. *Eur J Pharmacol*, 294, 547-53.
- KNUDSON, A. G., JR. 1971. Mutation and cancer: statistical study of retinoblastoma. *Proc Natl Acad Sci U S A*, 68, 820-3.
- KOLESNICK, R. N. & KRONKE, M. 1998. Regulation of ceramide production and apoptosis. *Annu Rev Physiol*, 60, 643-65.
- LARGENT, B. L., WIKSTROM, H., GUNDLACH, A. L. & SNYDER, S. H. 1987. Structural determinants of sigma receptor affinity. *Mol Pharmacol*, 32, 772-84.
- LAURINI, E., ZAMPIERI, D., MAMOLO, M. G., VIO, L., ZANETTE, C., FLORIO, C., POSOCCO, P., FERMEGLIA, M. & PRICL, S. 2010. A 3D-pharmacophore model for sigma2 receptors based on a series of substituted benzo[d]oxazol-2(3H)-one derivatives. *Bioorg Med Chem Lett*, 20, 2954-7.
- LAZARENO, S. & BIRDSALL, N. J. 2000. Effects of contamination on radioligand binding parameters. *Trends Pharmacol Sci*, 21, 57-60.
- LEITNER, M. L., HOHMANN, A. G., PATRICK, S. L. & WALKER, J. M. 1994. Regional variation in the ratio of sigma 1 to sigma 2 binding in rat brain. *Eur J Pharmacol*, 259, 65-9.
- LEVER, J. R., GUSTAFSON, J. L., XU, R., ALLMON, R. L. & LEVER, S. Z. 2006. Sigma1 and sigma2 receptor binding affinity and selectivity of SA4503 and fluoroethyl SA4503. *Synapse*, 59, 350-8.
- LIPINSKI, C. A., LOMBARDO, F., DOMINY, B. W. & FEENEY, P. J. 2001. Experimental and computational approaches to estimate solubility and permeability in drug discovery and development settings. *Adv Drug Deliv Rev*, 46, 3-26.
- LURJE, G. & LENZ, H. J. 2009. EGFR signaling and drug discovery. *Oncology*, 77, 400-10.
- MACH, R. H., GAGE, H. D., BUCHHEIMER, N., HUANG, Y., KUHNER, R., WU, L., MORTON, T. E. & EHRENKAUFER, R. L. 2005. N-[18F]4'

- fluorobenzylpiperidin-4-yl-(2-fluorophenyl) acetamide ([¹⁸F]FBFPA): a potential fluorine-18 labeled PET radiotracer for imaging sigma-1 receptors in the CNS. *Synapse*, 58, 267-74.
- MACH, R. H., HUANG, Y., BUCHHEIMER, N., KUHNER, R., WU, L., MORTON, T. E., WANG, L., EHRENKAUFER, R. L., WALLEN, C. A. & WHEELER, K. T. 2001. [[¹⁸F]N-(4'-fluorobenzyl)-4-(3-bromophenyl) acetamide for imaging the sigma receptor status of tumors: comparison with [¹⁸F]FDG, and [(¹²⁵I)]IUDR. *Nucl Med Biol*, 28, 451-8.
- MACH, R. H., HUANG, Y., FREEMAN, R. A., WU, L., BLAIR, S. & LUEDTKE, R. R. 2003. Synthesis of 2-(5-bromo-2,3-dimethoxyphenyl)-5-(aminomethyl)-1H-pyrrole analogues and their binding affinities for dopamine D2, D3, and D4 receptors. *Bioorg Med Chem*, 11, 225-33.
- MACH, R. H., SMITH, C. R., AL-NABULSI, I., WHIRRETT, B. R., CHILDERS, S. R. & WHEELER, K. T. 1997. Sigma 2 receptors as potential biomarkers of proliferation in breast cancer. *Cancer Res*, 57, 156-61.
- MACH, R. H. & WHEELER, K. T. 2009. Development of molecular probes for imaging sigma-2 receptors in vitro and in vivo. *Cent Nerv Syst Agents Med Chem*, 9, 230-45.
- MACH, R. H., WU, L., WEST, T., WHIRRETT, B. R. & CHILDERS, S. R. 1999. The analgesic tropane analogue (+/-)-SM 21 has a high affinity for sigma2 receptors. *Life Sci*, 64, PL131-7.
- MAEDA, D. Y., WILLIAMS, W., KIM, W. E., THATCHER, L. N., BOWEN, W. D. & COOP, A. 2002. N-arylalkylpiperidines as high-affinity sigma-1 and sigma-2 receptor ligands: phenylpropylamines as potential leads for selective sigma-2 agents. *Bioorg Med Chem Lett*, 12, 497-500.
- MARTIN, W. R., EADES, C. G., THOMPSON, J. A., HUPPLER, R. E. & GILBERT, P. E. 1976. The effects of morphine- and nalorphine- like drugs in the nondependent and morphine-dependent chronic spinal dog. *J Pharmacol Exp Ther*, 197, 517-32.
- MATSUMOTO, R. R., LIU, Y., LERNER, M., HOWARD, E. W. & BRACKETT, D. J. 2003. Sigma receptors: potential medications development target for anti-cocaine agents. *Eur J Pharmacol*, 469, 1-12.
- MATTSON, M. P. & CHAN, S. L. 2003. Calcium orchestrates apoptosis. *Nat Cell Biol*, 5, 1041-3.
- MAURICE, T. & LOCKHART, B. P. 1997. Neuroprotective and anti-amnesic potentials of sigma (sigma) receptor ligands. *Prog Neuropsychopharmacol Biol Psychiatry*, 21, 69-102.
- MAURICE, T., URANI, A., PHAN, V. L. & ROMIEU, P. 2001. The interaction between neuroactive steroids and the sigma1 receptor function: behavioral consequences and therapeutic opportunities. *Brain Res Brain Res Rev*, 37, 116-32.
- MAUVAIS-JARVIS, F. 2011. Estrogen and androgen receptors: regulators of fuel homeostasis and emerging targets for diabetes and obesity. *Trends Endocrinol Metab*, 22, 24-33.
- MCCANN, D. J., WEISSMAN, A. D. & SU, T. P. 1994. Sigma-1 and sigma-2 sites in rat brain: comparison of regional, ontogenetic, and subcellular patterns. *Synapse*, 17, 182-9.

- MCCONKEY, D. J. & ORRENIUS, S. 1996. The role of calcium in the regulation of apoptosis. *J Leukoc Biol*, 59, 775-83.
- MEI, J. & PASTERNAK, G. W. 2001. Molecular cloning and pharmacological characterization of the rat sigma1 receptor. *Biochem Pharmacol*, 62, 349-55.
- MENDELSON, L. G., KALRA, V., JOHNSON, B. G. & KERCHNER, G. A. 1985. Sigma opioid receptor: characterization and co-identity with the phencyclidine receptor. *J Pharmacol Exp Ther*, 233, 597-602.
- MICHELOT, J. M., MOREAU, M. F., VEYRE, A. J., BONAFIOUS, J. F., BACIN, F. J., MADELMONT, J. C., BUSSIERE, F., SOUTEYRAND, P. A., MAUCLAIRE, L. P., CHOSSAT, F. M. & ET AL. 1993. Phase II scintigraphic clinical trial of malignant melanoma and metastases with iodine-123-N-(2-diethylaminoethyl 4-iodobenzamide). *J Nucl Med*, 34, 1260-6.
- MIR, S. U., AHMED, I. S., ARNOLD, S. & CRAVEN, R. J. 2012. Elevated progesterone receptor membrane component 1/sigma-2 receptor levels in lung tumors and plasma from lung cancer patients. *Int J Cancer*, 131, E1-9.
- MOLTZEN, E. K., PERREGAARD, J. & MEIER, E. 1995. Sigma ligands with subnanomolar affinity and preference for the sigma 2 binding site. 2. Spiro-joined benzofuran, isobenzofuran, and benzopyran piperidines. *J Med Chem*, 38, 2009-17.
- MONNET, F. P., DE COSTA, B. R. & BOWEN, W. D. 1996. Differentiation of sigma ligand-activated receptor subtypes that modulate NMDA-evoked [3H]-noradrenaline release in rat hippocampal slices. *Br J Pharmacol*, 119, 65-72.
- NARAYANAN, S., BHAT, R., MESANGEAU, C., POUPAERT, J. H. & MCCURDY, C. R. 2011. Early development of sigma-receptor ligands. *Future Med Chem*, 3, 79-94.
- NEWMAN, J. D., ANTHONY, J. R. & DONOHUE, T. J. 2001. The importance of zinc-binding to the function of Rhodospirillum rubrum ChrR as an anti-sigma factor. *J Mol Biol*, 313, 485-99.
- NGUYEN, D. H. & HILDRETH, J. E. 2000. Evidence for budding of human immunodeficiency virus type 1 selectively from glycolipid-enriched membrane lipid rafts. *J Virol*, 74, 3264-72.
- NICHOLSON, H., COMEAU, A., MESANGEAU, C., MCCURDY, C. R. & BOWEN, W. D. 2015. Characterization of CM572, a Selective Irreversible Partial Agonist of the Sigma-2 Receptor with Antitumor Activity. *J Pharmacol Exp Ther*, 354, 203-12.
- NICOTERA, P. & ORRENIUS, S. 1998. The role of calcium in apoptosis. *Cell Calcium*, 23, 173-80.
- NORTH, W. G., GAO, G., MEMOLI, V. A., PANG, R. H. & LYNCH, L. 2010. Breast cancer expresses functional NMDA receptors. *Breast Cancer Res Treat*, 122, 307-14.
- NOVAKOVA, M., ELA, C., BOWEN, W. D., HASIN, Y. & EILAM, Y. 1998. Highly selective sigma receptor ligands elevate inositol 1,4,5-trisphosphate production in rat cardiac myocytes. *Eur J Pharmacol*, 353, 315-27.

- OGAWA, K., SHIBA, K., AKHTER, N., YOSHIMOTO, M., WASHIYAMA, K., KINUYA, S., KAWAI, K. & MORI, H. 2009. Evaluation of radioiodinated vesamicol analogs for sigma receptor imaging in tumor and radionuclide receptor therapy. *Cancer Sci*, 100, 2188-92.
- OLIFERENKO, S., PAIHA, K., HARDER, T., GERKE, V., SCHWARZLER, C., SCHWARZ, H., BEUG, H., GUNTHER, U. & HUBER, L. A. 1999. Analysis of CD44-containing lipid rafts: Recruitment of annexin II and stabilization by the actin cytoskeleton. *J Cell Biol*, 146, 843-54.
- OSTENFELD, M. S., FEHRENBACHER, N., HOYER-HANSEN, M., THOMSEN, C., FARKAS, T. & JAATTELA, M. 2005. Effective tumor cell death by sigma-2 receptor ligand siramesine involves lysosomal leakage and oxidative stress. *Cancer Res*, 65, 8975-83.
- PALESTINI, P., PITTO, M., TEDESCHI, G., FERRARETTO, A., PARENTI, M., BRUNNER, J. & MASSERINI, M. 2000. Tubulin anchoring to glycolipid-enriched, detergent-resistant domains of the neuronal plasma membrane. *J Biol Chem*, 275, 9978-85.
- PAN, Y. X., MEI, J., XU, J., WAN, B. L., ZUCKERMAN, A. & PASTERNAK, G. W. 1998. Cloning and characterization of a mouse sigma1 receptor. *J Neurochem*, 70, 2279-85.
- PATI, M. L., GROZA, D., RIGANTI, C., KOPECKA, J., NISO, M., BERARDI, F., HAGER, S., HEFFETER, P., HIRAI, M., TSUGAWA, H., KABE, Y., SUEMATSU, M. & ABATE, C. 2016. Sigma-2 receptor and progesterone receptor membrane component 1 (PGRMC1) are two different proteins: Proofs by fluorescent labeling and binding of sigma-2 receptor ligands to PGRMC1. *Pharmacol Res*, 117, 67-74.
- PATI, M. L., HORNICK, J. R., NISO, M., BERARDI, F., SPITZER, D., ABATE, C. & HAWKINS, W. 2017. Sigma-2 receptor agonist derivatives of 1-Cyclohexyl-4-[3-(5-methoxy-1,2,3,4-tetrahydronaphthalen-1-yl)propyl]piperazine (PB28) induce cell death via mitochondrial superoxide production and caspase activation in pancreatic cancer. *BMC Cancer*, 17, 51.
- PATRICK, S. L., WALKER, J. M., PERKEL, J. M., LOCKWOOD, M. & PATRICK, R. L. 1993. Increases in rat striatal extracellular dopamine and vacuous chewing produced by two sigma receptor ligands. *Eur J Pharmacol*, 231, 243-9.
- PELUSO, J. J., DECERBO, J. & LODDE, V. 2012a. Evidence for a genomic mechanism of action for progesterone receptor membrane component-1. *Steroids*, 77, 1007-12.
- PELUSO, J. J., GAWKOWSKA, A., LIU, X., SHIODA, T. & PRU, J. K. 2009. Progesterone receptor membrane component-1 regulates the development and Cisplatin sensitivity of human ovarian tumors in athymic nude mice. *Endocrinology*, 150, 4846-54.
- PELUSO, J. J., LODDE, V. & LIU, X. 2012b. Progesterone regulation of progesterone receptor membrane component 1 (PGRMC1) sumoylation and transcriptional activity in spontaneously immortalized granulosa cells. *Endocrinology*, 153, 3929-39.
- PERREGAARD, J., MOLTZEN, E. K., MEIER, E. & SANCHEZ, C. 1995. Sigma ligands with subnanomolar affinity and preference for the sigma 2

- binding site. 1. 3-(omega-aminoalkyl)-1H-indoles. *J Med Chem*, 38, 1998-2008.
- PRASAD, P. D., LI, H. W., FEI, Y. J., GANAPATHY, M. E., FUJITA, T., PLUMLEY, L. H., YANG-FENG, T. L., LEIBACH, F. H. & GANAPATHY, V. 1998. Exon-intron structure, analysis of promoter region, and chromosomal localization of the human type 1 sigma receptor gene. *J Neurochem*, 70, 443-51.
- QUICK, M. W. & LESTER, R. A. 2002. Desensitization of neuronal nicotinic receptors. *J Neurobiol*, 53, 457-78.
- QUIRION, R., BOWEN, W. D., ITZHAK, Y., JUNIEN, J. L., MUSACCHIO, J. M., ROTHMAN, R. B., SU, T. P., TAM, S. W. & TAYLOR, D. P. 1992. A proposal for the classification of sigma binding sites. *Trends Pharmacol Sci*, 13, 85-6.
- QUIRION, R., PILAPIL, C. & MAGNAN, J. 1987. Localization of kappa opioid receptor binding sites in human forebrain using [3H]U69,593: comparison with [3H]bremazocine. *Cell Mol Neurobiol*, 7, 303-7.
- RASTINEJAD, F., PERLMANN, T., EVANS, R. M. & SIGLER, P. B. 1995. Structural determinants of nuclear receptor assembly on DNA direct repeats. *Nature*, 375, 203-11.
- RODGERS, W. & ROSE, J. K. 1996. Exclusion of CD45 inhibits activity of p56lck associated with glycolipid-enriched membrane domains. *J Cell Biol*, 135, 1515-23.
- RODOT, S., DARICOURT, J., BUSSIERE, F., LACOUR, J. P., MIGNECO, O., THYSS, A., MICHELOT, J. M., BONAFIOUS, J. F., SCHNEIDER, M., BARETY, M. & ET AL. 1994. A radiolabelled iodobenzamide for malignant melanoma staging. *Melanoma Res*, 4, 307-12.
- ROE, M. W., LEMASTERS, J. J. & HERMAN, B. 1990. Assessment of Fura-2 for measurements of cytosolic free calcium. *Cell Calcium*, 11, 63-73.
- ROHE, H. J., AHMED, I. S., TWIST, K. E. & CRAVEN, R. J. 2009. PGRMC1 (progesterone receptor membrane component 1): a targetable protein with multiple functions in steroid signaling, P450 activation and drug binding. *Pharmacol Ther*, 121, 14-9.
- ROPERTO, S., COLABUFO, N. A., INGLESE, C., URRARO, C., BRUN, R., MEZZA, E., STAIBANO, S., RASO, C., MAIOLINO, P., RUSSO, V., PALMA, E. & ROPERTO, F. 2010. Sigma-2 receptor expression in bovine papillomavirus-associated urinary bladder tumours. *J Comp Pathol*, 142, 19-26.
- ROWLAND, D. J., TU, Z., XU, J., PONDE, D., MACH, R. H. & WELCH, M. J. 2006. Synthesis and in vivo evaluation of 2 high-affinity 76Br-labeled sigma2-receptor ligands. *J Nucl Med*, 47, 1041-8.
- RUGGERO, D. 2009. The role of Myc-induced protein synthesis in cancer. *Cancer Res*, 69, 8839-43.
- RYBCZYNSKA, A. A., DIERCKX, R. A., ISHIWATA, K., ELSINGA, P. H. & VAN WAARDE, A. 2008. Cytotoxicity of sigma-receptor ligands is associated with major changes of cellular metabolism and complete occupancy of the sigma-2 subpopulation. *J Nucl Med*, 49, 2049-56.

- SCHMIDT, H. R., ZHENG, S., GURPINAR, E., KOEHL, A., MANGLIK, A. & KRUSE, A. C. 2016. Crystal structure of the human sigma1 receptor. *Nature*, 532, 527-30.
- SEO, M. D., ENOMOTO, M., ISHIYAMA, N., STATHOPOULOS, P. B. & IKURA, M. 2015. Structural insights into endoplasmic reticulum stored calcium regulation by inositol 1,4,5-trisphosphate and ryanodine receptors. *Biochim Biophys Acta*, 1853, 1980-91.
- SEPULVEDA, M. I., LUMMIS, S. C. & MARTIN, I. L. 1991. The agonist properties of m-chlorophenylbiguanide and 2-methyl-5-hydroxytryptamine on 5-HT₃ receptors in N1E-115 neuroblastoma cells. *Br J Pharmacol*, 104, 536-40.
- SETH, P., FEI, Y. J., LI, H. W., HUANG, W., LEIBACH, F. H. & GANAPATHY, V. 1998. Cloning and functional characterization of a sigma receptor from rat brain. *J Neurochem*, 70, 922-31.
- SHIN, E. J., NAH, S. Y., CHAE, J. S., BING, G., SHIN, S. W., YEN, T. P., BAEK, I. H., KIM, W. K., MAURICE, T., NABESHIMA, T. & KIM, H. C. 2007. Dextromethorphan attenuates trimethyltin-induced neurotoxicity via sigma1 receptor activation in rats. *Neurochem Int*, 50, 791-9.
- SIDHU, A., KIMURA, K., UH, M., WHITE, B. H. & PATEL, S. 1998. Multiple coupling of human D5 dopamine receptors to guanine nucleotide binding proteins Gs and Gz. *J Neurochem*, 70, 2459-67.
- SIMONS, K. & IKONEN, E. 1997. Functional rafts in cell membranes. *Nature*, 387, 569-72.
- SINGER, S. J. & NICOLSON, G. L. 1972. The fluid mosaic model of the structure of cell membranes. *Science*, 175, 720-31.
- SMITH, S. M., WUNDER, M. B., NORRIS, D. A. & SHELLMAN, Y. G. 2011. A simple protocol for using a LDH-based cytotoxicity assay to assess the effects of death and growth inhibition at the same time. *PLoS One*, 6, e26908.
- SOBY, K. K., MIKKELSEN, J. D., MEIER, E. & THOMSEN, C. 2002. Lu 28-179 labels a sigma(2)-site in rat and human brain. *Neuropharmacology*, 43, 95-100.
- SPRUCE, B. A., CAMPBELL, L. A., MCTAVISH, N., COOPER, M. A., APPLEBY, M. V., O'NEILL, M., HOWIE, J., SAMSON, J., WATT, S., MURRAY, K., MCLEAN, D., LESLIE, N. R., SAFRANY, S. T., FERGUSON, M. J., PETERS, J. A., PRESCOTT, A. R., BOX, G., HAYES, A., NUTLEY, B., RAYNAUD, F., DOWNES, C. P., LAMBERT, J. J., THOMPSON, A. M. & ECCLES, S. 2004. Small molecule antagonists of the sigma-1 receptor cause selective release of the death program in tumor and self-reliant cells and inhibit tumor growth in vitro and in vivo. *Cancer Res*, 64, 4875-86.
- SU, T. P. 1982. Evidence for sigma opioid receptor: binding of [3H]SKF-10047 to etorphine-inaccessible sites in guinea-pig brain. *J Pharmacol Exp Ther*, 223, 284-90.
- SU, T. P., LONDON, E. D. & JAFFE, J. H. 1988. Steroid binding at sigma receptors suggests a link between endocrine, nervous, and immune systems. *Science*, 240, 219-21.

- SUZANNE, M. & STELLER, H. 2013. Shaping organisms with apoptosis. *Cell Death Differ*, 20, 669-75.
- SUZUKI, T. 2002. Lipid rafts at postsynaptic sites: distribution, function and linkage to postsynaptic density. *Neurosci Res*, 44, 1-9.
- TAM, S. W. 1985. (+)-[3H]SKF 10,047, (+)-[3H]ethylketocyclazocine, mu, kappa, delta and phencyclidine binding sites in guinea pig brain membranes. *Eur J Pharmacol*, 109, 33-41.
- TAN, D., TAN, S., ZHANG, J., TANG, P., HUANG, J., ZHOU, W. & WU, S. 2013. Histone trimethylation of the p53 gene by expression of a constitutively active prolactin receptor in prostate cancer cells. *Chin J Physiol*, 56, 282-90.
- TANG, L., GAMAL EL-DIN, T. M., PAYANDEH, J., MARTINEZ, G. Q., HEARD, T. M., SCHEUER, T., ZHENG, N. & CATTERALL, W. A. 2014. Structural basis for Ca²⁺ selectivity of a voltage-gated calcium channel. *Nature*, 505, 56-61.
- TANG, P., HUNG, M. C. & KLOSTERGAARD, J. 1996. Human pro-tumor necrosis factor is a homotrimer. *Biochemistry*, 35, 8216-25.
- TANIGUCHI, C. M., EMANUELLI, B. & KAHN, C. R. 2006. Critical nodes in signalling pathways: insights into insulin action. *Nat Rev Mol Cell Biol*, 7, 85-96.
- TANTRAL, L., MALATHI, K., KOHYAMA, S., SILANE, M., BERENSTEIN, A. & JAYARAMAN, T. 2004. Intracellular calcium release is required for caspase-3 and -9 activation. *Cell Biochem Funct*, 22, 35-40.
- THOMAS, G. E., SZUCS, M., MAMONE, J. Y., BEM, W. T., RUSH, M. D., JOHNSON, F. E. & COSCIA, C. J. 1990. Sigma and opioid receptors in human brain tumors. *Life Sci*, 46, 1279-86.
- TOBIN, A. B. 2008. G-protein-coupled receptor phosphorylation: where, when and by whom. *Br J Pharmacol*, 153 Suppl 1, S167-76.
- TORRENCE-CAMPBELL, C. & BOWEN, W. D. 1996. Differential solubilization of rat liver sigma 1 and sigma 2 receptors: retention of sigma 2 sites in particulate fractions. *Eur J Pharmacol*, 304, 201-10.
- TU, Z., DENCE, C. S., PONDE, D. E., JONES, L., WHEELER, K. T., WELCH, M. J. & MACH, R. H. 2005. Carbon-11 labeled sigma2 receptor ligands for imaging breast cancer. *Nucl Med Biol*, 32, 423-30.
- TU, Z., XU, J., JONES, L. A., LI, S., DUMSTORFF, C., VANGVERAVONG, S., CHEN, D. L., WHEELER, K. T., WELCH, M. J. & MACH, R. H. 2007. Fluorine-18-labeled benzamide analogues for imaging the sigma2 receptor status of solid tumors with positron emission tomography. *J Med Chem*, 50, 3194-204.
- ULUKAYA, E., COLAKOGULLARI, M. & WOOD, E. J. 2004. Interference by anti-cancer chemotherapeutic agents in the MTT-tumor chemosensitivity assay. *Chemotherapy*, 50, 43-50.
- VAN WAARDE, A., RYBCZYNSKA, A. A., RAMAKRISHNAN, N., ISHIWATA, K., ELSINGA, P. H. & DIERCKX, R. A. 2010. Sigma receptors in oncology: therapeutic and diagnostic applications of sigma ligands. *Curr Pharm Des*, 16, 3519-37.
- VAUPEL, D. B. 1983. Naltrexone fails to antagonize the sigma effects of PCP and SKF 10,047 in the dog. *Eur J Pharmacol*, 92, 269-74.

- VAZQUEZ, S. M., PIGNATARO, O. & LUTHY, I. A. 1999. Alpha2-adrenergic effect on human breast cancer MCF-7 cells. *Breast Cancer Res Treat*, 55, 41-9.
- VERI, M. C., DEBELL, K. E., SEMINARIO, M. C., DIBALDASSARRE, A., REISCHL, I., RAWAT, R., GRAHAM, L., NOVIELLO, C., RELLAHAN, B. L., MISCIA, S., WANGE, R. L. & BONVINI, E. 2001. Membrane raft-dependent regulation of phospholipase Cgamma-1 activation in T lymphocytes. *Mol Cell Biol*, 21, 6939-50.
- VILNER, B. J. & BOWEN, W. D. 1993. Sigma receptor-active neuroleptics are cytotoxic to C6 glioma cells in culture. *Eur J Pharmacol*, 244, 199-201.
- VILNER, B. J. & BOWEN, W. D. 2000. Modulation of cellular calcium by sigma-2 receptors: release from intracellular stores in human SK-N-SH neuroblastoma cells. *J Pharmacol Exp Ther*, 292, 900-11.
- VILNER, B. J., DE COSTA, B. R. & BOWEN, W. D. 1995a. Cytotoxic effects of sigma ligands: sigma receptor-mediated alterations in cellular morphology and viability. *J Neurosci*, 15, 117-34.
- VILNER, B. J., JOHN, C. S. & BOWEN, W. D. 1995b. Sigma-1 and sigma-2 receptors are expressed in a wide variety of human and rodent tumor cell lines. *Cancer Res*, 55, 408-13.
- VOGT, P. K. 1993. Cancer genes. *West J Med*, 158, 273-8.
- VON HALLER, P. D., DONOHOE, S., GOODLETT, D. R., AEBERSOLD, R. & WATTS, J. D. 2001. Mass spectrometric characterization of proteins extracted from Jurkat T cell detergent-resistant membrane domains. *Proteomics*, 1, 1010-21.
- WAJANT, H. 2002. The Fas signaling pathway: more than a paradigm. *Science*, 296, 1635-6.
- WATERHOUSE, R. N. & COLLIER, T. L. 1997. In vivo evaluation of [18F]1-(3-fluoropropyl)-4-(4-cyanophenoxymethyl)piperidine: a selective sigma-1 receptor radioligand for PET. *Nucl Med Biol*, 24, 127-34.
- WATERHOUSE, R. N., STABIN, M. G. & PAGE, J. G. 2003. Preclinical acute toxicity studies and rodent-based dosimetry estimates of the novel sigma-1 receptor radiotracer [(18)F]FPS. *Nucl Med Biol*, 30, 555-63.
- WHEELER, K. T., WANG, L. M., WALLEN, C. A., CHILDERS, S. R., CLINE, J. M., KENG, P. C. & MACH, R. H. 2000. Sigma-2 receptors as a biomarker of proliferation in solid tumours. *Br J Cancer*, 82, 1223-32.
- WOLFE, S. A., JR., CULP, S. G. & DE SOUZA, E. B. 1989. Sigma-receptors in endocrine organs: identification, characterization, and autoradiographic localization in rat pituitary, adrenal, testis, and ovary. *Endocrinology*, 124, 1160-72.
- WONG, E. H., KNIGHT, A. R. & WOODRUFF, G. N. 1988. [3H]MK-801 labels a site on the N-methyl-D-aspartate receptor channel complex in rat brain membranes. *J Neurochem*, 50, 274-81.
- WU, Z. S., CHENG, H., JIANG, Y., MELCHER, K. & XU, H. E. 2015. Ion channels gated by acetylcholine and serotonin: structures, biology, and drug discovery. *Acta Pharmacol Sin*, 36, 895-907.
- XU, J., ZENG, C., CHU, W., PAN, F., ROTHFUSS, J. M., ZHANG, F., TU, Z., ZHOU, D., ZENG, D., VANGVERAVONG, S., JOHNSTON, F., SPITZER, D., CHANG, K. C., HOTCHKISS, R. S., HAWKINS, W. G., WHEELER, K.

- T. & MACH, R. H. 2011. Identification of the PGRMC1 protein complex as the putative sigma-2 receptor binding site. *Nat Commun*, 2, 380.
- XU, R., LORD, S. A., PETERSON, R. M., FERGASON-CANTRELL, E. A., LEVER, J. R. & LEVER, S. Z. 2015. Ether modifications to 1-[2-(3,4-dimethoxyphenyl)ethyl]-4-(3-phenylpropyl)piperazine (SA4503): effects on binding affinity and selectivity for sigma receptors and monoamine transporters. *Bioorg Med Chem*, 23, 222-30.
- YAMAMOTO, H., HIGA-NAKAMINE, S., NOGUCHI, N., MAEDA, N., KONDO, Y., TOKU, S., KUKITA, I. & SUGAHARA, K. 2014. Desensitization by different strategies of epidermal growth factor receptor and ErbB4. *J Pharmacol Sci*, 124, 287-93.
- YEH, S. H., LIU, R. S., WU, L. C., YANG, D. J., YEN, S. H., CHANG, C. W., YU, T. W., CHOU, K. L. & CHEN, K. Y. 1996. Fluorine-18 fluoromisonidazole tumour to muscle retention ratio for the detection of hypoxia in nasopharyngeal carcinoma. *Eur J Nucl Med*, 23, 1378-83.
- ZENG, C., GARG, N. & MACH, R. H. 2016. The PGRMC1 Protein Level Correlates with the Binding Activity of a Sigma-2 Fluorescent Probe (SW120) in Rat Brain Cells. *Mol Imaging Biol*, 18, 172-9.
- ZENG, C., ROTHFUSS, J. M., ZHANG, J., VANGVERAVONG, S., CHU, W., LI, S., TU, Z., XU, J. & MACH, R. H. 2014. Functional assays to define agonists and antagonists of the sigma-2 receptor. *Anal Biochem*, 448, 68-74.
- ZENG, C., VANGVERAVONG, S., JONES, L. A., HYRC, K., CHANG, K. C., XU, J., ROTHFUSS, J. M., GOLDBERG, M. P., HOTCHKISS, R. S. & MACH, R. H. 2011. Characterization and evaluation of two novel fluorescent sigma-2 receptor ligands as proliferation probes. *Mol Imaging*, 10, 420-33.
- ZENG, C., VANGVERAVONG, S., XU, J., CHANG, K. C., HOTCHKISS, R. S., WHEELER, K. T., SHEN, D., ZHUANG, Z. P., KUNG, H. F. & MACH, R. H. 2007. Subcellular localization of sigma-2 receptors in breast cancer cells using two-photon and confocal microscopy. *Cancer Res*, 67, 6708-16.
- ZHANG, C., HU, J. J., XIA, M., BOINI, K. M., BRIMSON, C. & LI, P. L. 2010. Redox signaling via lipid raft clustering in homocysteine-induced injury of podocytes. *Biochim Biophys Acta*, 1803, 482-91.
- ZILFOU, J. T. & LOWE, S. W. 2009. Tumor suppressive functions of p53. *Cold Spring Harb Perspect Biol*, 1, a001883.
- ZITVOGEL, L., APETOH, L., GHIRINGHELLI, F., ANDRE, F., TESNIERE, A. & KROEMER, G. 2008. The anticancer immune response: indispensable for therapeutic success? *J Clin Invest*, 118, 1991-2001.
- ZUKIN, S. R., BRADY, K. T., SLIFER, B. L. & BALSTER, R. L. 1984. Behavioral and biochemical stereoselectivity of sigma opiate/PCP receptors. *Brain Res*, 294, 174-7.